Investigation of the mechanisms of repair following Ventilator Induced Lung Injury and the potential for Mesenchymal Stem Cells to enhance the repair process.

By Gerard Curley MB, BCh, BAO, FCARCSI

A Thesis Submitted in Fulfillment of the Requirements for the Degree of Doctor of Philosophy (Ph.D.)

Anaesthesia, School of Medicine

National University of Ireland, Galway

February 2012

Supervisor: Professor John G Laffey

Summary of Contents

Detailed Table of Contents

Acknowledgements

First and foremost I wish to gratefully acknowledge the expert advice and direction of Professor John G Laffey, who has given me unlimited support before, during and after this project, and without whose first-rate guidance the project would not have come to fruition.

I would like to acknowledge the contributions of the other members of the Lung Biology Group at NUI, Galway, in particular Dr Brendan Higgins, Dr Daniel O'Toole, and Dr James Devaney who shared with me their expertise in in vivo and in vitro laboratory techniques. I am also indebted to many other scientists in REMEDI, in particular Dr Eric Farrell, Ms Georgina Shaw, and Dr Aideen Ryan, for their guidance with regard to Mesenchymal Stem Cells

I am grateful to my fellow PhD students for their help and support in a variety of areas where their experience is far superior to mine, in particular Dr Maya Contreras, Ms Claire Masterson, Ms Patricia McHale, Dr Bilal Ansari and Dr Mairead Hayes.

I gratefully acknowledge the funding sources that made my Ph.D. work possible. My work was generously supported by a Molecular Medicine Ireland Clinician Scientist Fellowship Award, through the Higher Education Authority (PRTLI Cycle 4). The Lung Biology Group is also supported by funding from the European Research Council, Brussels, Belgium, under the Framework 7 Programme (Grant No: ERC-2007-StG 207777) and the Health Research Board, Dublin, Ireland (Grant No: RP/2008/193).

Finally, I wish to thank my family, in particular my wife Sarah, my son Harry, and daughters Molly and Zoe, for their patience, support and encouragement throughout these last four years.

Dedication

This work is dedicated to my wife Sarah, son Harry and daughters Molly and Zoe.

1.0 Thesis Abstract

Introduction: ARDS is a syndrome of acute respiratory failure that presents with progressive arterial hypoxemia, dyspnea, and a marked increase in the work of breathing. Virtually all patients with ARDS receive mechanical ventilation. However, the delivery of even "normal" tidal volumes may indeed have the potential to be quite injurious to the injured, mechanically ventilated ARDS lung. Lung ventilation volume increases lead to progressive epithelial cell deformation, with disruption of the alveolar-capillary barrier and injury to the alveolar epithelium. One of the most important mechanisms that determines the severity of lung injury is the magnitude of injury to the alveolar epithelial barrier. The possibility of repairing the epithelial injury at an early stage is a major determinant of recovery. Specific treatments to accelerate alveolar epithelial repair do not exist. Little is known at present about the cellular and molecular mechanisms of of efficient and aberrant alveolar epithelial repair in ALI/ARDS. Recent pre-clinical experimental studies indicate that bone-marrow derived mesenchymal stem cells (MSCs) may reduce the severity of Acute Lung Injury (ALI). However the potential for MSC's to enhance repair and recovery following ALI is not known.

Methods: We first described the factors important in the development of an animal model of recovery from VILI, allowing the study of the development and repair from this type of lung injury over time. We then sought to examine the pattern of inflammation, injury, and repair, the time course and mechanisms of resolution and repair, and the potential for fibrosis, following ventilation

induced lung injury (VILI). We then used our unique animal model of repair from VILI to test the reparative properties of MSCs, using different doses and timing of delivery. We also examined the potential for non-stem cells, and for MSC secreted products, to enhance repair in comparison to MSCs. The contribution of specific MSC secreted mediators was then examined in a wound healing model. Finally we examined different routes of administration of MSCs in our repair model.

Results: We defined factors that are important in the development of VILI and integral to developing a reliable, reproducible animal model that represents the disease, including younger animal age, peak pressures above a threshold value and higher inspiratory flow rates. We developed a cohort of animals with an homogenous injury, that was representative of stretch induced lung damage. High stretch ventilation caused a severe lung injury, activating a transient inflammatory and fibroproliferative repair response, which restored normal lung architecture without evidence of fibrosis. MSCs therapy enhanced repair following VILI. Specifically, MSCs improved oxygenation, lung compliance, reduced total lung water, decreased lung inflammation and histologic lung injury. MSC therapy attenuated alveolar TNF-alpha and IL-6 levels, but increased alveolar IL-10 concentrations. Conditioned MSC medium also enhanced lung repair and attenuated the inflammatory response to lung stretch. MSCs and their conditioned medium were twice as effective in healing alveolar epithelial wounds in comparison to fibroblasts and their conditioned medium controls. Antibodies to Keratinocyte Growth Factor, but not Hepatocyte Growth Factor, or Transforming Growth Factor-β, attenuated this effect on alveolar epithelial

repair of MSC conditioned medium. Finally, intratracheal MSC therapy and intra-tracheal conditioned MSC medium also enhanced lung repair and attenuated the inflammatory response to lung stretch.

Conclusion: This novel rat model of repair from VILI will serve to improve our knowledge of the mechanisms of repair as well as provide a useful paradigm for testing strategies to hasten recovery in ALI. In our studies of repair from VILI, multiple targets to hasten recovery were identified, and the potential for a more sustained fibroproliferative response was noted. MSCs, delivered systemically or locally, can modulate the inflammatory response to VILI, enhance alveolar fluid clearance and augment repair in the lung. The therapeutic effect appears to be mediated through paracrine factors secreted by MSCs. The ability of MSCs to enhance recovery after Ventilator Induced Lung Injury may in part be due to their abiltiy to enhance alveolar epithelial wound repair, and that this mechansim may result wholly or in part from the secretion of Keratinocyte Growth Factor by MSCs.

2.0 Introduction

2.1 The Acute Respiratory Distress Syndrome

Acute Lung Injury (ALI), and it's more severe subset Acute Respiratory Distress Syndrome (ARDS), is a syndrome of acute respiratory failure that presents with progressive arterial hypoxemia, dyspnea, and a marked increase in the work of breathing. Most patients require endotracheal intubation and positive pressure ventilation. In 2005, the incidence of ALI and ARDS in adults was estimated to be approximately 200,000 patients annually in the United States, with a mortality of approximately 40% [1]. Because of the aging population and the growing incidence of sepsis, this figure probably underestimates the actual incidence [2]. Despite major advances in management, the mortality of ARDS remains as high as 44% based on observational studies and 36% based on randomized controlled trials [3]. Although there are several clinical disorders associated with the development of ARDS, including sepsis, pneumonia, aspiration of gastric contents, and major trauma [4], the pathogenesis is common to all and involves inflammatory injury to the lung endothelium and epithelium, which causes a marked increase in lung vascular and epithelial permeability and the passage of protein-rich edema fluid into the air spaces. The initial lung injury can be compounded by Ventilator-Induced Lung Injury (VILI), particularly when high tidal volumes and inflation pressures are used [5].

Clinical recovery from ALI/ARDS depends on the use of lung-protective ventilation with lower tidal volumes and the reduction of airway pressures, which facilitate the resolution of inflammation, repair of the injured epithelium, and removal of edema fluid from the air spaces. Although there has been

considerable progress in understanding the pathogenesis of ALI/ARDS, there are several important gaps in our knowledge. In particular, the mechanisms that contribute to restoration of a normal alveolar epithelium require more study.

2.2 Ventilator Induced Lung Injury

Virtually all patients with ARDS receive mechanical ventilation. Regional alveolar overdistension during ventilation can induce excessive mechanical stresses to the extracellular matrix, leading to the development of interstitial edema, extra-cellular matrix fragmentation [6], epithelial injury, and biotrauma characterized by neutrophil infiltration and inflammatory cytokine production [6, 7].

2.2.1 What is Ventilator Induced Lung Injury?

Animal studies revealed that a ventilation strategy with lower tidal volumes and lower airway pressures was protective in ALI due to several mechanisms, including reduced lung endothelial injury, reduced lung epithelial injury, reduced lung inflammation, and accelerated resolution of alveolar edema [7, 8]. Thus, ventilation with higher tidal volumes and elevated airway pressures causes more lung inflammation and probably results in direct mechanical injury to the lung epithelium and endothelium as well.

2.3 The pathogenesis of VILI – Understanding the injury

VILI results from the action of mechanical forces on lung structures such as the epithelial cells, the endothelial cells, the extracellular matrix and the peripheral airways during mechanical ventilation. In particular, cyclic over-distension and

collapse/re-opening of airway units with each breath are two key pathophysiological mechanisms leading to VILI [9].

It is not possible to study the effects of isolated excess mechanical stretch injury on human lungs. However, extensive study of animal lungs injured by excessive ventilation has been carried out. Current mechanistic insights into VILI include ventilator induced pulmonary oedema, volutrauma, barotrauma, biotrauma, mechanotransduction and activation of inflammatory cells and mediators.

2.3.1 The concept of baby lung

Injured lungs are particularly susceptible to overdistension because the number of aerated and recruitable alveoli is decreased ("the baby lung concept") [10]. Within the baby lung, both fully aerated and nonaerated but recruitable respiratory units exist in close proximity. This has been confirmed by computerized tomography (CT) in patients with ARDS [11]. A preferential distribution of ventilation to the less injured units places these units at a higher risk for hyperinflation injury. Supporting this hypothesis is recent histologic and CT imaging data in a rat VILI model that demonstrates a regional redistribution of ventilation from atelectatic to non-atelectatic areas resulting in overinflation injury [12]. In this study, a combination of high tidal volume and lack of recruitment of atelectatic regions consistently demonstrated histologic evidence of alveolar injury as measured by hyaline membrane formation, inflammatory cell infiltration, and the presence of alveolar epithelial cell lesions. Markers of biotrauma such as cytokines IL-6, IL-1β, and myeloperoxidase were elevated as well. Clearly the delivery of what would be a "normal" tidal volume to a healthy

non-atelectatic lung, may indeed have the potential to be quite injurious to the injured, mechanically ventilated baby lung.

2.3.2 VILI – Early Studies

The potential for mechanical ventilation to induce harm has been a matter of concern from the earliest years of its introduction into medical practice. In 1964 Greenfield and colleagues [13] ventilated closed-chest dogs for 2 hours at 26–32 cm H_2O peak inspiratory pressure and allowed them to recover for 24 hours before subjecting them to thoracotomy. Zones of atelectasis were found at gross examination and the extracts of these lungs had increased surface tension, suggesting altered surfactant properties. A few years later in 1968, Sladen *et al* [14] reported that patients ventilated for long periods suffered from deteriorated lung function, an increased alveolar–arterial oxygen gradient, and a fall in respiratory system quasi-static compliance. Webb and Tierney [15] conducted the first comprehensive study in intact animals that unambiguously demonstrated that mechanical ventilation may produce pulmonary edema. They subjected rats to positive airway pressure ventilation with peak pressures of 14, 30, and 45 cm H_2O. Edema developed, occured more rapidly and was more severe in animals ventilated with 45 cm H_2O than in those ventilated with 30 cm H_2O peak pressure. Profuse edema and alveolar flooding developed within 13 to 35 min in animals ventilated with 45 cm H_2O peak pressure. No abnormality was observed after 1 h of ventilation with 14 cm H_2O peak pressure. These findings have been replicated in more detail in later studies [16-18].

2.3.3 Gross and microscopic pathology

Animal lungs injured by mechanical ventilation grossly display a pattern of atelectasis, severe congestion and enlargement because of oedema [15, 19, 20]. Ventilator-induced pulmonary edema is associated with severe endothelial and epithelial abnormalities, the structural counterpart of the alterations in permeability [16-18]. Electron microscope observations show discontinuities in alveolar type I cells in rabbits ventilated with moderate (20 cm H_2O) peak airway pressure for 6 hours [21]. Widespread alterations of endothelial and epithelial barriers were evidenced when a higher peak airway pressure was used [16-18]. Lungs of rats ventilated for short periods (5 to 10 min) with 45 cm H_2O peak airway pressure had endothelial abnormalities - some endothelial cells were detached from their basement membrane, resulting in the formation of intracapillary blebs. There were also occasional breaks in endothelial cells. Ventilation for longer periods resulted in alveolar flooding and diffuse alveolar damage [16]. There were profound alterations in the epithelial layer in addition to the capillary lesions. The severity of the alterations was unevenly distributed: the epithelial lining appeared to be intact in some areas, whereas there were discontinuities and sometimes almost complete destruction of type I cells in many others, leaving a denuded basement membrane. In contrast, type II cells always appeared to be preserved. Hyaline membranes filled the alveolar spaces in most of the sections examined of animals with severe alveolar edema [16, 17]. Endothelial breaks allowed direct contact between polymorphonuclear neutrophils and the basement membrane. Overall, this histologic pattern of injury is indistinguishable from that of ARDS.

2.3.4 VILI – pulmonary oedema

VILI induces alterations in microvascular permeability via several potential mechanisms. These range from a physiological increase in pore size with lung volume changes to direct mechanical injury, and loss of alveolar-capillary barrier function.

The increase in epithelial permeability to small hydrophilic solutes that occurs as lung volume increases is a physiologic phenomenon. The clearance of aerosolized 99mTc-DTPA increased when the functional residual capacity (FRC) was increased by positive end-expiratory pressure (PEEP) during mechanical ventilation [22], or spontaneous ventilation [23] in sheep. The same observation has been made in humans [24, 25]. Only major increases in lung volume alter epithelial permeability to large molecules during static inflation [26]. In contrast, prolonged cyclic lung inflation during mechanical ventilation produces major alterations in epithelial permeability to proteins, both large and small [27].

Work by Parker and colleagues [28] in isolated perfused dog lobes shows that increasing lung volume ultimately alters endothelial permeability to solutes of both small and large molecular weight and suggest the presence of an airway pressure threshold below which these modifications do not occur.

Direct mechanical injury is, however, the most likely cause of the rapidly developing pulmonary oedema exhibited in small animal species, such as in these studies, subjected to high lung stretch. Mead and colleagues [29] proposed that, at a transpulmonary pressure of 30 cmH_2O, the pressure across an atelectatic region surrounded by a fully expanded lung would be approximately 140 cmH_2O. In the heterogeneously injured lung, strain may therefore be greater

in areas where the inflated lung is adjacent to the atelectatic or fluid-filled lung due to interdependence. The potentially injurious effects of strain and shear force on lung epithelial and endothelial cells would be enough to damage alveolar barrier function and to lead to alveolar oedema and flooding. Indeed as mentioned above, alveolo-capillary barrier damage is obvious and extensive after VILI.

The presence of edema fluid in the airspaces is both an effect of lung injury and a potential mechanism by which VILI is amplified. Edema fluid fills alveoli and promotes airspace collapse by inactivating surfactant and filling airways [28, 30, 31]. This loss of lung volume leads to heterogeneity of the lung, resulting in even greater overdistention of the remaining lung units. Therefore, if the clearance of edema fluid from the distal airspaces is reduced, a vicious cycle of airspace edema leading to greater lung overdistention and shear stress will ensue [32]. For example, flooding distal lung units of rats with saline was found to act synergistically with high tidal volume ventilation to increase endothelial permeability to albumin [33]. In that study, the authors also found that permeability to albumin increased as the respiratory system compliance decreased, suggesting that a smaller lung volume was ventilated. As ventilated lung volume decreased, more injury resulted [33].

The clearance of edema from the airspaces requires the active transport of sodium across the epithelium. Lecuona and colleagues [34] reported that high tidal volume ventilation induced a reduction in energy-dependent sodium transport.

2.3.5 Volutrauma versus Barotrauma

Many studies suggest that high lung volumes (volutrauma), but not high intrathoracic pressures (barotraumas) per se, are crucial in the genesis of ventilator induced lung oedema. In one study where rats were subjected to large or low tidal volume ventilation, but with identical peak airway pressures (45cmH_2O), using thoracoabdominal strapping, the rats subjected to high tidal volume-high airway pressure ventilation developed permeability pulmonary oedema [17]. Strapped animals ventilated with a high airway pressure but a normal tidal volume had no oedema. To further corroborate these findings rats ventilated with high tidal volumes but negative airway pressures by means of an iron lung developed permeability oedema. Thus volutrauma rather than barotrauma appears to be responsible for ventilator induced pulmonary oedema. These findings have been replicated in several species using different approaches [35-37](59, 27, 76). Adkins et al [36] observed that in young rabbits with greater chest wall compliance lung capillary filtration coefficient increased more than in older rabbits ventilated with the same peak airway pressures.

2.3.6 PEEP and low volume injury

Ventilator induced pulmonary oedema is less severe when tidal volume is decreased and end-inspiratory lung volume is kept constant by increasing PEEP during high-volume ventilation [38]. Webb and Tierney [15] showed that oedema was lessened by 10 cmH_2O PEEP application during ventilation with 45 cmH_2O peak airway pressure. The authors attributed this beneficial effect of PEEP to the preservation of surfactant activity. Later studies exhibited

preservation of the alveolar epithelial layer in animals ventilated with PEEP in comparison to those ventilated with zero end-expiratory pressure (ZEEP) [17]. PEEP prevented repetitive opening and closing of terminal units, thereby decreasing shear stress at this level. Similar observations have been made by other investigators either in intact animals [39, 40] or in perfused canine lobes [41].

The flip-side of overinflation and overdistension, the potential for low-volume injury, was later given attention by the Slutsky group [42]. Their work in isolated rat lungs demonstrated that repetitive opening and collapse lead to a decrease in lung compliance and injury to the epithelial cells that line small airways and alveolar ducts. This hypothesis was validated by a series of elegant studies by Gaver et al. [43, 44].

2.3.7 The role of inflammatory mediators in VILI

Over the last decade, the bio-trauma hypothesis [45] postulated that mechanical ventilation causes the release of soluble mediators from the lungs into the bloodstream and that these circulating mediators cause injury in the lungs and in other organs. This hypothesis is attractive and plausible, but has not been proved.

The potential for increased local inflammation in response to excess mechanical stretch as a mechanism of lung injury propagation has been examined by Ranieri and colleagues [46]. They measured bronchoalveolar lavage (BAL) and plasma levels of several proinflammatory cytokines in 44 patients with ARDS who were randomized to receive mechanical ventilation with a conventional strategy (mean tidal volume, 11.1 ml/kg; mean PEEP, 6.5 cmH2O) or to receive a low tidal

volume, higher PEEP strategy of ventilation (mean tidal volume, 7.6 ml/kg; mean PEEP, 14.8 cmH2O). Broncho-alveolar lavage (BAL) fluid from patients in the lower tidal volume, higher PEEP group had significantly fewer neutrophils and lower concentrations of tumor necrosis factor alpha (TNF-α), IL-1β, IL-6, and IL-8. Plasma levels of IL-6 were also significantly lower in the patients that received protective ventilation [46]. Plasma IL-6 levels also declined in patients ventilated with low tidal volume compared with conventional tidal volume in the National Institutes of Health Acute Respiratory Distress Syndrome Network study [47]. In other clinical studies, elevations in pro-inflammatory cytokines correlate with increased patient mortality in ARDS [48, 49].

In experimental studies, high tidal volume, low PEEP ventilation induces the release of proinflammatory cytokines into the airspaces and bloodstream, as well as neutrophil infiltration into the lung, and the activation of lung macrophages [50]. Tremblay and colleagues [7] found that isolated, non-perfused rat lungs ventilated with a tidal volume of 40 ml/kg without PEEP for 2 hours had large increases in lavage concentrations of TNF-α, IL-1β, IL-6, and macrophage inflammatory peptide 2. Reduction of the tidal volume to 15 ml/kg or lower reduced the lavage concentrations of these mediators. The increase in these cytokines was greater if rats were pre-treated with endotoxin, but the differences among the groups persisted. High tidal volume ventilation also increased the expression of c-fos mRNA, a transcription factor important in the early stress response [7].

The potential importance of proinflammatory mediators in the development of VILI is also supported by data from experimental studies of the effects of anti-TNF-α antibody and IL-1 receptor antagonist on lung injury following surfactant

depletion. Imai and colleagues [51] reported that the pretreatment of surfactant-depleted rabbits with anti-TNF-α antibody prior to the initiation of mechanical ventilation resulted in less severe histologic lung injury and preserved oxygenation. In a similar model, IL-1 receptor antagonist pretreatment reduced endothelial albumin permeability and neutrophil infiltration [52].

However, several laboratory studies report minimal elevations in cytokine level despite severe lung injury [53-56], that together with the finding that exogenous cytokines do not necessarily produce lung injury [57] argues against an obligate pathogenic role.

In the clinical setting, the issue is also confounded. Some patients undergoing elective surgery have similar levels of circulating cytokines whether the ventilation parameters are injurious or 'protective' [58]; in addition, profound elevation in circulating cytokines can occur despite the use of 'protective' ventilation and the absence of structural lung injury [59]. Such lack of correlation in a variety of clinical and experimental settings suggests that these molecules may be markers of tissue inflammation or repair rather than pathogenic mediators. Thus, levels of circulating mediators might not reflect the net effect on tissue or cellular injury, and a simple correlation of a specific circulating cytokine level with the degree of injury cannot prove—and might not indicate—pathogenic effect. This also explains why mediator inhibition would have multiple and unpredictable effects.

Other mediators implicated in VILI include coagulation factors, such as plasminogen activator inhibitor-1, hormones, such as angiotensin-II and lipid derived mediators, such as cyclooxygenase and lipoxygenase [60].

To identify the cellular source of inflammatory cytokines in VILI, Pugin and colleagues [61] cultured human alveolar macrophages on flexible silastic membranes and exposed the cells to cyclic stretch for up to 32 hours. Cyclic strain induced an increase in the secretion of IL-8. When the macrophages were pretreated with lipopolysaccharide, TNF-α and IL-6 secretion also increased to a greater extent in strained cells compared with static cultures. The authors also noted that there was an increase in nuclear translocation of the transcription factor nuclear factor kappa-B (NFκB) in macrophages after 30 min of cyclic strain [61].

In another study by the same group [62], a variety of cell types, including macrophages, A549 cells, two endothelial cell lines, a bronchial epithelial cell line, and primary lung fibroblasts, were exposed to the same cyclic strain. Of these cell types, only macrophages and A549 cells secreted IL-8 in response to mechanical distention. The relative quantity of IL-8 secreted from macrophages was much greater than the amount secreted from A549 cells. In the absence of endotoxin stimulation, cytokines were not secreted in significant amounts from any of the other cell types [62]. The importance of this finding is highlighted by clinical data that demonstrate high levels of IL- 8 in pulmonary edema fluid from ventilated patients with ARDS [63, 64]. The alveolar macrophage may therefore be an important stretch-responsive cell in the initiation of the inflammatory response observed in VILI. This does not, however, rule out a possible role for other cell types in the propagation of early pro-inflammatory signaling in VILI.

2.3.8 The role of inflammatory cells in VILI

In addition to macrophages, polymorphonuclear leukocytes (PMNs) have been un-equivocally implicated in the pathogenesis of ALI and ARDS [65]. The current evidence seems to point to the role of PMNs as major effector cells in the generation of the tissue injury characteristic of VILI [66]. One of the first studies proposing that mechanical ventilation could lead to an inflammatory response used a model of neutrophil depletion by nitrogen mustard. Kawano et al. [67] demonstrated that the neutrophil-depleted animals had markedly improved oxygenation and decreased pathologic evidence of injury after lung lavage and/or mechanical ventilation versus a control group treated with the lavage and ventilatory protocol alone.

More recently, Zhang et al. [68] combined these two observations and examined the hypothesis that mechanical ventilation could lead to activation of PMNs in excess of that expected with ARDS alone. In these studies, PMNs isolated from normal human volunteers were incubated with BAL fluid from ARDS patients ventilated with either a conventional mechanical ventilation (CMV) or a protective ventilation strategy. Treated neutrophils were assessed post-incubation for evidence of PMN activation. This group [68] found that, in the conventional ventilation strategy group, all markers of neutrophil activation were increased more markedly than in the group ventilated with the protective strategy. These findings, although not conclusive, support the current evidence, which suggests that mechanical ventilation can lead to release of mediators that prime neutrophils, possibly providing a mechanism by which PMNs mediate tissue injury in VILI. Thus the role of PMNs in the pathogenesis of VILI may be regulated by their interaction with other cells, including epithelial cells and possibly vascular endothelial cells.

2.3.9 Mechano-transduction

Studies have also suggested that mechano-transduction, the conversion of externally applied forces on cells into activation of various cell signaling pathways and alterations in gene expression or cell structure, plays a role in VILI, and multiple stretch-activated signal transduction pathways (e.g., mitogen-activated protein kinases, stretch-sensitive ion channels, integrin receptors) have been identified [69]. In a seminal study using an isolated perfused rat lung model Parker et al. [70] abrogated the increase in microvascular permeability due to high pressure controlled ventilation (20 and 30 cmH_2O) with gadolinium (an inhibitor of endothelial stretch-activated cation channels). In a subsequent study Parker et al. [71] demonstrated in the same model that inhibition of phospho-tyrosine kinase increases the susceptibility of the lungs to high PIP injury; in contrast, inhibition of tyrosine kinase attenuates lung injury. The results of these studies lent further support to the contention that ventilation-induced changes in microvascular permeability are actively modulated by a molecular response to ventilation rather than simply a result of passive structural failure of the alveolar capillary membrane.

In addition to cell stretch and strain, cellular injury appears to play a pivotal role in the activation of these responses, and deformation-induced plasma membrane disruptions have been directly linked to the activation of pro-inflammatory signaling cascades including early stress response genes, chemokine receptors, and adhesion molecules [72]. In this setting, membrane disruption acts as a mechano-transducer or "damage sensor," whereby the influx of calcium after membrane injury leads to the upregulation of such mediators as fos and NF-κB

2.3.10 Cell membrane wounding and stress failure in VILI

Central to the pathophysiology of VILI is the lungs' response to deformation. Lung cells possess well developed mechanisms to buffer stress concentrations associated with cellular shape changes induced under these conditions. However, in the injured, mechanically ventilated lung, the forces acting on cells may be excessive compared to those experienced by the healthy lung. Increased levels of alveolar ventilation often impose cellular shape changes associated with lytic tensions in stress bearing structures such as the cytoskeleton and/or the plasma membrane.

The detailed morphological changes to the blood–gas barrier documented by Dreyfuss et al. [16] provide convincing electron micrographic evidence for dose- and time-dependent deformation-induced wounding at the cellular level as a result of mechanical ventilation. For example, the development of interstitial edema, plasma membrane blebbing, and loss of cellular contact with the basement membrane occurs after as little as a 5-min period of injurious ventilation [38]. Longer exposure at the same settings result in increasingly severe cellular injury including inter- and intracellular gap formations, denuded basement membranes, and finally, complete cellular destruction.

Electron microscopy provided the initial snapshots of cellular and plasma membrane wounding after injurious ventilation, but did not provide evidence of causality. To further explore this cause–effect relationship, Gajic et al. [73] perfused isolated, mechanically ventilated rat lungs with propidium iodide (PI). PI is a plasma membrane impermeant fluorophore utilized in studies of membrane integrity; its detection within the cell necessarily confirms a plasma

membrane disruption has occurred. This series of experiments yielded two important results. First, the number of subpleural cells with membrane defects increased with length of exposure and increasing tidal volume, confirming the dose-dependent qualitative observations under EM. Second, by infusing PI at varying points in the timecourse and then comparing the number of PI positive cells in each, it was inferred that the majority (60%) of injured cells were able to repair the defect in their plasma membranes. These cells remained wholly viable after wounding.

2.3.11 Summary of injury in VILI

Thus, many of the investigations cited above suggest physical disruption of the lung (e.g., capillary stress failure by alveolar overdistension) as one mechanism whereby mechanical ventilation produces lung injury [38, 73]. However, evidence of a potentially important role for ventilator-induced molecular and cell-mediated events in the pathogenesis of ventilator-induced injury is also quite convincing [51, 52, 67], as is the potential role of VILI in distal organ dysfunction [74].

2.4 Is VILI important in the clinical setting?

Mechanical ventilation is an indispensible component of basic life support strategies. Despite the essential nature of this mechanical respiratory support in the critically ill, it has become apparent that ventilators can damage the organ they seek to support. Clinicians have been aware for many years of the effects of clinical barotrauma in the lung, and the leakage of air due to disruption of the

airspace wall [75], the most serious of which is tension pneumothorax. Unlike the classical forms of macroscopic injury, the more subtle physiologic and morphologic alterations are not immediately obvious; however, several fundamental experimental studies have demonstrated that alterations in lung fluid balance, increases in endothelial and epithelial permeability and severe tissue damage can be observed after high stretch mechanical ventilation [16-18]. The possibility that mechanical ventilation can actually worsen acute lung disease is now accepted as reality [76].

Definitive clinical proof for this phenomenon came with the results of a single-center study in Brazil in 1998 [77] and from the multicenter National Heart, Lung and Blood Institute supported ARDS Network clinical trial in 2000 [47]. The multicenter ARDS Network trial of 861 patients demonstrated a marked reduction in mortality and in severity of lung injury with a lung-protective ventilatory strategy, and it provided convincing evidence that previously accepted ventilatory strategies using high tidal volumes and high airway pressures amplified lung injury in patients with ARDS.

2.4.1 Is VILI still a problem in the era of 'protective' ventilation?

Yes. More recent attempts to adjust ventilation strategies to further reduce harm have met with limited success [78-80]. Even with contemporary low stretch strategies, it appears difficult to avoid regional areas of high lung stretch [81]. Quantitative assessment of computed tomography images in humans with severe ARDS indicates that the amount of normally aerated tissue - the so called 'baby lung' - is variable, of the order of 200–500g, and may be as low as 200ml [82]. A 6 ml/kg tidal volume applied to these "baby lungs" can and does result in airway

pressures in the range of 30-35cm H_20 [83]. In this regard, the mean peak airway pressure in the treatment arm of the ARDS net low tidal volume study was 34cm H_2O [83]. Other diseased lung regions may be subject to even greater distention and greater regional intra-alveolar and airway pressures [84]

In addition, low stretch strategies may worsen atelectasis [85], which can also cause harm [86].

2.5 Therapeutic Strategies – Reduce Injury or enhance Repair

2.5.1 Time course of injury versus repair

The clinical course of patients with ALI or ARDS is variable and influenced by different factors. Typically, a stereotyped response to lung injury occurs, with transition from alveolar capillary damage to a fibroproliferative phase, independent of initial cause [87]. One of the most important mechanisms that determines the severity of lung injury is the magnitude of injury to the alveolar epithelial barrier [4]. The possibility of repairing the epithelial injury at an early stage is a major determinant of recovery. Specific treatments to accelerate alveolar epithelial repair do not exist, although progress in studies with experimental models of ALI suggests that specific treatment may be possible in the future [88]. Most of the treatment modalities tested to date were based on diminution of the inflammatory response in the lung in order to minimise the initial injury. However, an alternative therapeutic approach is to accelerate the repair process in the alveolar epithelium in the early stages of ALI/ARDS, to enhance the resolution of pulmonary oedema and improve outcomes in these patients [89]. Little is known at present about the cellular and molecular

mechanisms of alveolar epithelial repair in ALI/ARDS. In particular, soluble mediators that play a key role in alveolar epithelial repair in ALI/ARDS patients must be identified and characterised if novel therapeutic strategies are to be developed. Nevertheless, the repair phase may provide greater opportunities than the injury phase for therapeutic approaches to improve outcome from ALI/ARDS.

2.5.2 Normal repair mechanisms in the injured lung

Throughout adult life, multicellular organisms must maintain the structure and function of their tissues by generating new cells. In young animals, tissue damage can usually be repaired quickly, but this natural capacity may fail after repeated challenges during disease, and with age. These considerations drive us to understand the mechanisms by which adult organs normally achieve tissue homeostasis and repair, and to try to harness and augment these processes. Mammalian tissue regeneration may involve several mechanisms, including but not limited to compensatory hyperplasia, dedifferentiation and adult stem cells. The emerging picture is that different organs use different strategies to renew themselves, and that more diversity and flexibility underpin these renewal processes than previously imagined. Some organs, such as hair follicles, blood and gut, which constantly renew themselves throughout life, contain adult stem cells that are morphologically unspecialized, have a relatively low rate of division and are topologically restricted to localized regions known as ‘niches’ that tightly regulate their behavior [90].

The adult lung, on the other hand, is a vital and complex organ that normally turns over very slowly. However, when injury to the epithelium of the lung does

occur it has to be repaired as quickly as possible. For the most part, cell lineage tracing studies and the analysis of mouse lung injury models suggest that the adult lung epithelium is maintained by divergent progenitor cells residing in discrete microenvironmental niches along the proximal-distal axis of the respiratory tree [91], consistent with the existence of a "nonclassical" stem cell hierarchy in which relatively quiescent differentiated progenitor cells function as facultative stem cells [92]. In the proximal lung (trachea and main bronchi) it is likely that undifferentiated basal cells can function as classical stem cells, both self-renewing and giving rise to ciliated and secretory cells. In the more distal lung, where there are no basal cells, the evidence suggests that subpopulations of Clara cells in specific micro-environments can self-renew and give rise to different cell types after injury. In the alveoli, damaged type I cells can be restored from type II cells, although whether all type II cells have this capacity is not yet known [91]. The diversity of strategies for repair, and the different classes of stem cells in the lung are in sharp contrast to the situation in the intestine. Here, only a few stem cells are present near the base of the crypts, which appear to be responsible for replenishing the entire epithelium. This difference probably reflects the fact that when injury to the epithelium of the lung does occur it has to be repaired as quickly as possible. In this case, a situation in which multiple cell types can proliferate and function as progenitors for repair is probably an advantage. Also, the complex spatial organization of the lung and the sheer variety of cells that constitute the mature organ dictate that repair after injury may require multiple pools of progenitor cells capable of self-renewal and multipotency.

2.5.3 Dysregulated repair in ALI/ARDS

Physiological lung epithelial wound repair is a complex, highly orchestrated process presenting numerous points where dysregulation may occur, leading to the development of aberrant healing. Current studies are limited by a lack of relevant lung injury models, with much work relying on other organ models such as the skin or in vitro cultures. This thesis attempts to describe the processes required to heal a severe wound to the alveolar epithelium, characteristic of Acute Lung Injury and Ventilator Induced Lung Injury in particular, highlighting areas where dysregulation may occur, which in turn may lead to the development or continuation of a disease state, and also factors that may accelerate wound repair and recovery from severe injury.

2.6 Mesenchymal Stem Cells – Can they enhance repair?

Mesenchymal stem cells came to prominence for their potential to repair connective tissues such as bone, cartilage and bone marrow stroma. The multi-lineage differentiation potential of MSCs, together with their easy availability and extensive capacity for in vitro expansion, has led to their having now become part of the ever-expanding “stem cells can do it” hype, and it remains important to sort out broadly accepted and well supported facts from suggested possibilities. MSCs can differentiate to several cell types, but because MSCs produce important growth factors and cytokines, and may provide important cues for cell survival in damaged tissues, with or without direct participation in long-term tissue repair, they have become major cellular candidates in attempts to heal an expanding list of tissues. They are one of the few normal cell types that

have so far been produced in the large quantities needed for therapeutic development.

Mesenchymal Stem Cells offer considerable promise as a novel therapeutic strategy for ARDS and VILI. Resolution of the lung injury in ALI is impeded by destruction of the integrity of the epithelial barrier, which inhibits alveolar fluid clearance and depletes surfactant, destruction that is exacerbated by VILI [4]. Stem cells may restore epithelial and endothelial function, whether by differentiating into these cell types or via secretion of paracrine factors to enhance restoration of these tissues. ALI is characterized by an intense but transient inflammatory response. The immunomodulatory properties of MSCs may have therapeutic relevance. The relatively transient nature of the inflammatory process in ALI reduces the need for repeated therapies with the attendant risk of adverse immunological reactions. ALI is frequently associated with dysfunction of other organs. Stem cells offer the potential to decrease injury and/or restore function in diverse systemic organs, including the kidney [93], liver [94] and heart [95]. Stem cells may directly attenuate bacterial sepsis, the commonest and most severe [1] cause of ALI/ARDS, via a number of mechanisms, including enhancement of phagocytosis and increased bacterial clearance [96], and anti-microbial peptide secretion [97]. There is also the potential to further enhance the therapeutic effect of MSCs, by tranducing them to secrete disease modifying molecules. As stem cells home to sites of inflammation when administered intravenously following tissue injury [98], they may therefore provide an attractive vector for gene based therapies [99]. Finally, both the distal lung epithelium and the pulmonary endothelium are selectively

accessible to stem cell therapies, via the intra-tracheal route or as a result of the fact the entire cardiac output transits the pulmonary vasculature.

2.7 What are MSCs

2.7.1 Nomenclature

MSCs were initially described as a bone-marrow-derived mononuclear cell population that, when cultured ex vivo, adhered to plastic with a fibroblast-like morphology [100]. These cells were distinct from hematopoietic stem cells (HSCs) and could be identified by their capacity to adhere to plastic, to generate colony forming unit fibroblasts (CFU-F) in culture, as well as by their potential to differentiate into multiple lineages, and bone, cartilage and adipocyte cells in particular [101, 102]. It is also assumed that MSCs can undergo self-renewal, in particular since they can be maintained in culture for prolonged periods. Although bone marrow is the most often used source of MSCs, denominated bone-marrow-derived stem cells (BMSCs), MSCs with similar biological properties have also been isolated from other tissues including adipose tissue, skeletal muscle, dental pulp and cord blood [103-106]. Of special interest is adipose tissue since it represents an abundant and accessible source of MSCs denominated adipose-derived stem cells (ASCs) [106]. Depending on their origin, isolated populations show differences in proliferation and differentiation capacities, as well as in the expression of surface antigens. However, it is well acknowledged that, regardless of their origin, MSCs represent multipotent progenitors of mesoderm-derived (or even non-mesoderm-derived) tissues.

Different laboratories have indentified, under partly different handling or culture conditions, MSCs (or MSC-like cells) with specific properties and have assigned them different names (although differences can arise due to different isolation protocols, markers, culture conditions, etc.). These include mesenchymal stem cells (MSCs), a term originally coined by Caplan [101], mesenchymal stromal cells (MSCs) [107], bone marrow stromal cells (BMSCs) [108], marrow-isolated adult multipotent inducible cells (MIAMI) [109] and multipotent adult progenitor cells (MAPCs) [110]. All these meet the definition of MSC and although the Mesenchymal and Tissue Stem Cell Committee of the International Society for Cellular Therapy (ISCT) emphasizes the use of multipotent mesenchymal stromal cells in order to clarify MSC terminology [107], the term mesenchymal stem cells is widely used when referring to the acronym MSC.

2.7.2 Origin of MSCs

New insights suggest that MSCs are naturally found as perivascular cells, summarily referred to as pericytes, which are released at sites of injury, where they secrete large quantities of bioactive factors that are both immunomodulatory and trophic [111]. Many studies have pointed to pericytes as a potential source of MSCs [112, 113]. However, in the absence of specific and unique markers that would allow for a proper identification of MSCs in vivo, a histological localization of these cells is virtually impossible. Our knowledge of the developmental origin of MSCs is still quite limited. It is widely believed that MSCs derive from mesoderm; notably, however, a recent study showed that the earliest lineage providing MSC-like cells during embryonic trunk development is indeed generated from Sox1+ neuroepithelium rather than from mesoderm, at

least in part through a neural crest intermediate stage [114]. These early MSCs are then replaced, later in development, by MSCs from other origins. The potential link, if any, between these cells and the MSCs isolated according to Friedenstein's protocol [100] remains to be established.

2.7.3 Minimal criteria for MSC

Due to the lack of specific mesenchymal cell markers and the heterogeneity of the MSC populations, the Mesenchymal and Tissue Stem Cell Committee of the ISCT established three minimal criteria that MSCs isolated from human bone marrow and other mesenchymal tissues must fulfil in vitro: i) adherence to plastic in standard culture conditions, ii) display of a specific surface antigen expression pattern (CD73+ CD90+ CD105+ CD34- CD45- CD11b- CD14- CD19- CD79a- HLA-DR-), and iii) multipotency, that is, differentiation potential along the osteogenic, chondrogenic and adipogenic lineages should be demonstrated [115].

2.7.4 MSCs are heterogeneous

Despite these criteria, there may be more diversity among MSCs than we are aware of. The heterogeneity of the MSC population is revealed by *in vitro* differentiation assays, where most of the population shows a differentiation potential towards one or two different cell types, whereas only very few cells harbor a tripotent differentiation capacity [116]. These data might suggest a hierarchical structure of the MSC population, but the lack of specific surface markers hamper their identification and isolation.

Characterization is also hampered by the low frequency of these cells (0.01 - 0.001% within bone marrow, 0.00001 - 0.00003% in cord blood) [102, 108], and the lack of efficient *in vivo* transplantation models (such as for HSCs or mammary stem cells) to demonstrate the stem cell nature of each subpopulation.

2.8 Efficacy in reducing lung injury in pre-clinical models

MSCs have also been demonstrated to reduce mortality, improve alveolar epithelial barrier function and attenuate inflammation and lung injury in diverse pre-clinical ALI animal models. In 2003, Ortiz et al [117] reported that MSC therapy could reduce the degree of fibrosis in bleomycin-induced lung injury in mice, and that the effect did not primarily depend on engraftment, which was less than 5%, but rather on paracrine mechanisms. Xu et al [118] reported that intravenous administration of MSCs after intraperitoneal endotoxin decreased the influx of neutrophils into the air spaces of the lung and also reduced the quantity of pulmonary edema. In animal models where endotoxin [119] or live *Esherichia coli* bacteria [96] was administered by the intrapulmonary route, survival was significantly improved with MSC therapy compared with controls. MSCs reduced the quantity of pulmonary edema, the degree of histologic lung injury, and the concentration of lung pro-inflammatory cytokines. The number of bacteria recovered from the lung was less with MSC therapy than with saline or fibroblast controls [96]. In a mouse caecal ligation and puncture model of sepsis, Nemeth *et al* [120] determined that systemically administered MSCs, given either 24 hours prior to, or 1 hour after surgery, improved survival, reduced organ dysfunction including indices of ALI, reduced neutrophil oxidative injury and increased circulating neutrophils, while lowering bacterial counts in blood.

Two similar studies reported that MSCs or their secreted factors reduce lung inflammation and improve histologic lung injury in experimental rodent models of hyperoxia-induced bronchopulmonary dysplasia [121, 122], providing protection of lung vascular and alveolar structures, and preventing the development of pulmonary hypertension. Finally, in an experiment to provide more clinically relevant information regarding the potential of cell therapy in human ALI, Lee *et al* [123, 124] utilized the established *ex vivo* perfused human lung preparation to test the effects of MSC therapy. When the lung was treated 1 h after instillation of the endotoxin with intrabronchial allogeneic MSC, lung vascular permeability and extravascular lung water returned to normal levels, and the rate of alveolar fluid clearance increased to a normal level. Control studies with human fibroblasts showed no effect.

2.9 Why might MSCs be an effective therapeutic option for ALI?

MSCs offer considerable promise as a novel therapeutic strategy for ALI/ARDS for a number of reasons. ***First,*** MSCs offer the potential to differentiate into lung cells and directly replace damaged cells and tissues. ***Second,*** ALI is characterized by an intense but transient inflammatory response. While previous strategies to simply inhibit this response have met with failure, the more complex, 'immunomodulatory' properties of MSCs may be more effective. MSCs may be able to 'reprogramme' the immune response to reduce the destructive inflammatory elements while preserving the host response to pathogens. ***Third***, MSCs may be able to enhance the repair and resolution of lung injury. Resolution of the ALI/ARDS is impeded by destruction of the integrity of the epithelial barrier, which inhibits alveolar fluid clearance and depletes surfactant[125].

MSCs may restore epithelial and endothelial function, whether by differentiating into these cell types or via secretion of paracrine factors to enhance restoration of these tissues. ***Fourth,*** ALI/ARDS is frequently a component of a generalized process resulting in dysfunction and failure of multiple organs. MSCs have been demonstrated to decrease injury and/or restore function in the kidney [126, 127], liver [128, 129] and heart [130]. ***Fifth,*** stem cells may directly attenuate bacterial sepsis, the commonest [131] and most severe [132] cause of ALI/ARDS, via a number of mechanisms, including enhancement of phagocytosis and increase bacterial clearance[96], and anti-microbial peptide secretion [133]. ***Sixth,*** there is the potential to further enhance the therapeutic effect of MSCS, by tranducing them to secrete disease modifying molecules. As MSCs home to sites of inflammation when administered intravenously following tissue injury [134], they may therefore provide an attractive vector for gene based therapies [135]. ***Seventh,*** both the distal lung epithelium and the pulmonary endothelium are selectively accessible to stem cell therapies, via the intra-tracheal route[136] or as a result of the fact the entire cardiac output transits the pulmonary vasculature. ***Finally,*** stem cells are in clinical studies for a wide range of disease processes. The clinical potential of MSCs for ALI/ARDS has been considerably enhanced by a recent study demonstrating that human MSCs can reduce endotoxin induced injury to explanted human lungs [137].

Taken together, these findings suggest considerable hope for MSCs as a therapy for ALI/ARDS.

2.10 How might MSCs work to enhance repair

2.10.1 Migration to the site of injury

Transplanted MSCs have been shown to home to sites of damaged tissue. Bone fractures, infarcted heart muscle, rat ischemic brain and renal injury are all sites of localization of transplanted MSCs in animal models [138-141]. MSCs can be isolated from peripheral blood and can be found in increased numbers under stress of total body irradiation or hypoxia, implying that MSCs are part of the innate reparative response to injury, and that a natural trafficking signal to sites of tissue damage exists [142, 143]. MSCs express an assortment of chemokine receptors that allow for their migration in response to the chemokine-attractive gradients generated by the inflamed injured site. The functional chemokine receptors expressed by MSCs include CCR1, CCR7, CCR9, CXCR3, CXCR4, CXCR5 and CX3CR1 [144]. The CXCR4 receptor and its single, specific chemokine, stromal cell-derived factor 1 (SDF1/CXCL12) has an important role in the regulation of hematopoietic stem cells (HSC) and other stem cell trafficking, along with a part in controlling the metastasis of several types of cancer [145]. This signaling axis has been shown to regulate MSC localization to damaged heart tissue in a rat model of myocardial infarction and to fractured mouse tibias [138, 140]. Both in vitro and in vivo experiments with MSCs overexpressing CXCR4 have shown increased migration, localization and healing in the case of transplantation into mice suffering coronary occlusion-reperfusion injury [146, 147]. SDF1 expression is upregulated in rodent hearts following myocardial

infarction and this led to an increase in the number of MSCs recruited to the injured tissue [148, 149]. However, Ip et al. [150] showed that inhibition of CXCR4 in MSC had no effect on MSC migration to ischemic myocardium, but instead was dependent on integrin β1. Similarly, MSC homing to bone was improved with ectopic expression of integrin alpha4 and its association with integrin beta1 in mice [151]. The chemokine receptor CCR7 has been associated with MSC localization to CCL2-expressing skin wound sites [152]. The chemokine CCL2 (monocyte chemotactic protein 1 (MCP-1)) is also produced at sites of inflammation and reported to be critical for recruiting MSCs expressing its receptor CCR2 [153].

In their journey to the injured tissue, MSCs first adhere to vascular endothelial cells and cross the endothelial barrier to achieve transendothelial migration [154]. Studies investigating the mechanisms of adhesion between MSCs and microvascular endothelium indicate that MSCs display coordinated rolling and adhesion behavior on endothelial cells mediated by very late antigen-4/vascular cell adhesion molecule-1 (VLA-4/VCAM-1).

The innate ability of MSCs to target sites of injury and damage and the determination of the mechanisms involved will have important implications for the therapeutic use of MSCs.

2.10.2 MSC Plasticity- differentiation, transdifferentiation and engraftment

In developmental biology, cellular differentiation is the process by which a less specialized cell becomes a more specialized cell type. Occasionally cells believed to belong to a certain lineage have been observed to undergo an abrupt alteration in phenotype and exhibit a phenotype characteristic of a different cell

lineage. The process has been referred to as trans-differentiation [155, 156]. MSCs are multipotent cells that can be induced *in vitro* and *in vivo* to differentiate into a variety of mesenchymal tissues, including bone, cartilage, tendon, fat, bone marrow stroma and muscle [102]. Studies have also indicated that MSCs can transdifferentiate into cells of other lineages [157-159]. Chao et al. reported that MSCs derived from umbilical cord trans-differentiated into islet-like cell clusters *in vitro*, which could express insulin and glucagon, through stepwise culturing in neuron-conditioned medium [159]. Paunescu et al. reported that MSCs isolated from the sternum of patients could differentiate into epithelial-like cells and may thus serve as a cell source for tissue engineering and cell therapy of epithelial tissue [160]. MSCs can also differentiate into multiple skin cell types including keratinocytes and contribute to wound repair [152]. In addition, MSCs may be involved in angiogenesis, which is important for repair of wounded tissues. After proper induction, MSC-derived smooth muscle cells could form vessel walls that were substantially similar to native vessels when examined histologically and molecularly [161].

Much of the initial interest in adult stem cell therapy originated from the multi-potent nature of the bone marrow derived cells. Krause *et al.* [162] found that a single bone marrow derived hematopoietic stem cell could give rise to cells of multiple different organs including the lung. She reported up to 20% engraftment of bone marrow-derived cells in the lung, including epithelial cells, from a single hematopoietic precursor. That report stimulated additional investigations into the possibility that bone marrow-derived MSC might be able to regenerate the lung epithelium and/or endothelium as well. However, those results were questioned by multiple groups, who observed only engraftment of

leukocyte lineages [163], or low engraftment rates in lung injury models with observed rates of < 1% [117, 164, 165].

Although stem cell transdifferentiation has been well documented in a lot of in vitro studies, its contribution to tissue repair is thus at best controversial [166] because some researchers reported that only limited donor-derived cells were detected *in vivo* and evidence of the differentiation potential of MSCs in the human body is still lacking [167]. Nevertheless, differentiation of MSCs toward specific cell types in the *ex vivo* and *in vivo* animal models, even to a low degree, suggests an important biological phenomenon that may be exploited for cell replacement therapy, that is, induction of MSCs *in vitro* to a specific cell type and transplantation of these functional cells for cell replacement therapy. When migrating to injured tissue from systemic circulation, these cells may further differentiate into more mature, tissue-specific cells with sufficient functions after being exposed to a tissue-specific environment. However, notwithstanding this, and despite initial interest in their multi-potent properties, engraftment in the lung now does not appear to play the major beneficial role.

2.10.3 MSCs and the immune response

MSCs were first isolated from bone marrow, a key site of hematopoiesis in which MSCs are now thought to play a role [100]. HSCs require stromal supporting cells for proper differentiation and for the maintenance of the quiescent state within the endosteal niche of the bone marrow and both supporting functions can be carried out by the MSC-progeny, osteoblasts [168]. This has been the basis for the use of MSCs in combination with HSC transplantation in the hope of enhancing engraftment and proliferation of donor HSC which is under

investigation in several clinical trials [169]. As a possible consequence of this tight interaction with immune cell progenitors MSCs are non-immunogenic and can themselves modulate the immune response

Both *in vitro* co-culture experiments and *in vivo* models of immune/inflammatory disease suggest a clear and compelling profile of MSCs as potent modifiers of a wide range of targets within the innate and adaptive arms of the immune system [170, 171]. MSC immunomodulatory actions have been demonstrated in a wide range of disease states including sepsis, acute lung injury, acute myocardial ischemia, stroke, kidney injury, inflammatory bowel disease, graft-versus-host disease (GVHD), multiple sclerosis, diabetes mellitus, and organ transplantation [111, 171]. Clinical trials have been completed or are underway in several of these areas [172].

2.10.3.1 MSCs and innate immnity

The innate immune system provides effective antimicrobial defense against infectious agents but also acts as a barrier to allogeneic and xenogeneic transplantation. It is clear that allo-MSCs avoid acute rejection mechanisms normally mediated through the complement system, likely through secretion of Factor H [173] and expression of the complement control proteins CD55, CD46 and CD59 [174]. However, other aspects of complement, the anaphylotoxins C3a and C5a, may be involved in attracting and activating MSCs at sites of tissue damage [175].

Although initital *in vitro* observations suggested that MSCs were not susceptible to lysis by natural killer (NK) cells [176, 177], it is now apparent that in spite of

the suppression of proliferation, surface receptor expression, and effector functions of NK cells via prostaglandin E2 (PGE2) and 2,3-indoleamine dioxygenase, they can be lysed by activated NK cells [178-180]. Whether this interaction of MSCs with NK cells translates to the *in vivo* setting is unknown.

The interaction of MSCs with neutrophils has received scant attention. Raffaghello et al [181] recently reported that MSCs inhibited apoptosis and the oxidative burst of resting and activated neutrophils while preserving their phagocytic and chemotactic functions.

One aspect of MSC innate immune interaction that has received more study is the monocyte/macrophage. Recent evidence suggests that monocytes and macrophages may be "programmed" by their surrounding microenvironment either to mediate potent, locally destructive effects, appropriate for immediate clearance of dead cells and prevention of infection at a site of injury or to produce a range of anti-inflammatory, pro-regenerative factors, indicative of a central role in the resolution and repair phase of tissue injury [182-184]. Evidence is accumulating that MSCs are involved in this re-programming [120, 185, 186]. Most notably Nemeth *et al* demonstrated convincingly that both auto- and allo-MSCs reduced mortality from sepsis in a mouse model through a direct interaction with macrophages in the lung that resulted in enhanced production of interleukin (IL)-10 and was mediated through a complex monocyte/MSC crosstalk involving TLRs, tumour necrosis factor (TNF), nitric oxide and PGE2 [120].

Toll-like receptors are a type of pattern recognition receptor that recognize molecules that are broadly shared by pathogens, but distinguishable from host molecules. Recent work in this area has reinforced the concept of MSCs as cells

responsive to and modulatory of innate immunity [187-191]. MSCs express a range of TLRs, and signaling through these receptors influences migration, survival, differentiation, and immunosuppressive capacity. It is unclear whether signaling through these receptors downregulates MSC immune modulation (as has been shown with TLR3 and TLR4 ligands [188, 192] or further enhances MSC immune suppressive properties [189]. The enhanced immune modulation seen with IFN-γ [193] may be particularly effective in suppressing chronic inflammation seen in autoimmunity (not driven by pathogens) without impairing inflammatory responses essential to antimicrobial defense (where TLR ligands would be abundant).

Taken together with the previously discussed literature on MSC interactions with the complement system, NK cells, neutrophils, and ligands for TLRs, these studies paint a striking picture of the complexity of MSC cross-talk with the innate immune system and of the rich potential for harnessing these effects for therapeutic benefits.

2.10.3.2 MSCs and adaptive immunity - Dendritic cells

Dendritic cells (DCs) are the most potent of all antigen presenting cells, acting as a link between innate and adaptive immunity, and with the unique ability to activate both memory and naïve T-lymphocytes. It is not surprising that MSCs influence DC development, as both MSCs and many DC precursors are bone marrow residents. At the level of development, MSC co-culture strongly inhibits the initial differentiation of monocytes to immature DCs in vitro [194, 195]. This

effect is reversible [194] and can be replicated by MSC-derived soluble factors, including PGE2 and IL-6 [196].

MSCs suppress maturation marker expression, antigen presentation capability, and capacity to respond to lymph node–derived chemotactic signals—the three cardinal features of conventional DC maturation. Unlike suppression of T-cell proliferation in mixed lymphocyte reaction (MLR), both contact-dependent and soluble factors contribute to this immunomodulatory phenomenon.

DCs may also show an altered profile of cytokine expression in response to MSCs, with reduced IL-12 [197] and increased IL-10 [177] production. They may also become capable of indirect immune suppression through induction of regulatory T (treg) cells [194].

2.10.3.3 MSCs and adaptive immunity - T-regulatory cells

The two principal T cell suppressor populations are considered to be CD4+ $CD25^{high}$ FOXP3+ T cells that develop in the thymus (sometimes called natural Treg) and T cells that can develop from naïve T cells in the periphery (termed inducible or adaptive Treg). Treg cells play an important role in suppressing a range of autoimmune disease and in downregulation of inflammation. Treg cells achieve suppression by two principal mechanisms: bystander suppression involves the secretion of cytokines by antigen-activated tregs, such as IL-10 and TGF-β, that suppress local effector T cells [198-200]. In contrast, during infectious tolerance, activated Treg cells condition the host to promote further Treg cell populations of broader specificity [201-203].

MSCs can induce treg cells indirectly via DCs, as referred to above. It is now clear that MSCs can directly induce Treg cells in the absence of DCs [204]. The mechanisms responsible for induction of Treg cells by allogeneic human MSCs include cell contact, PGE2, and TGF-β1, which appear to play complementary, non-redundant roles [205, 206]. MSCs sustain Treg cell survival and the suppressor phenotype over time [207], the important implication being that MSCs may cast a regulatory or immunosuppressive shadow long after the original stromal cells have declined, reminiscent of infectious tolerance, and thus suggest a mechanism whereby MSCs with a brief persistence in vivo may have profound long-term effects.

2.10.3.4 MSCs and adaptive immunity - T-cell and B-cell effector responses

In *in vitro* experiments, MSCs block activation of T cells in response to a host of immunogenic stimuli by release of paracrine factors [171]. A diverse set of soluble factors have been proposed for this function, including TGF-β, IGF, VEGF, hepatocyte growth factor (HGF), IL-2, IL-10 and PGE2 possibly regulated by Toll-like receptors [171, 208]. Indoleamine 2, 3-dioxygenase is another soluble factor released by MSCs in response to IFN-λ that depletes T cell tryptophan levels leading to inhibition of T cell activation, proliferation and apoptosis [209].

Despite this, Krampera et al. have shown a requirement for direct MSC-T cell interaction to modulate the T cell reaction [210].

Thus, there is now a considerable body of data demonstrating that MSCs have potent direct suppressive influences on effector CD4+ T cells while promoting and sustaining Treg cells. Studies of MSC effects on B-cell function have produced

some conflicting results. *In vitro* experiments involving co-culture of human MSCs with purified B-cell populations under a variety of stimulatory conditions have predominantly shown inhibition of B-cell proliferation, differentiation, immunoglobulin production, and chemotaxis with preserved or improved cell survival [211-213]. Mediators that have been identified for MSC suppression of B-cell functions to date include alternatively cleaved CCL2 [214], IFN-γ, and PD1/PDL1 interaction [215].

In contrast, however, several groups have reported stimulatory effects of MSCs on *in vitro*–activated B cells or plasma cells from healthy humans [216] or patients with systemic lupus erythematosis [217]. The reasons for such apparently contradictory results are not entirely clear but may include variability in the sources and properties of MSCs as well as in the different antigen-dependent and polyclonal stimuli that have been used to activate B cells in culture.

Taken together, the existing literature regarding MSC effects on B-cell and plasma cell functions suggest a complex interaction that includes both inhibitory pathways of high clinical interest as well as the potential for stimulatory effects that could limit the benefit of MSC-based therapies for some immune/ inflammatory diseases.

2.10.3.5 Are MSCs immune-privileged?

The question of whether MSCs are truly immunoprivileged *in vivo* remains central to their efficacy, and to the therapeutic equivalence of allo- and auto-MSCs. A key issue is whether the inherent immune suppressive properties of

MSCs are sufficient to overcome the potent and diverse processes that are typically engendered by allogeneic cells in a healthy individual. In the majority of potential clinical applications it is not clearly known for how long MSCs need to persist in vivo in order to exert their maximal beneficial effects. For conditions in which a short-lived presence of MSCs within diseased tissue is of benefit, as in sepsis or ALI, it is, nevertheless, likely that strong immunogenicity of allo-MSCs will have a negative influence on the potency and duration of treatment effect as well as the feasibility of subsequent dosing. It is therefore important to define the extent and the limits of their immune privileged state.

As mentioned above much of the mechanistic basis for MSC immune modulation has been discovered, and some at least have been identified as operational *in vivo.* Furthermore, several studies have indicated that donor-specific MSC infusion prior to or at the time of allogeneic organ or tissue transplantation may delay rather than hasten allograft rejection [218]. In humans, donor MSCs have been reported to attenuate some aspects of GVHD following allogeneic hematopoietic stem cell transplantation [219]. More recent data from animal models also suggest that MSCs of allogeneic or xenogeneic source can effectively protect from death due to sepsis [120], neuronal loss following cerebral ischemia [185], and neurological injury in experimental autoimmune encephalomyelitis [220, 221] in comparable fashion to auto-MSCs.

Notwithstanding these results, the majority of studies that have carefully analyzed donor-specific responses in immune competent rodents, pigs, and non-human primates following allo-MSC administration have generated evidence of immunogenicity [221-230]. Notably, donor-specific antibody was observed in all studies in which allo-antibody assays were carried out. In several studies allo-

specific responses were relatively weak [222, 224, 229], whereas in others allo-MSCs proved to be strongly immunogenic and sensitizing against subsequent donor antigen exposure [225, 226, 230].

However, it is also evident that immunogenicity and therapeutic immune modulation can co-exist in vivo. In some disease models allo-MSCs and auto-MSCs were found to be of comparable efficacy despite eliciting anti-donor immune responses [221, 223], whereas in others, efficacy was lower for allo-MSCs compared with auto-MSCs [230, 231]. The parallel influences of immunogenicity and suppression may be especially beneficial for proposed therapies using MSCs in sepsis, where a functioning immune system is essential for host bacterial clearance.

Overall, it is reasonable to state at this time that MSCs have the capacity to initiate both cellular and humoral allo-immune responses in vivo but that, in some conditions, immunogenicity may be considerably attenuated compared with other allogeneic cell types because of inherent anti-inflammatory and immune modulatory properties.

Some additional important issues are linked to the basic question of the in vivo immunogenicity of allo-MSCs and its significance for their therapeutic application. It is of interest to know whether immunosuppressive therapies currently prescribed in organ transplantation can be effectively used to prevent anti-donor immune responses to allo-MSCs in vivo without diminishing therapeutic efficacy. In this regard, Poncelet *et al.* [232] have shown, in a miniature pig model of myocardial infarction, that the calcineurin inhibitor tacrolimus significantly attenuated the anti-donor antibody response to allo-MSCs delivered directly into the infarct. Recently, Ge et al. [233] also

demonstrated that a combination of allo-MSC infusion and low-dose sirolimus (rapamycin) therapy resulted in long-term survival of fully MHC-mismatched heart transplants in mice.

2.10.4 Impact of the microenvironment on the MSC

MSC therapy may be deployed, particularly in the case of ALI and sepsis, into sites of inflammation, rich in pro-inflammatory mediators such as IL-1, TNF and IFN-γ. The influence of this environment on MSC immune modulation, and whether anti-donor immune responses are heightened, is important to determine. Stimulation of MSCs with IFN-γ upregulates both MHC class I and II [234, 235], which may render these cells susceptible to rejection in an immune competent host, especially as an elevated MHC class I level makes the cells vulnerable to cytotoxic T-cell-mediated lysis *in vitro*. In the pig, Cho *et al*. [225] have demonstrated that both T-cell and antibody responses to allo-MSCs were enhanced *in vivo* by pre-exposure of MSCs to IFN-γ. Thus, there is evidence that in the setting of inflammation, allo-MSC immune rejection may be a more likely prospect. However, in contrast, it is well established that exposure of MSCs to some inflammatory signals, such as IFN-γ can enhance their suppressive effects on T cells, monocyte macrophages, and DCs [190, 193, 236, 237]. In models of GVHD, chronic obstructive pulmonary disease, and allergic airway disease, prestimulation of MSCs with IFN-γ improves the efficacy of cell therapy [237, 238]. While these results appear to be contradictory, they indicate that MSCs introduced into an inflammatory environment are responsive to and modulate their surroundings such that they may exert further beneficial immune

suppressive actions, or, on the other hand, they may be rendered more susceptible to lysis by cytotoxic T-cells and NK cells. These two processes may not be mutually exclusive, but they require more study in order to establish the safety and efficacy of MSCs for sepsis and ALI.

2.10.5 Paracrine vs contact dependent mechanisms

Much of current evidence for MSC mediated disease modification has focused on soluble factors. MSCs have the ability to secrete multiple paracrine factors such as growth factors [239], factors regulating endothelial and epithelial permeability [240], anti-inflammatory cytokines [120], and, more recently, antimicrobial peptides [97] that can potentially treat the major abnormalities that underlie ALI, including impaired alveolar fluid clearance, alveolar epithelial injury, altered lung endothelial permeability, dysregulated inflammation and infection. Another novel paracrine-dependent mechanism involves the release of membrane-derived microvesicles, a recently appreciated means of intercellular communication that involves horizontal transfer of mRNA and proteins between cells [127].

2.10.5.1 Key paracrine mediators

The list of soluble factors that are candidate mediators for MSC immune modulation includes transforming growth factor-β (TGF-β), prostaglandin E_2 (PGE_2), indoleamine 2,3-dioxygenase [209], interleukin-6 [196] interleukin-10 (IL-10), IL-ra and tumour necrosis factor-α-induced protein 6 (TSG-6) among others. In a mouse model of asthma injected MSCs decreased levels of Th2

cytokines (IL-4, IL-5, and IL-13) in bronchial lavage, and lowered serum levels of Th2 immunoglobulins (IgG1 and IgE), all through the secretion of TGF-β [241]. In a model of sepsis following cecal ligation and puncture (CLP) in mice, Nemeth *et al.* [120] found that bone marrow derived mouse MSC, activated by LPS or TNF-α, secreted PGE2, which reprogrammed alveolar macrophages to secrete IL-10. In bleomycin induced lung injury and fibrosis in mice, Ortiz *et al*. [242] found that mouse MSCs decreased subsequent lung collagen accumulation, fibrosis and levels of matrix metalloproteinases in part by IL-1ra secretion; IL-1ra is a cytokine that competitively competes with IL-1β for IL-1 receptor binding. IL-1β is one of the major inflammatory cytokines in pulmonary edema fluid in patients with ALI/ARDS [243]. Recently Danchuk *et al* [244] demonstrated that human MSCs delivered via either the intravenous or intraperitoneal route significantly attenuated LPS-induced inflammation in the lung. Knockdown of TSG-6 expression in hMSCs by RNA interference abrogated most of their anti-inflammatory effects. In addition, intra-pulmonary delivery of recombinant human TSG-6 reduced LPS-induced inflammation in the lung [244].

Bone marrow derived MSC are known to produce several epithelial specific growth factors, specifically keratinocyte growth factor (KGF), angiopoietin 1 (Ang1) and hepatocyte growth factor (HGF). In the *ex vivo* perfused human lung, the intra-bronchial instillation of human MSC 1 h following endotoxin-induced lung injury restored alveolar fluid clearance or the ability to resolve pulmonary edema fluid in part by the secretion of keratinocyte growth factor (KGF) [124]. In primary cultures of human alveolar type II cells, human MSC grown without cell contact in a Transwell plate restored the increase in epithelial permeability to protein caused by exposure to inflammatory cytokines in part by the secretion of

Ang1 [240]. This effect of MSC secreted Ang1 on lung permeability is supported by several recent studies, which demonstrated the therapeutic use of MSC (with and without transfection with human Ang1) in mice injured by LPS [99, 245, 246]. Another epithelial specific growth factor secreted by MSC is hepatocyte growth factor (HGF) [247]. Previously, HGF was found to stabilize integrity of pulmonary endothelial cells by the inhibition of Rho GTPase and the prevention of actin stress fiber formation and paracellular gaps among pulmonary endothelial cells injured by thrombin [248].

Recently, Krasnodembskaya et al reported that human bone marrow derived MSC can inhibit bacterial growth directly, and their antimicrobial effect is mediated in part through the secretion of an antimicrobial peptide LL-37, which was up-regulated upon bacterial stimulation [97]. They also demonstrated that LL- 37 secretion by MSC improved bacterial clearance *in vivo* in the mouse model of *E.coli* pneumonia, when MSC were administered intra-bronchially.

Further limiting the damage from inflammation in MSC-transplanted mice could be the ability of MSCs to regulate the oxidative state of the local environment. It has been proposed that MSCs secrete antioxidant molecules such as glutathione and disulfide cysteine, to maintain redox homeostasis, as seen when conditioned media from MSCs were able to rescue oxidized cells and in an endotoxin model of lung injury [249].

2.10.5.2 Role of cell-cell contact

Notwithstanding this, contact dependent mechanisms and soluble factors are thought to collaborate for the induction of MSC mediated immune suppression

[171]. Cell-cell contact mediated by adhesion molecules may play an important initial step in MSC mediated T-cell proliferation [250]. Nemeth *et al* demonstrated that macrophage reprogramming to an anti-inflammatory phenotype requires MSC contact and does not occur in response to conditioned medium [120]. In addition, new preliminary data suggest that MSC may enhance repair to the injured alveolar epithelium in a LPS-induced lung injury model in rats by the mitochondrial transfer of material from one cell to the other [244].

2.11 Summary

Ventilation Induced Lung Injury remains a persistant cause of ongoing injury to the lung in the setting of Acute Lung Injury. Therapies aimed at reducing this injury, including low tidal volume strategies and different levels of PEEP have appeared to have reached their maximum potential in terms of beneficial effect. An alternative approach is to focus on the repair process after VILI. Mesenchymal Stem Cells are an attractive therapeutic option, whose immune-modulating and reparative properties after VILI should be explored.

3.0 Aims and Hypotheses

3.1 Title

Investigation of the mechanisms of repair following Ventilator Induced Lung Injury and the potential for Mesenchymal Stem Cells to enhance the repair process.

3.2 Overall Aims

Development and characterization of a rodent model of recovery following Ventilator Induced Lung Injury (VILI), and determination of the efficacy, mechanism of action and optimal delivery strategy of Mesenchymal Stem Cells to enhance the repair process following VILI

3.3 Specific Aims

1. To establish a novel rodent model of recovery following VILI
2. To determine the role of the inflammatory and fibroproliferative response in repair following VILI.
3. To determine the potential for IV MSCs to enhance repair following VILI.
4. To determine the mechanisms by which intra-vascularly administered MSCs enhance recovery following VILI induced lung injury
5. To determine the potential for fresh versus stored Mesenchymal Stem Cells (MSCs) to enhance repair following VILI

6. To further elucidate the mechanisms by which MSCs enhance recovery following VILI induced lung injury, by examining effect on in vitro wound scratch model
7. To determine the potential for intra-tracheal MSCs to enhance repair following VILI
8. To compare the efficacy of intra-vascular versus intra-tracheal MSC administration in enhancing repair following VILI
9. To determine the mechanisms by which intra-tracheal administered MSCs enhance recovery following VILI

3.4 Specific Hypotheses

1. VILI can be induced in rats in a non-fatal model, allowing the study of the recovery phase from injury
2. VILI generates a sustained inflammatory and fibroproliferative response in the rat, and this results in disordered repair and lung fibrosis
3. MSCs enhance functional and structural recovery after VILI.
4. This effect of MSCs is mediated, at least in part, via secreted soluble factors
5. MSCs in culture have greater potential to enhance repair following VILI, than cryopreserved MSCs, thawed and administered immediately
6. MSCs and their conditioned medium enhance repair in alveolar epithelial monolayers subjected to wound scratch injury
7. The potential of MSCs to enhance pulmonary epithelial repair will be mediated in part via secretion of growth factors such as keratinocyte growth factor.

8. Intra-tracheal MSCs therapy will be as effective as intra-venous MSC therapy in enhancing repair following VILI.
9. The mechanism of action of intra-tracheal MSCs will be mediated, at least in part, via MSC secreted soluble factors

4.0 Methods and Materials

4.1 Animal Experiments

4.1.1 Permissions

All experiments were conducted under license from the Department of Health, Government of Ireland, and received approval from the Animal Care Research Ethics Committee of National University of Ireland, Galway.

All animal experiments were carried out using specific pathogen free adult male Sprague Dawley rats, obtained from Charles River Laboratories, Kent, United Kingdom.

4.2 VILI via tracheostomy Model

4.2.1 Surgical tracheostomy, and carotid arterial access

Anaesthesia was induced with intraperitoneal ketamine 80 mg.kg-1 (Ketalar, Pfizer, Cork, Ireland) and xylazine 8 mg.kg-1 (Xylapan, Vétoquinol, Dublin, Ireland). After confirmation of depth of anaesthesia by paw clamp, intravenous access was obtained via the dorsal penile vein and further anaesthesia was maintained with an intravenous Saffan infusion (Alfaxadone 0.9% and alfadolone acetate 0.3%; Schering-Plough, Welwyn Garden City, United Kingdom) at 5–20 $mg \cdot kg^{-1} \cdot h^{-1}$. Pre-tracheal fur was removed, and blunt dissection was carried out using arterial forceps through pre-tracheal muscles and fascia to reveal the trachea. The trachea was dissected out, and an incision was made between the 4^{th} and 5^{th} tracheal rings. A tracheostomy tube (2-mm internal diameter) was inserted and secured. Right sided pre-tracheal muscles and strap muscles of the

neck were retracted and the right sided carotid artery was located together with the vagus nerve and adherent sheath. The nerve and sheath were dissected from the length of visible carotid artery and intra-arterial access (22-gauge cannula; Becton Dickinson, Cowley, United Kingdom) was sited.

4.2.2 Baseline ventilation protocol

Intravenous access, tracheostomy and carotid artery canula were sited as above. After confirmation of depth of anesthesia by using paw clamp, Cisatracurium besilate (0.5 mg; Nimbex, GlaxoSmithKline, Dublin, Ireland) was administered intravenously to produce muscle relaxation.

The animals were ventilated by using a small animal ventilator (CWE SAR 830 AP, CWE Inc, Pennsylvania, USA) with an inspired gas mixture of 30% oxygen, respiratory rate of 80 breaths/min, tidal volume of 6 $ml.kg^{-1}$, and positive end-expiratory pressure of 2 cm H_2O. To minimize lung derecruitment, a recruitment maneuver consisting of a positive end-expiratory pressure of 10 cm H_2O for 25 breaths was applied every 5 min throughout the protocol. Animals were ventilated for 20 minutes using these settings. Depth of anesthesia was assessed every 10 min by monitoring the cardiovascular response to paw clamp. Body temperature was maintained at 36–37.5°C by using a thermostatically controlled blanket system (Harvard Apparatus, Holliston, MA) and confirmed with an indwelling rectal temperature probe. Systemic arterial pressure, peak airway pressures, and temperature were continuously measured throughout the experimental protocol. After 20 min, an arterial blood gas sample (100 microlitre) was drawn for blood gas measurement (ABL 705; Radiometer, Copenhagen, Denmark), and lung compliance was measured as described below.

4.2.3 Exclusion and termination criteria

Before entry into the experimental protocol, the following baseline values were required for continuation with the protocol: arterial oxygen tension greater than 120 mmHg, HCO_3^- greater than 20 mmol · l^{-1}, and temperature of 36.0–37.5°C. Where the criteria were not fulfilled, variables were reassessed after an additional 15 min, during which no specific interventions were performed. Failure to meet the criteria at this point mandated exclusion from the protocol. Thereafter, the experiment was terminated if at any stage during the protocol the mean arterial pressure (MAP) dropped below 30 mmHg for greater than 15 min.

4.2.4 Recovery from VILI via tracheostomy – ventilator settings

Once baseline criteria were attained, injurious ventilation was commenced. This consisted of various settings of high peak inspiratory pressure, respiratory rate, and inspiratory flow rate, and zero end expiratory pressure, to induce lung injury. Injury was induced using either FIO_2 0.3 or 0.21.

Once injury was achieved, the animals were ventilated using baseline ventilation settings as described above. To minimize lung derecruitment, a recruitment maneuver consisting of a positive end-expiratory pressure of 10 cm H_2O for 25 breaths was applied every 15 min throughout the recovery period.

4.2.5 Measurement of physiological variables

Intra-arterial blood pressure, peak airway pressures, and rectal temperature were recorded continuously for the duration of the protocol. Hourly assessment of oxygenation, ventilation, and acid-base status was carried out through blood gas analysis. Static inflation lung compliance was measured at baseline and hourly throughout the protocol. Compliance was measured immediately before a recruitment maneuver, ensuring a standardized lung volume history. Incremental 1-ml volumes of room air were injected *via* the tracheostomy tube, and the pressure attained 3 s after each injection was measured, until a total volume of 5 ml was injected.

4.2.6 Measurement of gas exchange using FIO_2 1.0

In order to calculate alveolar-arterial oxygen gradient, a period of ventilation using FIO_2 1.0 was necessary. This was accomplished over a 15 minute interval at the end of each protocol.

4.2.7 Euthanasia of animals

At the end of the treatment protocol, heparin (400 IU · kg^{-1}; CP Pharmaceuticals, Wrexham, United Kingdom) was then administered intravenously, and the animals were then killed by exsanguination.

4.3 VILI via Tracheal Tube Model

4.3.1 Oro-tracheal intubation protocol

Animals were anesthetized by inhalational induction with isoflurane and an intra-peritoneal injection of 40 $mg.kg^{-1}$ of ketamine (Pfizer, Kent, United

Kingdom) [251, 252]. Intravenous access was attained via tail vein with a 24G intravenous catheter (BD Insyte®; Becton Dickinson Ltd., Oxford, United Kingdom). Laryngoscopy was performed using an otoscope (Welch Allyn, Navan, Co Meath) and the trachea was intubated with a size 14G intravenous catheter (BD Insyte®; Becton Dickinson Ltd., Oxford, United Kingdom).

4.3.2 Injury and recovery protocol

Further anaesthesia was maintained with an intravenous Saffan infusion (Alfaxadone 0.9% and alfadolone acetate 0.3%; Schering-Plough, Welwyn Garden City, United Kingdom) at 5–20 mg · kg^{-1} · h^{-1} via tail vein canula. After confirmation of depth of anaesthesia by using paw clamp, Cisatracurium besilate (0.5 mg; Nimbex, GlaxoSmithKline, Dublin, Ireland) was administered intravenously to produce muscle relaxation. Baseline ventilation settings were similar to the tracheostomy protocol. The animals were ventilated by using a small animal ventilator (CWE SAR 830 AP, CWE Inc, Pennsylvania, USA) with an inspired gas mixture of 30% oxygen, respiratory rate of 80 breaths/min, tidal volume of 6 ml · kg^{-1}, and positive end-expiratory pressure of 2 cm H_2O. To minimize lung derecruitment, a recruitment maneuver consisting of a positive end-expiratory pressure of 10 cm H_2O for 25 breaths was applied every 5 min throughout the protocol. Animals were ventilated for 20 minutes using these settings. Depth of anesthesia was assessed every 10 min by monitoring the cardiovascular response to paw clamp. Body temperature was maintained at 36–37.5°C by using a thermostatically controlled blanket system (Harvard Apparatus, Holliston, MA) and confirmed with an indwelling rectal temperature

probe. Compliance was measured after 20 minutes as above, this time via the endo-tracheal tube.

4.3.3 Exclusion and termination criteria

Before entry into the experimental protocol, the following baseline values were required for continuation with the protocol: respiratory static compliance greater than 0.5mls/cmH_2O, and temperature of 36.0–37.5°C. Where the criteria were not fulfilled, variables were reassessed after an additional 15 min, during which no specific interventions were performed. Failure to meet the criteria at this point mandated exclusion from the protocol. Thereafter, the experiment was terminated if at any stage during the protocol the respiratory static compliance dropped below 0.3 ml/cmH_2O, an injury from which we had previously demonstrated was inconsistent with animal recovery.

4.3.4 Injurious ventilation protocol

Once baseline criteria were attained, injurious ventilation was commenced. This consisted of various settings of high peak inspiratory pressure, respiratory rate, and inspiratory flow rate, and zero end expiratory pressure, to induce lung injury. Injury was induced using either FIO_2 0.3 or 0.21. Different end-points for injury were used, either duration of injury or decrease in compliance by 50%.

4.3.5 Recovery from injury

Once animals had achieved the desired severity of lung injury, the severity of mechanical stretch was reduced to conventional protective seetings, anaesthesia was discontinued and the animals were allowed to recommence spontaneous respiration. Once spontaneous breathing was adequate (RR>60 bpm) ventilation was discontinued. The animals were extubated once fully awake and able to move limbs or head. They were subsequently placed in individually ventilated recovery cages (Tecniplast Inc., Buguggiate, Italy).

4.3.6 Assessment of injury and repair

At various time points (6 hours to 14 days depending on the protocol) following induction of VILI, the animals were re-anesthetized. A tracheostomy was inserted and carotid arterial access established, and the lungs were mechanically ventilated using baseline settings as above. Intra-arterial blood pressure, peak airway pressures and rectal temperature were recorded continuously. Static inflation lung compliance measurements were performed as described above. After 20 minutes, the inspired gas was altered to a FiO2 of 1.0 for 15 min, and an arterial blood sample was then taken for calculation of the alveolar–arterial oxygen gradient. At the end of the treatment protocol, heparin (400 IU · kg^{-1}; CP Pharmaceuticals, Wrexham, United Kingdom) was then administered intravenously, and the animals were then killed by exsanguination.

4.4 Tissue Sampling and Assays

Immediately postmortem, a thoracotomy was performed and the heart-lung block was dissected from the thorax. The following analysis was performed:

4.4.1 Wet:dry ratio

The right lower lobe was isolated, excised and weighed, and placed in a 4O°C oven. After 72 hours it was re-weighed for calculation of wet:dry ratio.

4.4.2 Bronchoalveolar lavage collection

Bronchoalveolar lavage (BAL) collection was performed as previously described [252]. 15mls of sterile NaCl 0.9% was injected via the tracheostomy into lung, in 5ml increments. These 5ml increments were allowed to return into a 15ml conical tube. 20 microlitres of this fluid was used undiluted for total cell count, and 1 ml was used for preparation of slides for differential cell count. Remaining BAL fluid was centrifuged at 1500g for 15 minutes, and the supernatant was collected and stored at -80°C for later analysis.

4.4.3 Total cell count

Total cell numbers per milliliter in the BAL fluid were determined. Each sample of undiluted BAL was counted twice for total cell count. A standard Neubauer hemocytometer counting chamber was used, counting cells in the four1/25 sq. mm corners plus the middle square in the central square. 10 microlitres of BAL fluid were pipetted underneath the haemocytometer coverslip. To obtain total cells per ml this total count was divided by 5 and multiplied by 10,000.

4.4.4 Differential cell count

1ml of undiluted BAL fluid was centrifuged at 15,000g for 1 minute. 750 microlitres was removed, and the remaining 250 microlitres was used to re-suspend the cell pellet. 50 microlitres of this concentrated cell suspension was pipetted into the funnel of a cytospin cartridge (Thermo-Fisher Scientific). The cartridge, along with a glass slide, were spun for 2 minutes at 200 rpm in the cytospin centrifuge (Thermo-Fisher Scientific). Cells were transferred to the glass slide, and fluid became adherant to the blotting paper on the underside of the cytospin cartridge. Slides were then stained using the Diff-Quik method. Slides were immersed 6 times in methanol, 5 times in eosin, and 3 times in methylene blue and allowed to dry. To obtain the differential cell count, 300 inflammatory cells (macrophages, neutrophils, lymphocytes or eosinophils) were identified in three different regions of the slide, and the number of neutrophils in each count was noted, to give the percentage neutrophil count. The total cell count was used to calculate the number of neutrophils per ml of BAL.

4.4.5 Protein assay

We used a commercially available protein assay kit - Micro BCA™ Protein assay kit (Pierce, Rockford, IL, USA). Each sample was examined in triplicate. Due to the high concentration of protein in the BAL, we first made a 1 in 10 dilution of each sample in PBS. We first prepared standards as outlined in kit instructions to give a working range of protein concentrations from 20-2000μg/ml. The

Working Reagent (WR) was prepared by mixing 50 parts of BCA™ Reagent A with 1 part of BCA™ Reagent B (50:1, Reagent A:B). We pipetted 25 µl of each standard or sample replicate into a microplate well (working range = 20-2,000 µg/ml). We then added 200 µl of the WR to each well and mixed the plate thoroughly on a plate shaker for 30 seconds. The plate was then covered and incubated at 37°C for 30 minutes before being cooled to room temperature. The absorbance of the samples was then measured at 560nm on a Wallace plate reader.

4.4.6 Enzyme-linked immunosorbent assay

We used commercially available enzyme linked immunoassay kits from R&D Systems Europe Ltd**,** Abingdon Science Park, Abingdon, OX14 3NB United Kingdom. Nunc (Denmark) 96 well flat bottomed ELISA plates were first coated with the binding antibody and coating buffer at 100 µl per well, wrapped in parafilm and left to incubate at 40C overnight. Plates were then subjected to three 300 µl per well washes with PBS Tween. Blocking buffer of 5% BSA 100 µl was added to each well and left for one hour at room temperature. A standard curve set of samples was constructed with 400 µl neat IL-6 or CINC1 at the top end of the range and 7 serial half dilutions of this then made with 5% BSA as the diluents. The plates were again subjected to three 150 µl per well washes with PBS Tween. Samples were then added in triplicate. Neat BAL was used and 25 µl of each was added to 75 µl of 5% BSA per well. The standard curve samples were added at this stage also at 90 µl per well. A 1 in 400 dilution of detection antibody was added to each well and left to incubate for 90 minutes. The plate underwent three 150 µl per well washes with PBS Tween. Strep –Hrp conjugate

solution (100 µl) was added to each well and the plate left for 20 minutes. The plate was again subjected to three 150 µl per well washes with PBS Tween. Substrate solution (100 µl) was added to each well and the plate left in the dark. Finally 50 µl of stop solution (1M H_2SO_4) was added to each well and the plate read at the Wallace plate reader. Absorbance readings at 450nm for 0.1 seconds and 550nm for 0.5 seconds were taken.

4.4.7 Multiplex bead array analysis of cytokines

We used the Bio-Plex 200 system (Bio-Rad Life Science, California, USA), a Luminex-based multiplex analysis system that permits the simultaneous analysis of up to 100 different biomolecules (i.e., proteins, peptides, or nucleic acids) in a single microplate well. Each assay was performed on the surface of a 6.5 µm polystyrene bead. The beads were filled with different ratios of two different fluorescent dyes, resulting in an array of 100 distinct spectral addresses. We utilized the Bio-Plex Rat Cytokine 9-Plex A Panel (Bio-Rad), with the following cytokines assayed: IL-1α, IL-1β, IL-2, IL-4, IL-6, IL-10, GM-CSF, IFN-γ and TNF-α. A work flow of the multiplex assay is provided in Figure 4-1 below.

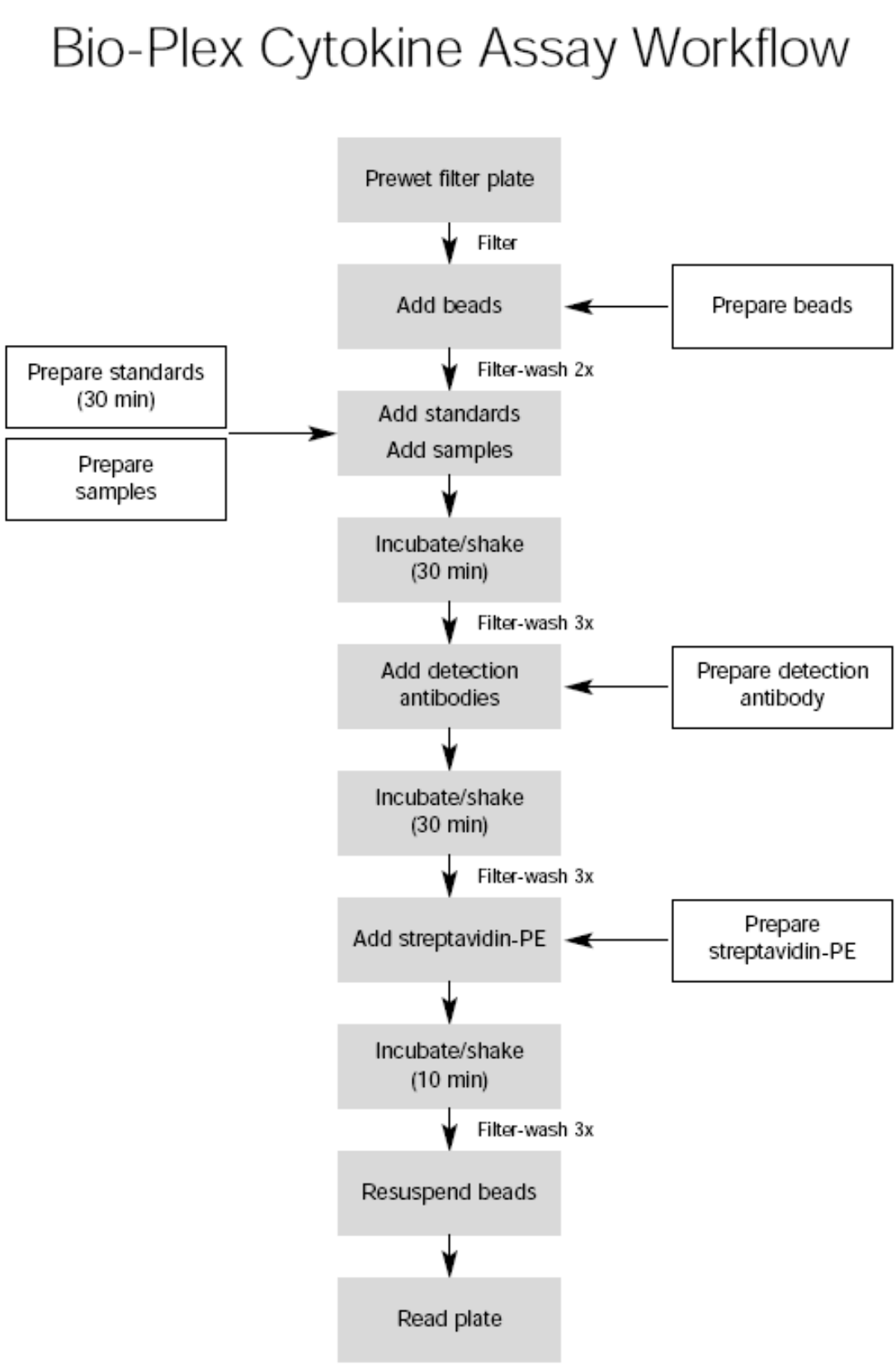

Figure 4-1 Work flow for multiplex cytokine assay

Neat BAL samples were thawed and vortexed. A standard curve using the high PMT setting and starting at a 10-fold lower concentration of cytokine as is recommended for serum, or plasma samples was used. Standard was reconstituted by adding 500µL of standard diluent to the standard vial. This was vortexed gently for 5 seconds and then incubated on ice for 30 min. A serial dilution was carried out as in Figure 4-2 below.

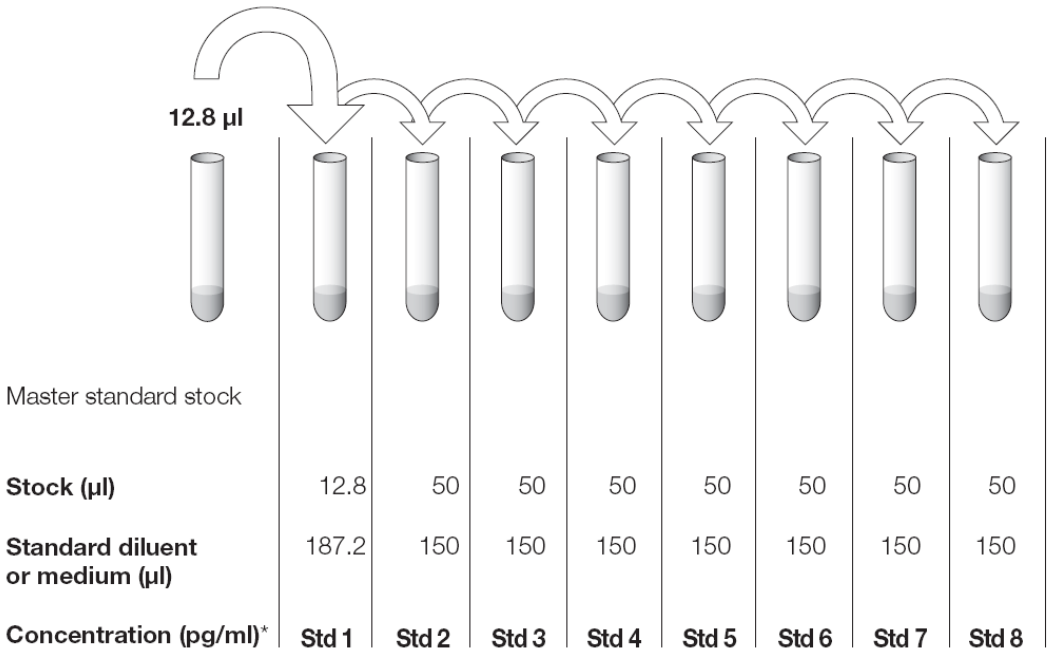

Figure 4-2 Performance of serial dilutions creation of a standard curve

The anti-cytokine bead (25x) stock solution was vortexed at medium speed for 20 sec and a 25-fold working dilution of the anti-cytokine bead (25x) stock solution in Bio-Plex Assay Buffer A was prepared. All unneeded wells were covered with plastic adhesive plate sealer. The vacuum pressure was set to 2 inches Hg using a standard flat bottom 96-well plate. The filter plate was pre-wet with 100 µl of Bio-Plex Assay Buffer. The bottom of the plate was blotted after this and every vacuum filtration. The working Bead solution was vortexed at

medium speed for 20 sec and 50μL was added to each well. The plate was then vacuum filtered and washed with Bio-Plx wash buffer. 50μL of standards and samples were then added to the wells, and these were incubated for 30 minutes at room temperature. The plate was filter washed 3 times with Bio-Plex wash buffer. 25μL of detection antibody was added to each well and incubated for 30 minutes at room temperature. After 3X wash, 50μL of streptavadin-PE was added to each well, and incubated for 10 minutes at room temperature. After a further 3X wash, the beads in each well were resuspended in 125μL of Bio-Plex Assay Buffer and the plate was read in the Bio-Plex 200 system.

4.4.8 Real-Time Polymerase Chain Reaction for Pro-Collagen Peptides

4.4.8.1 RNA extraction from tissue

200 mg of lung tissue from each animal's right lung was used to prepare cDNA. First RNA extraction from each sample was undertaken. Each tissue sample was placed in 15ml tubes and washed with PBS. Homogenization of the tissue was done using a Quiagen TissueRuptor™ (Quiagen, Venlo, Netherlands) with 1ml of TRIzol (Invitrogen) added per 100mg of tissue. Once the tissue was completely dissolved, phase separation was undertaken. Chloroform 200μl per ml TRIzol was added, vortexed for 15 seconds and left at room temperature for 2-3 minutes. Following centrifugation three phases were visible within each tube. The aqueous top phase was carefully removed to a new tube and 500 μl of isopropanol per 1 ml TRIzol was added. The samples were left to incubate at room temperature for ten minutes. The samples were then centrifuged at 12000g for 15 minutes at 4^0C. The supernatant was removed and the RNA pellet

washed with 80% alcohol and vortexed. The samples were again centrifuged at 7500g for 5 minutes at 4^0C. The supernatant was removed and the alcohol allowed to air dry for 2-3 minutes. The tubes were transferred to a 70^0C heat block and let sit for 2-3 minutes. The pellet was re-dissolved in 81 µl of DEPC water. DNAase treatment was completed using Ambion™ DNAase treatment kit. To each sample 8µl of 10X DNAase I Buffer and 2 µl of DNase I Enzyme were added. The sample was vortexed, spun and incubated at 42^0C for 25 minutes. Column purification was achieved using Qiagen's Rneasy Protocol. 350µl Buffer RLT (with BME-10µl/ml Buffer RLT) was added to each sample and then 250µl of 100% ethanol. The entire volume was applied to RNeasy column and spun full speed for 1 minute. The sample was reapplied to the RNeasy column and centrifuged. The column was transferred to a new 2ml collection tube. 750ul Buffer RPE was added and centrifuged at 12000g for 1 minute. The flow-through was discarded and 750ul Buffer RPE added and spun full speed for 1 minute. Flow through was discarded and the column transferred to a new labelled 1.5ml eppendorf. 56 µl DEPC H_2O was added and let sit for 2 minutes. The tube and column were spun at full speed for 2 minutes. The flow-through was collected, the column discarded and the sample stored on ice. Each sample of RNA was then quantified at Nanodrop spectrometry (Thermo Scientific Nanodrop 2000, Bishop Meadow Road, Loughborough, Leicestershire, UK).

4.4.8.2 cDNA synthesis

The previously prepared RNA was used to produce cDNA for use in quantitative real time PCR. cDNA was synthesized from the RNA using the ImProm-II™

reverse transcription system from Promega (Promega®, 2800 Woods Hollow Road Madison, WI, USA). This was carried out as follows.

- In tube "A", 3 µl of the RNA, 1µl of random primer and 1.8µl water was added. This mixture as incubated at 70^{o}C for 5 minutes and then immediately transferred to ice for 5 min.
- In tube "B" the following mixture was prepared. 3.7 µl water, 4 µl Improm-II 5X buffer, 4.8 µl $MgCl_2$, 1 µl dNTP mix, 0.5 µl recombinant RNasin ribonuclease inhibitor and 1 µl Improm-II RT.
- The contents of Tubes "A" and "B" were added to a PCR tube.
- The mixture was subjected to the following program in the thermocycler (Applied Biosystems Veriti Gradient Thermal Cycler, California, USA).
    - 25^{o}C for 5 minutes
    - 42^{o}C for 1 hr
    - 70^{o}C for 15 minutes
- A negative reaction was also setup. This reaction was the same as above with the substitution of water for RT.
- The resulting cDNA, was diluted 1:10 and stored at -20^{o}C until use for rt-PCR analysis.

4.4.8.3 rt-PCR analysis

Each cDNA sample was subjected to duplicate analysis. Quantitative PCR was performed for pro-collagen 1 and 3 genes, normalised against a GAPDH control

product. We looked for a comparison of fold induction of pro-collagen 1 and 3 amongst the 8 groups of animals, to detect fibroproliferation as a result of lung stretch.

4.4.8.4 Creation of the SYBR-Green Real-time PCR Reaction

There was a total volume of 10μL per reaction. A master-mix was made with the appropriate solutions, with 5μL of the master-mix added per reaction.

The master mix contained:

Fast SYBR® Green Master Mix (2x concentration; Applied Biosystems): 5μL

Distilled Water: 3.98μL

Forward primer (100uM): 0.01μL - final conc is 1μM

Reverse primer (100uM): 0.01μL - final conc is 1μM

Primer sequences from MWG-Biotech GmbH:

Quantitative primers

GAPDH RN Forward 5'-TTGTGAAGCTCATTTCCTGG-3'

GAPDH RN Reverse 5'-CATGTAGGCCATGAGGTCCA-3'

Pro-collagen I RN: Forward 5'-TCATCGAATACAAAACCACCA-3'

Pro-collagen I RN Reverse 5'-GCAGGGCCAATGTCCAT-3'

Pro-collagen III RN: Forward 5'-ACACACTGGTGAATGGAGCAA-3';

Pro-collagen III RN Reverse 5'-GCCAATGTCCACACCAAATT-3'

PCR was carried out in the StepOne Plus (Applied Biosystems) Fast-enabled Real Time PCR System in a MicroAmp™ Fast Optical 48-Well Reaction Plate. The comparative CT (ΔΔCT) method was used to determine the relative target

quantity in samples. Measurements were normalized using the endogenous GAPDH control. The PCR cycle durations and temperatures are outlined in Table 4-1 below.

Table 4-1 PCR cycle times and temperatures

Step	**Cycles**	**Time**	**Temperature**
Initial denaturation	1	3 min	95^0C
Denaturation Annealing Elongation	40	30 sec 30 sec 45 sec/kb	95^0C 45^0C 72^0C
Final Elongation	1	2 min	72^0C

4.4.9 Lung tissue collagen content using the Sircol assay

Lung tissue collagen content was determined using the Sircol collagen assay (Biocolor Ltd., Belfast, United Kingdom)[253] according to the manufacturers instructions. Lung homogenate (0.1mg/ml) was incubated in acid-pepsin at 4°C overnight. At a pepsin (Sigma-Aldrich) concentration of 0.1 mg/ ml 0.5M acetic acid the enzyme activity, at 4°C, is effective in removing the terminal non-helical telopeptides to release the collagen in lung into solution. A standard curve was constructed using 15, 30 and 50µg of Collagen Reference Standard (Biocolor) Sirius red reagent (50 µl) was added to each lung homogenate (50µl) and standard and mixed for 30 minutes. The collagen–dye complex was precipitated

by centrifugation at 16,000 *g* for 5 minutes and dissolved in 0.5 M NaOH. Finally, the samples were introduced into a microplate reader and the absorbance determined at 540 nm.

4.4.10 Tissue Western Blot analysis for MMPs

These assays were carried out in collaboration with Dr Cecilia O'Kane, Queens University Belfast. To determine relative concentrations of MMP-1, -3, -8, -13 and TIMP-2, total cell protein was extracted from thawed, homogenized lung tissue samples. For each sample, 0.2g of tissue was homogenized in 2mls of PBS and centrifuged at 15000g for 30 minutes. 1ml of supernatant protein was removed and its protein concentration determined using BCA protein assay kit (Pierce® BCA Protein Assay Kit, Thermo Scientific, 3747 N. Meridian Road PO Box 117 Rockford, Illinois, USA). For BAL samples, protein quantification was carried out on neat samples. 20µg of the total protein extract from each sample was loaded on a polyacrylamide gel (Precise™ Protein Gel, Pierce Biotechnology, 3747 N. Meridian Road PO Box 117 Rockford, Illinois USA) and electrophoresed in Tris-HEPES-SDS running buffer. Non-specific binding sites were blocked overnight in PBS/non-fat dry milk solution (5% w/v) at 4°C. Primary antibodies used were polyclonal rabbit anti-rat MMP-3Ab from Chemicon at 1/1000, polyclonal rabbit anti-rat MMP-8 Ab Chemicon, 1/1000, mouse anti-rat MMP-13 at 1/400 dilution, mouse anti-rat TIMP-2 at 1/1000 in blocking solution was applied for 12 hours followed by washing the blot paper with Tween 20/PBS (0.05% v/v). Subsequently the membrane was incubated with antigoat antibody conjugated to horseradish peroxidase (Cell Signaling Technology, 3 Trask Lane Danvers, MA 01923, United States) for 1 hour at a dilution of 1:2000 in blocking solution.

After a second set of washes the membrane was incubated with a chemiluminescent substrate (SuperSignal® West Pico, Pierce Biotechnology, Thermo Scientific) for 5 minutes and then visualised with Kodak Image Station 4000MM Pro (Carestream Health, Inc., Rochester, N.Y). During electrophoresis samples were alongside a standard aliquot of chemiluminescent marker (Pierce). Blots were photographed using darkroom software (UVP), and relative density of the bands obtained measured using Scion image analysis [254]. The density of the bands was compared with the density of the 50kDa band on the chemiluminescent marker to allow comparison between gels.

4.4.11 Gelatin zymography

These assays were carried out in collaboration with Dr Cecilia O'Kane, Queens University Belfast. Gelatin zymography to analyze MMP-2 and -9 concentrations was performed as previously described [255]. Twenty-microliter aliquots of BAL or homogenised tissue as above with 5× loading buffer (0.25 M Tris pH 6.8, 50% glycerol, 5% SDS, bromophenol blue) were run on 11% acrylamide gels impregnated with 0.1% gelatin at 180V for 3.5 hours (buffer 25 mM Tris, 190 mM glycine, 0.1% SDS). After incubation in 2.5% Triton X for 1 hour with agitation and two brief washes in collagenase buffer (55 mM Tris base, 200 mM sodium chloride, 5 mM calcium chloride, 0.02% Brij, pH 7.6), gels were incubated for 16 hours in fresh collagenase buffer at 37°C. Gelatinolytic activity was detected by a single step stain/de-stain method using 0.02% Coomasie blue in 1:3:6 acetic acid: methanol: water. All experimental samples were run in parallel with 2ng recombinant MMP-9 (Merck, Nottingham, UK) to standardize between

gels. Densitometric analysis was performed by digital image acquisition (UVP) followed by proteolytic band quantification with NIH Image version 1.61.

4.5 Histology

4.5.1 Preparation of lung tissue

The left lung was isolated and fixed for morphometric examination. The pulmonary artery was cannulated, the left atrium was incised, and the pulmonary circulation was perfused with normal saline at a constant hydrostatic pressure of 35 cm H2O until the left atrial effluent was clear of blood. The right lung was ligated and removed to be used for rt-PCR and Western Blot analysis. The left lung was then inflated through the tracheal catheter using paraformaldehyde (4% wt/vol) in phosphate-buffered saline (300 mOsmol) at a pressure of 25 cm H_2O. Paraformaldehyde was then instilled through the pulmonary artery catheter at a pressure of 62.5 cmH_2O. The left atrium was then tied off to prevent pulmonary venous inflow into the atrium, creating a constant distending pressure across the pulmonary vasculature, and maximally distending the pulmonary vessels. After 30 min, the pulmonary artery and trachea were ligated, and the lung was stored in paraformaldehyde for 24 h and then embedded in paraffin wax.

After fixation, the vertical axis of the left lung was identified. The lung was cut into six equal sections perpendicular to this axis using a sharp blade. (See **Figure** below for the division of the lung into sections.)

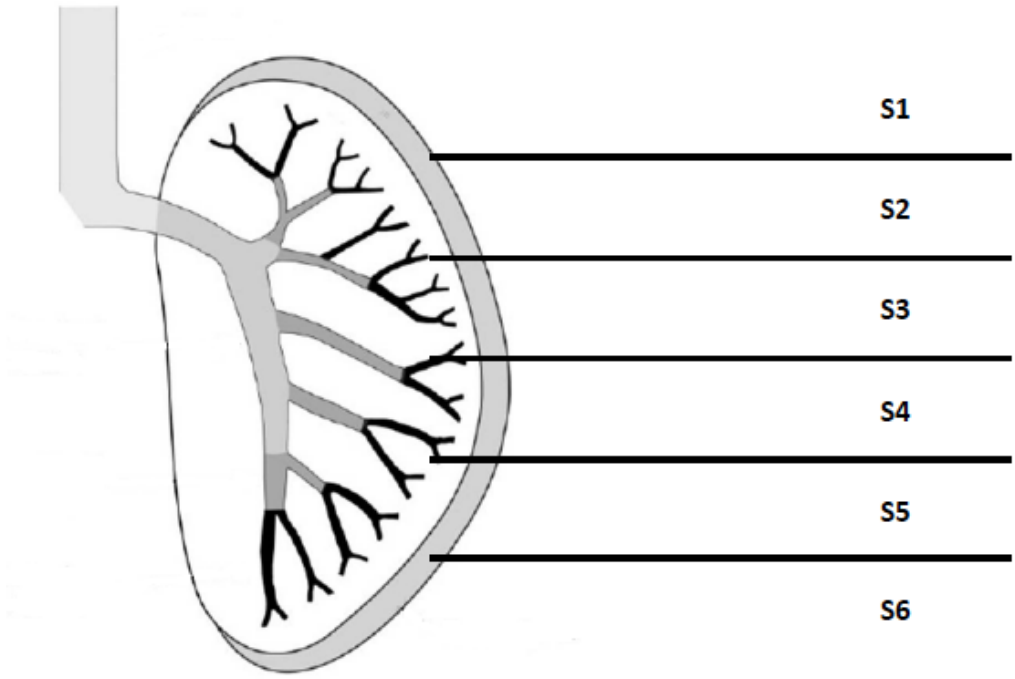

Figure 4-3 Division of lung into sections for paraffin embedding

4.5.2 Paraffin embedding

After sectioning the paraformaldehyde fixed lung, the sections were placed in an appropriately labelled histoprocessing cassette (Cat # M490-4, Histosette I, Simport Industries, 2588 Bernard-Pilon, Beloeil QC, J3CG 4S5, Canada). Also included in the cassette was a pencil inscribed label detailing the animal and section number. The sections were then placed in a histoprocessor (ASP 300 histoprocessor, Leica Microsystems, Wetzlar, Germany) on the factory preset "routine overnight" program. The following morning the cassettes were removed from the processor and the sections embedded in paraffin wax. Each section was orientated in a transverse manner, with its top as the cutting edge.

4.5.3 Slide preparation

Sections were cut at 7 μm using a microtome (Ergostar HM200, Microm Laborgerate GmbH, D69190 Walldorf, Germany) and placed on labelled glass slides. It is important to note that all labeling of slides was performed in a blinded manner.

4.5.4 Hematoxalin and Eosin Staining

The prepared slides were dried overnight at 37°C to facilitate adherence of the sections to the slides. The following morning the slides were heated at 60°C for 15 minutes in order to melt the wax. They were then put through two baths of xylene (Cat # 305756G, VWR International Limited, Poole, BH15 ITD, England) and graded alcohols (Cat # 1.00983.2500, Merck KGaA, 64271, Darmstadt, Germany) (100%, 90% and 70% respectively) to deparaffinize and rehydrate the tissue. The slides were then placed in a bath of hematoxylin for 3 minutes. These were rinsed in de-ionised water and dipped 8 times in acid alcohol, and rinsed again in de-ionised water. The slides were next placed in a bath of eosin (Cat # HT110232, Sigma-Aldrich Ireland Ltd. Dublin, Ireland) for 2 minutes. They were then dehydrated in 100% alcohol, 3 times, and two baths of xylene. Finally, they were then coverslipped and mounted in DPX (Cat # 360294H, VWR International Limited, Poole, BH15 ITD, England). Slides prepared in this manner were stored at room temperature, and protected from light.

4.5.5 Stereological Analysis

Slides prepared as described above were viewed at a 10X magnification under a

microscope (Model BX51, Olympus, Mason Technologies, Dublin 8, Ireland). Two fields of view from each slide were chosen at random and digitised using a digital camera (Olympus DP70, Mason technologies, Dublin 8, Ireland). Images were stored in eight-bit (256 level) format. The grid reference, *i.e.* X and Y grid coordinates for each image was recorded by referencing the scale attached to the microscope. A 100 point counting grid was overlaid on each image in AnalySISD (R) imaging software package (Version 1.20, Olympus, Soft Imaging System, Münster, Germany). Care was taken to ensure that the software was set to 10X magnification. Once this grid was superimposed over the image, a touch count was performed. At each of 100 intersection points on the grid, a record was taken for each of the following: acinar tissue, non-acinar tissue and airspace. The intraacinar tissue was defined as all tissues within the gas exchange portion of the lung, *i.e.*, respiratory bronchioles, alveolar ducts, alveolar sacs, and alveoli, including blood vessels contained within their walls. The intraacinar airspace was defined as all airspaces within the lumen of respiratory bronchioles, alveolar ducts, alveolar sacs, and alveoli. The totals were recorded and analysed using Minitab Statistical software.

4.5.6 Masson's Trichrome Staining for collagen

The prepared slides were dried overnight at 37°C to facilitate adherence of the sections to the slides. The following morning the slides were heated at 60°C for 15 minutes in order to melt the wax. They were then put through two baths of xylene (Cat # 305756G, VWR International Limited, Poole, BH15 ITD, England) and graded alcohols (Cat # 1.00983.2500, Merck KGaA, 64271, Darmstadt,

Germany) (100%, 90% and 70% respectively) to deparaffinize and rehydrate the tissue. The slides were then re-fixed in Bouin's solution (Picric Acid 75ml, Formaldehyde 25 ml, Glacial acetic acid 5ml, all Sigma Aldrich) for 1 hour at 56°C to imrove staining quality. Following this, they were rinsed under tap water for 10 minutes to remove the yellow colour. The slides were then stained in Weigert's iron hematoxylin working solution (hematoxylin 1g, 95% alcohol 100ml, 29% ferric chloride in water 4ml, distilled water 95ml, concentrated hydrochloric acid 1ml) for 10 minutes. Slides were once again rinsed in running warm tap water for 10 minutes. Following this they were washed in distilled water. Slides were then stained in Biebrich scarlet-acid fuchsin solution (1% Biebrich scarlet 90ml, 1% Acid fuchsin 10ml, glacial acetic acid 1ml, all Sigma Aldrich) for 10 minutes. Slides were washed in distilled water. Slides were then differentiated in phosphomolybdic-phosphotungstic acid solution (5% Phosphomolybdic acid 25 ml, 5% Phosphotungstic acid 25 ml, Sigma Aldrich) for 10-15 minutes or until collagen was not red. Slides were transferred directly to aniline blue solution (2.5g aniline blue in 100ml distilled water) and stained for 10 minutes. Slides were again rinsed in distilled water, and immersed in 1% acetic acid solution for 5 minutes, and once again rinsed in water. They were then dehydrated in 100% alcohol, 3 times, and two baths of xylene. Finally, they were then coverslipped and mounted in DPX (Cat # 360294H, VWR International Limited, Poole, BH15 ITD, England). Slides prepared in this manner were stored at room temperature, and protected from light.

4.5.7 Van Gieson Staining for Elastin Fibers

Solutions

5% alcoholic hematoxylin:

Hematoxylin ---------- 5 g

100% alcohol ---------- 100 ml

Mix to dissolve with the aid of gentle heat. Filter.

10% aqueous ferric chloride:

Ferric chloride ---------- 10 g

Distilled water ---------- 100 ml

Weigert's iodine solution:

Potassium iodide ---------- 2 g

Iodine ---------- 1 g

Distilled water ---------- 100 ml

The working solution, known as Verhoeff's Working Solution, was made up fresh as follows:

5% alcoholic hematoxylin ---------- 20 ml

10% ferric chloride ---------- 8 ml

Weigert's iodine solution ---------- 8 ml

Van Gieson's counterstain consisted of**:**

1% aqueous acid fuchsin ---------- 5 ml

Saturated aqueous picric acid ---------- 100 ml

The following morning after sectioning, the slides were heated at 60°C for 15 minutes in order to melt the wax. They were then put through two baths of xylene (Cat # 305756G, VWR International Limited, Poole, BH15 ITD, England)

and graded alcohols (Cat # 1.00983.2500, Merck KGaA, 64271, Darmstadt, Germany) (100%, 90% and 70% respectively) to deparaffinize and rehydrate the tissue. They were then stained in Verhoeff's solution for 1 hour until the tissue was completely black. Slides were then rinsed thoroughly in tap water. Differentiation was carried out by immersion in 2% aqueous ferric chloride (Sigma Aldrich) for 2 minutes. Slides were washed thereafter with tap water. The tissue was then treated in 5% sodium thiosulphate (Sigma Aldrich) for 1 minute. Slides were then counterstained in Van Giesen's solution for 5 minutes. They were then dehydrated in 100% alcohol, 3 times, and two baths of xylene. Finally, they were then coverslipped and mounted in DPX (Cat # 360294H, VWR International Limited, Poole, BH15 ITD, England). Slides prepared in this manner were stored at room temperature, and protected from light. The elastic fibers were stained blue-black and background was stained yellow.

4.5.8 Lung tissue Myofibroblasts – immunohistochemical staining with antibodies to α-smooth muscle actin

Paraffin-embedded tissue sections of 5μm in thickness were dewaxed and rehydrated. Antigen retrieval was performed by heating in citrate buffer. After quenching endogenous peroxidase activity and blocking nonspecific binding, sections were incubated with antibodies against alpha-smooth muscle actin (LSAB kit, Dako, CA, USA). Antibody binding was detected using horseradish peroxidase-labeled biotin streptavidin secondary antibodies (Dako) and immunostaining visualized using 3,3-diaminobenzidine chromogen (Dako). Positive cells were identified and counted in 15 areas from each lung at 20X magnification and compared to controls. Positive staining smooth muscle cells

located in the walls of arterioles were not included in counts.

4.5.9 Lung Tissue Collagen Quantification

Alveolar thickness and fibrosis were scored in ten random fields at three levels through a subset of lungs, according to the Ashcroft method (**Table 4-2**) [256], by a histopathologist blinded to the treatment groups. According to the scale defined by Ashcroft et al, lung sections may be assessed by a system of grades **(Table 4-2)**. If there is any difficulty in deciding between two odd-numbered grades, the field would be given the intervening even-numbered score. In every field, the predominant degree of fibrosis was recorded as that occupying more than half of the field area.

Table 4-2 Grading of fibrosis according to Ashcroft

Grade of fibrosis	Ashcroft Scale
0	Normal Lung
1	Minimal fibrous thickening of alveolar or bronchiolar vessels
2	None
3	Moderate thickening of walls without obvious damage to lung architecture
4	None
5	Increased fibrosis with definite damage to lung structure and formation of fibrous bands or small fibrous masses
6	None
7	Severe distortion of structure and large fibrous areas
8	Total fibrous obliteration of the field

4.5.10 Lung tissue elastin quantification

The lung parenchyma was also evaluated for the density of the elastic fibers. The proportion of fibers in the lung parenchyma was determined using the linear

point counting grid in 10 fields per subgroup of animals. The ratio between the number of points based on the colored fibers and the lung parenchyma was determined. These sections were also evaluated by a blinded histopathologist according to level of organization on a 4 point scale as follows: (1) Organised, (2) Mild disruption in organization, (3) Fiber disruption and disorganization evident and (4) Elastin fibers grossly disrupted throughout.

4.6 Mesenchymal Stem Cell Techniques

4.6.1 Rodent MSC isolation and culture

Mesenchymal Stem Cells were isolated from rat femora and tibiae under sterile conditions in the animal surgery room as previously described [257] with additional modifications. Briefly, male Sprague Dawley rats (8-12 weeks old) were euthanized by inhalation of CO_2. Incisions were made on both lower limbs to expose the tibiae and femora. Both bones were removed from the hind limbs and placed in ice cold sterile Tyrode's solution (Sigma, St. Louis, MO). The marrow was then flushed into a dish containing rMSC complete culture medium (Alpha-MEM Media (Gibco), F12-Ham Media (Gibco), 10% foetal bovine serum (FBS lot-selected for rapid growth of MSCs and maintenance of MSC pluripotency in culture), 1% antibiotic/antimycotic) and dispersed into a cell suspension. After centrifugation and filtration through a 100micron nylon mesh, a cell count was performed and the cells were transferred to a T-175 flask containing 30 mls of rMSC complete medium, at a density of $9x10^5$ cells/cm^2. On day 3 of culture in an atmosphere of 5% CO_2/90% humidity at 37^oC, medium and non-adherent cells were removed and fresh medium was added to each flask. Cells were ready

for subculture (usually after 16-17 days) when colonies began to exhibit a compact appearance and multi-layered growth or when the loosely formed colonies began to merge into a monolayer (<90% of confluence).

Thereafter, cells were ready to be passaged after 6/7 days culture, at 80% confluence. For passage, media was aspirated off and cells were washed with sterile PBS to remove any remaining serum. 8mls 0.25% trypsin/EDTA solution was added to the cells, which were incubated for 5 minutes at 37^{o} C. The enzymatic reaction was stopped by adding the same volume of rMSC media to cells. Cells were centrifuged at 400g for 5 min. Media was aspirated off the cell pellet which was resuspended in 1ml and a haemocytometer count was undertaken. Cells were furthered passaged or cryopreserved at -80^{o}C in 10% DMSO. Cells were expanded to passage 4, whereupon they were used for experiments. (See **Figure 7-1A** for MSCs in culture.)

4.6.2 Human MSC Isolation and Culture

Human MSCs were aspirated under sterile conditions from the iliac crests of healthy human volunteers. The obtained marrow was filtered with a 70 μm cell strainer (Falcon, USA) before centrifuging at 400 g for 10 min. Cell pellets were resuspended in media consisting MEM-α (Gibco), supplemented with 10% Fetal Bovine Serum (FBS) (Gibco, USA) and 1% antibiotics (streptomycin and penicillin) (Gibco, USA), and cultured in 175 cm^2 flasks at 37 °C in a humidified atmosphere containing 5% CO_2. At day 4, the cultures were washed with PBS to remove the non-adherent cells and further expanded until >80% confluence, when they were harvested and expanded in 175 cm^2 flasks. After subculture, these cells were designated as passage 1.

4.6.3 MSC differentiation

Osteogenic differentiation was induced by culturing rMSCs for up to 4 weeks in rMSC Complete Medium supplemented with dexamethasone, ascorbic acid and β-glycerophosphate as previously described [258]. To observe calcium deposition, cultures were stained with Alizarin Red stain (Sigma, St Louis, MA) ***(Figure 1b)***. To induce adipogenic differentiation, rMSCs were cultured for up to 4 weeks in medium supplemented with dexamethasone and insulin; adipocytes were discerned by staining with Oil Red O (Sigma) ***(Figure 1c)***. Chondrogenic capacity was assessed by addition of TGF-beta (Invitrogen) and staining with Toluidine blue ***(Figure 1d).***

4.6.4 Characterisation of MSCs

In accordance with the position statement for the minimal criteria to define an MSC [115], cells were labeled with monocloncal antibodies and analyzed with a FACScan (Becton Dickinson, Franklin Lakes, NJ) and CellQuest software as described [143]. The following monoclonal antibodies were used for phenotypic characterisation of MSCs : anti-rat CD29-FITC, anti-rat CD90-PE, anti-rat CD44H-FITC, anti-rat CD73-PE, anti-rat CD45-FITC, anti-rat CD71-PE, anti-rat CD80-PE, anti-CD106-PE (all from BD Biosciences, San Jose, CA), anti-rat MHC class I-FITC (AbD Serotec, Kidlington, UK), anti-rat MHC class II-PE (AbD Serotec). For staining, cells were washed with FACS buffer (PBS containing 2 % FCS and 0.1 % NaN_3, all from Sigma Aldrich, Dublin, Ireland) and incubated for 5 min on ice

with anti-rat CD32 (Fcg receptor; BD Biosciences) to reduce unspecific binding. Then, without washing, mAbs were added and the cells were incubated for 30 - 45 min on ice. Finally, unbound reagents were removed by washing twice with FACS buffer and the cells were resuspended in FACS buffer for analysis using a FACS Canto (BD Biosciences). In some cases, cells were fixed by adding 2 % PFA in FACS buffer. Data were analysed with Diva software (BD Biosciences) or FlowJo.

4.6.5 Fibroblast isolation and culture

Adult male Sprague Dawley rats were euthanized by CO_2 inhalation. The ventral surface of the rat was shaved and sprayed with 70% ethanol. Skin and subcutaneous tissue was removed and placed into 70% ethanol for 30 seconds. Fat and subcutaneous tissue was removed and the skin strips were placed in 0.25% trypsin (Sigma) overnight. The epidermis was then peeled from the dermal layer, and the dermal layer was placed on a scored 6 well plate (Sarstedt, Wexford, Ireland) in F-12/MEM-alpha medium supplemented with fetal calf serum (10%) and penicillin/streptomycin (1%).

Primary human lung fibroblasts were obtained from American Type Culture Collection (ATCC).

4.6.6 Conditioned Medium

Allogeneic human or rodent MSC, or human or rodent fibroblasts (2×10^6) were washed with PBS and cultured without serum for 24 h. The cells were again washed and the medium was then replaced, and the subsequent medium without

serum for the next 24h was used as the conditioned medium (CM). All conditioned medium was sterile-filtered through a 22μm filter to remove cellular debris. For the *in vivo* experiments 15 mls of this medium was concentrated using a 3000 kDa centrifugal concentrating filter (Amicon, Billerica, MA, USA) to give 500μL. For the *in vitro* experiments, medium was not concentrated.

4.6.7 Hypoxic treatment of human MSCs

To generate conditioned medium from hypoxic MSCs, cells were seeded at $9x10^5$ cells/cm^2 in 175cm^2 flasks and cultured under normal conditions for 24 hours. Cells were then washed with PBS, and cultured without serum under normal conditions for 24h. This medium was replaced with fresh serum free medium and the flasks were placed in the hypoxic chamber. Experiments were performed in an *in vivo 400* hypoxia chamber (Ruskinn Technologies, UK) at 37°C. MSCs were exposed to conditions of hypoxia (2.2% O_2, 5.5% CO_2, and 92.3% N_2) for 24 hours. Serum free medium was placed in the hypoxia chamber for a minimum of 3 hours to deplete the oxygen levels to the required 2.2%.

4.6.8 Cryopreservation and thawing of MSCs

To cryopreserve the cells, aliquots were resuspended in Freezing Medium (90% FBS and 10% DMSO) at a concentration of ~5 x 10^6 cells/mL. The vials were closed, placed on ice and transferred to a isopropyl alcohol lined freezing container ("Mr Frostie", Nalgene, Thermo Scientific), which lowers the temperature of the cell suspension at the rate of –1°C per minute to –80°C. The container was then placed in the –80°C freezer and from here into the vapor phase of liquid nitrogen of a Cryoplus 2 Storage container.

To thaw cryopreserved cells, vials were removed from liquid nitrogen vapour storage, placed in a 37 degree water bath and, together with rMSC Complete medium, were spun at 500g, washed in PBS and thereafter suspended in PBS for infusion, or in MSC medium for culture.

4.7 In vitro pulmonary epithelial wound healing experiments

To investigate the effects of MSCs on pulmonary epithelial wound repair, and the mechanisms underling these effects, we used a scratch injury model. The use of cell scratch models to examine epithelial repair began over 50 years ago [259] and has been validated in a number of settings [260, 261].

4.7.1 Pulmonary alveolar A549 cells

A549 cells were purchased from The European Collection of Cell Cultures (Porton Down, UK) as cryopreserved 90-passage culture and used at passages 91-95. These cells were passaged in growth medium (RPMI-1640, Sigma), supplemented with 10% fetal calf serum, penicillin G (100 U/ml) and streptomycin (100 μg/ml; GIBCO BRL, Grand Island, NY) at 37°C in a humidified incubator saturated with a gas mixture containing 5% CO_2 in air.

4.7.2 Scrape wounding and restitution of epithelial monolayer

All tissue culture work was carried out in a Herasafe Heraeus Class 2 Biosaefty cabinet supplied by Kendro Laboratory Products PLC . Bishop's Stortford, UK. A549 cells were grown to confluence in 24 well plates (Corning Ltd, Corning, NY) in appropriate growth medium. Once the cells had grown to confluence, a single

wound was made in each well, by scraping off cells with a 1000μl pipette tip. For the purposes of standardization, all wounds were made by the same investigator. A single downward vertical stroke was made in each well to create a wound. The medium was then aspirated, and the cells washed once with PBS. Washing with PBS removed those cells scraped from the plate surface and prevented their re-adherence to the plate. In each experiment a separate 24 well plate was created whereby three scrapes were immediately fixed for 10 minutes with 4% paraformaldehyde in PBS (w/v). These scrapes would serve as the size of the wound at time zero. Pre-equilibrated and prewarmed media was then added to the remaining wells.

Scratch wounds were incubated in 1ml of (i) MEM-α medium, (ii) human fibroblast conditioned medium, (iii) human MSC conditioned medium, or (iv) co-cultured with MSCs.

4.7.3 Neutralisation of growth factors in conditioned medium using monoclonal antibodies

MSC conditioned medium was incubated with specific monoclonal antibodies to inactivate keratinocyte growth factor (KGF), hepatocyte growth factor (HGF) and transforming growth factor – beta1 (TGF-β1) (Abcam, Cambridge, UK) respectively. Antibody concentrations were according to the manufacturers instructions to achieve maximum neutralization in the presence of expected concentrations of growth factors. For KGF this constituted 1μg/ml. For HGF, 1μg/ml, and for TGF-β1 2μg/ml. A549 wounds were exposed to MSC conditioned medium with and without antibodies to each candidate mediator, and the extent of wound closure assessed at 48 hours.

4.7.4 Co-cultures

Co-cultures were carried out with Corning HTS transwell plates (pore size 0.4μm, Corning, NY, USA). In the case of MSC co-cultures, MSCs were seeded at 1 x 10^3 cells/cm^2 in the inserts and maintained in human MSC medium for 3 days prior to co-culture, which allowed the mesenchymal stem cells to reach 70–80% confluence. Mesenchymal stem cell containing inserts were washed and then added to the A549 wells and flooded with fresh serum free medium. Similarly, as controls, human fibroblasts were seeded at 1 x 10^3 cells/cm^2 in a co-culture insert and maintained in MSC medium for 3 days prior to co-culture.

4.7.5 Assessment of pulmonary epithelial wound repair

At 24, 48 or 72 hours, the plates were removed from the incubator, the medium was aspirated, and the cells washed with PBS and fixed for 10 minutes with 4% paraformaldehyde in PBS (w/v). The epithelial monolayers were then stained with hemotoxylin and eosin to delineate the borders of the scrape wounds. Firstly the media from the wells was aspirated off and each well gently washed with PBS 1 ml per well. The cells were then fixed with 4% paraformaldehyde 200μml per well for 20 minutes. The wells were then washed again with 1 ml of PBS before hemotoxylin stain 200μml was added to each well for five minutes. The wells were then washed of excess hemotoxylin using water and acid alcohol 1% 300 μml added to each well. The wells were again washed with water before adding 200μml of eosin to each well for 5 minutes. The wells were again washed of excess eosin before being placed in a 37°C oven to dry.

The extent of epithelial restitution was determined by imaging each plate, following fixation of the monolayer, on a flatbed scanner (Canoscan 3200F, Canon Ireland Ltd), and assessing the area of each wound using edge-finding software (Photoshop v8.0, Adobe Systems Inc, San Jose, California). Briefly, scrape images were cropped to 5mm in length, and the Magic Wand tool, set to a constant tolerance, was used to determine the number of pixels still in the wounded area. The remaining wound area was then compared to the area of the wounds at baseline to determine the extent of wound restitution.

4.8 Data Analysis

All analyses were performed using SigmaStat® 3.5 (Systat Software, Point Richmond, CA). The distribution of all data was tested for normality using the Kolmogorov-Smirnov test. Results are expressed as mean (± SD) for normally distributed data, and as median (interquartile range) where non-normally distributed. Data were analyzed by Students t test, or one-way Analysis of Variance (ANOVA) followed by Student-Newman-Keuls test, or by one-way ANOVA on ranks followed by Dunns test. Underlying model assumptions were deemed appropriate on the basis of suitable residual plots. A two-tailed p value of <0.05 was considered significant.

5.0 Establishing an animal model of repair from Ventilator Induced Lung Injury

5.1 Abstract

Introduction: Ventilator induced lung injury (VILI) is a complication of mechanical ventilation, seen most frequently in patients with Acute Lung Injury (ALI). Most animal models developed to define its pathophysiology have focused on the acute (<24 h) phase of the injury. Here we describe the factors important in the development of a model of recovery from VILI, allowing the study of this type of lung injury over time.

Methods: Two different rodent models of injury were used. The first utilized mechanical ventilation via tracheostomy, with the injury and repair period confined to 10 hours or less. The second delivered injurious mechanical ventilation via endotracheal intubation, allowed the animal to recover and extubate after injury, and assessed the recovery period over a longer period, from 6 hours to 14 days. Factors assessed for their contribution to the development of injury and repair included animal age, peak inspiratory pressure, inspiratory flow rate, the use of supplemental oxygen, and the use of a threshold decrease in respiratory static compliance as opposed to a specific duration of VILI to define extent of injury.

Results: Younger animal age, peak pressures above a threshold value and higher inspiratory flow rates were all factors that resulted in more severe VILI in the rat. Animals injured via tracheostomy did not recover respiratory static compliance or gas exchange over an 8 hour period. However, animals injured via ET intubation, and allowed to recover, displayed significant injury after 6 hours,

and then recovered gradually over a 96 hour period, although structural changes were present in the lung up to this time point. Animals injured to a target of 50% reduction in respiratory static compliance displayed less variability in injury and repair than animals subjected to high stretch injury for a defined time period.

Conclusion: This long term low mortality rat model of repair from VILI will serve to improve our knowledge of the mechanisms of repair as well as provide a useful paradigm for testing strategies to hasten recovery in ALI.

5.2 Introduction

5.2.1 What relevance do animal models have to studying human disease?

Animal models provide a bridge between patients and the laboratory bench. Hypotheses generated in human studies can be tested directly in animal models, and the results of studies in more simple in vitro systems can be tested in animal models to assess their relevance in intact living systems. Mechanistic studies can be performed either by treating normal animals with inhibitors that block key steps in specific pathways or by creating animals with specific gene alterations to test the importance of single gene products or pathways. Without animal models there would be no way to test clinical hypotheses generated in patients using intact biological systems, and there would be no way to validate the importance of fundamental laboratory findings without going directly to human experimentation.

5.2.2 Modelling Acute Lung Injury in animals

Ideally, animal models of Acute Lung Injury (ALI) should reproduce the mechanisms and consequences of ALI in humans, including the physiological and pathological changes that occur. In humans, the definition of ALI is based on the following well-defined set of clinical parameters developed by the American European Consensus Conference [262], namely:

1. Acute onset
2. Radiological evidence of diffuse bilateral pulmonary infiltrates
3. A ratio of the partial pressure of arterial oxygen to the fraction of inspired oxygen (PaO_2/FIO_2) of less than 300

4. No clinical evidence for elevated pulmonary arterial pressure

However, these criteria cannot be directly translated to experimental animals. To simulate human ALI/ARDS, animal models should re-produce the acute injury to the epithelial and endothelial barriers in the lungs and the acute inflammatory response in the air spaces. Ideally, the injury should evolve over time if the animals are supported for prolonged periods.

The main features that characterize ALI in animal models have been identified, and the most relevant methods to assess these features outlined [263]. A series of questionnaires were distributed to a panel of experts in experimental lung injury. The Committee concluded that the main features of experimental ALI include histological evidence of tissue injury, alteration of the alveolar capillary barrier, presence of an inflammatory response, and evidence of physiological dysfunction; they recommended that, to determine if ALI has occurred, at least three of these four main features of ALI should be present. The Committee also identified key ‘‘very relevant’’ and ‘‘somewhat relevant’’ measurements for each of the main features of ALI and recommended the use of at least one ‘‘very relevant’’ measurement and preferably one or two additional separate measurements to determine if a main feature of ALI is present [263]

5.2.3 What are the features of Ventilator Induced Lung Injury in animal models?

Alterations in lung fluid balance, increases in endothelial and epithelial permeability, and severe tissue damage have been seen following mechanical ventilation in animals. The macroscopic and even microscopic damage observed

in VILI [17, 18, 38] is not specific. It closely resembles that observed in other forms of experimental acute lung injury. More importantly, it does not fundamentally differ from the diffuse alveolar damage observed during human acute respiratory distress syndrome. Thus, were VILI to occur in humans, it would be indistinguishable from most of the initial acute offending processes that lead to respiratory failure and the need for ventilator assistance. VILI also causes prominent changes in water and protein permeability as evidenced in isolated rat and mouse lungs by increased wet-to-dry weight ratios and microvascular filtration coefficients [264]. Recruitment of inflammatory cells as assessed by lung MPO assay or BAL neutrophil counts is generally evident [265]. Increased formation and release of cytokines from overventilated lungs has been reported in mouse and rat studies using isolated lung preparations, but may not be present in all models of VILI [7, 55]. Last, but not least, over-ventilation causes a steady decline in arterial oxygen saturation which typically results in severe hypoxemia within several hours [266].

5.3 Aims

5.3.1 To establish a consistent non-fatal stretch induced rodent lung injury

Taking these elements into account, we set about establishing a reproducible animal model of repair from ventilator induced lung injury. Our first task was to induce a severe but survivable stretch lung injury in animals. Such an injury would replicate the known physiologic features of VILI, including deteriorations in oxygenation and respiratory static compliance, alveolar fluid clearance and activation and recruitment of inflammatory cells and mediators. We aimed to

identify the important factors, both ventilator dependent and animal dependent, that determine injury during mechanical ventilation.

5.3.2 To develop a model of injury and repair from VILI over a 10 hour period

Having identified the factors important in the development of VILI in the rat, we then focused on establishing a repair phase after injury. We used direct physiologic measurements of recovery, such as oxygenation and compliance, as surrogate measures of repair of a damaged alveolar-capillary barrier. We postulated that after a return to protective lung ventilation after a period of injurious ventilation, physiologic recovery would occur over a period of hours, reflecting repair of the ventilator injured lung.

5.3.3 To develop a severe but recoverable VILI animal model

We then set about creating a model whereby animals could recover without the added injurious stimulus of low tidal volume mechanical ventilation. We postulated that a longer time period, and the removal of any injurious mechanical ventilatory stimulus, would expedite recovery.

5.3.4 To determine model reproducibility with a fixed duration of high lung stretch

Animal studies are fraught with high variability in the results, and this is true even under strictly controlled conditions and when all the animals are genetically identical [263]. We sought to quantify the degree of variability in

injury and recovery when injurious ventilation was applied for a pre-determined amount of time.

5.3.5 To determine model reproducibility with injury to a fixed severity of lung compliance decrement

Some physiological measures such as oxygenation are invasive, and the repeated sampling required to assess degree of injury may interfere with our recovery model. Respiratory static compliance represents the best available measure of lung injury. Changes in compliance represent the accumulation of pulmonary oedema as a result of damage to the alveolar-capillary membrane, as well as the influx of inflammatory cells into the alveolar space. These changes make the lung more difficult to expand and result in a decrease in compliance. Thus, compliance should represent the degree of injury in rats, and could be used to homogenize the injury among animals with different apparent susceptibility.

5.4 Methods

5.4.1 VILI via tracheostomy model

Animals were anaesthetized as described in Methods and Materials Section 4.2. A tracheostomy was inserted, and thereafter the carotid artery was canulated. The animals were ventilated for 20 minutes with settings RR 80 bpm, tidal volume 6ml/kg, PEEP 2.5 cmH_2O, FIO_2 0.3 as described in Section 4.2.2. After baseline ventilation, arterial blood gas sample analysis was performed and respiratory static compliance was assessed. Once these parameters met baseline criteria (see methods), injurious ventilation was commenced.

We used a variety of different injury settings in order to develop a significant lung injury using the criteria that has now been established [263]. We varied peak inspiratory pressure, respiratory rate, inspiratory flow rate, addition or not of supplemental oxygen and duration of injurious ventilation. The factors that were deemed important in the development of VILI in these animals are outlined below.

5.4.2 VILI via orotracheal intubation model

As described in Section 4.3, animals were anaesthetized with isoflurane and intravenous access was obtained. Laryngoscopy was performed and animals were orotracheally intubated with a size 14G catheter. Animals underwent baseline ventilation for 20 minutes. Injurious ventilation was commenced for 1-3 hours, using different settings. Anaesthesia was maintained using intravenous Saffan, and muscle relaxation was achieved with cis-atracurium. After the designated amount (time period or compliance decrement) of injurious

ventilation, animals were allowed to awaken and recover. Baseline ventilation was continued until there was adequate spontaneous respiratory effort. Once the animals were fully awake, they were extubated and returned to their cages. After a period of recovery, animals were once more anaesthetized, intravenous access was obtained and a tracheostomy and carotid arterial canula were inserted. Animals were ventilated for a 20 minute period with FIO_2 0.3 and for 15 minutes with FIO_2 1.0. Respiratory system static compliance and arterial blood gas measurements were obtained. Thereafter the animals were exsanguinated under deep anaesthesia, the heart lung block was dissected from the thorax, and wet:dry measurements and BAL collection were performed to assess inflammatory cell infiltration (as described in methods section).

5.4.3 Series (i): Examination of factors contributing to injury severity in rats during mechanical ventilation

5.4.3.1 Series (i-a) Effect of animal age

Young rats (4-6 weeks) were ventilated at the same injurious settings as older rats (12-16 weeks), with Pinsp=25cmH_2O, RR=15, FIO_2=0.3, Inspiratory flow=0.5L/min, over a period of 2 hours.

5.4.3.2 Series (i-b) Variation in tidal volumes

In these studies we employed continuous flow, time-cycled, pressure-control ventilation (PCV). We measured the tidal volumes produced at baseline and at the onset of injurious ventilation, and looked at how these volumes changed over time as injury developed, using settings Pinsp=25cmH_2O, RR=15, FIO_2=0.3,

inspiratory flow=0.5L/min, over a period of 2 hours, in animals ventilated via trachestomy. Volumes were measured with both a paediatric volumeter (Draeger, Germany) and through displacement of water from a filled bottle with an escape tube.

5.4.3.3 Series (i-c) Effect of inspiratory flow/ rate of rise on development of VILI

Using ventilator settings Pinsp=25cmH_2O, RR=15, FIO_2=0.3, we investigated the effects of two different flow rates, 0.5L/min versus 0.6L/min, on the development of VILI in animals via tracheostomy.

5.4.3.4 Series (i-d) Determination of the importance of peak pressure settings in development of VILI

We subjected both animals who had tracheostomy and carotid arterial canulation and orotracheally intubated animals alone to different levels of peak pressures with the same respiratory rate in order to develop a significant, reproducible but survivable injury. Animals were subjected to peak pressures of 25, 27.5, 30 and 35 cmH_2O, for up to 4 hours of mechanical ventilation.

5.4.3.5 Series (i-e) Investigation of the importance of respiratory rate in VILI development

We subjected animals to different respiratory rates with the same peak pressure in order to develop a significant, reproducible but non-fatal injury. Animals were subjected to respiratory rates of 15, 18 and 20 breaths per minute, for up to 4 hours of mechanical ventilation.

5.4.3.6 Series (i-f): The importance of duration of injurious ventilation in modeling repair from VILI

We looked at different durations of injurious mechanical ventilation in animals via tracheostomy, including 1 hour, 1.5 hours, 2 hours, 3 hours and 4 hours, using the settings Pinsp=25cmH_2O, RR=15, FIO_2=0.3, Inspiratory flow=0.5L/min.

5.4.3.7 Series (i-g) Effect of supplemental oxygen in development of VILI

We subjected animals to injurious mechanical ventilation, with FIO_2 = 0.21 or 0.3, using the settings Pinsp=25cmH_2O, RR=15, inspiratory flow=0.5L/min.

5.4.4 Series (ii): Developing a model of injury and repair from VILI over a 10 hour period

As described in Section 4.2, animals were anaesthetized, venous access was obtained, and a tracheostomy was inserted. A carotid arterial canula was inserted. After a period of baseline ventilation, injurious ventilation was commenced, for a period of 60-120 minutes. Respiratory static compliance measurements and blood gas analysis were performed at regular intervals. Thereafter, animals were ventilated with baseline protective lung ventilation settings for various time periods from 4-8 hours, to identify whether physiologic recovery was evident.

5.4.5 Series (iii): To induce a severe but recoverable VILI in animals via oro-tracheal intubation

This series aimed to put together the insights gained in prior experiments to develop a model where the animals stustianed a severe, but non-fatal, lung

injury, from which they could recover. Animals were anesthetized as described in Section 4.2, and subjected to injurious ventilation for 1, 2 and 3 hours. Animals underwent mechanical ventilation with a variety of peak pressures from 25cmH_2O up to 40cmH_2O. Respiratory rate (18 bpm), inspiratory flow rate (0.5L/min) and FIO_2 (0.3) were kept constant. After the designated period of injurious ventilation, animals were allowed to awaken and recover. Baseline ventilation was continued until there was adequate spontaneous respiratory effort. Once the animals were fully awake, they were extubated and returned to their cages. Recovery was assessed at 24 hours post injury.

5.4.6 Series (iv): Use of lung compliance as endpoint to titrate severity of VILI

Animals were anaesthetized, oro-tracheally intubated and subject to injurious mechanical ventilation until respiratory static compliance decreased by 50%. They were then recovered and extubated. Recovery was assessed over different time periods, at 6, 24, 48 and 96 hours. At these time intervals post injury, animals were anaesthetized, a tracheostomy and carotid arterial canula was inserted, and respiratory static compliance, blood gases, inflammatory cell infiltration and wet:dry ratio were assessed.

5.5 Results

5.5.1 Series (i-a): Young rats had more severe injury than older rats

Despite identical ventilation settings, younger (4 week old) animals had worsened oxygenation and respiratory static compliance after 2 hours of VILI, in comparison to older (12 week) animals **(Figure 5-1)**. Wet:dry ratios, and inflammatory cell infiltration were also worse in this group **(Figure 5-1)**.

5.5.2 Series (i-b): Tidal volumes declined over time during pressure controlled injurious ventilation

Baseline tidal volumes in a 400g rat were 3.125 mls per breath. At a Pinsp of 30cmH_2O the tidal volume rose to 16mls, (40mls per kg in a 400g rat). After 1 hour of ventilation this tidal volume had decreased to 14mls (30mls/kg), and after 2 hours of ventilation tidal volumes had fallen to 10mls (25mls/kg).

5.5.3 Series (i-c): Higher inspiratory flow rates caused more severe VILI

Increasing the inspiratory flow rate from 500ml/min to 600ml/min, without changing the other ventilation settings, reduced the time to development of lung injury. After 2 hours of injurious ventilation, animals ventilated with the higher inspiratory flow rate had worsened respiratory static compliance and oxygenation in comparison to the lower flow rate group **(Figure 5-2)**.

5.5.4 Series (i-d): Peak pressure is an important determinant of VILI, although there may be a VILI threshold

Oro-tracheal intubated animals subjected to peak pressures of 25, 27.5 and 30 cmH_2O did not develop measurable injury after 90 minutes of VILI, and did not have detectable injury after up to 4 hours of mechanical ventilation. However, animals subjected to peak pressures of $35cmH_2O$ developed significant and measurable injury after 90 minutes **(Figure 5-3)**.

Animals that underwent tracheostomy and carotid arterial canulation differed in their susceptibility to VILI. Peak pressures used to injure animals that were oro-tracheally intubated resulted in rapid development of pulmonary oedema and cardiovascular compromise and collapse in these animals. Animals ventilated at peak pressure of 30 and $35cmH_2O$ did not survive 1 hour of this injurious ventilation. However, similar to the orotracheal group, a threshold was present, and animals ventilated with peak pressure of $20cmH_2O$ did not develop measurable injury at 90 minutes **(Figure 5-4)**. Animals ventilated between these two extremes developed measureable injury after 90 minutes.

5.5.5 Series (i-e) Respiratory rate does not appear to affect the development of VILI

Alterations in respiratory rate between 15-20 breaths per minute did not demonstrably alter the injury for a given inspiratory pressure.

5.5.6 Series (i-f) Injurious ventilation produced a step-wise deterioration in respiratory static compliance over time

Animals ventilated via tracheostomy developed a step-wise decrement in respitatory compliance at a P_{insp} of 25cm H_2O. In contrast, animals ventilated with lower inspiratory pressure of 20cm H_2O did not develop measurable injury, even over several hours **(Figure 5-4).**

5.5.7 Series (i-g) Supplemental Oxygen (FiO_2 0.3) appears to reduce the severity of VILI

Animals ventilated with room air demonstrated more severe injury than animals ventilated with the same settings using supplemental oxygen. The addition of supplemental oxygen allowed the animals to tolerate a longer time period of high stretch ventilation. Thus, although animals subject to excess lung stretch using FIO_2 0.21 developed gas exchange abnormalities faster than those using FIO_2 0.3, this was not accompanied by a significant inflammatory cell infiltrate. Animals who underwent high lung stretch ventilation without the addition of supplemental oxygen experienced critical deteriorations in oxygenation after less than an hour of ventilation. This was likely an insufficient time period at injurious ventilation to develop an inflammatory response. The addition of supplemental oxygen allowed a longer period of injurious mechanical ventilation and the development of a significant inflammatory response **(Figure 5-5)**.

Compliance was also worse in the animals that were ventilated with room air **(Figure 5-5).**

5.5.8 Series (ii): VILI induced lung injury severity continues to worsen even with lung protective ventilation

Gas exchange abnormalities, and worsening of respiratory static compliance were evident after a period of injurious ventilation, as was evident in our previous pilot studies **(Figure 5-6)**. After commencement of protective lung ventilation, gas exchange was improved after 1 hour. This likely reflects the addition of PEEP and lung recruitment, and is unlikely to represent repair to the injured lung in the form of re-absorption of oedema fluid or reconstitution of damaged alveolar units. Moreover, respiratory static compliance continued to deteriorate over the next 4-8 hours, showing no significant improvement over this time period. This likely reflects a worsening of pulmonary oedema and an accumulation of inflammatory cells after the injurious stimulus has been removed. Obvious physiological recovery reflecting lung repair did not occur.

5.5.9 Series (iii): VILI can be induced in animals via an oro-tracheal tube, facilitating animal recoverey

Animals underwent mechanical ventilation with a variety of peak pressures from 25cmH_2O up to 40cmH_2O. Changes in respiratory static compliance were not evident after 3 hours of ventilation with peak pressures up to and including

30cmH_2O **(Figure 5-3A)**. Wet:Dry ratios, oxygenation and compliance were within normal range after 24 hours

However, ventilation with peak pressures of 35cmH_2O resulted in significant changes in compliance after 90 minutes of injury **(Figure 5-3A)**. Animals could be extubated after a short period of recovery at baseline ventilation. Recovery assessment after 24 hours revealed significant gas exchange abnormalities, ongoing alveolar-capillary barrier dysfunction as assessed by wet: dry ratio and significant inflammatory cell recruitment **(Figure 5-7)**. Ventilation with peak pressure of 40cmH_2O resulted in injury after only 20 minutes of ventilation. We deemed this unsuitable due to the likely non-inflammatory nature of the injury in such a short time frame.

Using time as a marker of degree of injury during high stretch mechanical ventilation, the variability among animals in terms of injury was very wide **(Figure 5-7)**. This variability is borne out by the fact that some animals had completely normal physiologic parameters after 24 hours, while other animals remained severely injured, and 2 died after injury.

5.5.10 Series (iv-a): Respiratory static compliance is a reliable measure of degree of lung injury

Animals were injured to the same degree, despite the fact that the time to achieve injury, as measured by respiratory static compliance, was different in each animal. The variability in measures of injury and repair at harvest was less than that when animals were injured for defined time intervals **(Figure 5-8)**. There was no mortality in the "injury to compliance target" group, while two animals died in the VILI for 90 minutes group.

5.5.11 Series (iv-b) VILI injured animals progressively improve lung function following resumption of spontaneous ventilation

High stretch ventilation caused a severe injury as evidenced by worsening of physiologic indices of lung function. Physiologic indices demonstrated maximal injury at 6 hours following VILI, while lung function had largely returned to normal by 96 hours. Arterial oxygen tension decreased significantly following VILI, compared to sham animals (**Figure 5-8**). Arterial PO_2 was lowest at 6 hours post injury, remained low at 24 and 48 hours post VILI, and then progressively returned to baseline levels. The arterial oxygen tension had recovered to levels seen in uninjured animals by 96 hours post VILI. The alveolar-arterial oxygen gradient followed a similar pattern, with complete recovery demonstrable at 96 hours following VILI (**Table 6-1)**.

Static lung compliance decreased significantly following VILI, with the maximal decrement evident at 6 hours (**Figure 5-8**). Static compliance had improved by 24 hours, but did not return to normal until 14 days post VILI. BAL protein concentrations (**Figure 5-8**), and lung wet: dry weight ratios (**Figure 5-8**) were maximally increased at 6 hours, remained abnormal at 24 hours, and then decreased progressively.

5.6 Discussion

Defining the factors that are important in the development of VILI is integral to developing a reliable, reproducible animal model that represents the disease. Moreover, the ability to develop a cohort of animals with an homogenous injury, that is representative of stretch induced lung damage, enables us to test innovative therapies in rats that can be translated into better therapies for human diseases.

5.6.1 Justification for use of the Sprague Dawley rat

We choose to use adult male Sprague Dawley rats for this model. We did this for a number of reasons. First, our laboratory has extensive experience with this species of animal in diverse ALI models [252, 267, 268]. Second, animal size is an important consideration in selecting animal models of ALI. This is especially true when physiological parameters such as arterial oxygen tension and mean arterial pressure are monitored [269]. Rats are large enough to allow arterial canula placement and venous access readily. Body size makes the measurement of physiological parameters in mice difficult. Measurement of respiratory static compliance can be accomplished easily in the rat. We chose to model VILI in the rat to enable us to test ongoing physiologic injury and recovery readily. Size is also an important consideration for the collection of blood. It is easier to obtain sufficient quantities of blood or to obtain multiple blood samples in larger species such as the rat, rabbit or nonhuman primates. The ability to obtain multiple blood samples is important when the study design requires monitoring of physiological parameters, such as blood gases, plasma cytokines, and

leukocyte counts over time. A severe lung injury is survivable in these animals, thus allowing us to assess what happens in the recovery phase. Housing and feed costs are minimal in rats. Also, ethical considerations would limit larger animal numbers. Chemical assay availability is limited in other animal species. Problems relating to the use of rats to model VILI include the precipitous development of pulmonary oedema, which can compromse cardio-respiratory function, and is not representative of what occurs in larger animals and humans.

5.6.2 VILI in different animal species

A number of different animal species have been used to study lung injury, yet there are important and sometimes major differences among animal species in responses to injury, particularly injury in response to microbial products. There are significant differences between the pathologic appearance of the lungs of small animals, such as rats, [15-17] and those of larger ones [270] at the early stage of VILI. These differences are probably related to the differing durations of the challenge. Oedema develops so rapidly (a few minutes) in small animals in these studies that there is not enough time for the development of noticeable inflammation and neutrophil infiltration of lung tissue. In contrast, the several hours necessary to produce patent edema in larger animals is sufficient for activation, adherence, and significant migration of neutrophils into airspaces [270].

There are many other examples of the slower appearance of VILI in intact large animals. Carlton and coworkers [37] found an increase in the extravascular lung water to dry lung weight ratio of only 19% in intact lambs ventilated with 58 cm H_2O peak inspiratory pressure for 6 h. Microscopic examination was either

normal or showed only mild perivascular edema, but no alveolar edema. Alveolar flooding occurred in sheep, but after 18 h of ventilation with a peak inspiratory pressure of 50 cm H_2O [271]. Whereas ventilation may produce severe edema in small animals in less than 1 h, ventilation for 24 h or more with similarly high airway pressures is necessary in larger animals.

Thus, in our studies, a balance was struck between developing a significant injury, but doing this over a time frame sufficient to generate an inflammatory response

5.6.3 Justification for use of a single injury model

No single animal model reproduces all of the characteristics of ALI/ARDS in humans, and most of the existing animal models are relevant for only limited aspects of human ALI/ ARDS [272]. Nevertheless, if the characteristics of an animal model are well understood, and the results are interpreted within the limits of the specific model, animal studies can provide focused tests of key elements of the lung injury response in humans

5.6.4 Age of animal species in modeling repair from ALI

We found animal age to be a confounding factor, in that animals behaved somewhat the opposite of what one would expect, taking longer to injure with age. Age is associated with compromised physiologic and immunologic function [273]. Age dependent changes in respiratory and cardiovascular reserve are well documented [274, 275]. The age-dependent deterioration of the immune system results in increased susceptibility to viral and bacterial infections, opportunistic

infections, reactivation of latent viruses, decreased responses to vaccination, autoimmune diseases, and neoplasias in humans and animals [276]. In addition, there is an age-dependent systemic inflammatory state in humans and animals even in the absence of disease [277]. The lungs of aged individuals also exhibit an elevated basal inflammatory state [278], which is primed to respond in an overexuberant manner following an infection or injury. Regardless of whether local (organ specific) or systemic, the elevated inflammatory state is characterized by elevated basal levels of the proinflammatory mediators IL-6, IL-8, IL-1, and TNF-α [279]. Additionally, after caecal ligation and puncture or injection of lipopolysaccharide (LPS), lungs obtained from aged mice have a greater elevation in IL-6 than young mice given the same challenges [279]. These studies indicate that advanced age is associated with elevated baseline levels of pro-inflammatory cytokines in the lung before injury and enhanced production of these factors after injury in the lung and at other sites.

Thus, it could be assumed that young rats would be less susceptible to VILI than older rats. However, this was not the case as illustrated in **Figure 5-1.** Young rats (4-8 weeks) injured earlier than older rats for a given peak pressure.

This apparent anomaly can be explained by respiratory mechanics and the pivotal role of lung distention in VILI. The lung and chest wall compliance of younger animals is larger, thus allowing greater distention for the same peak airway pressure. This has been previously observed by Adkins and colleagues [36], who observed that the lung capillary filtration coefficient increased more in young rabbits than in adult ones after 30 to 55 cm H_2O peak pressure ventilation, probably because of greater lung stretch for the same peak airway pressure in younger compliant lungs and chest wall.

5.6.5 Ventilator settings in VILI: Pressure Control Ventilation vs Volume Control Ventilation

In these studies we have employed continuous flow, time-cycled, pressure-control ventilation (PCV). In this mode, the assistance provided by the ventilator is controlled in two ways. The magnitude of each inflation is determined by the change in airway pressure, i.e. the difference between PIP and the baseline or positive end-expiratory pressure (PEEP). The VT for any breath depends on both this pressure difference, which drives gas movement, and the lung compliance. Thus, VT is indirectly determined when the PIP and PEEP are set. VT is not consistent when compliance changes. Thus, as compliance deteriorates during VILI, VT is reduced. We found this to be an important factor in our model in prior studies. The precipitious development of pulmonary oedema that is a feature of VILI in small animals as mentioned above, can lead to cardio-respiratory compromise rapidly. However, gradually lessening the injurious stimulus as lung damage progresses prevents a rapid deterioration and allows the development of an inflammatory response over time that may be more representative of VILI in humans.

5.6.6 The importance of inspiratory flow/ rate of rise in producing VILI

Besides the lung distention that occurs during mechanical ventilation, the rate at which lung volume increased was also an important determinant of injury in our model. Increasing the flow rate from 500ml/min to 600ml/min reduced the time to development of lung injury **(See Figure 5-2)**. This phenomenon has also been observed in rabbits. Peevy and coworkers [280] determined the capillary

filtration coefficient in isolated perfused rabbit lungs ventilated with various tidal volumes and inspiratory flow rates. They found that, for the same peak airway pressure of 53 cm H_2O small tidal volume ventilation (9 to 12 ml/kg BW) with a high flow rate (8.3 L/min) increased the filtration coefficient to the same extent (about 6 times baseline value) as ventilation with a markedly higher VT (25 to 35 ml/kg) but a low inspiratory flow rate (1.9 L/min).

5.6.7 The importance of peak pressure settings as a threshold for development of VILI

There is no well-defined pressure or volume above which manifestations of VILI, such as pulmonary oedema, begin to occur as the lung is over-expanded. The presence of an airway pressure threshold is, however, suggested by some of our initial studies. We subjected orotracheally intubated animals to different levels of peak pressures with the same respiratory rate in order to develop a significant, reproducible but non-fatal injury. Animals subjected to peak pressures of 25, 27.5 and 30 cmH_2O did not develop measurable injury after up to 3 hours of mechanical ventilation **(Figure 5-3)**. However, animals subjected peak pressures of 35cmH_2O developed significant and measurable injury after 90 minutes.

Animals that underwent tracheostomy and carotid arterial canulation differed in their susceptibility to VILI. Peak pressures used to injure animals that were orotracheally intubated resulted in rapid development of pulmonary oedema and cardiovascular compromise and collapse in tracheostimized animals. There may be a number of explanations for this. Animals subjected to surgical dissection develop more severe lung injury for a given pulmonary insult versus animals intact before injury. Ventilation via a surgical tracheostomy may result

in less leak during pressure control ventilation, and higher rate of rise of peak pressure.

These findings are corroborated in studies on isolated lungs by Parker and colleagues [28] and by the work by Carlton and coworkers [37] in intact animals. Carlton and coworkers produced graded increases in VT in lambs and studied their effect on lymph flow and protein concentration. Peak inspiratory pressure (and therefore VT) was increased in three successive steps (each of 4 h) from baseline (16 cm H_2O) to 61 cm H_2O. There was no change in lymph flow or protein composition during the first two steps (33 and 43 cm H_2O peak inspiratory pressure).

Nevertheless, pulmonary edema has been regularly produced with airway pressure levels lower than those used in this study. A peak inspiratory pressure of only 30 cm H_2O was enough in another study using rats [15]. Similarly, intact rats developed moderate pulmonary edema after 1 h of mechanical ventilation with a VT of 20 ml/kg BW [281]. Consistent with the absence of a well-delimited pressure or volume threshold, Tsuno and coworkers [20] found that ventilating sheep with a peak inspiratory pressure of 30 cm H2O for more than 40 h invariably resulted in increased wet lung weight and gross pathologic alterations. Finally, stable (2 h) isolated perfused rat lung preparations could not be obtained when peak airway pressure was above 13 cm H_2O [30] (a pressure level which nevertheless resulted in a greater inflation than in closed-chest animals).

5.6.8 Positive End Expiratory Pressure

While the degree of stretch to which animals are subject is central to the pathogenesis of VILI, it also appears likely that unstable lung units in ARDS may be damaged by repeated opening and closing during tidal ventilation. PEEP may prevent diffuse alveolar damage in experimental models during prolonged ventilation at high lung volumes by stabilizing distal units [17]. Thus, in order to maximize the injury and so that the model would be as representative as possible of what is happening in unstable lung units, we decided to utilize zero PEEP during the injurious ventilation phase.

5.6.9 Duration of injurious ventilation required to produce injury

As mentioned above, smaller animal species are more prone toward developing VILI. For this reason, and also for reasons of practicality, it is difficult to examine separately the effects of a given regimen of pressure and volume during mechanical ventilation and those of time. Changes in respiratory static compliance occurred within 60-90 minutes in most of our protocols using rats ventilated via tracheostomy. This was desirable in order to allow a sufficient time for recovery in these animals. Longer time periods using lower peak pressures may have resulted in equal injuries. However, our experience in animals ventilated and injured via oro-tracheal intubation is that a threshold may exist below which even hours of high peak pressure ventilation may not produce lung injury in small animals **(Figure 5-3 and 5-4)**.

5.6.10 VILI induced lung injury does not resolve despite "protective ventilation"

Gas exchange abnormalities, and worsening of respiratory static compliance were evident after a period of injurious ventilation, as was evident in our previous pilot studies **(Figure 5-6)**. After commencement of protective lung ventilation, gas exchange was improved after 1 hour. This likely reflects the addition of PEEP and lung recruitment, and is unlikely to represent repair to the injured lung in the form of re-absorption of oedema fluid or reconstitution of damaged alveolar units. Moreover, respiratory static compliance deteriorated over the next 4-8 hours, showing no significant improvement over this time period. This likely reflects a worsening of pulmonary oedema and an accumulation of inflammatory cells after the injurious stimulus has been removed.

Obvious physiological recovery reflecting lung repair did not occur. We may assume this was so for two reasons. Firstly, injury and recovery are not mutually exclusive processes, and both can occur at the same time, injury and repair ongoing side by side [282]. Physiological recovery or dysfunction reflects the balance between the two processes at any one time. Measurable recovery after severe lung injury evidently requires a longer time period than even up to 10 hours. Secondly, recovery requires the removal of the injurious stimulus. It is apparent that even low-tidal volume ventilation can cause activation of inflammatory pathways [283]. Furthermore, ventilation in the setting of severe lung injury can result in a synergistic injurious effect, as when combined with bacterial induced lung injury [284]. The same may be true of even low tidal volume ventilation in the setting of VILI. Rather than facilitate repair, low tidal volume mechanical ventilation after induction of a stretch induced injury may

encourage an ongoing inflammatory response and inhibit restoration of physiologic function.

5.6.11 Using compliance as a measure of degree of injury

We sought a more reliable injury severity parameter, in order to decrease the marked variability seen with fixed time ventilation protocols. Other physiological measures such as oxygenation are invasive, and the repeated sampling required to assess degree of injury may have interfered with our recovery model. Respiratory static compliance represented the best available measure of lung injury. Changes in compliance represent the accumulation of pulmonary oedema as a result of damage to the alveolar-capillary membrane, as well as the influx of inflammatory cells into the alveolar space. These changes make the lung more difficult to expand and result in a decrease in compliance. Thus, compliance should represent the degree of injury in rats, and could be used to homogenize the injury among animals with different apparent susceptibility.

Animals were injured to the same degree, despite the fact that the time to achieve injury, as measured by respiratory static compliance, was different in each animal **(Table 6-1)**. The variability in measures of injury and repair at harvest was less than that when animals were injured for defined time intervals **(Figure 5-8)**. However, some variability remained.

This variability may be explained by differences in the ability to repair injured lung among individual animals. We did not detect differences in respiratory system static compliance at baseline, thus the degree of lung expansion and stretch would have been similar in each rat. Despite this, the time to achieve injury differed substantially among animals. Similarly, the ability to remove

pulmonary oedema fluid, and repair a damaged alveolar-capillary barrier likely differed in each individual animal, despite similar age, weight, genetic background etc. However, these differences were minimized by our VILI model.

5.6.12 Summary and conclusions

In conclusion, studies in animal models are essential to our understanding of the pathophysiology of ALI and the development of novel therapeutic strategies for human ALI/ARDS. VILI remains a clinically relevant phenomenon, which can cause further lung and end organ damage in ALI. Modeling the recovery phase from VILI in the rat requires an understanding of the factors that contribute to the initial injury in this animal, in order to develop a reproducible, significant and survivable injury. The model we have created allows us to study the repair phase from injury, and also to develop strategies to enhance this repair phase.

5.7 Figures

Figure 5-1 Younger rats are more susceptible to injury

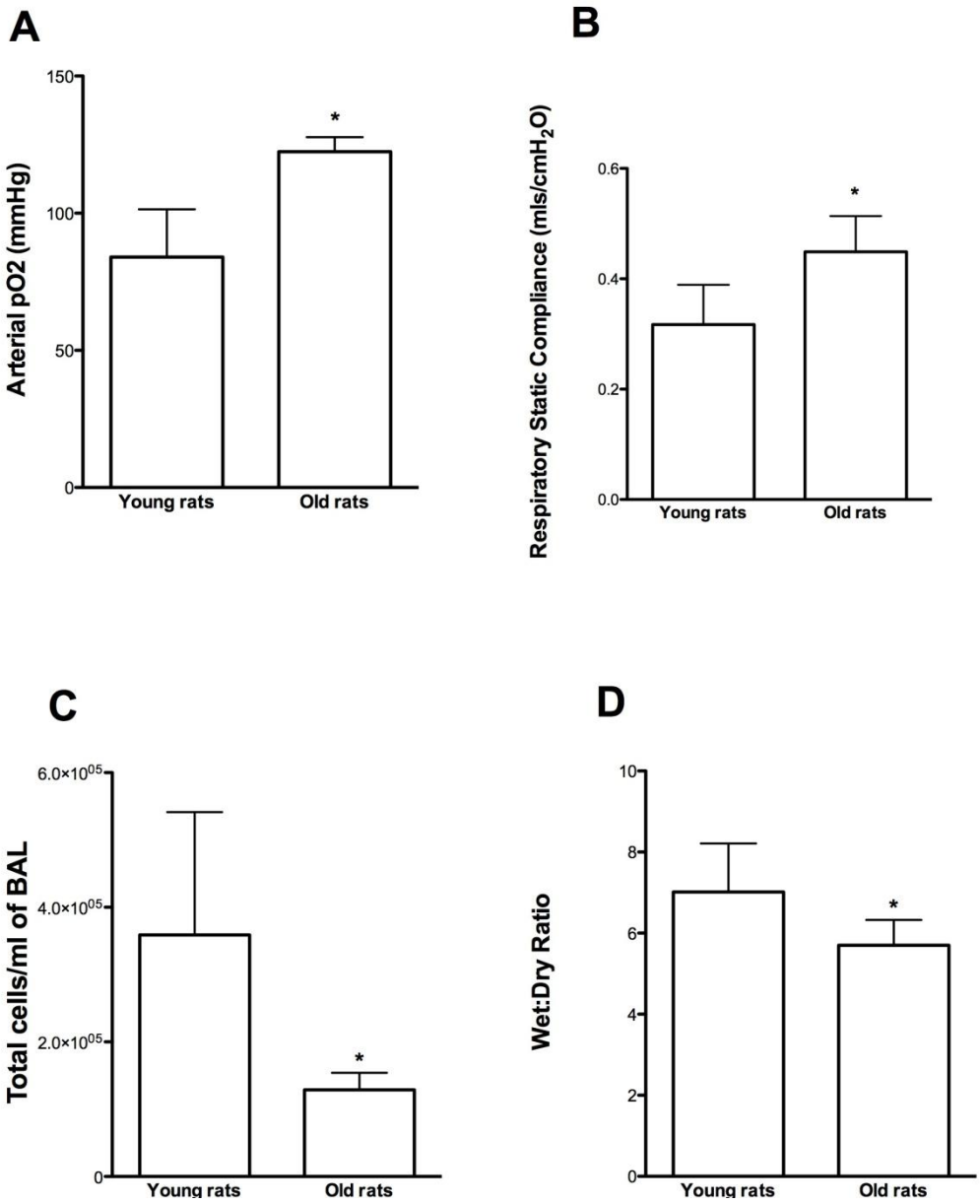

Panel A: Histogram representing arterial oxygen partial pressures of young (4 weeks) versus old (12 weeks) rats measured at an FiO2 of 0.3 after 2 hours of VILI

Panel B: Histogram representing static lung compliance of young (4 weeks) versus old (12 weeks) rats measured after 2 hours of VILI

Panel C: Histogram representing total inflammatory cells in BAL of young (4 weeks) versus old (12 weeks) rats measured after 2 hours of VILI

Panel D: Histogram representing wet:dry weight ratios of young (4 weeks) versus old (12 weeks) rats measured after 2 hours of VILI

Abbreviations: BAL, bronchoalveolar lavage * Significantly different ($P<0.05$, Students t test)

Figure 5-2 Higher inspiratory flow rates result in worse injury

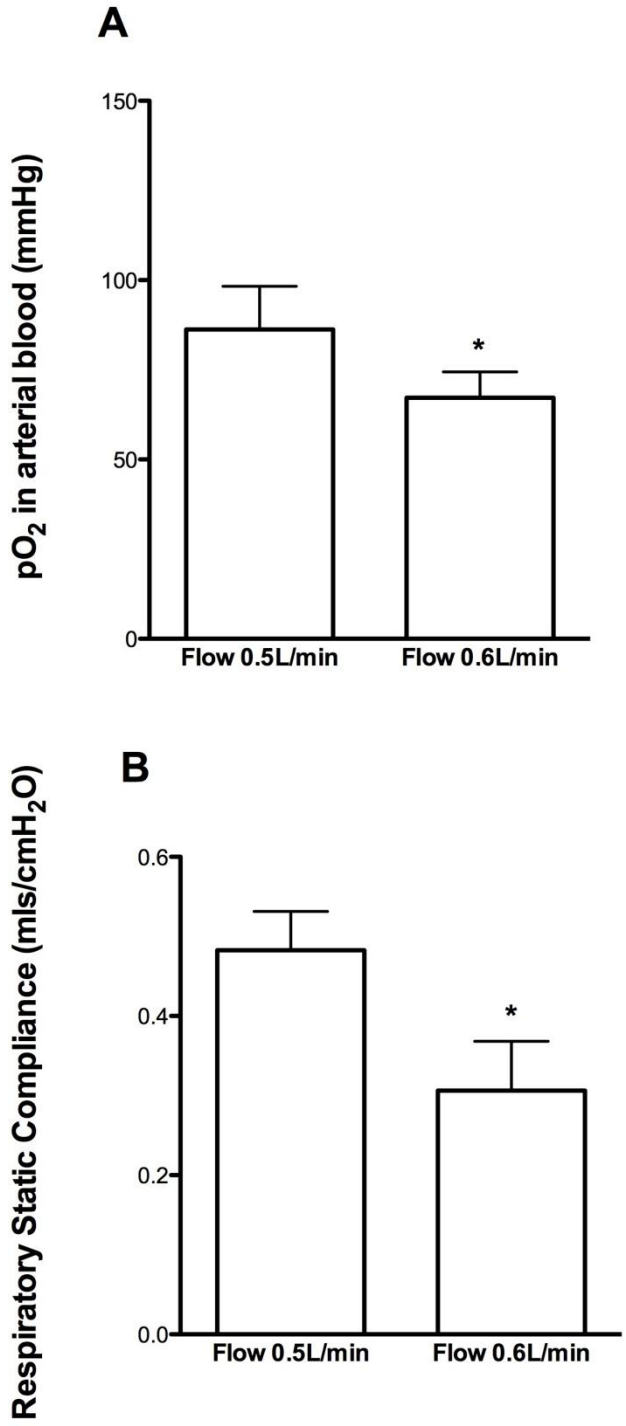

***Panel A*:** Histogram representing arterial oxygen partial pressures of rats after 2 hours of VILI using inspiratory flow rates of either 500ml/min or 600ml/min, measured at an FiO_2 0.3

Panel B: Histogram representing static lung compliance of rats after 2 hours of VILI using inspiratory flow rates of either 500ml/min or 600ml/min.

* Significantly different ($P<0.05$, Students t test)

Figure 5-3 There is a peak pressure threshold for injury

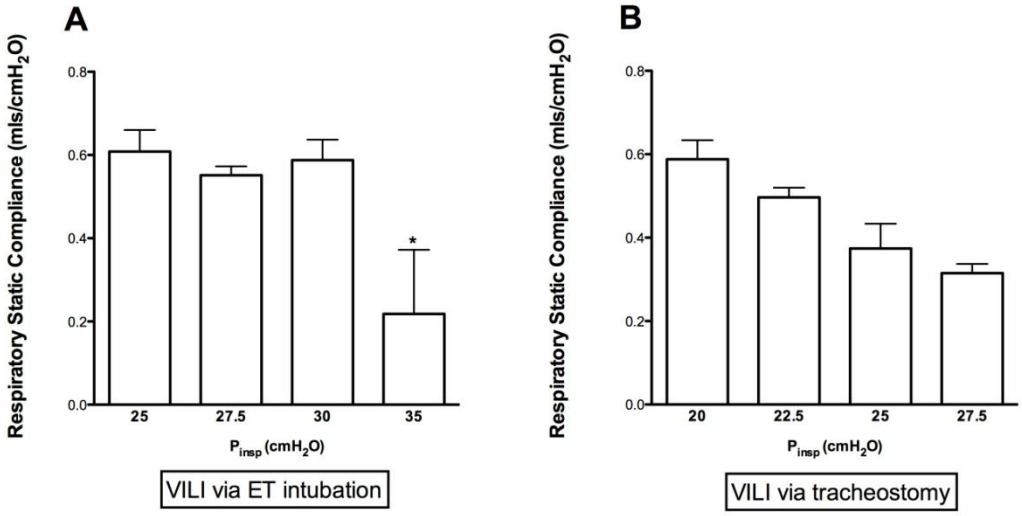

***Panel A*:** Histogram representing static lung compliance of rats after 90 minutes of VILI via orotracheal intubation using peak inspiratory pressures of either 25, 27.5, 30 or 35 cmH_2O.
***Panel B*:** Histogram representing static lung compliance of rats after 90 minutes of VILI via tracheostomy using peak inspiratory pressures of either 20, 22.5, 25 or 37.5 cmH_2O.
* Significantly different ($P<0.05$, ANOVA and Student-Neuman-Keuls) (N=3-4/group)

Figure 5-4 There is a peak inspiratory pressure threshold for injury

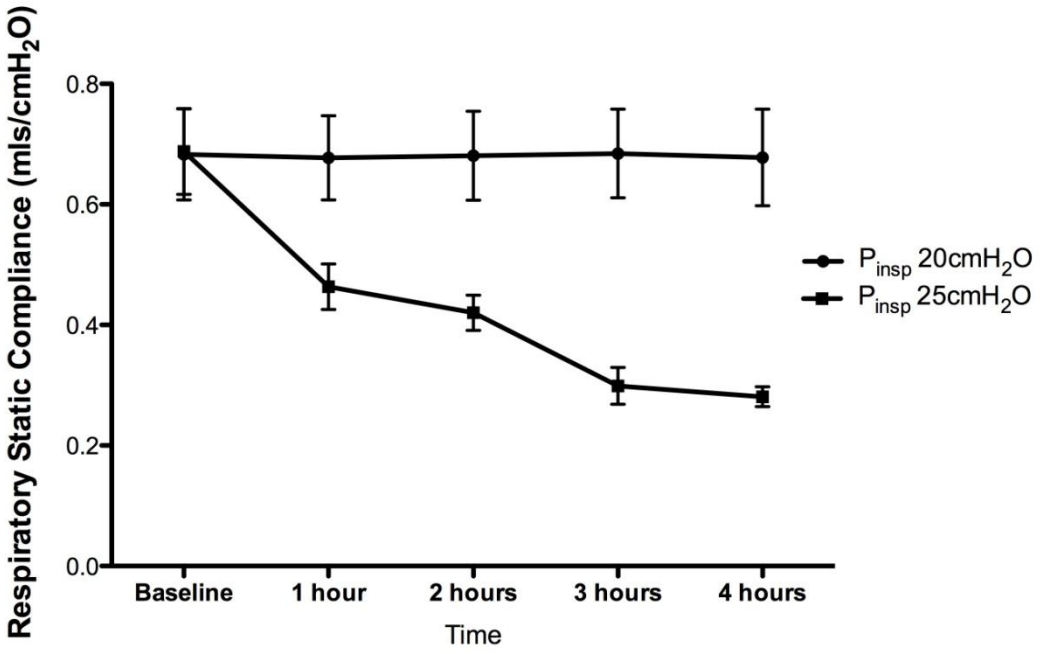

Figure 5-4: Line graph representing static lung compliance of rats during 4 hours of VILI via tracheostomy using peak inspiratory pressures of either 20 or 25 cmH_2O. **(N=4/group)**

Figure 5-5 VILI is worsened in room air

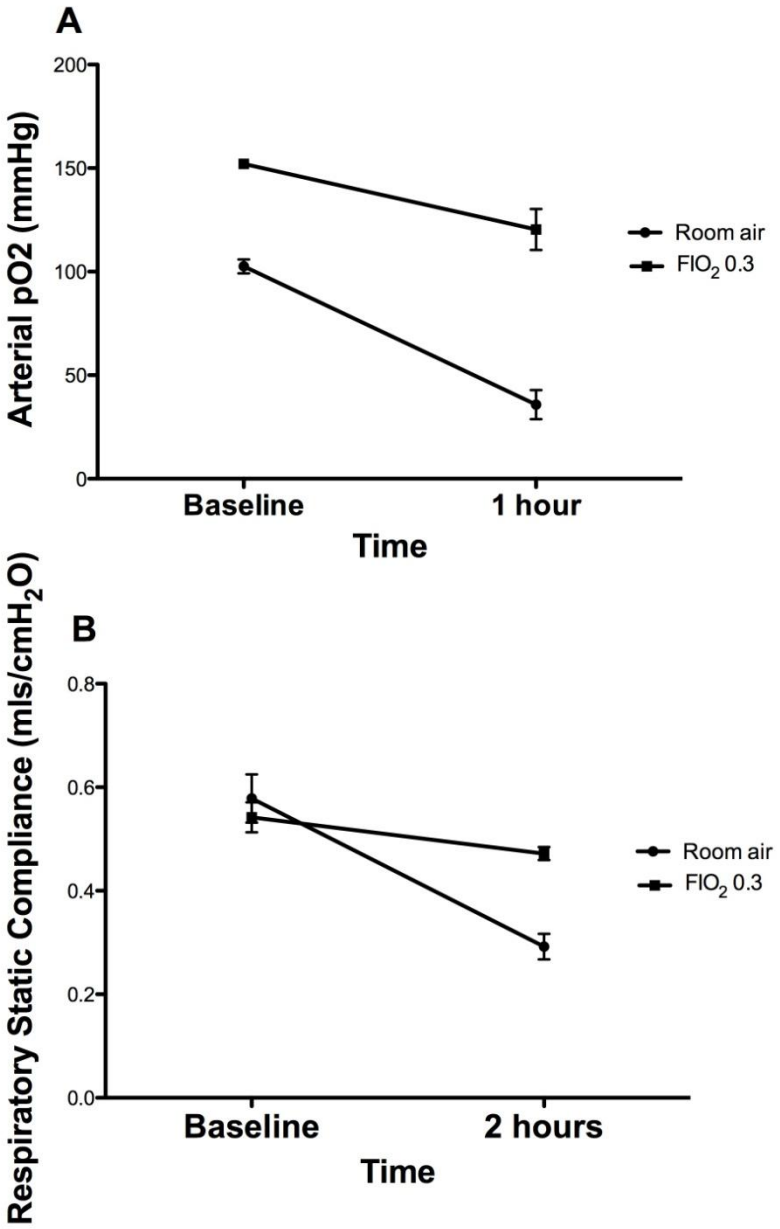

Panel A: Line graph representing arterial oxygen partial pressures of rats after 1 hour of VILI using either FiO2 0.3 or room air

Panel B: Line graph representing static lung compliance of rats after 1 hour of VILI using either FiO2 0.3 or room air (N=3-4/group)

Figure 5-6 Animals do not exhibit recovery during protective ventilation after VILI

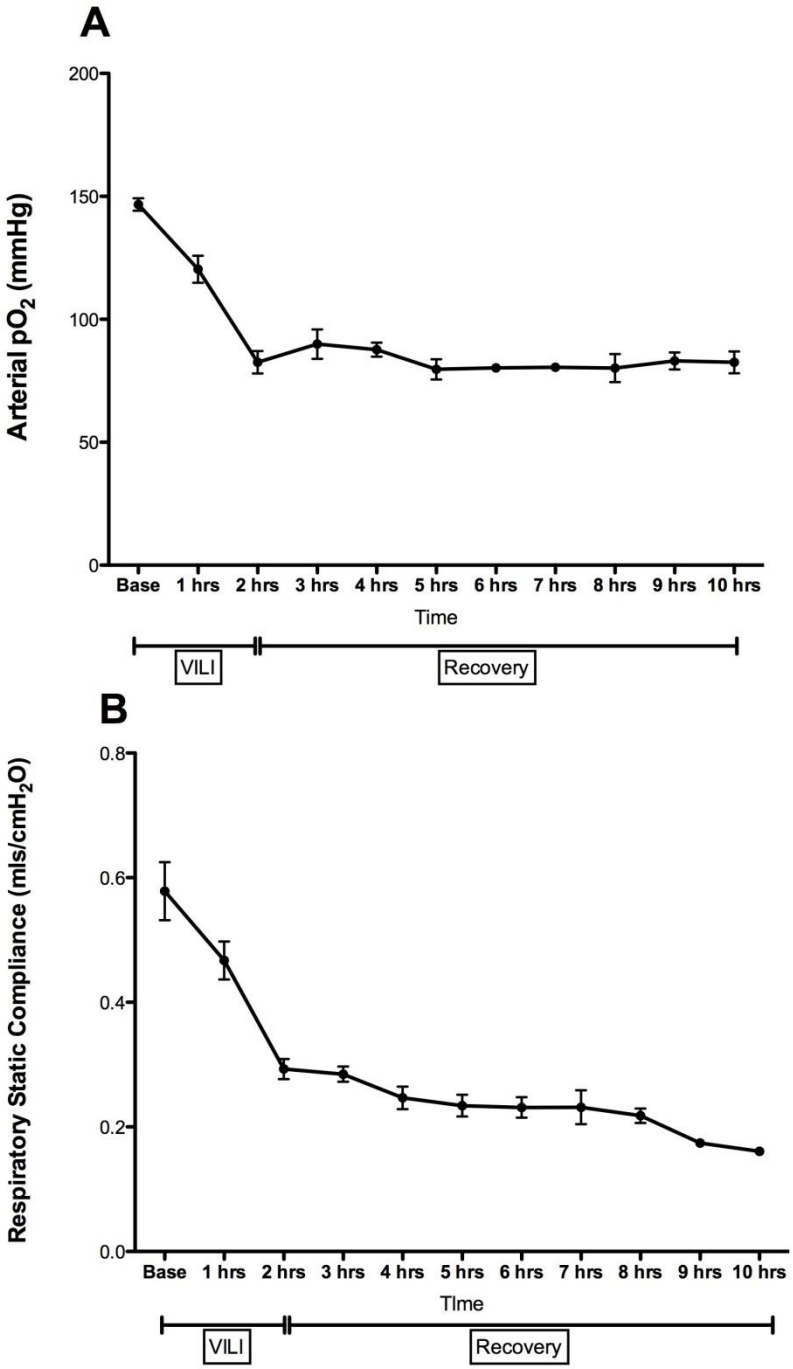

***Panel A*:** Line graph representing arterial oxygen partial pressures of rats during 2 hours of VILI, and afterawards for up to 8 hours using lung protective ventilation using FiO_2 0.3

***Panel B*:** Line graph representing static lung compliance of rats during and after 2 hours of VILI (N=3-4/group)

Figure 5-7 Variability is high when time is used as a marker of injury

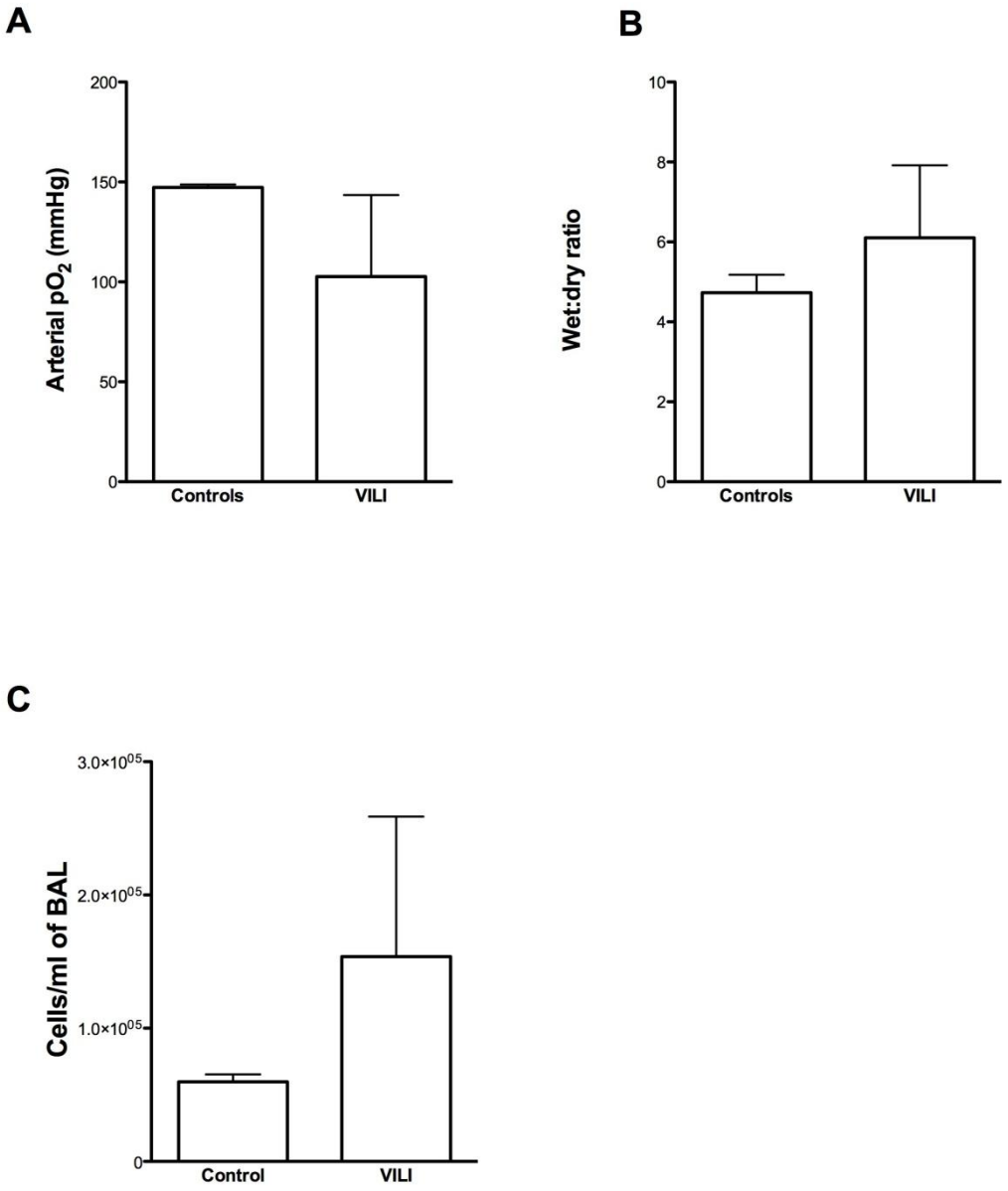

***Panel A*:** Histogram representing arterial oxygen partial pressures of rats 24 hours after being subject to 90 minutes of VILI, measured at an FiO_2 of 0.3

***Panel B*:** Histogram representing lung wet:dry weight ratios of rats 24 hours after being subject to 90 minutes of VILI

***Panel C*:** Histogram representing total inflammatory cells in BAL of rats 24 hours after being subject to 90 minutes of VILI

Abbreviations: Control, animals that received sham ventilation N=4 per group

Figure 5-8 Pattern of recovery from VILI over time

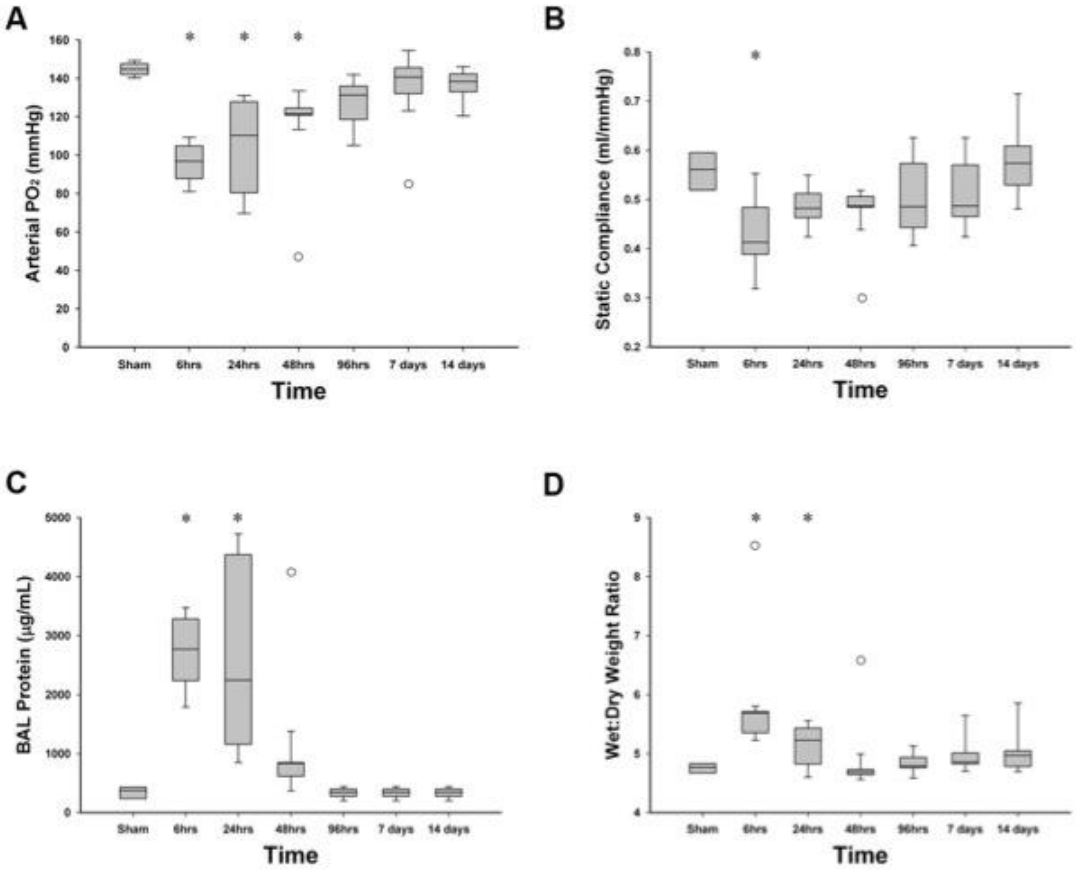

***Panel A*:** Box plot representing arterial oxygen partial pressures measured at an FiO_2 of 0.3 with sham and low stretch ventilation, and at each time point following VILI.

***Panel B*:** Box plot representing static lung compliance with sham and low stretch ventilation, and at each time point following VILI.

***Panel C*:** Box plot representing BAL protein concentrations with sham and low stretch ventilation, and at each time point following VILI.

Panel D: Box plot representing wet:dry weight ratios with sham and low stretch ventilation, and at each time point following VILI.

Abbreviations: Sham, animals that received sham ventilation; Vent, animals that received low stretch ventilation; BAL, bronchoalveolar lavage

Note: Open circles represent outlying data points.

*** Significantly different from sham and low stretch ventilated animals (P<0.05, ANOVA).**

6.0 Evolution of the inflammatory and fibroproliferative responses during resolution and repair following Ventilator Induced Lung Injury in the Rat

6.1 Abstract

Introduction: The time course and mechanisms of resolution and repair, and the potential for fibrosis following ventilation induced lung injury (VILI) are unclear. We sought to examine the pattern of inflammation, injury and repair and fibrosis following VILI.

Methods: 60 anesthetized rats were subject to: (1) high stretch; (2) low stretch; or (3) sham ventilation, and randomly allocated to undergo periods of recovery of 6, 24, 48, 96 hours, 7 days and 14 days. Animals were then re-anesthetized, and the extent of lung injury, inflammation and repair determined.

Results: No injury was seen following low stretch or sham ventilation. VILI caused severe lung injury, maximal at 24 hours, but largely resolved by 96 hours. Arterial oxygen tension decreased from a mean (SD) of 144.8 (4.1) mmHg to 96.2 (10.3) mmHg 6 hours post VILI, before gradually recovering to 131.2 (14.3) mmHg at 96 hours. VILI induced an early neutrophilic alveolitis, a later lymphocytic alveolitis, followed by a monocyte/macrophage infiltration. Alveolar tumor necrosis factor-α, interleukin-1β and transforming growth factor-β1 concentrations peaked at 6 hours, and returned to baseline within 24 hours, while interleukin-10 remained elevated for 48 hours. VILI generated a marked but transient fibroproliferative response, which restored normal lung architecture. There was no evidence of fibrosis at 7 and 14 days.

Conclusions: High stretch ventilation caused severe lung injury, activating a transient inflammatory and fibroproliferative repair response, which restored normal lung architecture without evidence of fibrosis.

6.2 Introduction

An important advance in the management of patients with Acute Lung Injury or Acute Respiratory Distress Syndrome (ALI/ARDS) has been the realisation that mechanical ventilation, the 'supportive' therapy necessary to sustain life, can overstretch and damage lungs and worsen ARDS – this is termed Ventilation Induced Lung Injury (VILI). The importance of VILI in the clinical setting is emphasized by the finding that ventilatory strategies that minimize lung stretch, by means of reduced ventilation intensity, have improved patient outcome from ARDS[285]. However, despite recent advances in the understanding of the pathophysiology of this disease, there remains no specific therapy for ALI/ARDS.

One potential explanation for the failure to translate advances in our understanding of the pathogenesis of ALI/ARDS into effective therapeutic strategies is the fact that many mechanistic and preclinical translational studies focus on the role of inflammation in the injury phase, while relatively little is known about the processes that facilitate repair and recovery following lung injury. Consequently, little is known about the effects of therapeutic strategies that inhibit lung injury on the repair process following injury. An alternative approach may be to modulate the repair process in ARDS. However, relatively little is known about the cellular and molecular mechanisms that mediate alveolar regeneration and repair.

Of importance, abnormal or dysregulated repair processes may result in fibroproliferation, causing distortion of the alveolar architechture and increasing morbidity and mortality in patients following ALI/ARDS [286]. Fibroproliferation has been demonstrated from the earliest phases of ALI/ARDS [286]. The factors influencing progression to fibrosis versus resolution of the

injury are incompletely understood. In particular, the effect of excessive lung stretch on lung remodelling and fibroproliferation, and the potential for mechanical stretch to lead to disordered repair and lung fibrosis, is not known. Cytokines, chemokines and growth factors released as part of the inflammatory response to lung stretch, together with inflammatory cell recruitment, may also play a role in the progression from resolution to fibroproliferation [47]. Specifically, transforming growth factor-β (TGF-β) plays a critical role in the fibroproliferative responses of the lung [287, 288], promoting fibroblast recruitment and activation [289], inducing collagen synthesis and inhibiting collagenase production [290], and inducing fibroproliferation [291]. Matrix metalloproteinases (MMPs) and their tissue inhibitors (TIMPs) may play a key role in remodelling following VILI. Increased MMP levels are seen in ventilated patients [292-294], as well as in experimental models of VILI [295], while MMP inhibition decreases lung injury [295, 296]. However, the precise roles of these factors in the resolution and repair process following VILI are unclear

We wished to characterize the inflammatory and fibroproliferative responses during resolution and repair following VILI. We hypothesized that VILI generates a sustained fibroproliferative response, and that this results in disordered repair and lung fibrosis. We established a non-lethal rodent model of repair following VILI, similar to that previously described [297], and characterized the inflammatory, repair and pro-fibrotic responses, and the time course of injury resolution, and the potential for a sustained fibrotic response following high stretch mechanical ventilation.

6.3 Methods

All work was approved by the Animal Ethics Committee of the National University of Ireland, Galway and conducted under license from the Department of Health, Ireland. Specific-pathogen-free adult male Sprague-Dawley rats (Harlan, Bicester, United Kingdom) weighing between 350–450g were used in all experiments. With the exception of the collection of the physiologic data, investigators were blinded to group allocation for all analyses.

6.3.1 High and Low Stretch Ventilation Protocols

For a more complete description, please refer to Section 4.3. Briefly, anesthesia was induced, intravenous access was obtained via tail vein, laryngoscopy was performed (Welch Allyn Otoscope®, Buckinghamshire, United Kingdom) and the animals were intubated with a size 14 intravenous catheter (BD Insyte®, Becton Dickinson Ltd, Oxford, United Kingdom). The animals were ventilated using a small animal ventilator (CWE SAR 830 AP, CWE Inc, Ardmore, PA). Anesthesia was maintained with repeated intravenous boli of alphaxalone/ alphadolone 10-12mg/kg (Saffan®, Schering Plough, Welwyn Garden City, United Kingdom) and muscle relaxation was achieved with cis-atracurium besylate 0.5mg.kg^{-1} (GlaxoSmithKline, Dublin 16, Ireland).

The animals were then allocated to ventilation under conditions of high lung stretch or to low stretch 'protective' ventilation. The high stretch mechanical ventilation protocol comprised of the following settings: FiO_2 of 0.3, inspiratory pressure 35 cmH_2O, respiratory rate of 18 min^{-1}, and positive end-expiratory pressure of 0 cmH_2O. When static compliance had decreased by 50%, high stretch ventilation was discontinued, and the animals were allowed to recover,

and subsequently returned to their cages. The 'low stretch' protocol comprised of the following settings: Fi_{O2} of 0.3, respiratory rate 80.min $^{-1}$, tidal volume 6 ml.kg^{-1} and positive end-expiratory pressure of 2cm H_2O. An additional group, which was not subjected to anesthesia or mechanical ventilation, was also included as an uninjured 'sham' comparison.

6.3.2 Assessment of injury, inflammation and repair: Anaesthesia and dissection

At 6, 24, 48 and 96 hours and at 7 and 14 days following ventilation or sham procedure, the animals were anesthetized with intraperitoneal ketamine 80 mg·kg^{-1} and xylazine 8 mg·kg^{-1}. After confirming depth of anesthesia by absence of response to paw compression, intravenous access was gained via the dorsal penile vein and anesthesia maintained with repeated intravenous boli of alfaxadone/ alfadadolone. Following this a tracheotomy tube (1mm internal diameter) was inserted and secured and intra-arterial access (22 or 24 gauge cannulae, Becton Dickinson, Franklin Lakes, NJ) was sited in the carotid artery. Sterile technique was utilized during all manipulations. Following confirmation of the absence of a hemodynamic response to paw clamp, cis-atracurium besylate 0.5mg.kg^{-1} was administered intravenously to achieve muscle relaxation, and the lungs were mechanically ventilated (Model 683; Harvard Apparatus, Holliston, MA) at a respiratory rate of 80.min $^{-1}$, tidal volume 6 ml.kg^{-1} and positive end-expiratory pressure of 2cm H_2O for 20 minutes, and indices of lung damage and repair assessed as described below.

6.3.3 Measurement of Physiologic Variables

Intra-arterial blood pressure, peak airway pressures and rectal temperature were recorded continuously. Arterial blood gas analysis was performed following commencement of mechanical ventilation. Static inflation lung compliance measurements were performed by injecting incremental 1 ml volumes of room air via the tracheotomy tube, and measuring the pressure attained 3 seconds after each injection, until a total volume of 5 ml was injected (See Section 4.2.5). At the end of the protocol, the inspired gas was altered to a FiO_2 of 1.0 for 15 min, and an arterial blood sample was then taken for calculation of the alveolar–arterial oxygen gradient. Heparin (400 $IU.kg^{-1}$, CP Pharmaceuticals, Wrexham, United Kingdom) was then administered intravenously, and the animals were then killed by exsanguination.

6.3.4 Tissue Sampling and Assays

Immediately post-mortem, the heart–lung block was dissected from the thorax and bronchoalveolar lavage (BAL) collection was performed as previously described [298, 299] in Section 4.4.2. Total cell numbers per milliliter in the BAL fluid were counted, and differential cell counts were performed (See Section 4.4.3). The concentrations of interleukin (IL) -1β, IL-6, tumor necrosis factor-α and IL-10 in BAL fluid were determined using a commercially available bio-plex multiplex bead based rat cytokine assay system (Bio-Rad Life Science, Hercules, CA) as described in Section 4.4.7. The concentration of total protein in BAL fluid was determined using a Micro BCA™ Protein assay kit (Pierce, Rockford, IL,) as

previously described[300] and in Section 4.4.5. The concentration of transforming growth factor-β1 (TGF-β1) and keratinocyte growth factor (KGF) in BAL fluid was determined using commercially available rat and human respectively, quantitative sandwich enzyme-linked immunosorbent assay (R and D systems, Abingdon, United Kingdom). This KGF assay has been validated for use in rats[301].

BAL fluid and homogenate MMP -2, and -9 concentrations were measured by gelatin zymography as previously described[302] and in detail in Section 4.4.11 . Briefly, to determine relative concentrations of MMP-1, -3, -7, -8, -12,-13 and TIMP-2, BAL was mixed in 1:1 ratio with βmercaptoethanol buffer as previously described[303] and 50μl loaded onto a 10% polyacrylamide gel. For homogenates an aliquot containing 50μg total protein as determined by Bradford assay, was loaded onto a 10% polyacrylamide gel, and Western blotting carried out as previously described[304]. Proteins were detected by chemiluminescence (Supersignal West pico/femto Chemiluminescent substrate kit, Pierce, Rockford, IL). Primary antibodies used were polyclonal rabbit anti-rat MMP-3 antibody at 1/1000, polyclonal rabbit anti-rat MMP-8 antibody, 1/1000, mouse anti-rat MMP-13 at 1/400 dilution, mouse anti-rat TIMP-2 at 1/1000 dilution (all United Chemi-Con, Rosemont, IL). During electrophoresis samples were placed alongside a standard aliquot of chemiluminescent marker (Pierce, Rockford, IL). Blots were photographed using darkroom software (UVP, Cambridge, United Kingdom), and relative density of the bands obtained measured using Scion image analysis [304]. The density of the bands was

normalized with the density of the 50kDa bands on the chemiluminescent marker lane to allow comparison between gels.

TIMP-1 was measured using an anti-rat TIMP-1 ELISA (R&D Systems) according to the manufacturer's instructions. Samples were diluted 1/20 -1/100: the lower limit of detection for the assay was 31.25pg/ml.

Wet/Dry lung weights were determined by tying off and removing the lowest lobe of the right lung, prior to BAL collection, and drying the lung at 37^{o}C for 72h before reweighing.

6.3.5 Histologic tissue preparation

The left lung was isolated and fixed for morphometric examination as previously described[305, 306] and in detail in Section 4.5.1. Briefly, the pulmonary circulation was first perfused with normal saline at a constant hydrostatic pressure of 25cm H_2O until the left atrial effluent was clear of blood. The left lung was then inflated through the tracheal catheter using paraformaldehyde (4% wt.vol^{-1}) in phosphate buffered saline (300mOsmol) at a pressure of 25cm H_2O. Paraformaldehyde was then instilled through the pulmonary artery catheter at a pressure of 62.5cm H_2O. After 30 minutes, the pulmonary artery and trachea were ligated, and the lung was stored in paraformaldehyde. After 24 hours, the lung was cut into six sections (See Figure 4-1), paraffin treated and embedded in wax. Sections were cut at 7 μm using a microtome (Ergostar HM200, Microm Laborgerate GmbH, D69190 Walldorf, Germany) and placed on labelled glass slides.

6.3.6 Stereological Analysis

The extent of histologic lung damage was determined using quantitative stereological techniques as previously described[251, 267] and in detail in Section 4.5.5.

6.3.7 Masson's trichrome staining for collagen in lung tissue

This is described in detail in Section 4.5.6. Briefly, 7 μm tissue sections were de-paraffinized and re-hydrated. They were then immersed in Weigert's hematoxylin, Biebrich scarlet-acid fuchsin solution, and phosphomolybdic acid solution.

6.3.8 Van Gieson Staining for Elastin Fibers

This is described in detail in Section 4.5.7. Briefly, 7 μm tissue sections were de-paraffinized and re-hydrated. They were then stained in Verhoeff's solution for 1 hour until the tissue was completely black. Slides were then counterstained in Van Giesen's solution for 5 minutes.

6.3.9 Lung tissue Myofibroblasts

This is described in detail in Section 4.5.8. Briefly, paraffin-embedded tissue sections of 5μm in thickness were dewaxed and rehydrated. Antigen retrieval was performed by heating in citrate buffer. After quenching endogenous peroxidase activity and blocking nonspecific binding, sections were incubated with antibodies against alpha-smooth muscle actin (LSAB kit, Dako, Carpinteria, CA). Antibody binding was detected using horseradish peroxidase-labeled biotin

streptavidin secondary antibodies (Dako) and immunostaining visualized using 3,3-diaminobenzidine chromogen (Dako). Positive cells were identified and counted in 15 areas from each lung at 20X magnification and compared to controls. Positive staining smooth muscle cells located in the walls of arterioles were not included in counts.

6.3.10 Pro-collagen 1 and 3 Transcription

This is described in detail in Section 4.4.8. Briefly, total RNA was extracted from the lungs of rats using Tri-Reagent (Sigma-Aldrich, Wicklow, Ireland) as previously described [255]. 1μg of the RNA was reverse transcribed using an Improm II Reverse Transcription System (Promega, Southampton, United Kingdom). The complementary DNA, diluted 1:20, was amplified using polymerase chain reaction (PCR) primers to pro-collagen I peptide: forward 5'-TCATCGAATACAAAACCACCA-3'; reverse 5'-GCAGGGCCAATGTCCAT-3'; pro-collagen III peptide: forward 5'-ACACAC TGGTGAATGGAGCAA-3'; reverse 5'-GCCAATGTCCACACCAAATT. Real time PCR was performed using Fast SYBER Green Mastermix (Applied Biosystems, Carlsbad, CA) using the StepOne Plus Fast enabled Real time PCR System (Applied Biosystems, Carlsbad, CA). After normalizing data to GAPDH messenger RNA levels, expression relative to control rats was calculated by the comparative C_t (cross over threshold) method.

6.3.11 Lung tissue Collagen Content

The Sircol collagen assay (Biocolor Ltd., Belfast, United Kingdom) is described in detail in Section 4.4.9. Briefly, lung homogenate was incubated in acid-pepsin

overnight. Sirius red reagent (50 µl) was added to each lung homogenate (50 µl) and mixed for 30 minutes. The collagen–dye complex was precipitated by centrifugation at 16,000 *g* for 5 minutes and dissolved in 0.5 M NaOH. Finally, the samples were introduced into a microplate reader and the absorbance determined at 540 nm.

6.3.12 Data Presentation and Analysis

All analyses were performed using SigmaStat® 3.5 (Systat Software, Point Richmond, CA). A two-tailed p value of <0.05 was considered significant. See Section 4.8 for further details.

6.4 Results

60 animals were entered into this study. Four animals underwent low stretch ventilation while 4 underwent sham ventilation, and were assessed 6 hours later. The remaining 52 animals were subjected to VILI, allowed to recover, and randomized to assessment at the pre-defined timed points. Four animals did not survive the high stretch ventilation protocol due to the severity of the injury induced, leaving 48 animals that recovered post VILI and that were subsequently assessed. There were no differences between the groups at baseline with regard to animal weight and duration of injurious ventilation required to induce injury (**Table 6-1**).

6.4.1 Injury and Recovery Profile

No lung injury was seen following protective ventilation compared to sham uninjured animals (**Table 6-1; Figures 6-1 and 6-2**). In contrast, high stretch ventilation caused severe derangement of physiologic indices of lung function, with maximal injury seen at 6-24 hours, and resolution of physiologic indices largely complete by 96 hours post VILI. Arterial oxygen tension was lowest at 6 hours post injury, remained low at 24 and 48 hours, and progressively returned to baseline levels by 96 hours (**Figure 6-1 Panel A**). The alveolar-arterial oxygen gradient followed a similar pattern (**Table 6-1)**. Static lung compliance decreased statistically significantly following VILI, with the maximal decrement evident at 6 hours (**Figure 6-1 Panel B**). Static compliance was improved at 48 hours, but did not return to normal until 14 days. BAL protein concentrations (**Figure 6-1 Panel C**), and lung wet: dry weight ratios **(Figure 6-1 Panel D)**

were maximally increased at 6 hours, remained abnormal at 24 hours, and then decreased progressively.

VILI caused progressive derangement of histological indices of lung injury, which was maximal at 48 hours, and which did not resolve until 7 days later. Quantitative stereological analysis demonstrated progressive increases in acinar tissue volume fraction (**Figure 6-2 Panel A**) and decreases in acinar air-space volume fraction (**Figure 6-2 Panel B**). Representative samples of the lung histology at each time point following VILI are given in **Figure 6-2 Panels C-H**.

6.4.2 Indices of Inflammation and Repair following VILI

No evidence of injury, inflammation or repair was seen following low stretch ventilation compared to sham uninjured animals (**Table 6-1; Figures 6-1, 6-2 and 6-3**). In contrast, high stretch ventilation resulted in a marked inflammatory and reparative response.

Inflammatory cells: BAL neutrophil counts increased rapidly following VILI, peaking at 24 hours and had returned to levels seen in sham and low stretch ventilation animals by 96 hours (**Figure 6-3 Panel A**). BAL lymphocyte counts increased more gradually following VILI, peaking at 24 hours and remaining raised at 48 hours before returning to levels seen in sham and low stretch ventilation animals at 7 days (**Figure 6-3 Panel B**). BAL monocyte/macrophage counts peaked at 48 hours following VILI, remained raised at 96 hours and did not return to uninjured levels until 14 days following VILI **(Figure 6-3 Panel C)**. BAL MMP-8 and MMP-9 levels peaked at 6 – 24 hours and decreased to uninjured levels by 96 hours (**Figure 6-3 Panels D–F**). There was no statistically

significant change in lung homogenate MMP-8 and -9 concentrations during the injury and resolution following VILI.

Inflammatory Cytokines: BAL tumour necrosis factor-α and IL-1β concentrations peaked at 6 hours following VILI, and had returned to uninjured levels at 24 hours (**Figure 6-4 Panels A-B**). BAL IL-6 also peaked at 6 hours but remained statistically significantly elevated at 24 hours, before returning to uninjured levels at the later time points (**Figure 6-4 Panel C**). BAL IL-10 concentrations also peaked at 6 hours and had returned to uninjured levels within 48 hours (**Figure 6-4 Panel D**).

Repair Mediators: BAL TGF-β concentrations peaked at 6 hours following VILI, and progressively decreased at the later time points, returning to pre-injury levels by 96 hours (**Figure 6-4 Panel E**). Interestingly, BAL KGF increased later following VILI, and was statistically significantly elevated at 14 days, but not at the earlier time points (**Figure 6-4 Panel F**).

6.4.3 Fibroproliferative response following VILI

High stretch ventilation caused a marked fibroproliferative response (**Table 6-1; Figure 6-5**). In contrast, no fibroproliferative response was seen following low stretch ventilation compared to sham uninjured animals.

Indices of Fibrosis: Tissue pro-collagen I peptide mRNA content increased dramatically post VILI, with a maximal increase at 48 and 96 hours (**Figure 6-5 Panel A**). In contrast, at 7 and 14 days pro-collagen I mRNA content was decreased compared to uninjured animals. Masson's Trichrome stained lung sections demonstrated patchy collagen accumulation in areas of injured lung

(Figure 6-6). Despite this, there was no change in tissue pro-collagen III messenger RNA (**Figure 6-5 Panel B**) or total lung collagen protein (**Figure 6-5 Panel C**) following VILI, and stereological assessment of lung tissue did not demonstrate an overall increase in lung collagen **(Figure 6-6 Panels A and B)**. Lung tissue myofibroblast content was increased at 6 to 96 hours and decreased to pre-injury levels at 7 and 14 days (**Figure 6-5 Panel D and Figure 6-6**). A decrease in the density of elastic fibers was seen in the group exposed to VILI, although this was not significant **(Figure 6-7)**. In addition, an abnormal structural disorganization of elastin fibers in the lung parenchyma was also observed in the VILI exposed animals, which persisted out to 96 hours post injury **(Figure 6-7).**

MMP-3, a stromelysin largely derived from fibroblasts [307], followed a similar time course to that seen with lung myofibroblasts, with rising levels in BAL (and homogenate - not shown) at 6 hours, peaking at 48 hours and reaching baseline by 96 hours (**Figure 6-8 Panels A and B**). BAL MMP-13, a fibroblast collagenase,[308] was statistically significantly increased following VILI, peaking at 24hrs and subsequently fell to baseline (**Figure 6-8 Panels B and C**). Most of the MMP-13 identified was present as a cleaved (<30kDa) product (**Figure 6-8 Panel B**). BAL TIMP-1 was undetectable in BAL following sham or protective ventilation, but increased rapidly following VILI, was statistically significantly elevated at 6 and 24 hours before decreasing to baseline by 96 hours (**Figure 6-8 Panel D**). Lung homogenates, in contrast, contained readily detectable levels of TIMP-1 at baseline. TIMP-2 was undetectable in BAL or homogenate (data not shown).

MMP-7, a key regulator of fibrosis, was also significantly elevated in BAL, decreasing progressively at later time points **(Figure 6-9).** MMP-2, a collagenase, was increased at 6 hours only, and not at the other time points **(Figure 6-9)**. MMP-12 (macrophages metalloelastase) was increased at all time points out to 96 hours **(Figure 6-9).**

6.5 Discussion

A greater understanding of the cellular and molecular mechanisms that mediate alveolar epithelial regeneration and repair following lung injury is essential to the development of therapies that target this phase of ALI/ARDS. Much of the long term morbidity following ALI/ARDS results from limitations in functional capacity due in part to ongoing impairment of respiratory function[309]. Despite this, most experimental studies concentrate on the early 'injury' phases of ALI/ARDS. Only one study to date has examined the pattern of resolution of ventilation induced ALI [297]. In these studies, we sought to characterise the inflammatory and fibroproliferative responses during resolution and repair following VILI, and determine whether high stretch is a sufficient stimulus to generate a fibroproliferative response and result in disordered repair and lung fibrosis.

6.5.1 Injury and Recovery Profile

Animals subjected to 'protective' ventilation did not sustain a detectable lung injury when assessed 6 hours post ventilation compared to unventilated sham animals. In contrast, high stretch ventilation caused a severe lung injury as evidenced by worsening of physiologic indices such as oxygenation, static lung compliance and lung wet: dry weight. Physiologic derangements were maximal at 6 hours, and then progressively resolved over the next 96 hours. In contrast, histological evidence of injury evolved more slowly and persisted for up to 7 days. Most interestingly, therefore, these data indicate that restoration of physiologic function occurs rapidly despite histological evidence of an ongoing

response to the injury. Nin et al demonstrated resolution of injury induced by 60 minutes of high lung stretch over a 24-72 hour time period [297]. The longer resolution phase in our studies may be due to the fact that the injurious stimulus was applied for a longer time period.

6.5.2 Cytokine, Chemokine, and Leukocyte profile

Cytokines, chemokines and growth factors released as part of the inflammatory response to excessive lung stretch play a key role in the repair process[47]. Conversely, dysregulated release of these mediators may result in the progression from injury resolution to fibroproliferation[47]. Overexpression of IL1-β and tumor necrosis factor-α causes varying degrees of lung fibrosis in preclinical models[310, 311]. In these studies, animals subjected to low stretch ventilation did not manifest an inflammatory response when assessed 6 hours post ventilation compared to unventilated sham animals. This suggests that while low stretch ventilation may activate innate immunity[312], any response is relatively short lived following discontinuation of ventilation. In contrast, VILI caused a marked but transient response in multiple mediators, including TNF-α, IL-1β, IL-6 and IL-10, which resolved progressively with restoration of lung function. The time course of IL-6 increase and resolution was similar to that previously demonstrated [297]. Interestingly, resolution of inflammation mirrored the time profile of injury and recovery of physiologic – rather than histologic – indices.

Alveolar concentrations of TGF-β, which plays a critical role in the pathogenesis of lung fibrosis[288-290], increased in the early phases following VILI. However,

the elevation of TGF-β was transient, and mirrored closely the time profile seen with pro-inflammatory cytokines. In contrast, alveolar concentrations of KGF, an epithelial specific growth factor produced by mesenchyme, that may be an important endogenous stimulus for alveolar epithelial proliferation and repair[301], was increased later in the repair process, becoming significantly elevated only at day 14 post VILI. KGF may therefore have a role in suppressing fibroproliferation after stretch injury.

VILI resulted in rapid alveolar neutrophilic infiltration, which peaked at 24 hours then decreased, returning to baseline levels by 96 hours. Neutrophils phagocytoze debris, and produce lipid and protein mediators important in orchestrating tissue repair. Alveolar lymphocytes, which are important in mediating resolution of lung injury by modulating innate immune responses[313], accumulated more gradually and remained elevated at 96 hours, a pattern consistent with previous studies[314]. Alveolar monocytes/macrophages, which induce neutrophil apoptosis [315] and phagocytosis of inflammatory cells[316], and are pivotal in the progression to lung repair[315], peaked at 48 hours, and remained elevated up to 7 days. The pattern of monocyte/macrophage infiltration mirrored the resolution of histological evidence of injury, suggesting a role in regulating the repair process.

6.5.3 Role of MMPs in Repair following VILI

A favorable balance of matrix metalloproteinases (MMPs) to their tissue inhibitors (TIMPs) is believed necessary to facilitate cell detachment from the basement membrane and migration during wound healing[317]. Conversely, an

imbalance between collagen catabolizing MMPs and their specific inhibitors, TIMPs, can result in excessive collagen production and/or breakdown. MMPs have been implicated in the pathogenesis of ARDS, and may contribute to loss of the alveolo-capillary barrier and intercellular junctions[318]. MMPs are raised in ARDS patients [293] and in experimental models of VILI[295]. Interestingly, some MMPs, such as MMP-9, appear to exhibit a protective profile in ALI[319].

In our studies, alveolar concentrations of MMPs and their TIMPs showed dynamic changes after VILI, but all, apart from MMP-12, had decreased to pre-injury levels by 96 hours. Alveolar concentrations of the collagenase MMP-8 and the gelatinolytic enzyme MMP-9, which are produced by neutrophils[320], exhibited similar time profiles to that seen with neutrophil infiltration. MMP-3, a stromelysin largely derived from fibroblasts[307], and the fibroblast collagenase MMP-13[308], followed a similar time course. MMP-8 and MMP-13 are the major collagenolytic species in rats. Despite a relatively small increase in MMP-13 compared with MMP-8, most of the MMP-13 present was in the active small (<30kDa) form, indicating the potential for rapid collagen degradation. MMP-9 is produced by epithelium, neutrophils and macrophages[319], it can damage basement membrane contributing to alveolar edema, but is also necessary for epithelial repair[319]. MMP-3 is produced predominantly by stromal cells in the lung, particularly when activated by inflammatory cytokines[304]. It cleaves and activates collagenases that degrade type I collagen, and may have some type IV collagenolytic activity, therefore contributing to basement membrane dysfunction[321]. The time course of rising MMP-3 in the BAL and homogenates was consistent with an increase in the number of myofibroblasts detected and suggests these are the predominant source of MMP-3 in this model.

MMP-7 was increased at 6 hours and decreased progressively out to 96 hours, although remained significantly elevated in comparison to controls. The enzyme encoded by the Mmp7 gene (also called matrilysin-1) is strongly induced in injured alveolar epithelium, degrades proteoglycans, fibronectin, and elastin, and is involved in wound healing [322]. Proteoglycans in the lungs serve important functions, such as regulation of water homeostasis, maintenance of tissue structure and function, modulation of the inflammatory response, and tissue repair and remodelling [323, 324]. Our findings are in line with recent observations reported by Moriondo et al. [325] who found that healthy rats ventilated for 4 h with high VT had increased pulmonary proteoglycans and activated MMPs. MMP-7 is a target gene of the WNT signaling pathway and has recently been identified as a key regulator of pulmonary fibrosis [326]. The progression of lung injury during VILI may involve an imbalance between the activation of MMPs and changes in the local mechanical environment of the lung. The increased up-regulation of MMP7 that we found supports a role for this enzyme in perpetuating lung inflammation and remodeling after injurious mechanical ventilation.

MMP-2 (gelatinase-A) is constitutively expressed by endothelial and epithelial cells. MMP-2, together with MMP-9, plays an important role in peri-cellular basement membrane turnover by degrading the main components of the basement membrane [327]. MMP-2 is localized in areas of fibroproliferation and basal membrane disruption [328] and shows intense activity in experimental models of pulmonary fibrosis [329, 330]. The release of MMP-2 in response to cell stretch may play a role in further lung injury.

Macrophage metalloelastase, also identified as MMP-12, has been previously described as a key factor of pathological progressive proteolytic destruction of ECM. Indeed, MMP-12 has been reported to be essential in tissue remodelling associated with emphysema in mice exposed to cigarette smoke [331]. In addition, an increased expression of MMP-12 in macrophages from patients with COPD was recently reported [332]. MMP-12 has potent extracellular matrix re-modeling properties due to its specific elastolytic activity, but may also participate to the inflammatory process through the activation of TNF-alpha [333]. Moreover, MMP-12 presents potent direct pro-inflammatory properties including the ability to induce neutrophil influx, cytokine and chemokine production [334]. MMP- 12 seems to be involved in numerous models of acute lung inflammation [333, 335]. Although the role of MMP-12 in animal models of emphysema is well documented, its involvement in VILI is not clear. Here we demonstrate an increased level of MMP-12 in lung homogenate up to 96 hours after injury. MMP-12 plays a role in mediating elastin fragmentation in cigarette smoke injured lungs [331]. Similarly, elastin fragmentation in this model of VILI (See below) may also be linked to MMP-12 and further monocyte accumulation in lung in response to excess stretch.

TIMP-1 and -2 are the major secreted inhibitors of MMPs in humans[319]. Rising levels of TIMP-1 are consistent with an increasing fibroblast population in lung tissue. However, it may also reflect mononuclear cell infiltration of the lung, as monocytes and macrophages are potential potent producers of TIMP-1, albeit to a lesser extent than fibroblasts. TIMP-2 was not detectable in this model.

6.5.4 Evidence for Fibroproliferation during Repair following VILI

Fibroproliferation is an early response to lung injury[286]. The factors influencing progression to fibroproliferation versus resolution and reconstitution of normal pulmonary parenchymal architecture are poorly understood. In particular, the role of mechanical stretch in initiating and potentiating pulmonary fibrotic change is unknown. Of interest, a recent in vitro study demonstrated how cyclic mechanical stretch can induce epithelial to mesenchymal transition in alveolar type II epithelial cells, providing a putative link between lung stretch and fibrosis [336].

Our findings demonstrate that stretch-induced lung injury causes a pronounced early pro-fibrotic stimulus. Tissue pro-collagen I messenger RNA increased dramatically, with a maximal increase seen at 48 to 96 hours. In contrast, at 7 and 14 days following VILI, pro-collagen I messenger RNA was decreased compared to that seen in uninjured animals. This suggests that transcription of collagen I is initially stimulated but later suppressed following VILI. Lung tissue myofibroblasts, which are considered the key effector cell in lung fibrogenesis, followed a similar pattern, increasing early following injury before decreasing to pre-injury levels in the later stages.

Later studies at one and two weeks following VILI did not provide any evidence that high lung stretch results in lung fibrosis. Indeed, total lung collagen content was not increased at the later time points, suggesting that active resorption of collagen may have occurred during the later phases of the resolution process. Taken together, these findings strongly suggest that sufficient collagenases (such as MMP-3, MMP-8 and MMP-13) are produced in a timely fashion to limit collagen deposition in the lung.

6.5.5 Limitations

A number of limitations need to be considered prior to consideration of the clinical implication of these findings. First, the model chosen was an isolated high stretch model. While high tidal volume ventilation can directly cause ALI/ARDS, particularly in patients undergoing cardiac [337] and thoracic surgery [338], and in critically ill patients that do not have pre-existing ALI/ARDS [339], VILI is generally seen in the context of other disease processes such as sepsis, in the clinical setting. However, we wished to focus solely on determining whether high lung stretch alone can generate a sustained fibroproliferative response resulting in an ongoing fibrotic response. This approach was necessary to elucidate the role of excessive lung stretch in contributing to disordered repair in the setting of ALI/ARDS. Second, high airway pressures, well beyond that seen clinically, were used to cause a severe stretch induced injury in these studies. However, ventilation with a peak inspiratory pressure as high as 45 cm H_2O is commonly used in pre-clinical studies to induce VILI [15, 16, 340]. This practice is supported by evidence that regional lung areas may be subject to gross overdistension in ALI/ARDS patients [341]. Quantitative assessment of computed tomography images in humans with severe ARDS indicates that the amount of normally aerated tissue - the so called 'baby lung' - is variable, of the order of 200–500g, and may be as low as 200ml [82]. A 6 ml/kg tidal volume applied to these "baby lungs" can and does result in airway pressures in the range of 30-35cm H_20 [83]. In this regard, the mean peak airway pressure in the treatment arm of the ARDS net low tidal volume study was 34cm H_2O [83]. Other

diseased lung regions may be subject to even greater distention and greater regional intra-alveolar and airway pressures [84].

Third, we did not provide a low stretch ventilation control group for each time point. However, our finding that 'protective' ventilation did not result in detectable injury, inflammatory or fibroproliferative response at 6 hours suggests that any response seen is transient, and that any additional information from these groups would be minimal. Fourth, the inclusion of groups with additional injury types and with differing degrees of stretch induced injury would have provided useful additional comparison groups. However, this would have required a large number of additional groups and are best examined in future studies. The duration of injurious ventilation in these studies was brief and longer durations of injurious ventilation might lead to a different pattern of resolution and repair. Lastly, the observational design of these studies precludes assessment of a cause and effect relationship between the mediator profile and the time course of injury and repair following VILI.

6.5.6 Clinical Implications

Our data suggest that repair following VILI demonstrates a pronounced early pro-inflammatory and pro-fibrotic phenotype. However, this is balanced by later events, such as MMP-3, MMP-8 and MMP-13 secretion that results in collagen reabsorption, and does not lead to an increase in lung fibrosis in the setting of uncomplicated VILI. The result is a well regulated process that restores lung architecture and function. High lung stretch alone, particularly when not sustained, may not constitute a sufficient stimulus to produce lung fibrosis. Nevertheless, there is clear potential for additional stimuli, such as infection or

additional episodes of stretch induced injury to disrupt this finely balanced process. Finally, we here establish a relevant pre-clinical model of the repair and resolution phase of VILI that can be used to test the efficacy of strategies targeted at this phase of the disease process.

6.5.7 Conclusions

These studies establish a rodent model of repair following VILI and characterize the time course of injury and repair following VILI. High lung stretch causes severe injury, resulting in a pronounced early pro-inflammatory and pro-fibrotic phenotype, but this response is balanced by later events that result in restoration of normal lung architecture and function.

6.6 Figures

Table 6-1 Baseline characteristics and physiologic variables

Variable	Sham	6 Hours	24 Hours	48 hours	96 hours	7 Days	14 Days
Number of animals	4	8	8	8	8	8	8
Animal Weight (g)	401±14	351 ± 15	339 ± 23	344 ± 30	348 ± 11	374 ± 18	393 ± 17
Animal survival (%)	4/4 (100%)	8/8 (100%)	8/8 (100%)	8/8 (100%)	8/8 (100%)	8/8 (100%)	8/8 (100%)
Duration of VILI (minutes)	0	95 ± 15	109 ± 58	119 ± 51	98 ± 10	146 ± 41	148 ± 31
Final arterial pO_2 (mmHg, $fIO_2 = 1$)	513.9 ± 20.8	318.6 ± 94.3	324.3 ± 158	402.7 ± 141.4	465.5 ± 19.4	413.7 ± 81.7	392.2 ± 54.7
Final alveolar-arterial Oxygen Gradient (mmHg)	157.3 ± 21.3	348.9 ± 94	348.9 ± 158.4	265.6 ± 134.5	207.6 ± 17.7	258.9 ± 82.3	278.8 ± 54.5
Mean Arterial Pressure (mmHg)							
Final	127 ± 11	138 ± 16	123 ± 16	111 ± 16	138 ± 10	130 ± 26	138 ± 9
Arterial pH							
Final	7.4 ± 0.03	7.39 ± 0.03	7.44 ± 0.04	7.42 ± 0.04	7.46 ± 0.01	7.41 ± 0.03	7.41 ± 0.01
Arterial PCO_2 (mmHg)							
Final	33.64 ± 2	35 ± 3.11	30.37 ± 2.13	34.16 ± 4.91	31 ± 0.38	32.57 ± 1.65	33.43 ± 2.6
Serum Bicarbonate (mMol/L)							
Final	22.8 ± 0.65	21.7 ± 1.6	22 ± 0.89	22.7 ± 1	23.5 ± 0.6	21.9 ± 0.8	21.8 ± 0.4

Serum Base Excess Final	2.9 ± 0.6	3.6 ± 2	3.8 ± 1	2.5 ± 1.2	2.3 ± 0.7	3.7 ± 0.9	3.7 ± 0.8
Total Cell Count in BAL (cells per ml)	67,500 ± 3,415	262,667 ± 127,549	499,143 ± 170,598	339,625 ± 99,543	200,000 ± 88,121	111,313 ± 14,361	88,125 ± 36,170

Data are expressed as mean±SD. Final data is data collected upon completion of the experimental protocol.

* Significantly different from Sham ($P < 0.05$).

Figure 6-1 Physiologic variables after VILI

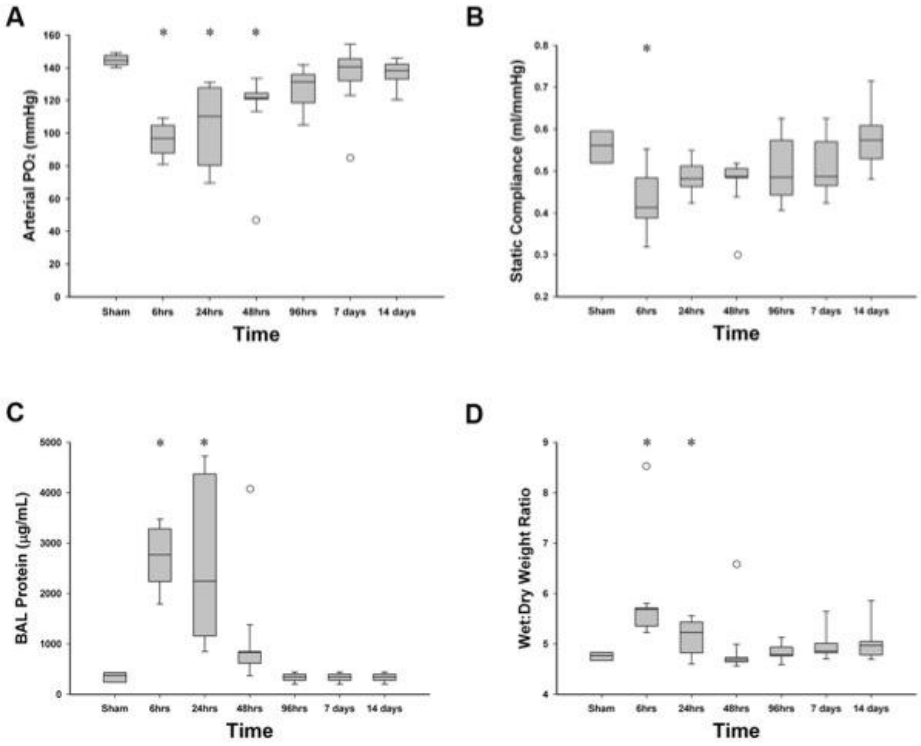

Figure 6-1

***Panel A*:** Box plot representing arterial oxygen partial pressures measured at an FiO_2 of 0.3 with sham and low stretch ventilation, and at each time point following VILI.

***Panel B*:** Box plot representing static lung compliance with sham and low stretch ventilation, and at each time point following VILI.

***Panel C*:** Box plot representing BAL protein concentrations with sham and low stretch ventilation, and at each time point following VILI.

***Panel D*:** Box plot representing wet:dry weight ratios with sham and low stretch ventilation, and at each time point following VILI.

Abbreviations: Sham, animals that received sham ventilation; Vent, animals that received low stretch ventilation; BAL, bronchoalveolar lavage

Note: Open circles represent outlying data points.

*** Significantly different from sham and low stretch ventilated animals (P<0.05, ANOVA and Student-Neuman-Keuls).**

Figure 6-2 Histology after VILI

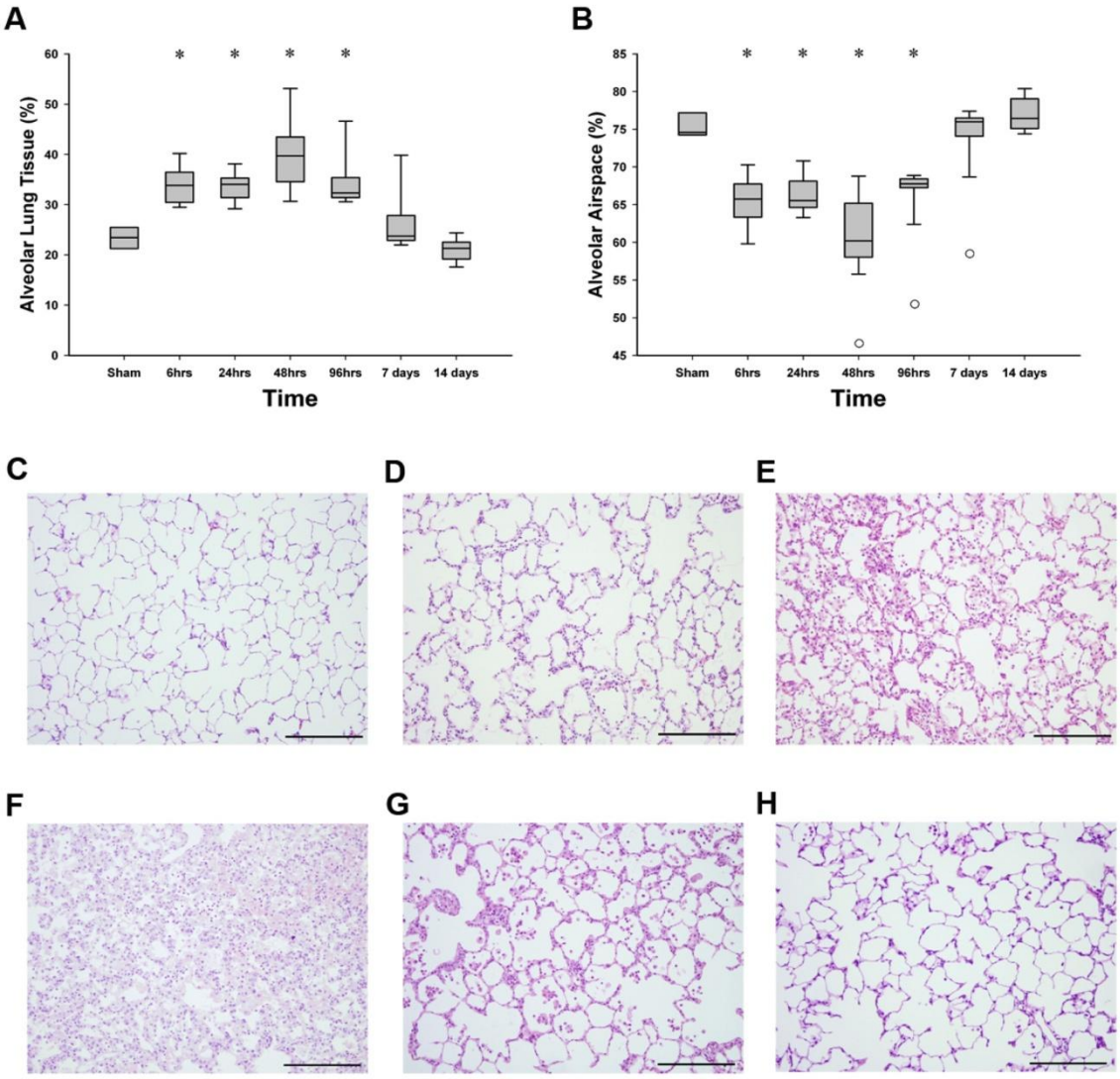

Figure 6-2

***Panel A*:** Box plot representing alveolar lung tissue with sham and low stretch ventilation, and at each time point following VILI.

***Panel B*:** Box plot representing alveolar airspace with sham and low stretch ventilation, and at each time point following VILI.

Panels C - H: Photomicrographs of representative sections of lung tissue. Panel C is an image from a sham uninjured lung, Panels D – H are from lungs at 6 hours, 24 hours, 48 hours, 96 hours and 7 days following VILI respectively. The degree of wall thickness and inflammatory cell infiltrate is maximal at 48 hours with progressive resolution at the later time points.

Notes: Open circles on box lots represent outlying data points. The scale bar represents 200micrometer.

Abbreviations: Sham, animals that received sham ventilation; Vent, animals that received low stretch ventilation * Significantly different from sham and low stretch ventilated animals ($P<0.05$, ANOVA and Student-Neuman-Keuls).

Figure 6-3 Inflammatory cells and MMPs in BAL after VILI

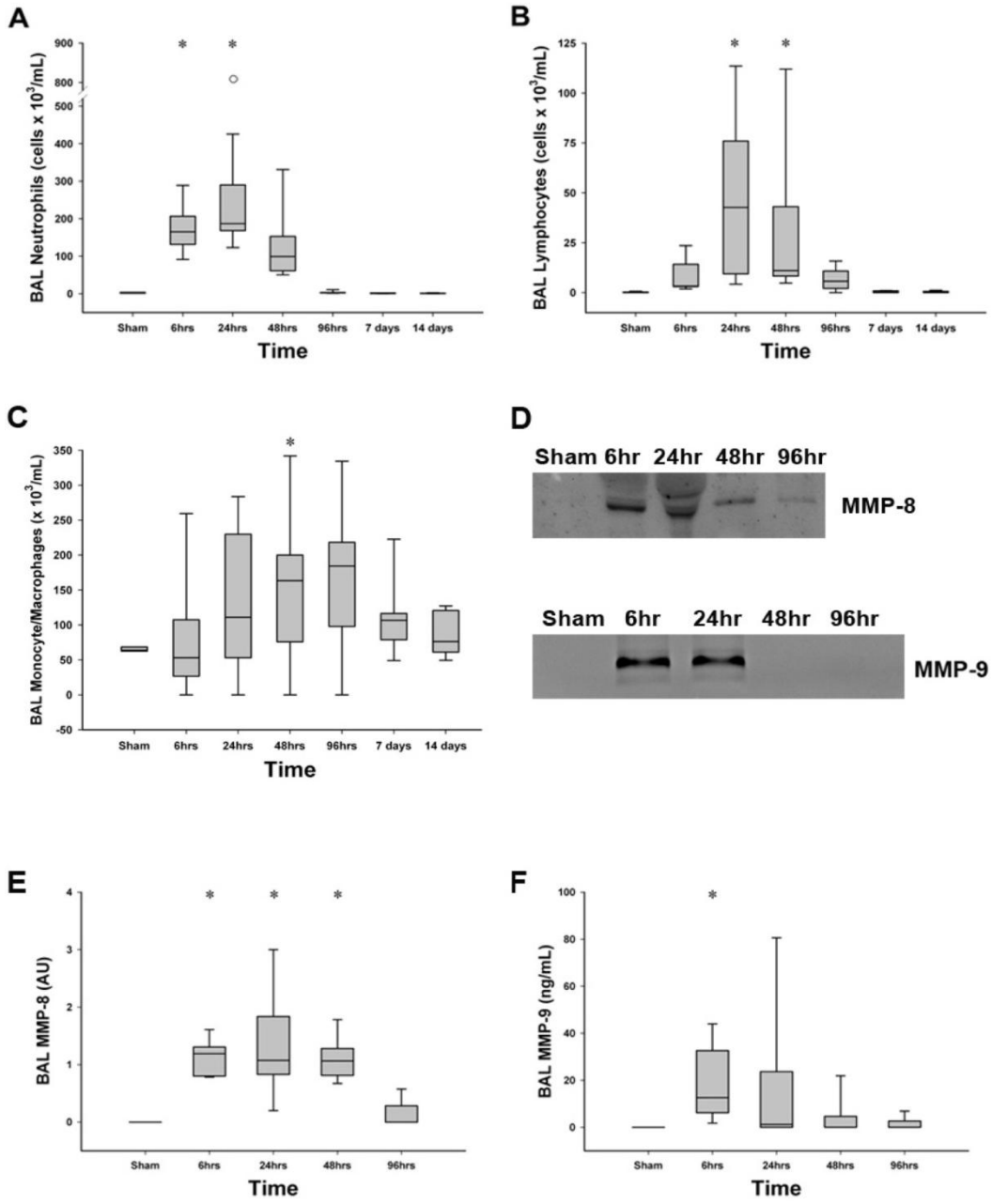

Figure 6-3

Panel A: Box plot representing bronchoalveolar lavage neutrophil counts with sham and low stretch ventilation and at each time point following VILI.

Panel B: Box plot representing bronchoalveolar lavage lymphocyte counts with sham and low stretch ventilation and at each time point following VILI.

Panel C: Box plot representing bronchoalveolar lavage monocyte/macrophage counts with sham and low stretch ventilation and at each time point following VILI.

Panel D: Representative western blots of bronchoalveolar lavage MMP-8 and MMP-9 with sham and low stretch ventilation and at each time point following VILI.

Panel E: Box plot representing densitometry of western blot bronchoalveolar lavage MMP-8 with sham and low stretch ventilation and at each time point following VILI.

Panel F: Box plot representing bronchoalveolar lavage MMP-9 concentrations with sham and low stretch ventilation and at each time point following VILI.

Abbreviations: Sham, animals that received sham ventilation; Vent, animals that received low stretch ventilation; BAL, bronchoalveolar lavage; AU, arbitrary units.

Note: Open circles represent outlying data points.

*** Significantly different from sham and low stretch ventilated animals (P<0.05, ANOVA)**

Figure 6-4 Cytokines in BAL after VILI

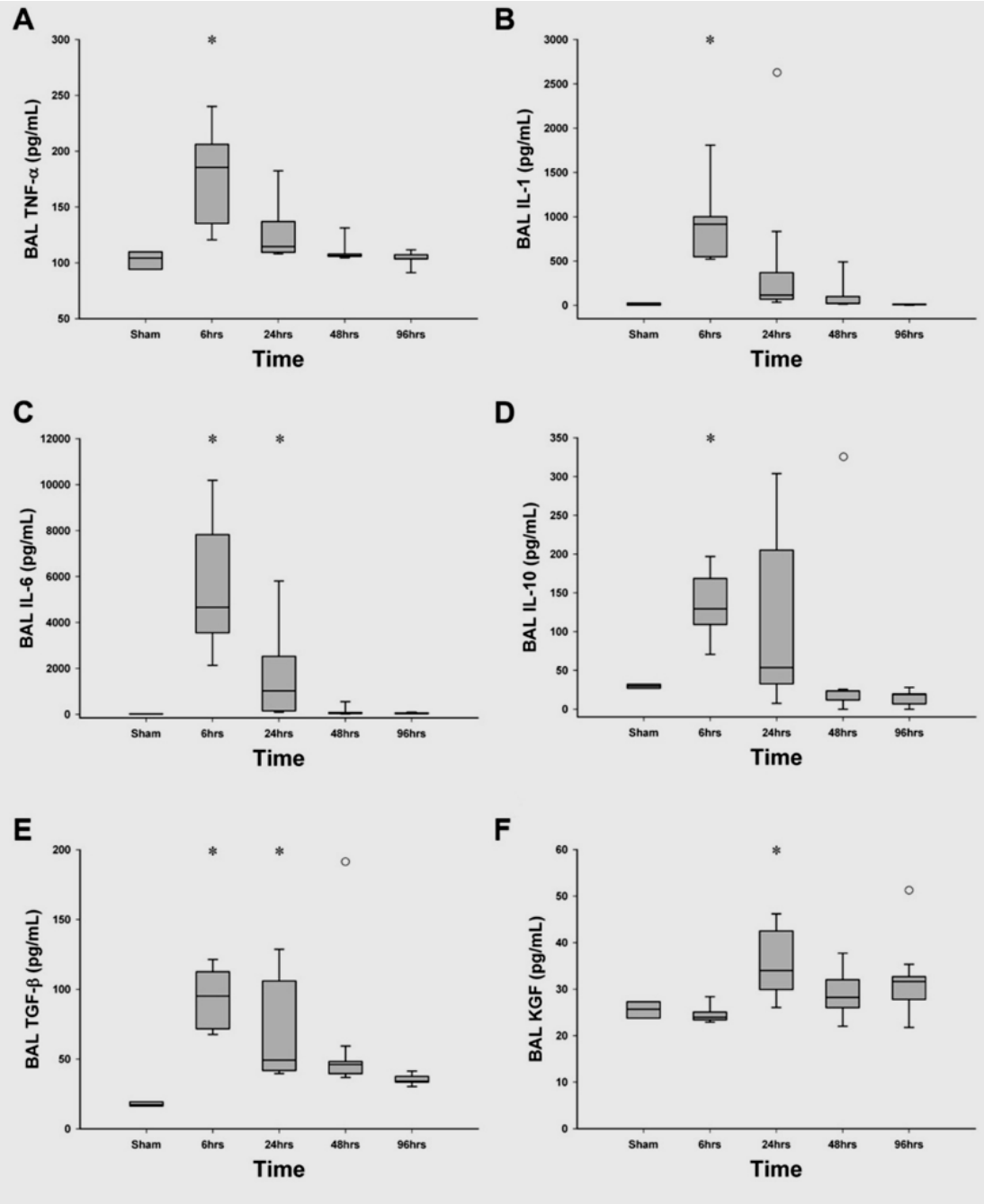

Figure 6-4

Panel A: Box plot representing bronchoalveolar lavage TNFa concentrations with sham and low stretch ventilation and at each time point following VILI.

Panel B: Box plot representing bronchoalveolar lavage IL-1β concentrations with sham and low stretch ventilation and at each time point following VILI.

Panel C: Box plot representing bronchoalveolar lavage IL-6 concentrations with sham and low stretch ventilation and at each time point following VILI.

Panel D: Box plot representing bronchoalveolar lavage IL-10 concentrations with sham and low stretch ventilation and at each time point following VILI.

Panel E: Box plot representing bronchoalveolar lavage TGF-b concentrations with sham and low stretch ventilation and at each time point following VILI.

Panel F: Box plot representing bronchoalveolar lavage KGF concentrations with sham and low stretch ventilation and at each time point following VILI.

Abbreviations: Sham, animals that received sham ventilation; Vent, animals that received low stretch ventilation; BAL, bronchoalveolar lavage.

Note: Open circles represent outlying data points.

* Significantly different from sham and low stretch ventilated animals ($P<0.05$, ANOVA and Student-Neuman-Keuls).

Figure 6-5 Fibroproliferation after VILI

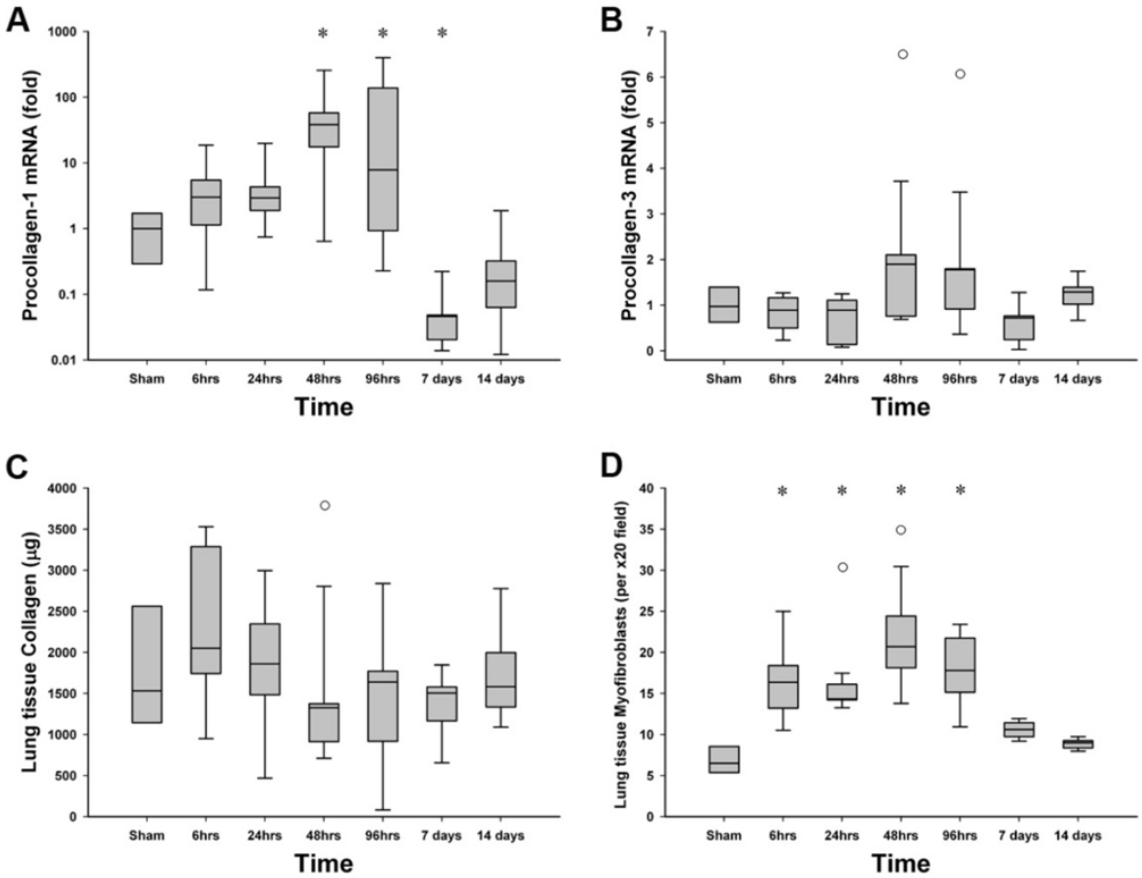

Figure 6-5

Panel A*:* Box plot representing lung tissue procollagen I mRNA content with sham and low stretch ventilation and at each time point following VILI.

Panel B*:* Box plot representing lung tissue procollagen III mRNA content with sham and low stretch ventilation and at each time point following VILI.

Panel C*:* Box plot representing lung tissue collagen content with sham and low stretch ventilation and at each time point following VILI.

Panel D*:* Box plot representing lung tissue myofibroblast counts with sham and low stretch ventilation and at each time point following VILI.

Abbreviations: Sham, animals that received sham ventilation; Vent, animals that received low stretch ventilation.

Note: Open circles represent outlying data points.

*** Significantly different from sham and low stretch ventilated animals (P<0.05, ANOVA Student-Neuman-Keuls).**

Figure 6-6 Collagen and myofibroblasts after VILI

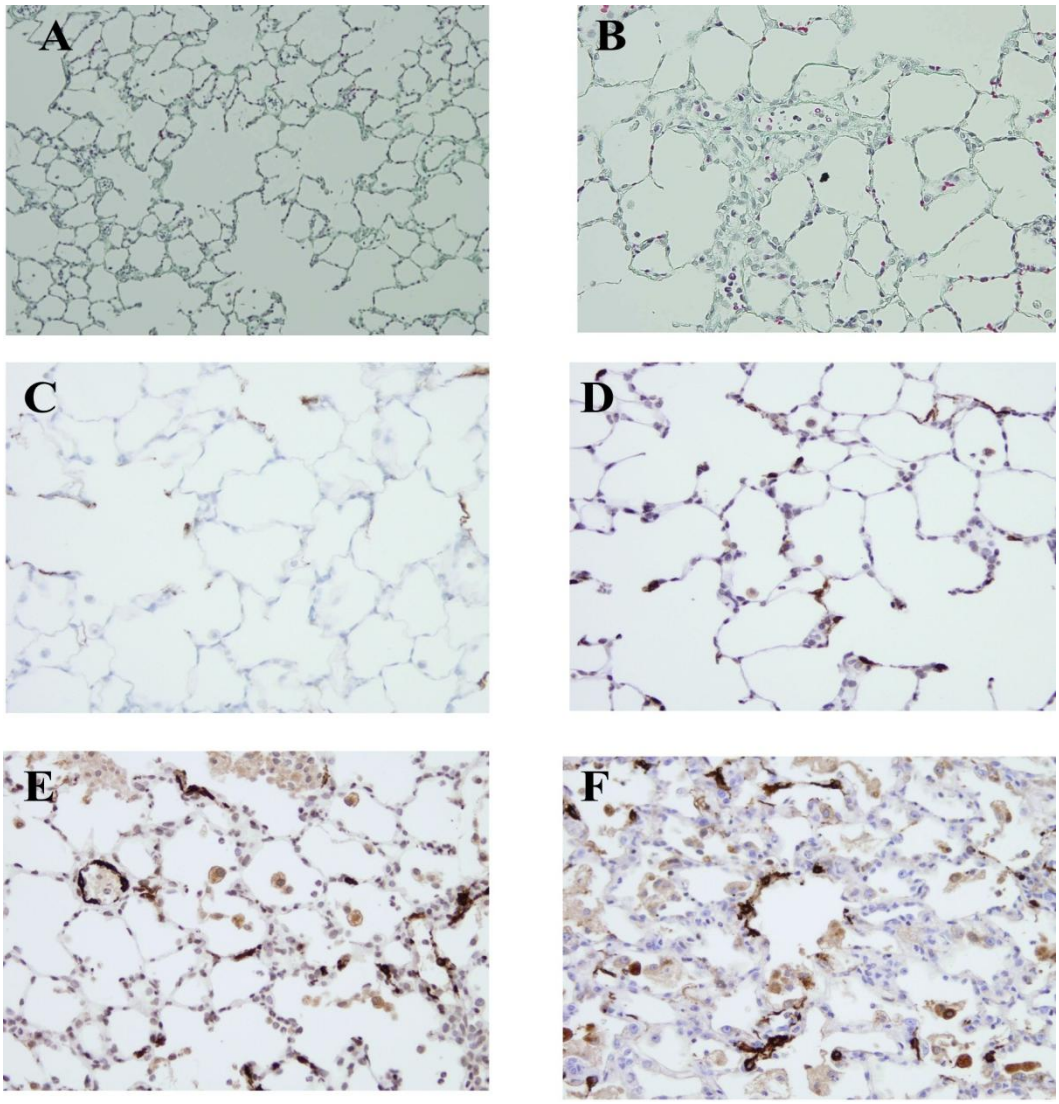

Figure 6-6

Panels A and B: Photomicrographs of representative masson trichrome stained sections of lung tissue. Panel A is an image from a sham uninjured lung, Panel B is from a lung 48 hours after injury

Panels C-F: Photomicrographs of representative alpha-smooth muscle actin immuno-stained sections of lung tissue. Panels C is from a sham ventilated animal, Panels D-F are from lungs at 6 hours, 24 hours and 48 hours, following VILI respectively.

Figure 6-7 Elastin after VILI

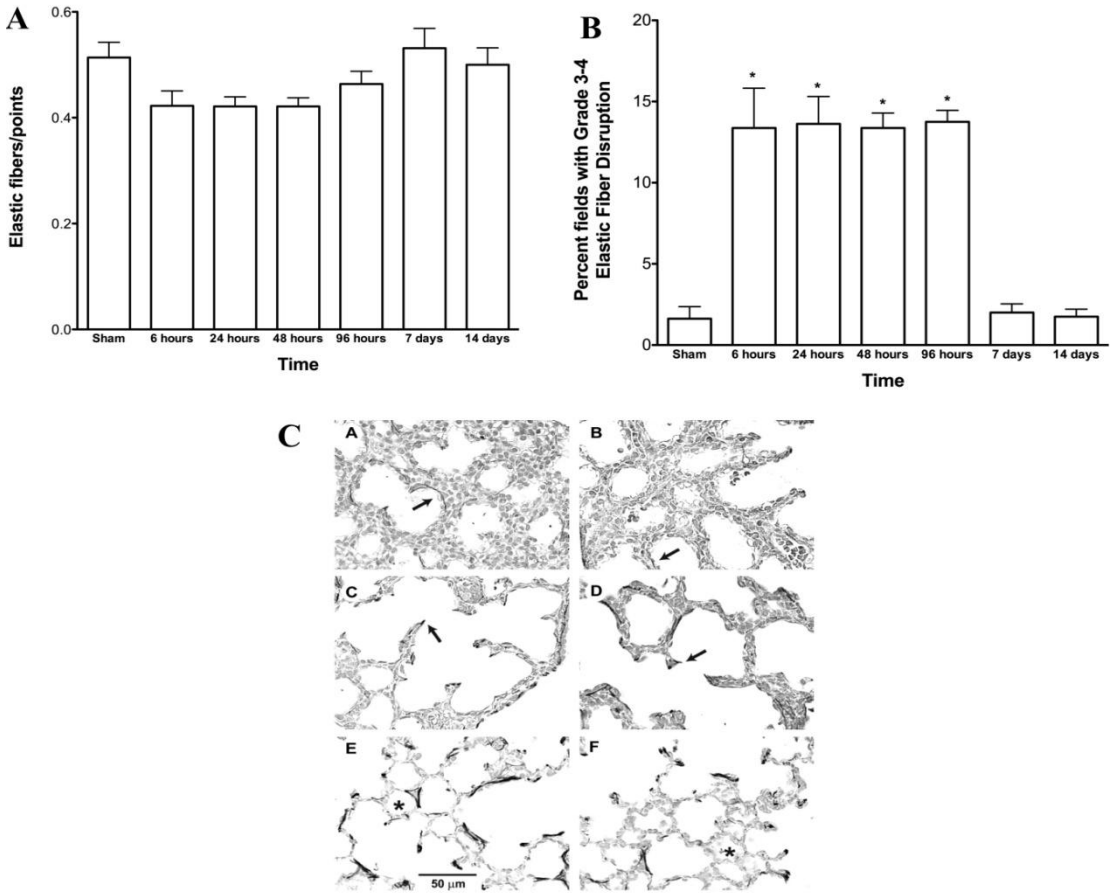

Figure 6-7

Panel A: Histogram representing ratio of elastic fiber per point count in lung tissue at different time points after VILI

Panel B: Histogram representing percentage lung fields graded as having either moderate or severely disrupted elastin stained fibers at different time points after VILI

Panel C: Photomicrographs of representative Van Gieson stained sections of lung tissue. Panels F is from a sham ventilated animal, Panels A-E are from lungs at 6 hours, 24 hours, 48 hours, 96 hours and 7 days following VILI respectively. Arrows indicate disrupted elastic fibers.

Figure 6-8 MMPs after VILI

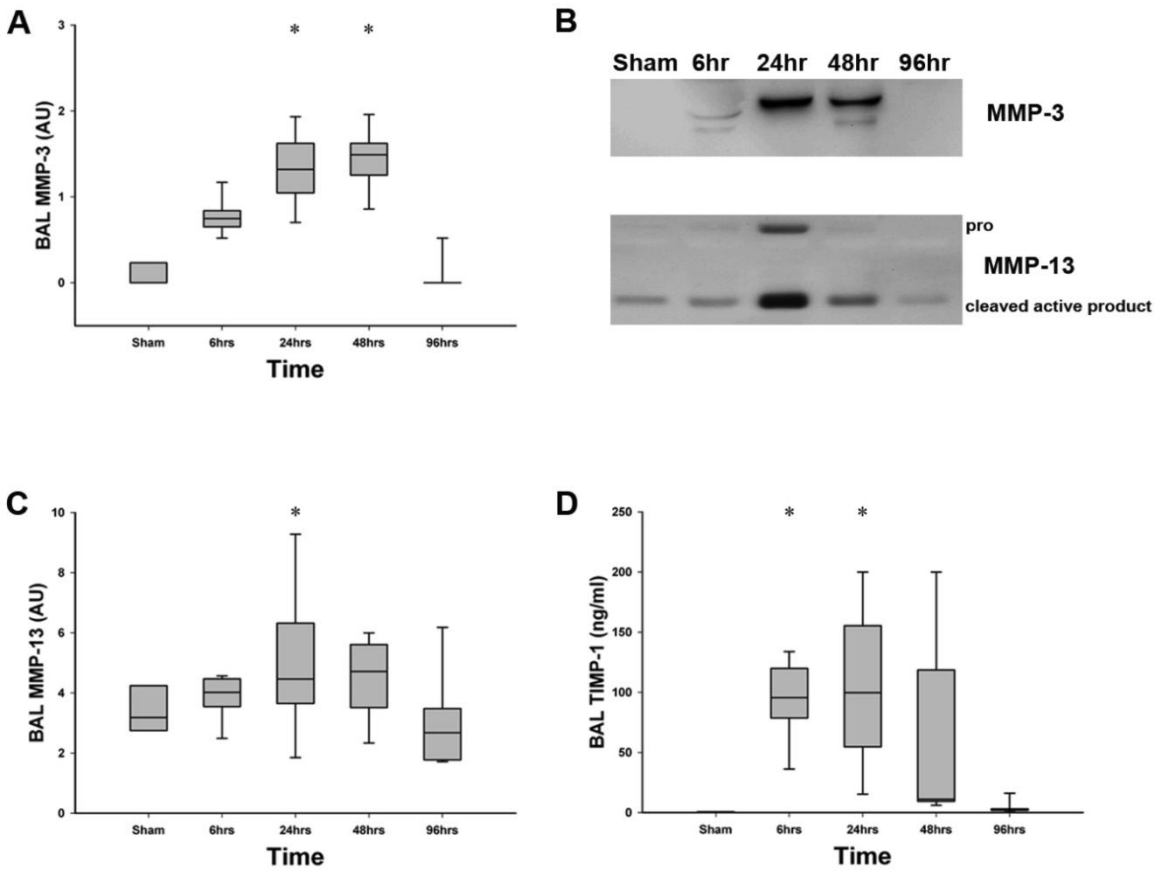

Figure 6-8

Panel A: Box plot representing bronchoalveolar lavage MMP-3 concentrations with sham and low stretch ventilation and at each time point following VILI.

Panel B: Representative western blot of bronchoalveolar lavage MMP-3 and -13 with sham and low stretch ventilation and at each time point following VILI.

Panel C: Box plot representing bronchoalveolar lavage MMP-13 concentrations with sham and low stretch ventilation and at each time point following VILI.

Panel D: Box plot representing bronchoalveolar lavage TIMP-1 concentrations with sham and low stretch ventilation and at each time point following VILI.

Abbreviations: Sham, animals that received sham ventilation; Vent, animals that received low stretch ventilation; BAL, bronchoalveolar lavage; AU, arbitrary units.

Note: Open circles represent outlying data points.

* Significantly different from sham and low stretch ventilated animals ($P<0.05$, ANOVA and Student-Neuman-Keuls).

Figure 6-9 MMPs in BAL after VILI

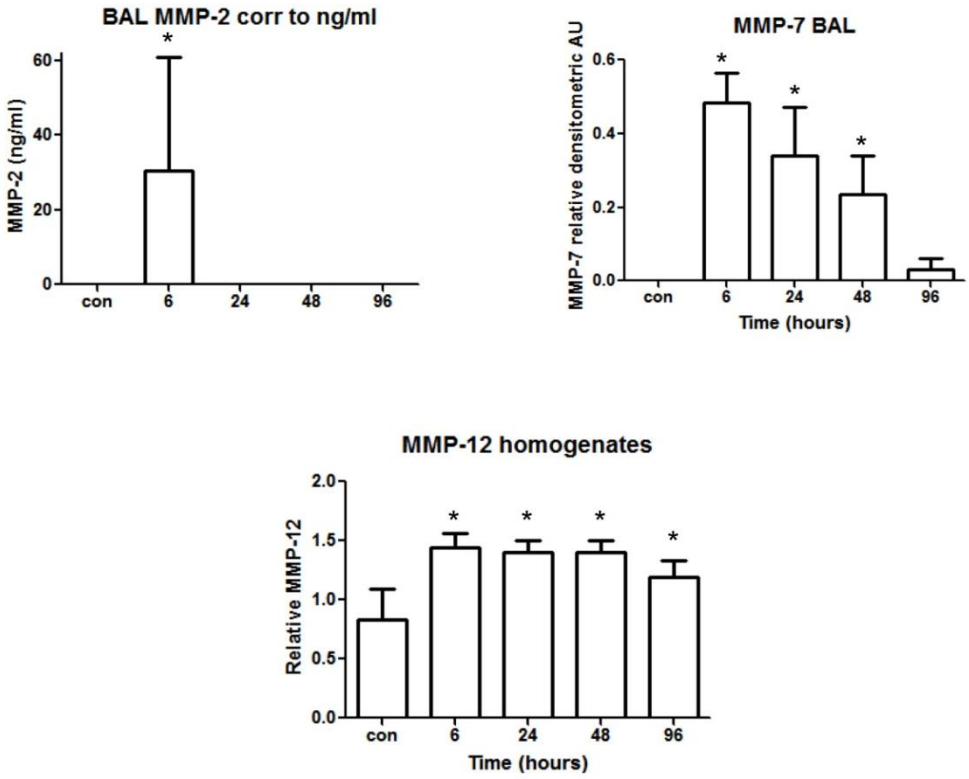

Figure 6-9

Panel A: Histogram representing concentration of MMP-2 in BAL at different time points (hours) after VILI

Panel B: Histogram representing concentration of MMP-7 in BAL at different time points (hours) after VILI

Panel C: Histogram representing concentration of MMP-12 in lung homogenate at different time points (hours) after VILI

* Significantly different from sham and low stretch ventilated animals ($P<0.05$, ANOVA and Student-Neuman-Keuls).

7.0 The role of Mesenchymal Stem Cells during recovery and resolution following Ventilator Induced Lung Injury

7.1 Abstract

Introduction: Recent pre-clinical experimental studies indicate that bone-marrow derived mesenchymal stem cells (MSCs) may reduce the severity of Acute Lung Injury (ALI). Intra-tracheal and systemic administration of MSCs reduced pulmonary oedema and pro-inflammatory cytokines, and improved survival in murine *E. coli* and systemic sepsis induced ALI. However the potential for MSC's to enhance repair and recovery following ALI is not known.

Objectives: We wished to evaluate the role of MSCs in modulating inflammation and enhancing repair after Ventilator Induced Lung Injury (VILI).

Methods: We used our animal model of repair from VILI to test the reparative properties of MSCs. Adult male Sprague Dawley rats were anaesthetised, orotracheally intubated and subjected to injurious mechanical ventilation to produce a severe ALI. Following recovery, the animals received two intravenous injections of MSCs (2 X 10^6 cells) immediately post injury and at 24 hours. Control animals received saline alone. Animals were harvested at 48 hours, and the extent of recovery following ALI was assessed. Subsequent experiments elucidated the mechanisms by which MSC's enhance repair, by examining the potential for non-stem cells, and for MSC secreted products, to enhance repair in comparison to MSCs.

Results: MSCs therapy enhanced repair following VILI. Specifically, MSCs improved oxygenation, lung compliance, reduced total lung water, decreased lung inflammation and histologic lung injury. MSC therapy attenuated alveolar TNF-alpha and IL-6 levels, but increased alveolar IL-10 concentrations. Conditioned MSC medium also enhanced lung repair and attenuated the inflammatory response to lung stretch.

Conclusion: MSCs can modulate the inflammatory response to VILI, enhance alveolar fluid clearance and augment repair in the lung. The therapeutic effect appears to be mediated through paracrine factors secreted by MSCs.

7.2 Introduction

Acute Lung Injury (ALI) and Acute Respiratory Distress Syndrome (ARDS) are devastating diseases with a mortality of up to 40% [342], and for which there are no therapies [343]. Mortality from ALI/ARDS has fallen [344], through both superior supportive care for sepsis, trauma and pneumonia, and the demonstation that mechanical ventilation, while necessary for survival, has the capacity to cause significant harm [77, 345]. The importance of Ventilator Induced Lung Injury is underscored by the fact that ventilation strategies that reduce lung stretch save lives [77, 345]. The mechanisms whereby ventilation contributes to lung injury are increasingly well understood [38, 346]. However, more recent attempts to adjust ventilation strategies to further reduce harm have met with limited success [78-80]. Even with contemporary low stretch strategies, it appears difficult to avoid regional areas of high lung stretch [81]. In addition, low stretch strategies may worsen atelectasis [85], which can also cause harm [86].

An alternative approach is to develop strategies that enhance lung repair following VILI. Mesenchymal stem cells (MSCs) are fibroblast-like cells characterized by their ability to self-renew and undergo differentiation into mesenchymal lineage cell types including bone, cartilage, adipose tissue, muscle and tendon [347]. MSCs can differentiate to several other cell types [160], but because MSCs produce important growth factors and cytokines, and may provide important cues for cell survival in damaged tissues, with or without direct

participation in long-term tissue repair, they have become major cellular candidates in attempts to heal an expanding list of tissues [348]. They are also one of the few normal cell types that have so far been produced in the large quantities needed for therapeutic development.

MSCs can be isolated from peripheral blood and can be found in increased numbers under stress of total body irradiation or hypoxia, implying that MSCs are part of the innate reparative response to injury, and that a natural trafficking signal to sites of tissue damage exists [142, 143]. Also, transplanted MSCs appear to target sites of injury and damage, including lung [117, 139, 140].

MSC immunomodulatory actions have been demonstrated in a wide range of disease states including sepsis, acute lung injury, acute myocardial ischemia, stroke, kidney injury, inflammatory bowel disease, graft-versus-host disease (GVHD), multiple sclerosis, diabetes mellitus, and organ transplantation [111, 171]. Clinical trials have been completed or are underway in several of these areas [172]. Although early, uncontrolled clinical case series provided exciting evidence of therapeutic benefits, the resulting optimism for off-the-shelf allo-MSC therapy has become tempered by the outcomes of recent, larger clinical trials in which allo-MSC products proved disappointing in terms of efficacy despite achieving safety endpoints [172].

On the other hand, the application of MSC therapy in human wounds show excellent results from studies in the last 3 years [349-351]. Recent studies have demonstrated that treatment of cutaneous wounds with MSCs accelerates wound healing kinetics and increases epithelialization and angiogenesis [349, 352, 353], suggesting that MSCs enhance wound repair by at least two different

mechanisms: differentiation and paracrine interactions with specific cell types in the cutaneous wound [354].

MSCs have demonstrated promise in a number of pre-clinical ALI/ARDS studies [96, 99, 120, 355-357] and appear to exert immuno-modulatory [194], anti-inflammatory [120] and regenerative [354] effects, and may orchestrate repair of diseased or injured tissues [358].

The potential for MSCs to augment wound healing and repair after stretch induced lung injury is not known. We hypothesized that MSCs would enhance functional and structural recovery after VILI. We further hypothesized that this effect would be mediated, at least in part, via MSC secreted soluble factors.

7.3 Methods

7.3.1 Mesenchymal Stem Cell Isolation and Culture

This is described in detail in Section 4.6.1. Briefly, mesenchymal stem cells were isolated from rat femora and tibiae under sterile conditions in the animal surgery room as previously described [257]. Cells were ready for subculture (usually after 16-17 days) when colonies began to exhibit a compact appearance and multi-layered growth or when the loosely formed colonies began to merge into a monolayer (<90% of confluence). Thereafter, cells were ready to be passaged after 6/7 days culture, at 80% confluence. Cells were expanded to passage 4, whereupon they were used for experiments. (See **Figure 7-1** for MSCs in culture.) MSCs were characterized according to international guidelines [115](**Section 4.6.3** and **Figures 4-1 and 4-2**).

7.3.2 Rat Dermal Fibroblasts

Dermal fibroblasts were isolated and cultured from adult male Sprague Dawley rats as described in Section 4.6.5.

7.3.3 Cryopreservation and thawing of rat MSCs and fibroblasts

To cryopreserve the cells, aliquots were re-suspended in Freezing Medium (90% FBS and 10% DMSO) and placed in the –80^{o}C freezer and from here into the vapor phase of liquid nitrogen of a Cryoplus 2 Storage container as described in Methods and Materials 4.6.8.

To thaw cryopreserved cells, vials were removed from liquid nitrogen vapour storage, placed in a 37 degree water bath and, together with rMSC Complete medium, were spun at 500g, washed in PBS and thereafter suspended in PBS for infusion.

7.3.4 Conditioned Medium

As described in detail in Section 4.6.6, allogeneic rat MSC (2×10^6) were cultured without serum for 24 h. The medium was then replaced, and the subsequent medium without serum for the next 24 h was used as the conditioned medium (CM). 15mls of this medium was concentrated using a 3000 KDa centrifugal concentrating filter (Amicon, Billerica, MA, USA) to give 500 microlitres.

7.3.5 Rodent Ventilator Induced Injury Protocol

As described in detail in Section 4.3, anesthesia was induced with intraperitoneal ketamine 80 $mg.kg^{-1}$ (Ketalar, Pfizer, Cork, Ireland) and xylazine 8 $mg.kg^{-1}$ (Xylapan, Vétoquinol, Dublin, Ireland). After confirmation of depth of anesthesia by paw clamp, intravenous access was obtained via tail vein, laryngoscopy was performed and the animals were intubated with a size 14G intravenous catheter (BD Insyte®, Becton Dickinson Ltd, Oxford, UK). The lungs were ventilated using a small animal ventilator (CWE SAR 830 AP, CWE Inc, Pennsylvania, USA). Anesthesia was maintained with repeated boli of Saffan® (alfaxadone 0.9% and alfadadolone acetate 0.3%; Schering Plough, Welwyn Garden City, UK) and muscle relaxation was achieved with cis-atracurium besylate $0.5mg.kg^{-1}$ (GlaxoSmithKline, Dublin, Ireland). The animals were then subjected to a high stretch mechanical ventilation protocol (Fi_{O2} 0.3, inspiratory pressure 35 cmH_2O,

respiratory rate 18 min^{-1}, and positive end-expiratory pressure 0 cmH_2O). When static compliance had decreased by 50%, high stretch ventilation was discontinued and animals were extubated, allowed to regain consciousness, and entered into the treatment protocol.

7.3.6 Assessment of Injury and Repair

As described in detail in Section 4.2, at 48 hours following VILI induction, animals were re-anesthetized. A tracheostomy was inserted and carotid arterial access established, and the lungs were mechanically ventilated (Model 683; Harvard Apparatus, Holliston, MA) at a respiratory rate of 80 min^{-1}, tidal volume 6 $ml.kg^{-1}$ and positive end-expiratory pressure 2 cmH_2O. Intra-arterial blood pressure, peak airway pressures and rectal temperature were recorded continuously. Static inflation lung compliance measurements were performed as previously described [251, 298]. After 20 minutes, the inspired gas was altered to a Fi_{O2} of 1.0 for 15 min, and a final arterial blood sample was taken. Heparin (400 $IU.kg^{-1}$, CP Pharmaceuticals, Wrexham, U.K.) was then administered intravenously, and animals were killed by exsanguination.

Immediately post-mortem, the heart–lung block was dissected and bronchoalveolar lavage (BAL) collection was performed as previously described [306, 359]. BAL differential cell counts were performed. Protein concentration was determined using a Micro BCA™ Protein assay kit (Pierce, Rockford, IL, USA).[300] BAL IL-1β, IL-6, TNF-α and IL-10 concentrations were determined using quantitative sandwich enzyme-linked immunosorbent assays (R and D systems, Abingdon, UK).[301]

Wet/dry lung weights were determined using the lowest lobe of the right lung as described in Section 4.4.1 [305]. The left lung was isolated and fixed for morphometric examination, and the extent of histologic lung damage was determined using quantitative stereological techniques as previously described [305, 306] and in Section 4.5.

7.3.7 Series 1: Determination of the immediate safety and tolerability of different doses of cryopreserved MSCs in uninjured ventilated rats

In this series, following induction of anaesthesia, intra-venous access, tracheostomy and carotid arterial access was established. Ventilation was commenced using "Baseline Ventilation" settings as described in Section 4.2.2. After 20 minutes of baseline ventilation, arterial blood gas analysis was performed and respiratory static compliance were assessed. Once baseline criteria were met (See Section 4.2.2), animals received a single dose of thawed MSCs, either $4x10^6$, $5x10^6$ or $6x10^6$, N=3 per group. Animals were ventilated for 4 hours, with hourly assessment of arterial blood gases and respiratory static compliance. Thereafter, the animals were sacrificed by exsanguination. Post-mortem, the right lower lobe was isolated for wet:dry ratio, and BAL was performed for total and differential cell count.

7.3.8 Series 2: Determination of the ongoing safety and tolerability of different doses of cryopreserved MSCs in uninjured ventilated rats

In a second series to determine the safety of MSCs, animals were anaesthetized, intravenous access was attained via tail vein, and the animals were oro-

tracheally intubated using a 14G canula. After 90 minutes of baseline ventilation, animals were given intra-venous injections of either $4x10^6$ or $5x10^6$ thawed MSCs, N=3 per group. The animals were then recovered and extubated. Once fully awake, they were returned to their cages. At 48 hours after injury, assessment of injury and repair was carried out as described above and in General Methods.

7.3.9 Series 3: Determination of safety and tolerability of different doses of cryopreserved MSCs in VILI injured rats

In this series, animals were anaesthetized, intravenous access was established via tail vein, and the animals were orotracheally intubated with a 14G canula. After 20 minutes of baseline ventilation (see Section 4.2.2), the animals were subjected to injurious high stretch ventilation, with ventilator settings Pinsp 35 cmH_2O, RR 18, PEEP 0 cmH_2O and FIO_2 0.3. Once compliance had decreased by 50%, injurious ventilation was discontinued and the animals were recovered and extubated. On recovery, the animals received injections of either $4x10^6$ MSCs or $5x10^6$ MSCs. Once fully awake they were returned to their cages. At 48 hours after injury, assessment of ongoing injury and repair was carried out as described above and in General Methods.

7.3.10 Series 4: Determination of safety and tolerability of divided doses of cryopreserved MSCs in VILI injured rats

In this series, animals were anaesthetized, intravenous access was established via tail vein, and the animals were orotracheally intubated with a 14G canula. After 20 minutes of baseline ventilation (see General Methods), the animals were

subjected to injurious high stretch ventilation, with ventilator settings Pinsp 35 cmH_2O, RR 18, PEEP 0 cmH_2O and FIO_2 0.3. Once compliance had decreased by 50%, injurious ventilation was discontinued and the animals were recovered and extubated. On recovery, the animals received injections of $2x10^6$ MSCs. Once fully awake they were returned to their cages. At 24 hours post injury, the animals were anaesthetized again, the tail vein was canulated, and a further injection of $2x10^6$ MSCs was administered. The animals were once again returned to their cages. 48 hours after injury, assessment of ongoing injury and repair was carried out as described above and in General Methods.

7.3.11 Series 5: Determination of potential for cryopreserved MSCs to enhance repair post VILI

In this series, animals were anaesthetized, the tail vein was canulated, and injurious ventilation was commenced via oro-tracheal canula. The animals were injured until their compliance fell by 50%. The animals were then recovered. Once animals were awake and self ventilating they were randomly allocated to receive a tail vein injection of either: (1) 2×10^6 of thawed cryopreserved MSCs suspended in 500μL PBS; or (2) 500μL PBS alone, and were returned to cages. 24 hours later they received a second injection of thawed cryopreserved MSCs, or vehicle, and the extent of repair following VILI assessed at 48 hours.

7.3.12 Series 6: Determination of potential for non-cryopreserved MSCs to enhance repair post VILI

Animals were anaesthetized and injured by mechanical ventilation as above, until compliance fell by 50%. They were then recovered. Once animals were

awake and self ventilating, they were randomly allocated to receive a tail vein injection of either: (1) 2 x 10^6 allogeneic non-cryopreserved rat MSCs suspended in 500µL PBS; or (2) 500µL PBS alone, and were returned to their cages. 24 hours later they were re-anaesthetized, the tail vein was cannulated, and a second injection of MSCs, or vehicle was administered. The animals were once again recovered and returned to their cages, and the extent of repair following VILI assessed at 48 hours.

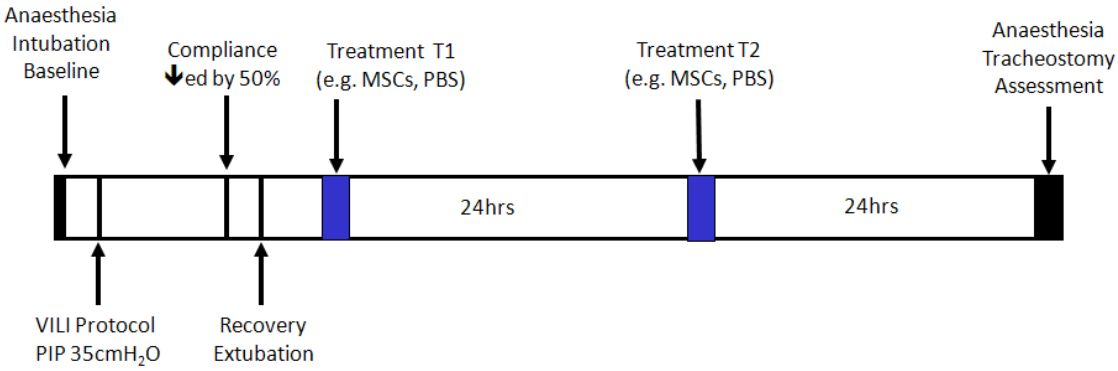

7.3.13 Series 7: Determination of the mechanism by which MSCs enhance repair

In this series, animals were injured via mechanical ventilation until lung compliance was reduced by 50%. Once animals were awake and self-ventilating, they were randomly allocated to receive a tail vein injection of either: (1) 2 x 10^6 non-cryopreserved MSCs suspended in 500µL PBS; (2) 500µL PBS; (3) 2 x 10^6 rat dermal fibroblasts suspended in PBS; or (4) 500µL of conditioned medium, and were returned to cages. 24 hours later they were re-anaesthetized, and a

second injection of MSCs, vehicle, fibroblasts or medium was administered. The extent of recovery and repair following VILI was assessed at 48 hours.

7.3.14 Statistics

The distribution of all data was tested for normality using Kolmogorov-Smirnov tests. Results are expressed as mean (± SD) for normally distributed data, and as median (interquartile range, IQR) where non-normally distributed. Data were analyzed by one-way ANOVA followed by Dunnets test, or by one-way ANOVA on ranks followed by Dunns test, with the vehicle group as the control group in each analysis. Comparisons between 2 groups were made using unpaired, two-tailed Student's t tests. Underlying model assumptions were deemed appropriate on the basis of suitable residual plots. A two-tailed p value of <0.05 was considered significant.

7.4 Results

7.4.1 Series 1: Determination of the immediate safety and tolerability of different doses of cryopreserved MSCs in uninjured ventilated rats

Animals tolerated the three different doses of MSCs, with no change in peak airway pressure, mean arterial pressure or respiratory static compliance **(Figure 7-3A)**. There was no perturbation in arterial blood gas measurements throughout the 4 hour duration of the protocol **(Figure 7-3B)**. Post-mortem, wet:dry ratios and inflammatory cell counts were indistinguishable from that of uninjured ventilated controls **(Figure 7-3C and D)**.

7.4.2 Series 2: Determination of the ongoing safety and tolerability of different doses of cryopreserved MSCs in uninjured ventilated rats

Animals tolerated the two different doses of MSCs and all survived to 48 hours. Assessment of injury and repair at 48 hours revealed no derangement in arterial blood gases or lung compliance, and no change in wet:dry ratio or inflammatory cell infiltration **(Figure 7-4)**.

7.4.3 Series 3: Determination of safety and tolerability of different doses of cryopreserved MSCs in VILI injured rats

12 animals were entered into this study, N=6 per group. 5 animals in each group died after the injection of MSCs. 4 in the $4x10^6$ group, and 4 in the $5x10^6$ group died immediately after injection of MSCs. 1 in the $4x10^6$ group survived for 2 hours, and 1 in the $5x10^6$ group survived for 6 hours.

7.4.4 Series 4: Determination of safety and tolerability of divided doses of cryopreserved MSCs in VILI injured rats

4 animals were entered into this study. All animals tolerated the injections of MSCs after injury, and at 24 hours post injury.

7.4.5 Series 5: Determination of potential for cryopreserved MSCs to enhance repair post VILI

Cryopreserved MSCs (cpMSCs) were stored in the vapour phase of liquid nitrogen. They were thawed on the morning of administration and injected post injury suspended in PBS. cpMSCs resulted in reduced inflammatory cell infiltration in lung tissue overall, and reduced neutrophil infiltration, from 1.0249 x 10^5/ml to 0.4592 x 10^5/ml ($P<0.05$) **(Figure 7-5A)**. cpMSCs also improved alveolar fluid clearance as measured by wet:dry ratio **(Figure 7-5B).** However, other measures of functional improvement, including Alveolar-arterial oxygen gradient and respiratory static compliance, were unchanged by cpMSCs **(Figure 7-5C and D)**.

7.4.6 Series 6: Determination of potential for non-cryopreserved MSCs to enhance repair post VILI

MSCs improve arterial oxygenation and lung static compliance: Arterial oxygenation was restored in the group that received MSCs, as measured by Alveolar-arterial oxygen gradient ($p<0.05$). **(Figure 7-6A)** Further functional recovery in lung physiology in response to rMSC treatment after VILI was

demonstrated by significant improvements ($p<0.01$) in respiratory system static compliance in comparison to vehicle controls **(Figure 7-6B).**

***MSCs enhance recovery of microvascular permeability*:** Pulmonary edema and total protein in BAL fluid were assessed 48 hr after VILI as measures of lung injury and vascular leak. VILI-injured rats displayed substantial pulmonary edema as indicated by an increased lung wet/dry weight ratio. Treatment with rMSCs significantly decreased the pulmonary edema 48 hrs post injury ($p<0.05$) **(Figure 7-6C)**. A similar pattern was seen in the total protein concentrations in BAL fluid **(Figure 7-6D),** consistent with a decrease in microvascular permeability.

MSCs decrease lung Inflammation: The total cell count in the BAL fluid was increased approximately 2-3 fold 48 hr after VILI (data not shown)**.** A significant portion of this increase was due to infiltration of neutrophils. MSCs resulted in reduced inflammatory cell infiltration in lung tissue overall, and reduced neutrophil infiltration, from 7.377×10^4/ml to 1.183×10^4/ml ($P<0.05$) **(Figure 7-7A)**.

To determine if rMSCs also affected expression of cytokines important in VILI, BAL fluid was analyzed by ELISA. Treatment with MSCs after VILI resulted in a significant decrease in TNF-α in BAL ($p<0.05$), with a non-significant downward trend in IL-6 levels. IL-10 levels were elevated in the group that received cell therapy ($p<0.05$), a finding consistent with other work in the field **(Figure 7-7B,C and D)**.

MSCs decrease histologic injury: Quantitative stereological analysis demonstrated that there was significant recovery in MSC treated rats in terms of alveolar tissue volume fraction or alveolar air-space volume fraction **(Figure 7-8)**

7.4.7 Series 7: Determination of the mechanism by which MSCs enhance repair

Conditioned medium from MSCs enhanced recovery following VILI to an extent comparable to that seen with MSC therapy. Animals that received MSCs and conditioned medium demonstrated functional improvements after VILI in terms of respiratory system static compliance ($p<0.01$) in comparison to vehicle and fibroblast controls **(Figure 7-9A).** MSCs and MSC conditioned medium administration also reduced lung total cell and neutrophil infiltration **(Figure 7-9B)**. These effects were accompanied by significant reductions in BAL IL-6 and TNF-α **(Figure 7-9C and D)** in the MSC and conditioned medium groups, and significant increases in serum but not BAL levels of IL-10 **(Figure 7-9E).**

7.5 Discussion

MSCs can be isolated from several sources, most commonly the bone marrow [360] but also placenta, adipose tissue, and human cord blood, periosteum, synovial fluid, muscle, hair follicles, root of deciduous teeth, articular cartilage, placenta, dermis, umbilical cord Wharton's jelly, lung, liver and spleen [171, 347]. From an immunologic perspective, allogeneic MSC are usually well tolerated by the host and have a low immunogenicity pattern because of constitutive low expression of MHC I and II proteins, and, in general, the lack of T-cell costimulatory molecules, such as CD80 and CD86 [234]. In addition, MSCs can be rapidly expanded *in vitro* while maintaining their multipotent properties [358]. The interest in MSCs as cellular therapy arises from numerous *in vivo* studies showing that MSCs avoid allorecognition, home to sites of injury, and suppress inflammation as well as immune responses. Preclinical studies have established that mesenchymal stem cell therapy may be effective for acute lung injury based on studies with endotoxin administered directly into the lungs of rodents [355] or into the perfused human lung [137]. Based on mouse studies, bone marrow-derived mesenchymal stem cells may be beneficial in sepsis [96, 120]. Here we have examined the effects and mechanisms of action of MSCs in a mechanical stretch induced model of ALI; specifically we look at both functional recovery and mechanistic aspects of MSC therapy, in a non-sepsis induced model of lung injury.

7.5.1 MSCs and dose

A major question surrounding the use of MSCs in clinical trials relates to appropriate dosing. What is the optimal dose of MSCs to gain maximum benefit

in a particular disease? Should there be repeated dosing, and how often and how far apart should these be? Increasing the dose brings with it the danger of embolic phenomena, especially in lung, and attendant right ventricular strain. In these studies we demonstrate the safety of MSC doses of up to $6x10^6$ in healthy uninjured rats. However, even doses of $4x10^6$ were not tolerated in animals after VILI. This is likely due to increased right ventricular strain in the setting of pulmonary oedema in VILI, and provides a note of caution in extrapolating doses used in other medical conditions such as Crohn's disease or myocardial infarction to the setting of ALI.

7.5.2 MSCs and immunomodulation

MSCs reduce the severity of organ injury as well as enhance recovery in this rodent model of Ventilator Induced Lung Injury. A major characteristic of MSC has been the immunomodulatory properties of the cells. Multiple studies have demonstrated that MSC possess potent immunosuppressive effects by inhibiting the activity of both innate and adaptive immunity, by effects on T cells, B cells, dendritic cells, monocytes, neutrophils, and macrophages [177, 194, 211, 361]. In this model MSC therapy potently inhibited inflammatory cell infiltration, specifically neutrophillic infiltration, into the lung after stretch induced lung injury. Neutrophil infiltration mediates many of the destructive effects of ALI, through release of oxygen free radicles, NO intermediates, pro-inflammatry cytokines. MSC therapy reduced TNF-α and IL-6 levels in BAL, two markers of disease severity, as well as orchestrators of injury in themselves.

The beneficial effect of MSCs on improved lung function following VILI was accompanied by an increase in BAL IL-10 levels, suggesting a role for IL-10 in

mediating the recovery in this model. IL-10 is a cytokine secreted predominantly by monocytes that downregulates the expression of TH1 cytokines, MHC class II antigens and costimulatory molecules on macrophages. IL-10 has also been reported to inhibit the rolling, adhesion and transepithelial migration of neutrophils [362]. In a model of sepsis following cecal ligation and puncture (CLP) in mice, Nemeth *et al*. [120] found that bone-marrow-derived MSCs, activated by LPS or TNFα, secreted prostaglandin E2, which reprogrammed alveolar macrophages to secrete IL-10. The beneficial effect of MSCs on mortality and improved organ function following sepsis (CLP) was eliminated by macrophage depletion or pretreatment with antibodies to IL-10 or the IL-10 receptor. In a model of acute lung injury by intratracheal *E. coli* endotoxin in mice, Gupta et al [355] found that intrapulmonary MSC improved survival and lung injury in association with a decrease in MIP-2 and TNFα levels in the bronchoalveolar lavage fluid (BAL) and elevated levels of IL-10 in both the plasma and BAL fluids.

7.5.3 MSCs and alveolar barrier function

Impaired alveolar fluid clearance (AFC, i.e., the resolution of pulmonary edema) is common in patients with ALI/ARDS. The level of AFC impairment has significant prognostic value in determining morbidity and mortality [363, 364]. Our results demonstrate that MSCs improved AFC and reduced levels of pulmonary oedema after VILI. Recently, the ability of human MSCs to restore alveolar epithelial fluid transport and lung fluid balance via secretion of KGF was demonstrated in an elegant study employing an *ex vivo* perfused human lung preparation injured by *E. coli* endotoxin [137].

MSCs reduced protein concentrations in BAL fluid after VILI. Another possible mechanism through which MSC may be beneficial is through therapeutic effects on the injured lung endothelium. The integrity of the lung microvascular endothelium is essential to prevent the influx of protein-rich fluid from the plasma as well as inflammatory cells which may further aggravate the ability of the lung epithelium to reduce alveolar edema. Several paracrine soluble factors, such as Ang1 and KGF, are potentially important in these effects [365].

These effects on alveolar fluid clearance and barrier permeability may mediate much of the functional improvement after VILI, manifest by improved oxygenation and an increase in respiratory system static compliance. Further improvement in function may come from including alveolar epithelial type II cell hyperplasia and differentiation, surfactant production [366], anti-apoptotic effects [367] and increased transcription and/or translation of the major sodium and chloride transport proteins [368, 369].

7.5.4 MSC secreted mediators

Interestingly, the cultured medium of the MSCs was also effective in improving recovery from VILI. The cultured medium improved respiratory static compliance, reduced inflammatory cell infiltration of the lung and reduced BAL pro-inflammatory cytokine levels. These findings appear to suggest that paracrine factors secreted by MSCs play a critical beneficial role in mediating recovery from VILI. Bone marrow derived MSC are known to produce several epithelial specific growth factors and other bioactive molecules such as KGF, PGE2, HGF, EGF, TGF-β1, sTNFR1, Ang1 and STC-1 that may also contribute to the immunomodulatory functions as well as enhance repair of injured lung [120,

240, 355, 370-373]. Recently, the ability of human MSCs and their conditioned medium to restore alveolar epithelial fluid transport and lung fluid balance via secretion of KGF was demonstrated in an elegant study employing an *ex vivo* perfused human lung preparation injured by *E. coli* endotoxin [137]. Our findings further corroborate this evidence.

A more precise understanding of the mechanisms underlying the therapeutic effect of MSCs in models of lung injury is needed. While most investigators have invoked both the immunomodulatory and growth factor production properties of MSCs to explain the protective effects, the exact mechanisms responsible for these effects remain unclear. For example, MSCs secrete or induce production of a variety of soluble factors such as IL-10, PGE2, TGF-β, KGF and others, but it is not known which of these factors is essential to the protection provided by MSCs. In addition, another major question is whether the effect is produced predominantly through cell-contact-dependent or -independent mechanisms or both, and whether or not the functional behavior of the cells changes depending on the alveolar milieu. Answering these questions will determine whether the effect of MSCs can be replicated with a mixture of recombinant soluble factors secreted by MSCs or with MSC-conditioned medium alone. Our study adds to the accumulating evidence that secreted paracrine factors are responsible for the therapeutic effects of MSCs. Furthermore, we have shown that these cells and their secreted factors are reparative in a non-sepsis mediated model of lung injury.

7.5.5 Cryopreservation of MSCs

Finally, formulating a cryopreservation protocol for MSCs is required because these cells cannot survive for long periods under *in vitro* culture conditions. Slow rate cooling methods using dimethylsulfoxide (DMSO) as a cryoprotectant have been used for a wide variety of MSC lines established from bone marrow [374]. Slow freezing reduces ice crystal formation and eliminates toxic and osmotic damage to cells through exposure to low concentrations of cryoprotectants while slowly decreasing temperatures [375]. However, it is difficult to completely eliminate injury by intracellular ice formation. Resuscitated MSCs can be subcultivated for many passages without a noticeable loss of viability and capability of osteogenic differentiation [376]. However, the effects of immediate injection post cryopreservation, and whether cells require a period of time in culture to activate them, or avoid senescence, is unknown. Here, we show that cryopreserved MSCs retain the ability to reduce inflammatory cell infiltration into the lung and enhance alveolar fluid clearance; these effects occur without any observable functional improvements, such as on gas exchange or respiratory system compliance, effects which were observed in animals who received MSCs fresh from culture in series 6 and 7. These results indicate that a period of time in culture may be necessary to activate these cells after cryopreservation, and have implications for the conduct of clinical trials of MSCs as cell therapy for ALI.

7.5.6 Conclusion

In conclusion, we have shown that bone marrow-derived MSCs enhance recovery after VILI when administered into the systemic circulation of the VILI injured rat. The mechanism for this effect is largely due to the secretion of paracrine soluble factors by the MSCs themselves. Our data show, to our knowledge for the first time, that MSC therapy may represent an innovative approach for treatment of VILI and ARDS, which continue to be a major cause of morbidity and mortality in critically ill patients.

7.6 Figures

Figure 7-1 MSC differentiation

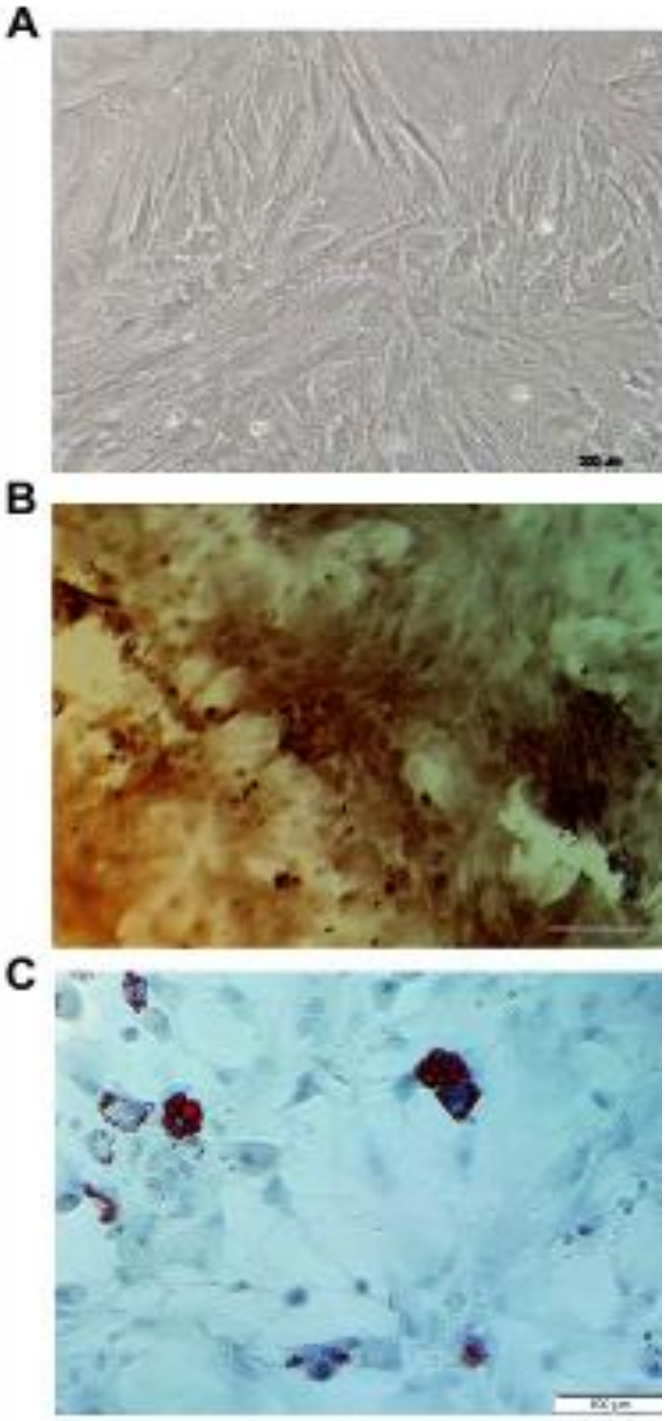

Figure 7-1: Differentiation of rat MSCs

Passage 2 bone marrow (BM)-derived adherent cells (Figure 4-1A), after culture in differentiation medium, were stained for alizarin red (Osteogenic staining, Figure 4-1B), oil red O (Adipocyte staining, Figure 4-1C) and safranin O (Chondrocyte staining, data not shown). All experiments were performed in triplicate.

Figure 7-2 MSC characterisation

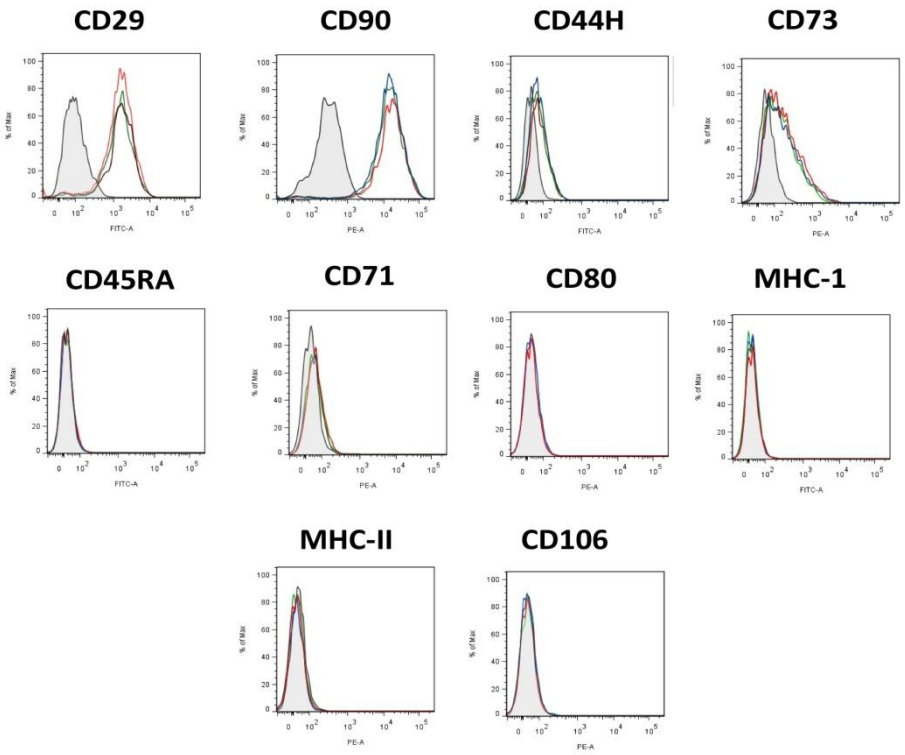

Figure 7-2: Characterization of surface markers on rat MSCs

The rat MSCs used in these studies were CD29, CD90, CD44H, CD73 positive and CD45RA, CD71, CD80, MHCI, MHCII, CD106 low or negative. Shown are FACS histograms of Sprague Dawley MSCs (passage 3) stained with antibodies against surface markers as indicated (colored) or with appropriate isotype controls (gray). Each colored line indicates replicates.

Figure 7-3 Safety and tolerability of MSCs

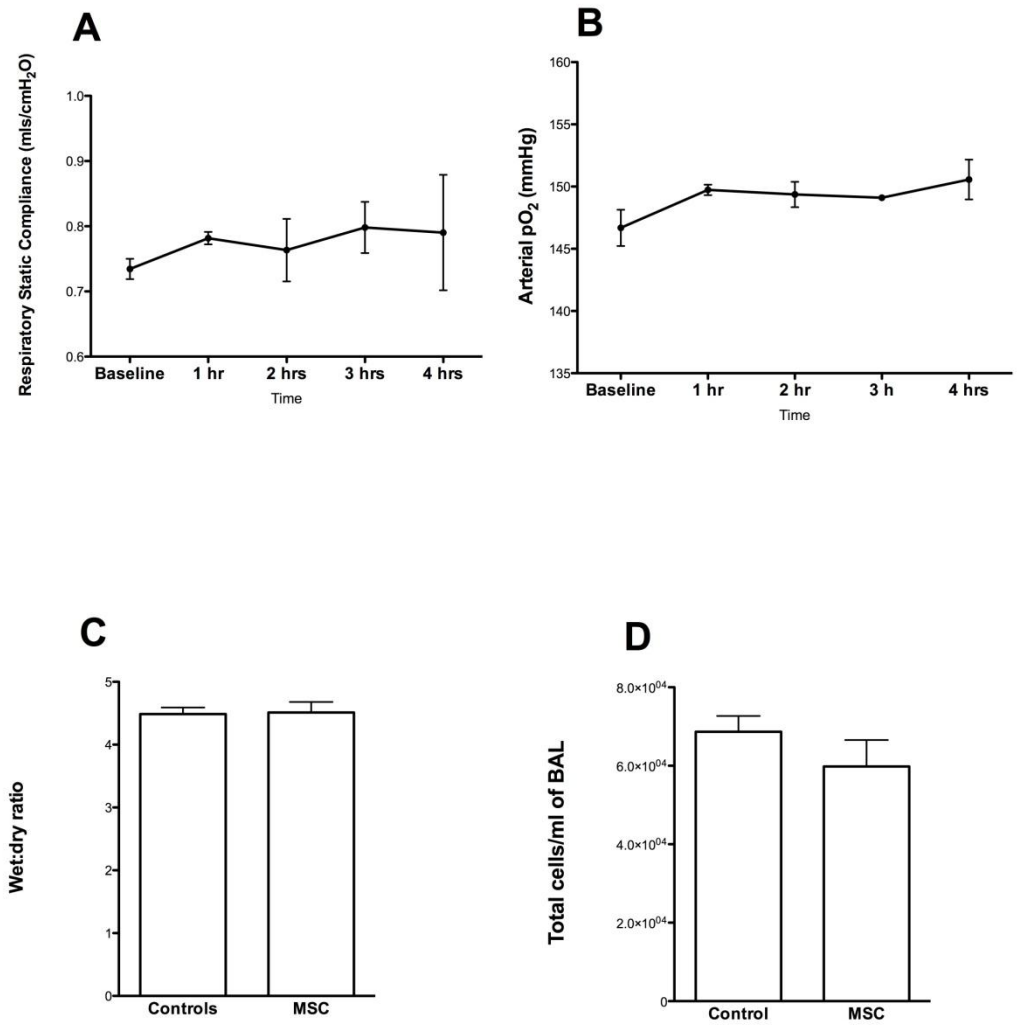

Figure 7-3

***Panel A*:** Line graph representing static lung compliance of rats during protective lung ventilation and after receipt of MSCs

***Panel B*:** Line graph representing arterial oxygen partial pressures of rats during protective lung ventilation and after receipt of MSCs

Panel C: Histogram representing wet:dry weight ratios of lungs of rats after receipt of MSCs and 4 hours of protective lung ventilation

Panel D: Histogram representing total inflammatory cells in BAL of rats after receipt of MSCs and 4 hours of protective lung ventilation

Abbreviations: BAL, bronchoalveolar lavage, MSCs, mesenchymal stem cells

Figure 7-4 Safety and tolerability of MSCs

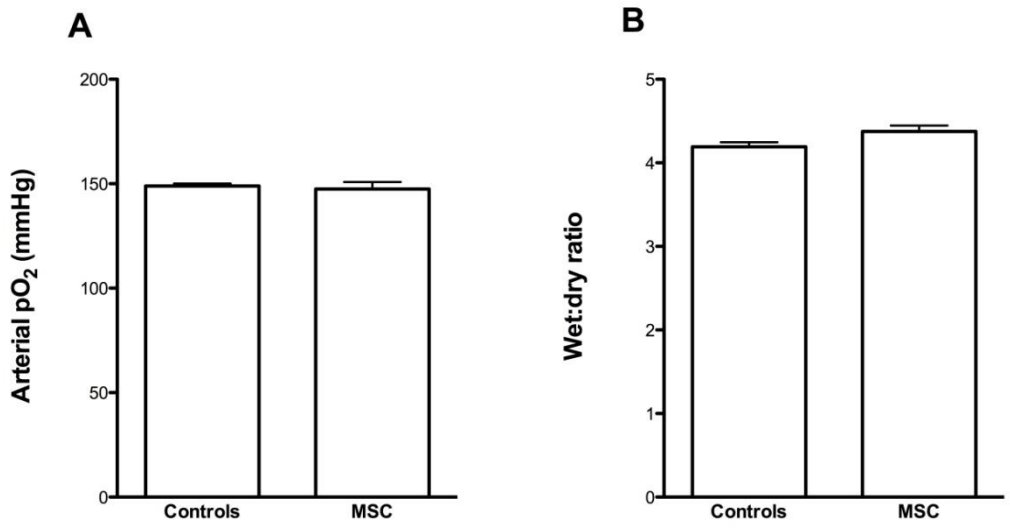

Figure 7-4

Panel A*:** Histogram representing arterial oxygen partial pressures of rats 48 hours after receipt of MSCs***

***Panel B*:** Histogram representing wet:dry weight ratios of lungs of rats 48 hours after receipt of MSCs

Abbreviations: MSCs, mesenchymal stem cells

Figure 7-5 MSCs improve physiologic variables after VILI

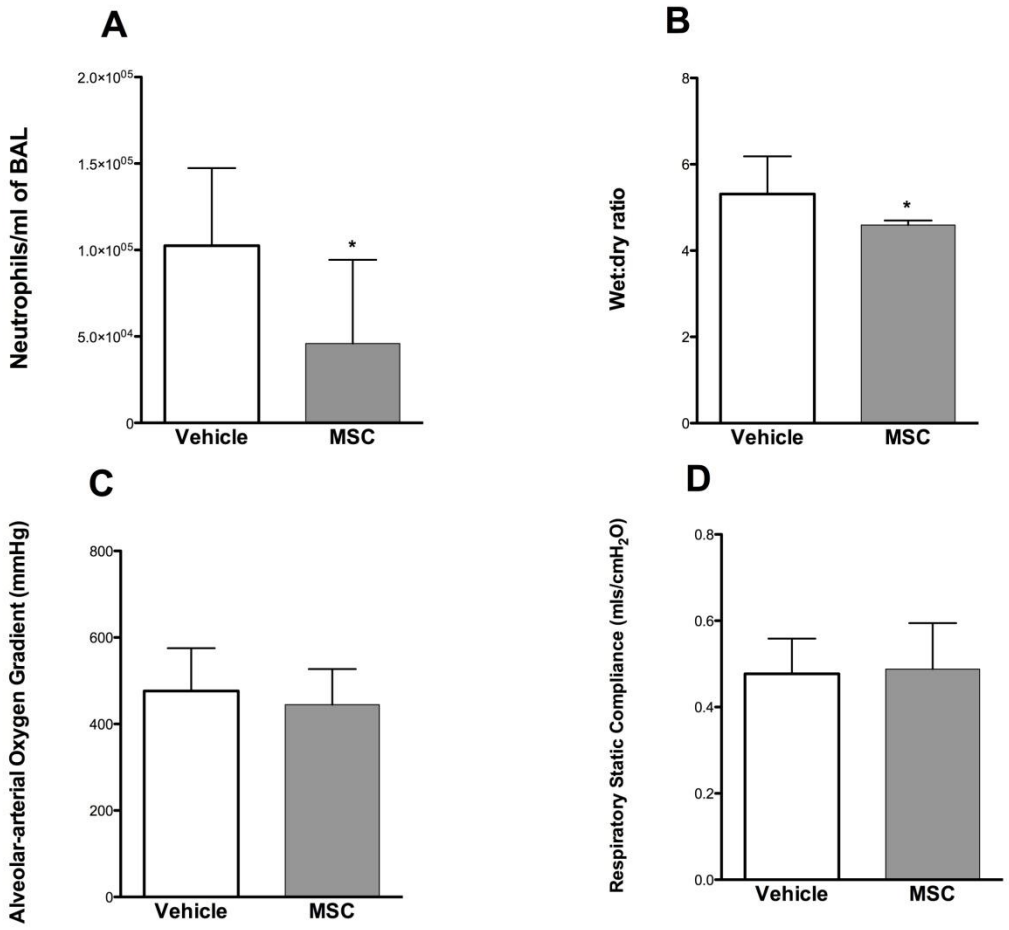

Figure 7-5

***Panel A*:** Histogram representing neutrophils in BAL of rats 48 hours after being subject to VILI.

***Panel B*:** Histogram representing lung wet:dry weight ratios of rats 48 hours after being subject to VILI.

Panel C: Histogram representing Alveolar-arterial oxygen gradient in rats 48 hours after being subject to VILI

Panel D: Histogram representing respiratory static compliance in rats 48 hours after being subject to VILI

Abbreviations: Vehicle, animals that received phosphate buffered saline; MSC, animals that received divided doses of mesenchymal stem cells

* Significantly different from vehicle ($P<0.05$, Students t test)

Figure 7-6 MSC therapy enhances resolution following Ventilation induced Lung Injury

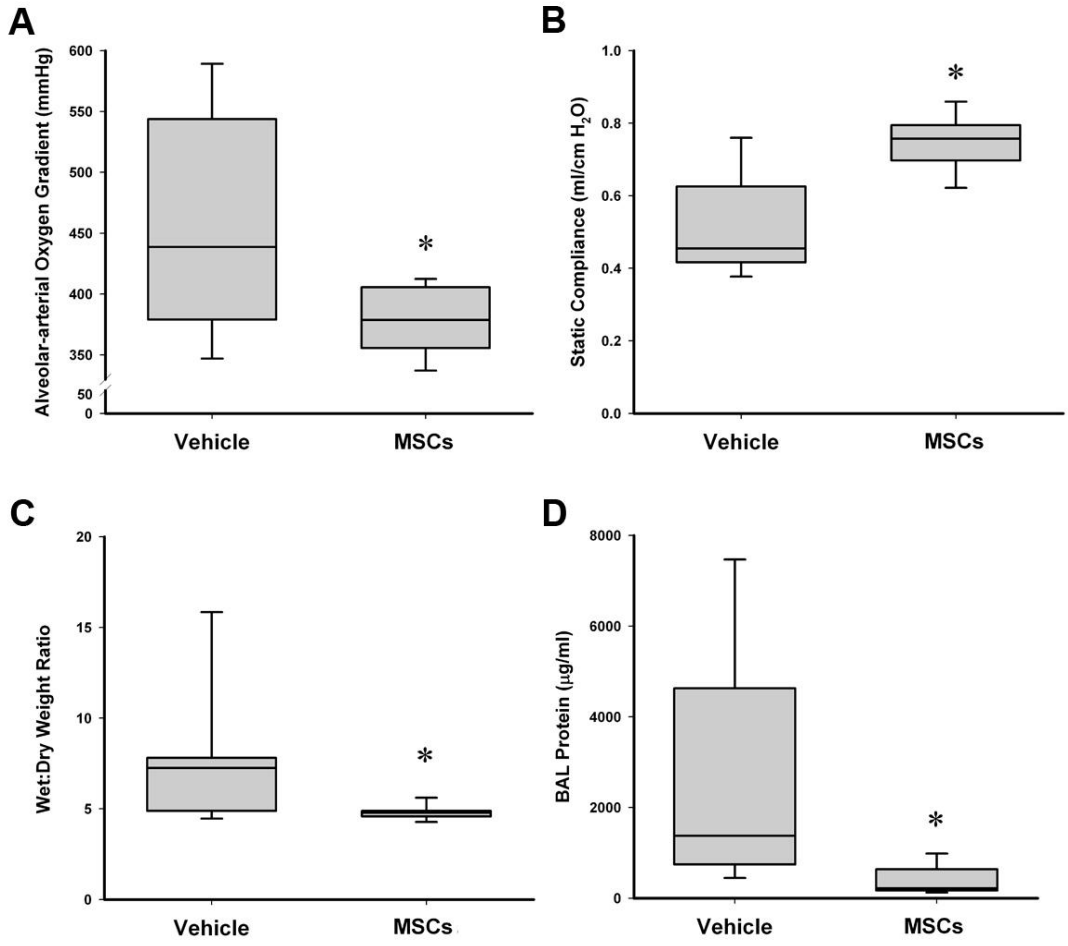

Figure 7-6: MSC therapy enhances resolution following Ventilation induced Lung Injury. MSC therapy decreased alveolar-arterial oxygen gradient **(Panel A),** increased static lung compliance **(Panel B),** and reduced lung wet:dry weight ratios **(Panel C**), and BAL protein concentrations **(Panel D),** 48 hours following induction of severe stretch induced lung injury, compared to vehicle.

Abbreviations: Vehicle: animals that received vehicle; MSCs, animals that received MSCs. BAL: bronchoalveolar lavage.

* Significantly ($P<0.05$) different from vehicle, Students-t test.

Figure 7-7 MSC therapy modulates the inflammatory response to VILI

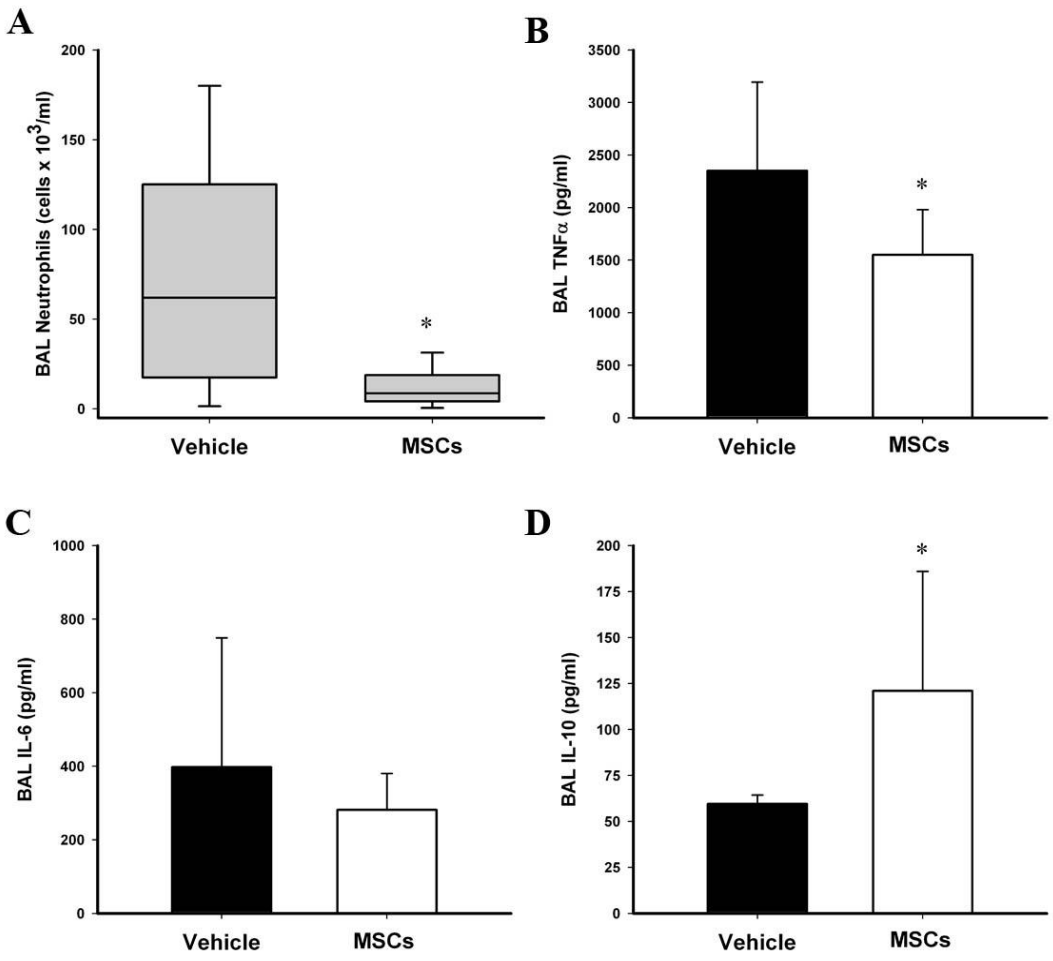

Figure 7-7: MSC therapy modulates the inflammatory response to VILI.

MSC therapy decreased BAL neutrophil counts **(Panel A),** and BAL TNF-a concentrations **(Panel B)**, did not alter BAL IL-6 concentrations **(Panel C)**, and increased BAL IL-10 **(Panel D)** concentrations, 48 hours following induction of severe stretch induced lung injury, compared to vehicle

Abbreviations: Vehicle: animals that received vehicle; MSCs, animals that received MSCs. BAL: bronchoalveolar lavage.

* Significantly ($P<0.05$) different from vehicle, Students-t test.

Figure 7-8 MSC therapy enhances the resolution of structural lung injury following VILI

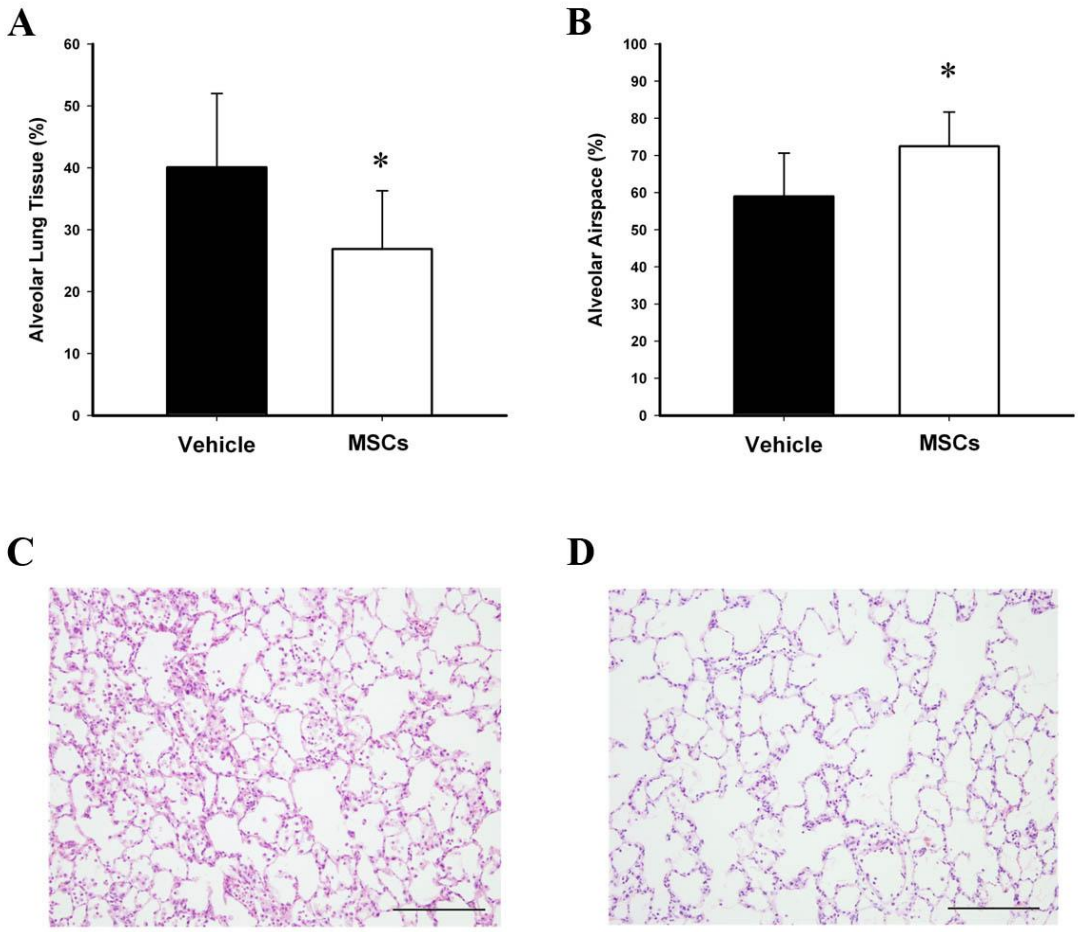

Figure 7-8: MSC therapy enhances the resolution of structural lung injury following VILI. MSC therapy enhanced resolution of histologic injury as evidenced by decreased alveolar lung tissue **(Panel A)** and increased alveolar airspace fraction **(Panel B)**. Representative photomicrographs of lung from a vehicle treated **(Panel C),** and MSC treated **(Panel D)** animal demonstrate greater resolution of lung injury with MSCs at 48 hours. Scale bar is 200mm Abbreviations: **Vehicle: animals that received vehicle; MSCs, animals that received MSCs. BAL: bronchoalveolar lavage.**

*** Significantly (P<0.05) different from vehicle.**

Figure 7-9 MSCs exert benefits via a paracrine mechanism

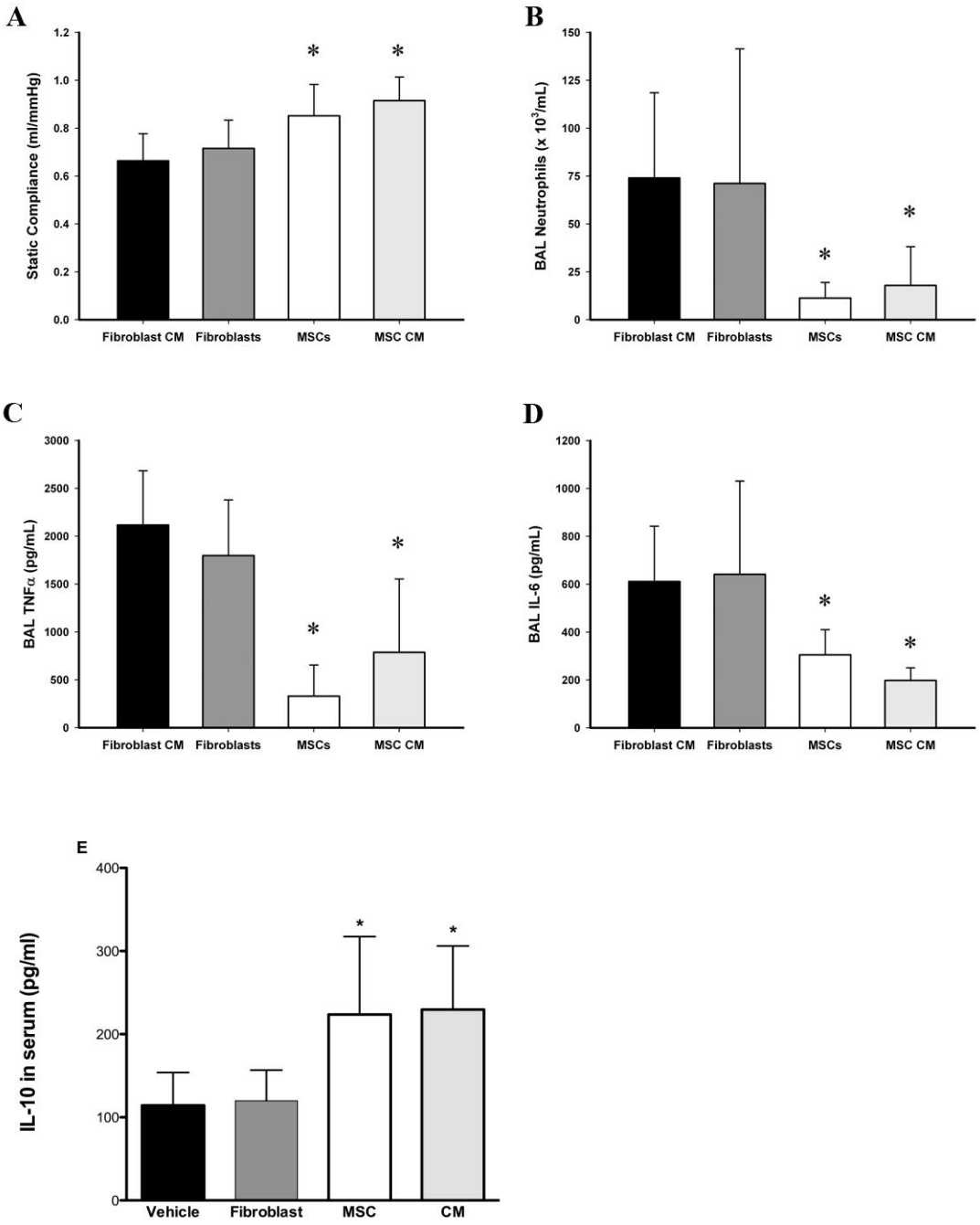

Figure 7-9: MSCs exert benefits via a paracrine mechanism

Both MSCs and MSC conditioned medium enhanced recovery of static lung compliance **(Panel A)**, decreased BAL neutrophil counts **(Panel B)** and BAL TNF-alpha **(Panel C)** and BAL IL-6 **(Panel D)**and increased serum IL-10 **(Panel E)** concentrations 48 hours following injury compared to animals that received fibroblasts or vehicle.

Abbreviations: Fibroblast CM: animals that received fibroblast conditioned medium; Fibroblasts: animals that received fibroblasts; MSCs, animals that received MSCs. MSC CM: animals that received MSC conditioned medium; BAL: bronchoalveolar lavage; TNF-α, tumor necrosis factor-a; IL-6, interleukin-6

* Significantly ($P<0.05$) different from Fibroblast CM and fibroblast groups (ANOVA and Student-Neuman-Keuls).

8.0 The investigation of the effects of mesenchymal stem cells in pulmonary epithelial wound repair in vitro

8.1 Abstract

Introduction: In patients with acute lung injury (ALI) or acute respiratory distress syndrome (ARDS), extensive damage to the alveolar epithelial and endothelial barrier is observed, resulting in the influx of protein-rich oedema fluid into the air spaces. Efficient alveolar epithelial repair is crucial to ALI/ARDS patients' recovery. MSCs and their conditioned medium can enhance repair in other organs, but their ability to enhance wound repair in the lung is unknown. While MSCs and MSC conditioned medium are effective in enhancing recovery after Ventilator Induced Lung Injury (VILI) in rodents, the precise mediator(s) responsible for this effect remains unclear.

Methods: We tested the ability of MSCs and their conditioned medium to enhance repair in A549 epithelial monolayer scratch wounds. We used different time periods for wound repair, and generated conditioned medium over different time periods, and in conditions of hypoxia, in order to maximize the reparative effects. We then used monoclonal antibodies to candidate mediators in MSC conditioned medium gain insight into specific repair mechanisms.

Results: MSCs and their conditioned medium were twice as effective in healing alveolar epithelial wounds in comparison to fibroblasts and their conditioned medium controls. Antibodies to Keratinocyte Growth Factor, but not Hepatocyte Growth Factor, or Transforming Growth Factor-β, attenuated this effect on alveolar epithelial repair of MSC conditioned medium.

Conclusion: These results suggest that the ability of MSCs to enhance recovery after Ventilator Induced Lung Injury may in part be due to their abiltiy to enhance alveolar epithelial wound repair, and that this mechansim may result wholly or in part from the secretion of Keratinocyte Growth Factor by MSCs.

8.2 Introduction

Injury to the lung epithelium may be caused by viral and bacterial infection, inflammation and oxidative stress, allergic reactions, physical trauma (as in mechanical ventilation), cancer or pathology of unknown origin [377]. In order to maintain effective lung function and to prevent progressive infection and further damage, any epithelial injury must be repaired, and epithelial integrity restored, as quickly as possible. In health, this process is likely to happen continuously at a background level in order to maintain homeostasis. However, in acute lung injury, the repair processes may not be able to adequately offset the injurious process, and aberrant repair causes a failure to restore normal epithelial integrity, leading to loss of lung function. Moreover, the processes characterizing lung injury and repair are modulated by ongoing external pro-injurious or anti-injurious stimuli (e. g. ongoing infection, Ventilator Induced Lung Injury or/and resuscitation) and are a result of genetic factors [378]. Repetitive biochemical and biophysical stimuli not only play a role in the natural history of ALI/ARDS but, when treated, can lead to improved clinical outcomes [47].

Wound repair is a complex, highly orchestrated process with numerous levels of control that operate in synchrony to facilitate physiological wound repair [379]. Dysregulation at any stage of this process could cause pathological wound repair, which may be critical in the pathophysiology of a number of lung diseases, including ALI [89]. Owing to the complex and often pleiotropic nature of factors in the wound process, it is likely that any therapeutics developed will have to be highly targeted towards specific cell populations, as well as temporally and spatially accurate.

Abundant evidence demonstrates the therapeutic potential of bone marrow-derived multipotent mesenchymal stromal cells for repair and regeneration of damaged tissue due to injury or disease. Indeed, MSCs ameliorate tissue damage in almost all of the major organs of the body including heart, brain, lung, liver, kidney, eye and skin [380]. Differentiation and paracrine signaling have both been implicated as mechanisms by which MSCs improve tissue repair [348]. Current data suggest that the contribution of MSC differentiation is limited due to poor engraftment and survival of MSCs at the site of injury [117]. Much of the current research now focuses on defining the MSC secretome and identifying the target cells at the site of injury that are responsive to MSC paracrine signaling [381].

Owing to issues of scale, it becomes progressively more difficult to investigate wound resolution in the lower regions of the bronchial tree. This issue regarding the lack of suitable models is not small airway and alveolar specific, as the entire field of pulmonary epithelial wound repair research is limited by a lack of suitable models. The majority of wounding work has been carried out in animal skin and corneal models or in human cells in vitro, partly due to the ease of access and visualization. We utilized the best available model of alveolar epithelial injury and repair in vitro to assess the efficacy of MSCs and their conditioned medium.

We hypothesized that MSCs in co-culture, and their conditioned medium, would enhance repair in alveolar epithelial monolayers subjected to wound scratch injury. We also investigated the mechanisms of this enhanced repair with the use of antibodies to candidate mediators secreted by MSCs.

8.3 Methods

8.3.1 MSC Harvest and Cell Culture

Human MSCs were aspirated from the iliac crests of healthy human volunteers as described in Section 4.6.2. Cells were thawed and expanded in tissue-cultured treated flasks (Sarstedt) at a density of 500,000 cells/150 cm2. Cells were passaged every 3– 4 days by trypsinization when they reached 70 – 80% confluence and used for the experimental protocols between passages 2 and 3. Between each passage, viability was measured with trypan blue exclusion. MSCs were cultured in α-minimum essential medium (MEM) without ribonucleosides or deoxyri- bonucleosides containing 2 mM L-glutamine, 10% FBS, penicillin, and streptomycin. Primary human lung fibroblasts and A549 lung adenocarcinoma cells were obtained from American Type Culture Collection (ATCC), the A549s as cryopreserved 90 passage culture and used at passages 91-95. MSCs were characterized according to international guidelines [115] (See **Figure 7-1** and **7-2** and Section 4.6.3). Cells were cultured in a humidified incubator at 5% CO_2 and 37°C under sterile conditions.

8.3.2 MSC co-culture

To study the effects of MSC and wound repair on the A549 monolayers injured by wound scratch, we developed a co-culture system with the Transwell inserts (0.4μm pore size and collagen I-coated, Costar, Corning) in 24-well plates. Mesenchymal stem cells were seeded at $3x10^3$ cells/cm^2 in the inserts and maintained in MSC medium for 6 days prior to co-culture, which allowed the

mesenchymal stem cells to reach 70–80% confluence in an undifferentiated state. Stem cell containing inserts were then added to the A549 scratched wells and flooded with fresh medium. Controls consisted of primary human fibroblasts seeded at 1×10^3 cells/cm^2 in a cell culture insert and maintained in medium for 6 days prior to co-culture.

8.3.3 Conditioned Medium

Human or rodent MSCs and fibroblasts (2×10^6) were washed and cultured without serum for 24 h. The cells were again washed and the subsequent serum-free medium for the next 24, 48 or 72 hours was used as the conditioned medium (CM). Cells were also cultured in hypoxic conditions (FIO_2 0.02) (See Section 4.6.7).

8.3.4 Wound Repair Experiments

This model is described in detail in Section 4.7. Briefly, single wounds were made in confluent A549 monolayers in 24 well plates with a 1000μL pipette tip [255]. Wounds were exposed to different conditions as per group allocation, for different time periods.

In ***the first experiment*** wounds were incubated in (i) MEM-α medium, (ii) 24 hour exposed human fibroblast conditioned medium, (iii) 24 hour exposed human MSC conditioned medium, or (iv) co-cultured with MSCs, or co-cultured with fibroblasts. Wounds were exposed to these conditions for 48 hours.

In ***the second experiment*** wounds were incubated in (i) MEM-α medium, (ii) 48 hour exposed human fibroblast conditioned medium, (iii) 48 hour exposed human MSC conditioned medium, or (iv) co-cultured with MSCs. Wounds were exposed to these conditions for 48 hours.

In ***the third experiment*** wounds were incubated in (i) MEM-α medium, (ii) 72 hour exposed human fibroblast conditioned medium, (iii) 72 hour exposed human MSC conditioned medium, or (iv) co-cultured with MSCs. Wounds were exposed to these conditions for 48 hours.

In ***the fourth experiment*** wounds were incubated in (i) MEM-α medium, (ii) 48 hour exposed human fibroblast conditioned medium, (iii) 48 hour exposed human MSC conditioned medium, or (iv) co-cultured with MSCs. Wounds were exposed to these conditions for 72 hours.

In ***the fifth experiment*** MSC conditioned medium was incubated with monoclonal antibodies to inactivate keratinocyte growth factor (KGF), hepatocyte growth factor (HGF) and transforming growth factor–β (TGF-β) (Abcam, Cambridge, UK) respectively. Antibody concentrations were according to the manufacturers instructions to achieve maximum neutralization. A549 wounds were exposed to MSC conditioned medium with and without antibodies to each candidate mediator, and the extent of wound closure assessed at 48 hours.

Wounds were exposed to MSC conditioned medium with and without antibodies to each candidate mediator. At 48 hours, the extent of epithelial restitution was determined (Photoshop v8.0, Adobe Systems Inc, San Jose, California).

8.3.5 Assessment of wound repair

At 48 or 72 hours later, the monolayers were fixed with 4% paraformaldehyde in PBS (w/v), and stained with hemotoxylin and eosin. The extent of epithelial restitution was determined by imaging each plate on a flatbed scanner and assessing the area of each wound using edge-finding software (Photoshop v8.0, Adobe Systems Inc, San Jose, California). Additional detail in regard to these cell lines and the wound assessment technique is provided in Chapter 2.

8.3.6 Statistical Analysis

Data was analyzed using Sigma Stat (San Jose, California, USA). The distribution of all data was tested for normality using Kolmogorov-Smirnov tests. Data were analyzed by one-way ANOVA followed by Dunnets test, or by one-way ANOVA on ranks followed by Dunns test, with the vehicle group as the control group in each analysis. Comparisons between 2 groups were made using unpaired, two-tailed Student's t tests. A two-tailed p value of <0.05 was considered significant.

8.4 Results

8.4.1 MSC conditioned medium enhances A549 wound closure

MSC–CM increased the rate of wound closure in alveolar epithelial A549 monolayers subjected to scratch injury in comparison to fibroblast CM and fresh medium controls **(Figure 8-1A)**. The rate of wound closure seen with MSC conditioned medium was similar to that seen in MSC co-cultures **(Figure 8-1A)**.

8.4.2 48 hour and 72 hour conditioned medium does not provide additional benefit to A549 wound closure than 24 hour conditioned medium

48 and 72 hour MSC–CM increased the rate of wound closure in alveolar epithelial A549 monolayers subjected to scratch injury in comparison to fibroblast CM and fresh medium controls **(Figure 8-1B)**. The rate of wound closure seen with 48 and 72 hour MSC conditioned medium was not superior to that observed with 24 hour CM (**Figure 8-1B**).

8.4.3 Wounds exposed for longer periods to MSC conditioned medium continue to have enhanced wound closure

In wounds exposed to MSC–CM for 72 hours, the beneficial effect continued, resulting in almost complete wound closure in some wells, in contrast to wounds incubated with fresh medium or fibroblast conditioned medium **(Figure 8-2A)**.

8.4.4 Conditioned medium produced from cells grown in hypoxia does not enhance A549 wound repair

MSC–CM produced during exposure of MSCs to hypoxia did not increase the rate of wound closure in alveolar epithelial A549 monolayers subjected to scratch injury in comparison to fibroblast CM and fresh medium controls **(Figure 8-2B)**.

8.4.5 MSCs enhance pulmonary epithelial wound repair via a KGF dependent mechanism

In subsequent studies, prior incubation of MSC-CM with antibodies to neutralize KGF attenuated its beneficial effects on wound repair (**Figure 8-3**). In contrast, incubation of MSC-CM with antibodies to neutralize HGF and TGF-β did not alter wound repair (**Figure 8-3**). MSC and fibroblast conditioned medium were assayed for the concentration of KGF. Our MSC-CM contained over five times more KGF than that secreted by fibroblasts over a 24 hour period **(Figure 8-4)**.

8.5 Discussion

Repair, remodeling, and regeneration of the respiratory system for the restoration of normal function after injury represent the holy grail of modern pulmonary biology. After injury, lung epithelium may either activate the necessary repair and regeneration pathways for proper repopulation of lost epithelial cells or undergo an aberrant remodeling and differentiation process, which represents the final common pathway for many types of parenchymal pulmonary diseases, including idiopathic interstitial pneumonia, autoimmune-related fibrosis, and bleomycin pulmonary toxicity, to the chronic obstructive pulmonary diseases (COPDs), including emphysema and chronic asthma as well as late phases of ALI/adult respiratory distress syndrome (ALI/ARDS) [382]. The above results provide a therapeutic basis for the use of mesenchymal stem cells to influence alveolar epithelum toward repair after injury. A promising therapeutic approach may be to use stem cells, or their secreted mediators, to regenerate or repair the damaged lung. Much work has been done on the potential for exogenous stem cells including mesenchymal stem cells, endothelial progenitor cells and embryonic stem cells to restore alveolar barrier function in the injured lung [383]. A multicenter Phase II trial of MSCs (Prochymal®, Osiris Therapeutics Inc., Columbia, US) is currently in progress for patients with moderate to severe COPD (NCT00683722), underlining the therapeutic potential of exogenous stem cells.

8.4.1 How does the lung repair itself?

While the healthy lung can effectively regenerate and repair itself, this regenerative capacity may diminish with age and with repeated challenge, such as during disease. In addition, disorders or failure of lung regeneration may contribute to the pathogenesis of several lung diseases.

Mammalian tissue regeneration appears to involve several mechanisms, including but not limited to compensatory hyperplasia, de-differentiation and adult stem cells. The emerging picture is that different organs use different strategies to renew themselves, and that more diversity and flexibility underpin these renewal processes than previously imagined. Some organs, such as hair follicles, blood and gut, which constantly renew themselves throughout life, contain adult stem cells that are morphologically unspecialized, have a relatively low rate of division and are topologically restricted to localized regions known as 'niches' that tightly regulate their behaviour [90]. In the intestine, for example, only a few stem cells are present near the base of the crypts, which appear to be responsible for replenishing the entire epithelium. In contrast, the adult lung normally regenerates very slowly [91]. However, when injury to the lung does occur, particularly if widespread, it has to be repaired rapidly if the organism as a whole is to survive. The need to rapidly regenerate an organ that normally regenerates slowly may pose particular difficulties.

For the most part, cell lineage tracing studies and the analysis of mouse lung injury models suggest that the adult lung epithelium is maintained by divergent progenitor cells residing in discrete microenvironmental niches along the proximal-distal axis of the respiratory tree [91], consistent with the existence of a "nonclassical" stem cell hierarchy in which relatively quiescent differentiated progenitor cells function as facultative stem cells [92]. In the proximal lung

(trachea and main bronchi) it is likely that undifferentiated basal cells can function as classical stem cells, both self-renewing and giving rise to ciliated and secretory cells. In the more distal lung, where there are no basal cells, the evidence suggests that subpopulations of Clara cells in specific micro-environments can self-renew and give rise to different cell types after injury. In the alveoli, the site of major injury during ALI, damaged type I cells can be restored from type II cells, although whether all type II cells have this capacity is not yet known [91]. MSCs may be able to modulate this process, through secretion of paracrine factors, one of which we have confirmed to be Keratinocyte Growth Factor.

8.4.2 How is KGF involved in repair of injured lung?

Keratinocyte Growth Factor (KGF) was first isolated from a human embryonic lung fibroblast line by Rubin et al. [384] in 1989. Unlike other members of the FGF family, KGF has epithelial specificity; KGF is expressed predominantly by mesenchymal cells, and its receptor (KGF receptor; KGFR) is expressed only in epithelial cells. This epithelial specificity suggests that KGF may play an important role in mesothelial-epithelial interactions [385].

The protective effect of exogenous KGF has been demonstrated in a variety of acute lung injury models. Panos et al. [386] pre-treated rats intratracheally with 5 mg/kg of recombinant human KGF. They had far better survival and virtually no histological changes when exposed to 120h of hyperoxia compared with untreated animals. Intratracheal KGF has since been shown to have a protective effect in lung injury induced by acid instillation [387], in an ANTU model of increased permeability pulmonary edema [369, 388], and in a rat model of

ventilator-induced lung injury [389]. Intratracheal KGF has also been shown to ameliorate radiation pneumonitis [390], bleomycin-induced lung injury [391], and Pseudomonas aeruginosa pneumonia [392], when given before the insult.

KGF has a wide variety of effects on lung epithelial cells that may mediate its protective effect in acute lung injury. One of the earliest observations was that both in vivo and in vitro administration of KGF cause alveolar epithelial type II cell proliferation [393, 394]. In vivo, intratracheal administration in rats stimulates reproducible type II cell hyperplasia that peaks at 2 days. Proliferation of type II cells is accompanied by migration to cover the alveolar epithelial barrier with type II cells, a process that histologically resembles reactive type II hyperplasia seen in human lungs after an injurious stimulus [395].

8.4.3 Summary and conclusion

Therefore, the activity of MSC-CM on scratch wound closure may more readily be attributed to stimulation of cell migration and/or proliferation, or perhaps even survival. There are several MSC secreted growth factors and chemokines that are likely targets for this stimulatory activity of wound closure in A549 scratch assays, although our experiments with the use of neutralising antibodies to KGF identify this factor as particularly relevant in this regard.

8.5 Figures

Figure 8-1 MSCs and MSC conditioned medium enhance pulmonary epithelial wound closure

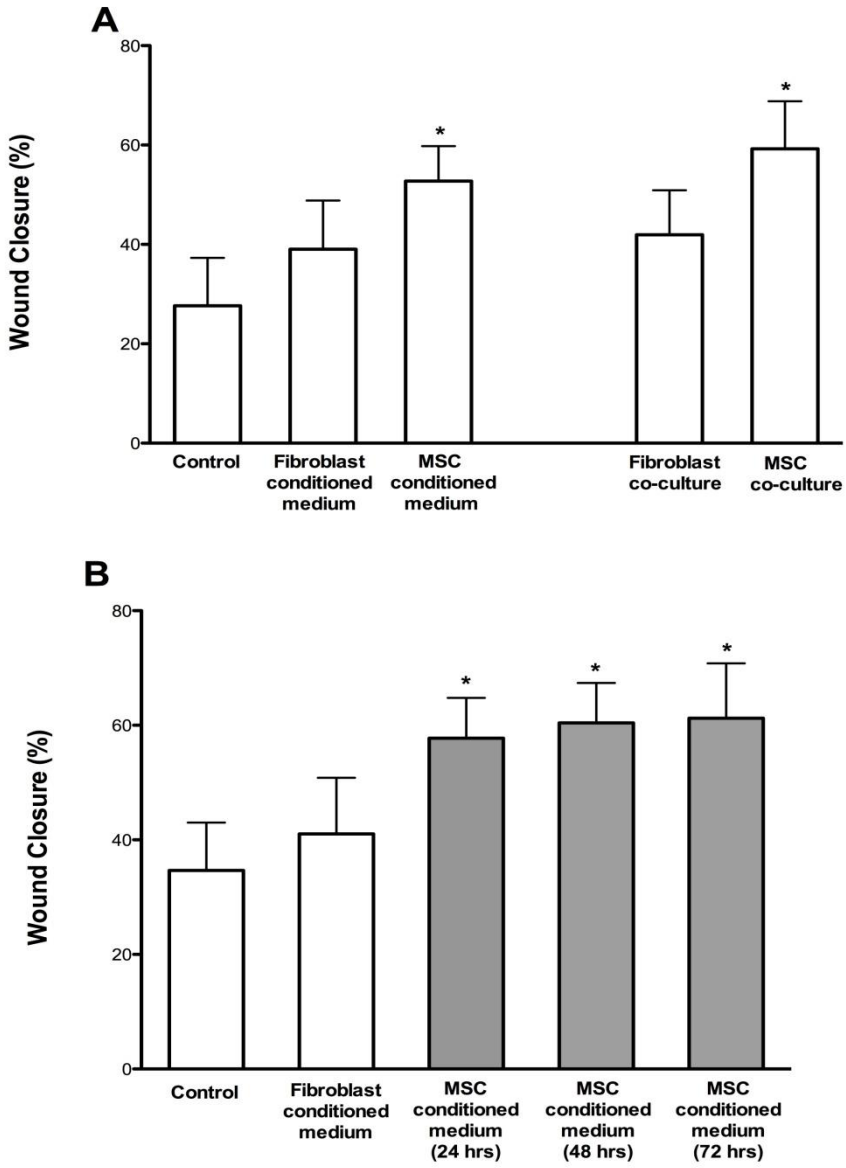

Figure 8-1: MSCs and MSC conditioned medium enhance pulmonary epithelial wound closure
In pulmonary epithelial layers, both MSCs and MSC conditioned medium enhanced wound closure **(Panel A)**.
48 hour or 72 hour conditioned medium does not provide additional benefit to A549 wound closure over 24 hour conditioned medium **(Panel B)**.
Abbreviations: CM, conditioned medium
* Significantly different from Fibroblast CM or control group ($p < 0.05$) (ANOVA and Student-Neuman-Keuls)

Figure 8-2 pulmonary epithelial wound closure in response to MSC and hypoxia conditioned MSC medium

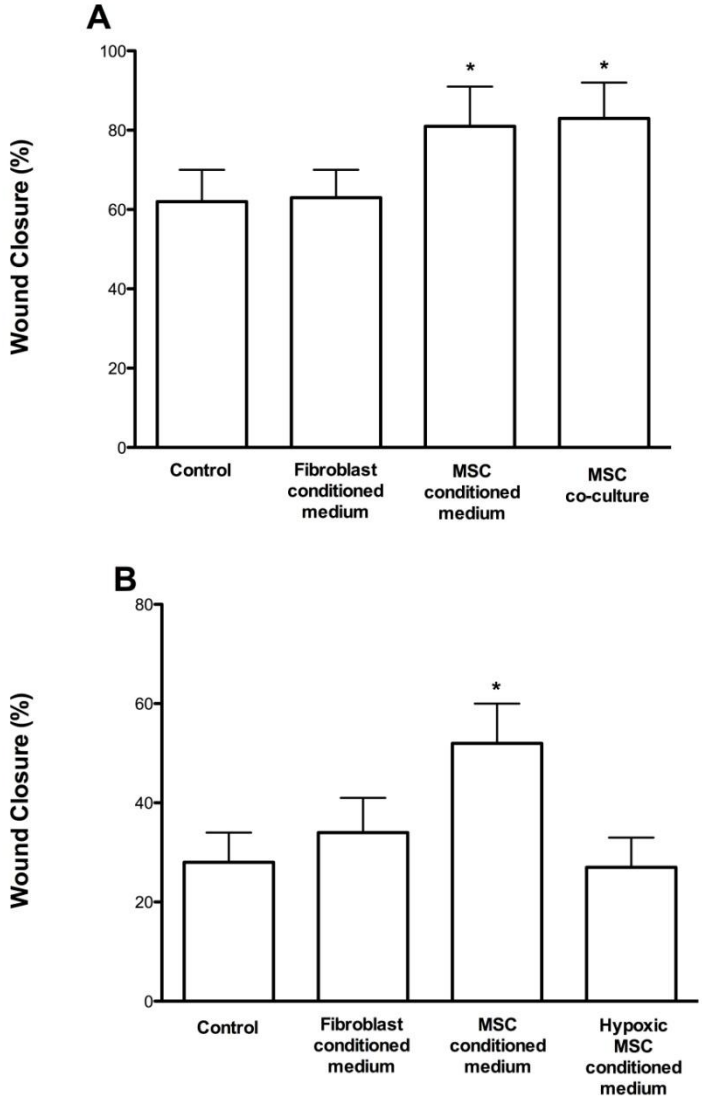

Figure 8-2

Panel A: Histogram demonstrating that the effects of MSCs and MSC conditioned medium on pulmonary epithelial wound closure continues up to 72 hours

Panel B: Histogram demonstrating that conditioned medium produced from MSCs grown in hypoxia does not enhance A549 wound repair

* Significantly different from Fibroblast CM or control group ($p < 0.05$) (ANOVA and Student-Neuman-Keuls)

Figure 8-3 MSCs enhance pulmonary epithelial wound closure via a KGF dependent mechanism

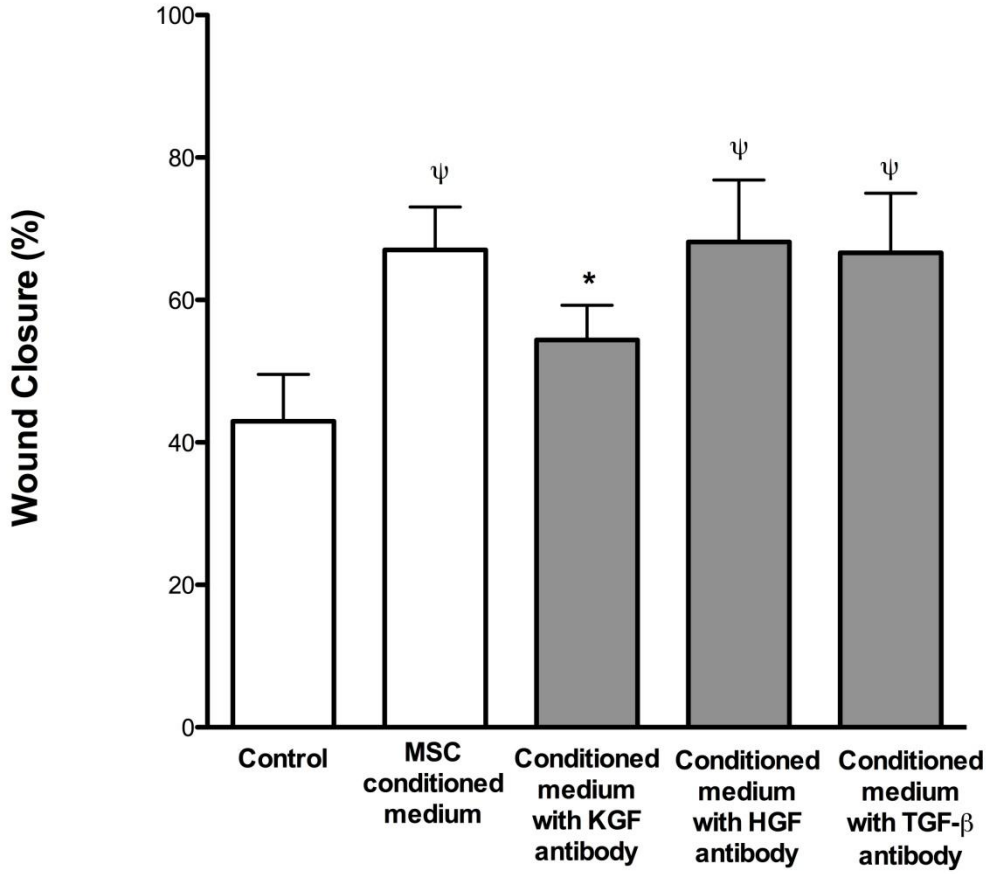

Figure 8-3: MSCs enhance pulmonary epithelial wound closure via a KGF dependent mechanism

In pulmonary epithelial layers, both MSCs and MSC conditioned medium enhanced wound closure Incubation of MSC conditioned medium with antibodies to neutralise KGF, but not HGF or TGF-β, attenuated its effect on wound healing.

Abbreviations: CM, conditioned medium KGF, keratinocyte growth factor, HGF, hepatocyte growth factor, TGF-β, transforming growth factor-β

* Significantly different from MSC CM groups; ψ Significantly different from control group $p<0.05$

Figure 8-4 MSC conditioned medium secretes KGF

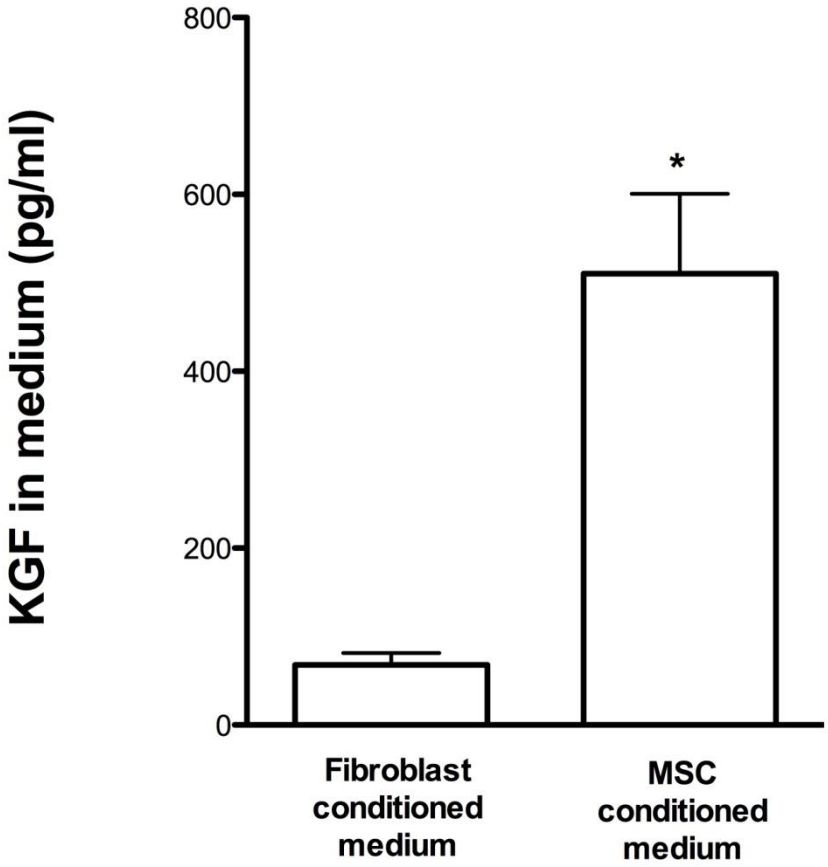

Figure 8-4

Histogram demonstrating the concentration of Keratinocyte Growth Factor in Fibroblast versus MSC conditioned medium

* Significantly different from fibroblast conditioned medium group, $p<0.05$ (Students-t test)

9.0 The role of intra-tracheal delivery of Mesenchymal Stem Cells during recovery and resolution following Ventilator Induced Lung Injury

9.1 Abstract

Introduction: Recent pre-clinical experimental studies indicate that bone-marrow derived mesenchymal stem cells (MSCs) may reduce the severity of Acute Lung Injury (ALI). Both intra-tracheal and systemic administration of MSCs reduced pulmonary oedema and pro-inflammatory cytokines, and improved survival in murine *E. coli* and systemic sepsis induced ALI. Our recent work has indicted that intravenous delivery of MSCs can also enhance repair after ALI. However the optimal route of delivery of MSCs in order to enhance repair in the ventilator injured lung is unknown.

Objectives: We wished to evaluate the role of intra-tracheal delivery of MSCs in modulating inflammation and enhancing repair after Ventilator Induced Lung Injury (VILI).

Methods: Adult male Sprague Dawley rats were anaesthetised, orotracheally intubated and subjected to injurious mechanical ventilation to produce a severe ALI. Following recovery, the animals received intra-tracheal instillation of MSCs, (4 X 10^6 cells), rat dermal fibroblasts (4 X 10^6 cells), or conditioned medium. Another group were given IV MSCs. Controls received vehicle, or no intervention. Animals were harvested at 48 hours, and the extent of recovery following ALI was assessed.

Results: Intratracheal MSCs therapy enhanced repair following VILI. Specifically, MSCs improved oxygenation, lung compliance, reduced total lung water, decreased lung inflammation and histologic lung injury. Intra-tracheal MSC therapy attenuated alveolar TNF-alpha and IL-6 levels, but did not alter alveolar IL-10 concentrations. Intra-tracheal conditioned MSC medium also enhanced lung repair and attenuated the inflammatory response to lung stretch.

Conclusion: Intra-tracheal MSCs can modulate the inflammatory response to VILI, enhance alveolar fluid clearance and augment repair in the lung. The therapeutic effect appears to be mediated through paracrine factors secreted by MSCs.

9.2 Introduction

Mechanical ventilation can be life-saving in acute respiratory failure, but may actually contribute to lung injury [46, 74]. Cyclic lung stretch during mechanical ventilation induces tissue disruption and destruction, and activates pro-inflammatory pathways, promoting the formation of pulmonary edema and neutrophil infiltration [16, 33].

The possibility that mechanical ventilation can actually worsen acute lung disease is now accepted as reality [76]. The importance of Ventilator Induced Lung Injury (VILI) is underscored by the fact that ventilation strategies that reduce lung stretch save lives [47, 77].

Previous studies have demonstrated the ability of murine mesenchymal stem cells (MSCs) to attenuate inflammation and lung injury in rodent models of Acute Lung Injury (ALI) [99, 119]. Recently, the ability of human MSCs to restore alveolar epithelial fluid transport and lung fluid balance via secretion of keratinocyte growth factor (KGF) was demonstrated in an elegant study employing an *ex vivo* perfused human lung preparation injured by *E. coli* endotoxin [137]. Our group has also recently demonstrated the ability of MSCs to enhance epithelial and endothelial repair via paracrine KGF secretion after a severe mechanical ventilation induced lung injury [396]. These studies have ignited much interest in human MSCs (hMSCs) as cellular therapy for ALI.

Little is known regarding the optimal delivery strategy for mesenchymal stem cells. The optimal cell delivery technique is that which provides the most therapeutic benefit, i.e. recovery of lung function. However, the relationship between cell retention, engraftment, timing of delivery, and subsequent therapeutic benefit remains unknown. Local delivery is theoretically more

attractive than systemic in that larger numbers of cells may potentially be administered to specific regions of interest within the target organ, ie the lung. Clinically, local cell delivery can be achieved by direct injection into the trachea via an endotracheal tube in patients ventilated for ALI.

On the other hand, systemic MSC infusion has been shown to be safe in clinical trials in human disease, such as in myocardial infarction [130], graft versus host disease [397] and stroke [398]. Intravenous delivery of cells has been promulgated as a simple delivery strategy for the lung that allows non-invasive repeated administration of large numbers of cells [399]. Numerous studies have shown that systemically infused MSCs are initially trapped in the vasculature of the lung [400]. Moreover, the ability of MSCs to home to injured tissues [98] may obviate the need for local delivery strategies, and may result in localized therapeutic benefit irrespective of mode of delivery .

We wished to ascertain whether our findings that IV MSCs can enhance wound repair in the lung [396] could be reproduced or enhanced with the use of intra-tracheal delivery. We hypothesized that intra-tracheal delivery of MSCs would enhance recovery and repair after Ventilator Induced Lung Injury. We also postulated that intra-tracheal delivery of MSCs would reduce cellular and biochemical measures of lung inflammation.

9.3 Methods

9.3.1 Mesenchymal Stem Cell Isolation and Culture

As described in detail in Section 4.6.1, Mesenchymal Stem Cells were isolated from rat femora and tibiae under sterile conditions in the animal surgery room as previously described [257]. Cells were ready for subculture (usually after 16-17 days) when colonies began to exhibit a compact appearance and multi-layered growth or when the loosely formed colonies began to merge into a monolayer (<90% of confluence). Thereafter, cells were ready to be passaged after 6/7 days culture, at 80% confluence. Cells were expanded to passage 4, whereupon they were used for experiments. (**Figure 7-1** for MSCs in culture.) MSCs were characterized according to international guidelines [115] **(Figure 7-1 and 7-2).**

9.3.2 Rat Dermal Fibroblasts

Section 4.6.5 describes isolation and culture of fibroblasts from adult male Sprague Dawley rats. Briefly, fat and subcutaneous tissue was removed from skin strips obtained from the abdominal wall of euthanized animals, and these were placed in 0.25% trypsin (Sigma) overnight. The epidermis was then peeled from the dermal layer, and the dermal layer was placed on a scored 6 well plate (Sarstedt, Wexford, Ireland) in F-12/MEM-α medium supplemented with fetal calf serum (10%) and penicillin/streptomycin (1%).

9.3.3 Conditioned Medium

As described in detail in Section 4.6.6, allogeneic rat MSCs (2×10^6) were cultured without serum for 24 h. The medium was then replaced, and the

subsequent medium without serum for the next 24 h was used as the conditioned medium (CM). 15mls of this medium was concentrated using a 3000 KDa centrifugal concentrating filter (Amicon, Billerica, MA, USA) to give 500 microlitres.

9.3.4 Rodent Ventilator Induced Injury Protocol

We utilized our established model of repair from VILI as described in detail in Section 4.3 [401]. Anesthesia was induced with intraperitoneal ketamine 80 $mg.kg^{-1}$ (Ketalar, Pfizer, Cork, Ireland) and xylazine 8 $mg.kg^{-1}$ (Xylapan, Vétoquinol, Dublin, Ireland). After confirmation of depth of anesthesia by paw clamp, intravenous access was obtained via tail vein, laryngoscopy was performed and the animals were intubated with a size 14G intravenous catheter (BD Insyte®, Becton Dickinson Ltd, Oxford, UK). The lungs were ventilated using a small animal ventilator (CWE SAR 830 AP, CWE Inc, Pennsylvania, USA). Anesthesia was maintained with repeated boli of Saffan® (alfaxadone 0.9% and alfadadolone acetate 0.3%; Schering Plough, Welwyn Garden City, UK) and muscle relaxation was achieved with cis-atracurium besylate $0.5mg.kg^{-1}$ (GlaxoSmithKline, Dublin, Ireland). The animals were then subjected to a high stretch mechanical ventilation protocol (Fi_{O2} 0.3, inspiratory pressure 35 cmH_2O, respiratory rate 18 min^{-1}, and positive end-expiratory pressure 0 cmH_2O). When static compliance had decreased by 50%, high stretch ventilation was discontinued and animals were entered into the treatment protocol.

9.3.5 Intra-tracheal cell and conditioned medium delivery

After injury, and while undergoing lung protective ventilation during the recovery from injury phase, animals were randomized to receive (i) no intra-tracheal therapy, (ii) intra-tracheal vehicle alone (PBS, 300μL), (iii) intra-tracheal fibroblasts ($4x10^6$), (iv) intra-tracheal MSCs ($4x10^6$), (v) intra-tracheal conditioned medium (300μL) or (vi) intravenous MSCs ($4x10^6$) (See **Figure 9-1**)

9.3.6 Assessment of Injury and Repair

As described in Section 4.3.6, at 48 hours following VILI induction, animals were re-anesthetized. A tracheostomy was inserted and carotid arterial access established, and the lungs were mechanically ventilated (Model 683; Harvard Apparatus, Holliston, MA) at a respiratory rate of 80 min^{-1}, tidal volume 6 $ml.kg^{-1}$ and positive end-expiratory pressure 2 cmH_2O. Intra-arterial blood pressure, peak airway pressures and rectal temperature were recorded continuously. Static inflation lung compliance measurements were performed as previously described [251, 298]. After 20 minutes, the inspired gas was altered to a Fi_{O2} of 1.0 for 15 min, and a final arterial blood sample was taken. Heparin (400 $IU.kg^{-1}$, CP Pharmaceuticals, Wrexham, U.K.) was then administered intravenously, and animals were killed by exsanguination.

Immediately post-mortem, the heart–lung block was dissected and bronchoalveolar lavage (BAL) collection was performed as previously described [306, 359] in Section 4.4.2. BAL differential cell counts were performed as in Section 4.4.4. Protein concentration was determined using a Micro BCA™ Protein

assay kit (Pierce, Rockford, IL, USA) see Section 4.4.5.[300] BAL IL-1β, IL-6, TNF-α and IL-10 concentrations were determined using quantitative sandwich enzyme-linked immunosorbent assays (R and D systems, Abingdon, UK)[301] as outlined in Section 4.4.6.

Wet/dry lung weights were determined using the lowest lobe of the right lung as previously described [305] in Section 4.4.1. The left lung was isolated and fixed for morphometric examination, and the extent of histologic lung damage was determined using quantitative stereological techniques as described in Section 4.5 [305, 306].

9.4 Results

40 animals were entered into the experimental protocol. All survived the injury and subsequent treatment allocation. 8 animals each were entered into the fibroblast, vehicle control, intra-tracheal MSC and intra-tracheal conditioned medium groups; 4 animals each were entered into the IV MSC and no therapy groups.

9.4.1 IT MSCs and IT conditioned medium improve physiologic lung function after VILI

Arterial oxygenation was restored in the group that received IT MSCs, and in the group that received IT conditioned medium, as measured by arterial blood gases and Alveolar-arterial oxygen gradient ($p<0.05$). **(Figure 9-2A)** Further functional recovery in lung physiology in response to IT rMSC treatment after VILI was demonstrated by significant improvements ($p<0.01$) in respiratory system static compliance in comparison to vehicle and VILI only controls **(Figure 9-2B).**

9.4.2 IT MSCs and IT conditioned medium improve alveolar epithelial barrier function after VILI

IT rMSCs and IT conditioned medium improved lung microvascular permeability, as evidenced by a decrease in lung wet:dry weight ratios **(Figure 9-3A)** and a decrease in alveolar fluid protein concentrations in comparision to controls **(Figure 9-3B)**.

9.4.3 IT MSCs and conditioned medium reduce inflammatory cells and cytokines in the lung after VILI

IT rMSCs and IT conditioned medium reduced both total BAL cell count and BAL neutrophil counts **(Figure 9-4A and B).** Alveolar concentrations of TNF-α **(Figure 9-5A)** and IL-6 **(Figure 9-5B)**, were decreased following rMSC and rMSC conditioned medium treatment. In contrast, alveolar concentrations of the anti-inflammatory cytokine IL-10 were not altered in response to rMSC and conditioned medium therapy **(Figure 9-5C***)*.

9.5 Discussion

With a mortality exceeding that of breast cancer or HIV/AIDS [1], the development of effective methods of delivery of novel therapies to the lungs during Acute Lung Injury is an immediate and important task of medical research. The recent success of cell therapy in experimental lung injury research has come about using both intra-tracheal and systemic delivery approaches [117, 119]. Our group has recently demonstrated for the first time the ability of intravenous MSCs to enhance repair in the lung after a high stretch mechanical ventilation induced lung injury [396]. This was achieved through more effective restoration of epithelial and endothelial barrier function, due in part to enhanced wound repair in response to secretion of KGF by MSCs, as well as a marked down-regulation of inflammation and an increase in the anti-inflammatory cytokine IL-10. We wished to determine whether intra-tracheal administration of MSCs or their conditioned medium would be as effective as systemic administration in promoting wound repair in the lung, and in diminishing the associated inflammatory response, after mechanical ventilation induced injury.

9.5.1 Intra-tracheal delivery of MSCs is as effective is systemic delivery in enhancing repair from VILI

In this study both IT MSCs and IT conditioned medium were as effective as IV MSCs in improving physiologic function after severe VILI. Both groups improved measures of alveolar epithelial and endothelial barrier function including wet:dry ratios and BAL protein concentrations. Local release in the lung of inflammatory cytokines was reduced in both intra-tracheal therapy groups also, in comparison to controls. However, the increase in BAL and systemic

concentrations of the anti-inflammatory cytokine IL-10 was not observed in the intra-tracheal therapy groups, in comparison to the increase observed in BAL and systemic IL-10 in the MSC group. These findings suggest that a threshold concentration of MSCs in the systemic circulation is a pre-requisite for significant or sustained IL-10 release.

9.5.2 What is the optimal route of delivery for MSC therapy

This study supports the idea that the intra-tracheal route is a viable alternative to the intravenous route for MSC delivery to promote repair in the lung. The intra-tracheal route of delivery allows direct access to the region that has sustained injury – the alveolar epithelium and endothelium. Local cell delivery to the lung may enhance cell retention in the lung, increase the concentration of secreted paracrine mediators in the lung responsible for beneficial effect, and decrease the need for high cell dose, and thus limit the potential adverse side effects of the treatment, such as embolic phenomena. This mode of delivery may have increased efficacy to repair the injured lung.

Although IV delivery of cells has been promoted as a potential simple delivery strategy, this method is not without its risks. While MSCs are known to hone to injured organs [140] including the lung [402], MSCs are also trapped in the vasculature of the lung even without it having sustained injury [140]. Cell entrapment in the lung might be explained because expanded MSCs are relatively large, activated, and express adhesion molecules. Because of this, they may not be able to pass the capillaries in the lung, and many of them become trapped. Indeed MSCs are of a size (10–20 μm) that could cause capillary plugging.

Development of capillary obstruction following IV cellular delivery may mitigate the potential improvement in lung function afforded by MSC delivery. The finding of reduced blood flow by angiography in a study of intra-coronary MSC administration after myocardial infarction, as well as immunohistochemical evidence of microvascular plugging alerts us to a potential limitation of IV MSC infusion [403].

Other organs such as the liver, spine, and spleen were also noted to have increased uptake after IV administration [404]. The effects of remote organ engraftment are unknown and may be benign; however, engraftment may result in uncontrolled cellular growth, differentiation, or malignant transformation in remote organs. Given the functional plasticity of such cells, the potential effects of such remote delivery should be considered when designing clinical studies.

On the other hand, the branching nature of the human tracheo-bronchial tree makes access to the alveolar epithelium difficult, particularly in the fluid filled ARDS lung. Injection of cells directly into the lung in the setting of severe lung injury may cause a dangerous if only transient decline in gas exchange and lung compliance. The findings of more effective anti-inflammatory action in terms of increased IL-10 in the group that received IV MSCs raises the possibility that this mode of delivery allows increased modulation of damaging inflammation, which may be relevant in the setting of accompanying distal organ dysfunction in ARDS.

9.5.3 MSCs secrete paracrine mediators

The mechanisms involved are poorly understood; however, increasing data suggests that the protective effects of MSCs are largely mediated through production of paracrine mediators [137, 348]. Our study once again confirms this hypothesis, with conditioned medium mimicking the beneficial effects of direct cell therapy in the ventilator injured lung. The anti-inflammatory effects of murine MSCs in the lung have been associated with MSC secretion of interleukin 1 receptor antagonist (IL1Ra) [242], TGF-β1 [241], and TSG-6 [244]. MSCs secrete other bioactive molecules such as HGF, EGF, sTNFR1, Ang1 and STC-1 that may also contribute to the immunomodulatory functions as well as enhance repair of injured lung [381]. Cells have been delivered intra-tracheally, intravenously and intra-peritoneally, to achieve therapeutic effect [244]. Intravenous or intra-alveolar administration of MSCs modulates both the inflammatory process and, as we have shown here, tissue remodeling, in experimental models of ALI despite minimal, if any engraftment [117, 357].

9.5.4 Summary and conclusions

In summary, we have used our established animal model of repair after VILI [401] to investigate the efficacy of IT delivery of MSCs and their conditioned medium to enhance recovery after mechanical stretch induced injury in the rat lung. Both IT MSCs and conditioned medium were as effective as IV MSCs in promoting restoration of function after VILI, and in reducing inflammatory cells and cytokines in the lung. However, IV MSCs increased IL-10 in the lung, a finding that was not reproduced in the IT MSC or conditioned medium groups,

raising the possibility that systemic delivery results in more pronounced modulation of inflammation, which may be beneficial in critical illness and multi-organ failure.

9.6 Figures

Figure 9-1 Experimental design

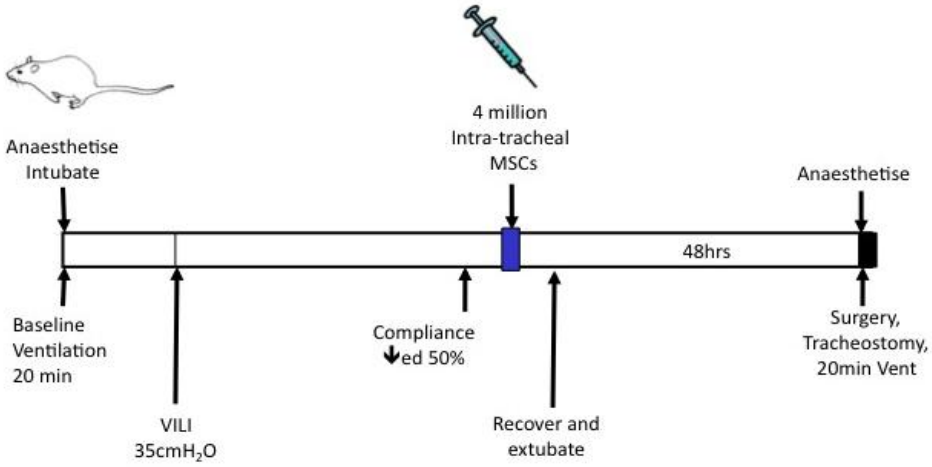

Figure 9-1
Flow diagram indicating timelines for experimental interventions.

Figure 9-2 MSC's and MSC conditioned medium enhances Lung Repair.

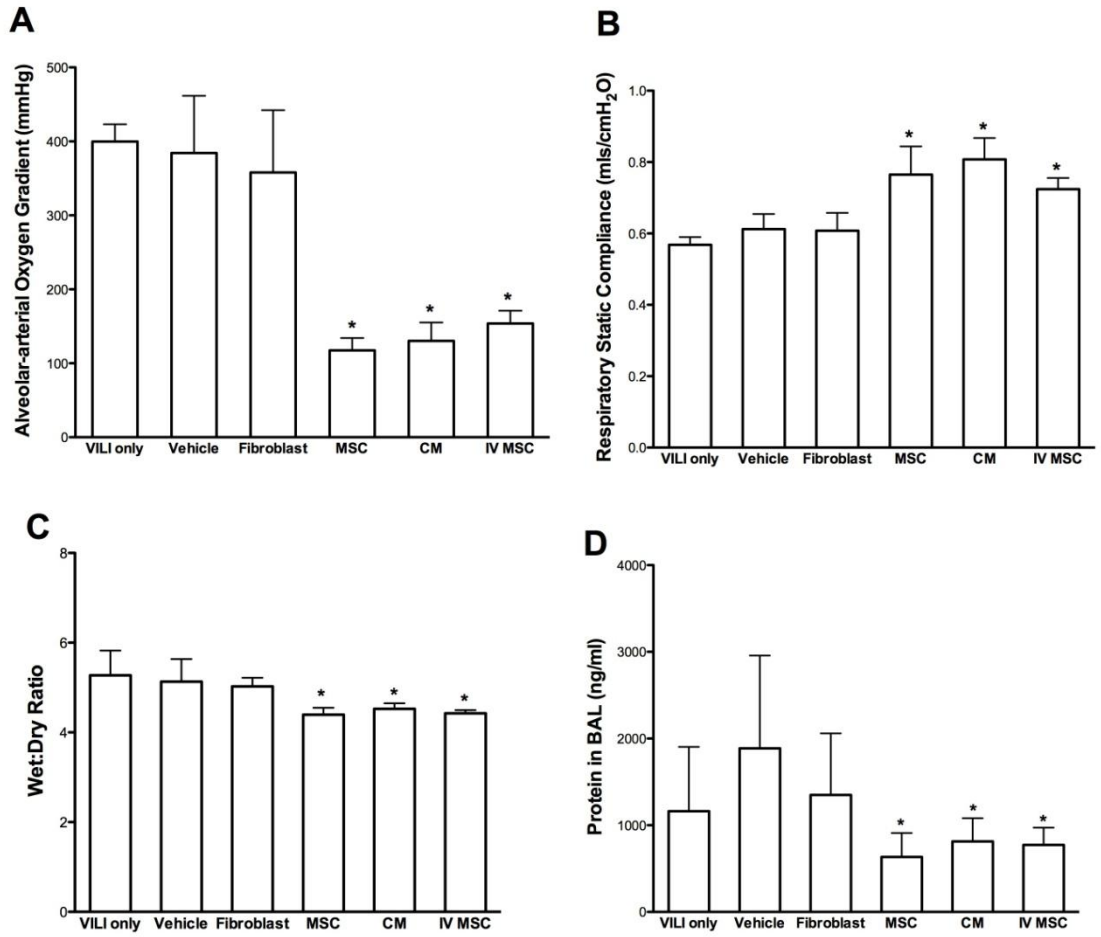

Figure 9-2: MSC's and MSC conditioned medium enhances Lung Repair.

IT and IV MSC therapy and MSC conditioned medium each decreased (P<0.001) alveolar-arterial oxygen gradient **(Panel A)**, increased (P<0.001) static lung compliance **(Panel B)**, reduced (P<0.001) lung wet:dry weight ratios **(Panel C)**, and decreased (P=0.007) BAL protein concentrations **(Panel D)**, 48 hours following induction of severe stretch induced lung injury, compared to the other groups.

Abbreviations: VILI only, no treatment given, Vehicle, treatment with vehicle alone; Fibroblast, intra-tracheal fibroblast therapy; MSCs, intra-tracheal MSCs; CM, intra-tracheal MSC conditioned medium; IV MSC, intravenous MSCs; BAL, bronchoalveolar lavage.

* Significantly (P<0.05) different from Vehicle, fibroblast and VILI only groups (ANOVA and Student-Neuman-Keuls).

Figure 9-3 MSC's and conditioned medium modulates the cellular inflammatory response to VILI.

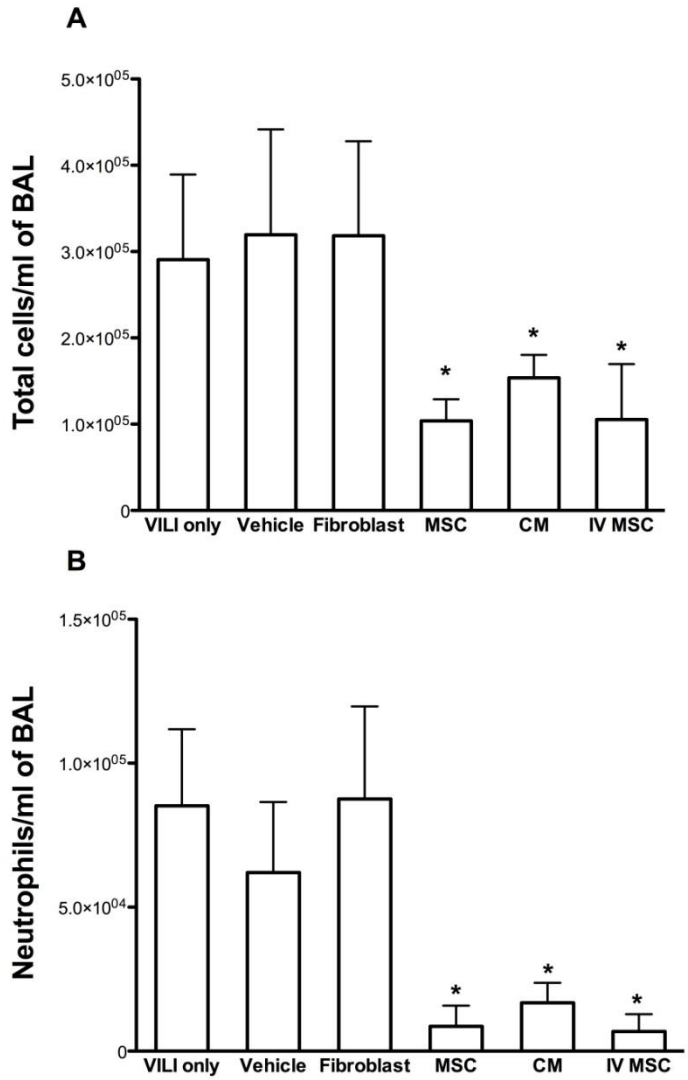

Figure 9-3: MSC's and conditioned medium modulates the cellular inflammatory response to VILI.

IT and IV MSC therapy and MSC conditioned medium each decreased (P<0.001) BAL total cell counts **(Panel A),** and decreased (P<0.001) BAL neutrophil counts **(Panel B)** 48 hours following induction of severe stretch induced lung injury, compared to the other groups.

Abbreviations: VILI only, no treatment given, Vehicle, treatment with vehicle alone; Fibroblast, intra-tracheal fibroblast therapy; MSCs, intra-tracheal MSCs; CM, intra-tracheal MSC conditioned medium; IV MSC, intravenous MSCs; BAL, bronchoalveolar lavage.

* Significantly (P<0.05) different from Vehicle, fibroblast and VILI only groups (ANOVA and Student-Neuman-Keuls).

Figure 9-4 MSC's and MSC conditioned medium modulates the cytokine response to VILI.

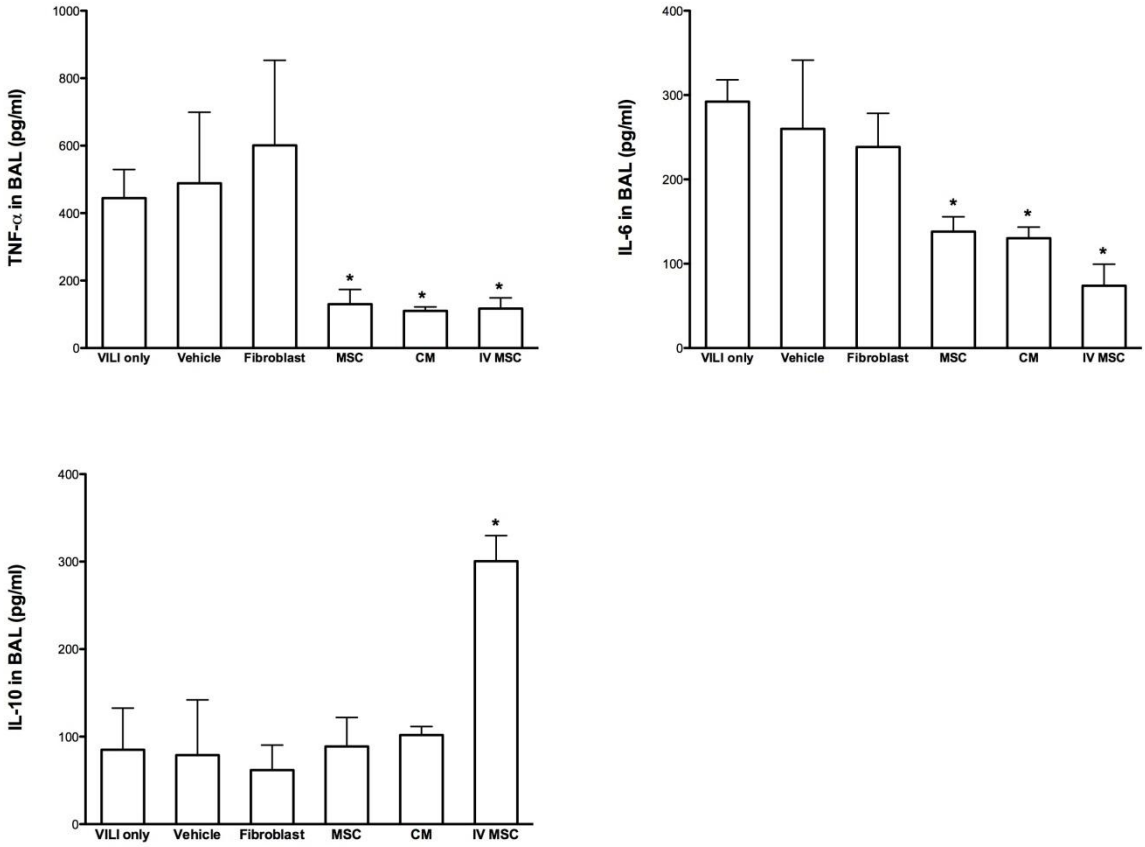

Figure 9-4: MSC's and MSC conditioned medium modulates the cytokine response to VILI.

IT and IV MSC therapy and MSC conditioned medium each decreased (P<0.001) BAL TNF-a concentrations **(Panel A),** and decreased (P<0.001) BAL IL-6 concentrations **(Panel B)**. IV MSCs, but not IT MSCs or IT conditioned medium, increased (P<0.001) BAL IL-10 **(Panel C)** concentrations, 48 hours following induction of severe stretch induced lung injury, compared to the other groups.

Abbreviations: VILI only, no treatment given, Vehicle, treatment with vehicle alone; Fibroblast, intra-tracheal fibroblast therapy; MSCs, intra-tracheal MSCs; CM, intra-tracheal MSC conditioned medium; IV MSC, intravenous MSCs; BAL, bronchoalveolar lavage.

* Significantly (P<0.05) different from Vehicle, fibroblast and VILI only groups (ANOVA and Student-Neuman-Keuls).

10.0 Discussion

10.1 Repair, remodeling and regeneration of the injured lung

Repair, remodeling and regeneration of the respiratory system for the restoration of normal function after injury represent the holy grail of modern pulmonary biology [405]. The lung is extremely complex, and development and repair require interaction among more than 40 different cell lineages [405]. The complex nature of both lung structure and injury repair mechanisms impact the ability of the lung to effect efficient repair.

Most patients with ARDS survive the acute phase, but many go on to die, often with evidence of pulmonary fibrosis [48]. Pulmonary fibrosis was found in open-lung biopsies of 53% of ventilated patients who had ARDS for 5 days [406]. Transbronchial lung biopsy revealed that 64% of patients with ARDS who were ventilated for an average of 12 days developed pulmonary fibrosis, and their mortality rate was 57% compared with 0% in patients without pulmonary fibrosis [382]. The mechanisms underlying the fibrotic phase of ARDS are largely unknown. Some investigations have focused on the underlying immune cell response in the acute phase of ARDS as a key factor in the development of fibrosis [407]. Another possibility relates to the role of the alveolar epithelium, which has largely been thought of as a passive bystander in the development of chronic pulmonary fibrosis. However, recent studies have suggested that ongoing alveolar epithelial cell apoptosis and retarded wound repair may play an important role in the pathogenesis of pulmonary fibrosis [408-410].

Our studies with a novel animal model of repair from VILI highlight some potential targets to augment repair processes, reveal several mechanisms that could contribute to aberrant repair, and demonstrate the potential of mesenchymal stem cells as a therapy after injury, one aspect of which is more efficient pulmonary epithelial wound repair.

10.2 How have our studies of the repair phase of ARDS contributed to current knowledge?

10.2.1 VILI induces a marked inflammatory response that may worsen lung and systemic organ injury

Over the last decade, the bio-trauma hypothesis [45] postulated that mechanical ventilation causes the release of soluble mediators from the lungs into the bloodstream and that these circulating mediators cause injury in the lungs and in other organs. Apart from contributing to lung injury, the bio-trauma hypothesis also postulates that lung-borne mediators might be implicated in the development of distant organ dysfunction.

This hypothesis is attractive and plausible, but has not been proven. Moreover, several laboratory studies report minimal elevations in cytokine level despite severe lung injury [54-56]. The finding that exogenous cytokines do not necessarily produce lung injury [57] also argues against an obligate pathogenic role.

Our studies confirm that excessive lung stretch induces the release of several pro-inflammatory cytokines coincident with the recruitment of inflammatory cells into the lung. While the peak levels of TNF-α were modest, the levels of IL-

1β and IL-6 were markedly elevated at 6 hours, at levels sufficient to cause lung injury and inflammation observed in other animal models [310, 311]. Our model indicates that a further episode of mechanical injury or repeated stretch of already damaged lung has the potential to result in a sustained pro-inflammatory environment, with consequent adverse effects on alveolar epithelial and endothelial permeability, and persistence of activated inflammatory cells.

Elevation in cytokine levels is associated with lung injury in laboratory [411, 412] and clinical [46, 285, 413] studies, and is associated with worse morbidity and mortality [414, 415]. Anti-cytokine strategies such as antibodies (e.g., against TNF-α [51], MIP-2 [53] and pre-B-cell colony-enhancing factor [416]), blockade with soluble receptors (e.g., soluble TNF-α receptors [417]) or receptor antagonists (e.g., recombinant interleukin-1 receptor antagonists [52]), antibodies to nuclear factor kappa-B (NFκB) [418] and steroids [419] have all conferred protection in experimental models. However, such associations do not prove causation, and there is substantial evidence against a simple pathogenic role.

An exemplar cytokine is TNF-α. It is an important early pro-inflammatory mediator, is expressed and secreted very early in the course of VILI, as in our model, and is biologically active (confirmed by cytotoxicity assay) in concentrations that are below detection limits of commonly used assays [411]. TNF-α acts on two receptors: p55 and p75, which have opposing effects [420]. The former promotes pulmonary edema, but the latter is protective and has a higher binding affinity; thus, TNF-α can have contrasting effects depending on its concentration [420].

10.2.2 The inflammatory response to VILI is pro-fibrotic

Over-expression of the cytokines TNF-α, IL-1β and IL-6 has been shown to induce an acute inflammatory response with variable degrees of alveolar destruction [310, 311], along with a graded fibrotic response ranging from marginal (TNF-α) to severe (IL-1β). The degree of fibrosis in these models was found to correlate directly to both the amount and duration of expression of active TGF-β1. While the level of expression of cytokines IL-1β and IL-6 after severe lung stretch in our model was of the magnitude required to produce an inflammatory response, the amount of TGF-β1 produced was not. The critical role of TGF-β1 in fibrogenesis has been demonstrated by over-expression of active TGF-β1 in rat lung, resulting in prolonged and severe interstitial and pleural fibrosis [421]. TGF-β1-induced fibrosis developed and progressed without extensive inflammation [421]. It is apparent from ours and other studies that induction of lung fibrosis is not directly dependent on the degree or characterization of the inflammatory response, but rather, the amount and length of TGF-β1 induced downstream of cytokine signaling.

It is apparent that excessive or recurring inflammatory events can cause excessive wound-healing responses that lead to the development of fibrosis. Either eliminating the causative agent, such as VILI, or treatments with anti-inflammatory agents such as corticosteroids may help restore the balance.

10.2.3 Diverse roles of TGF-β1 in VILI

TGF-β1 is a critical mediator that initiates and terminates tissue repair and whose sustained production underlies the development of tissue fibrosis [422]. In ALI the role of TGF-β1 has been most thoroughly evaluated during the late phase of tissue repair, where it plays a critical role in the development of the fibroproliferative response [423, 424]. In our model, TGF-β1 was elevated early, an increase that was not sustained at later time points. In patients with early ARDS, high concentrations of TGF-β1 in bronchoalveolar lavage fluid are correlated with decreases in the PaO_2/FIO_2 ratio [425], suggesting an important role for TGF-β1 before the fibroproliferative process can be clinically relevant. TGF-β1 has been implicated in the pathogenesis of pulmonary oedema in ARDS. Increased TGF-β1 induced permeability of both the endothelium and epithelium may contribute to alveolar flooding in bleomycin- or endotoxin-induced ALI by increasing the gaps between endothelial cells [426]. As the increase in TGF-β1 in our model coincided with the maximum degree of alveolar epithelial and endothelial barrier dysfunction, a role for this cytokine in the permeability alterations of VILI should be explored.

10.2.4 MMPs may be necessary for repair, but are implicated in fibrosis

The balance of MMPs to TIMPs [427] and collagens to collagenases vary throughout the injury and wound healing response, shifting from pro-synthesis and increased collagen deposition, towards a controlled balance, with no net increase in collagen. An imbalance between collagen-catabolizing MMPs and their specific inhibitors, TIMPs, can result in excessive collagen breakdown [428].

This is not to say that MMPs are not necessary; MMPs can disrupt the basement membrane and allow the influx of inflammatory cells. The basement membrane, which forms the ECM underlying the epithelium and endothelium of parenchymal tissue, precludes direct access to the damaged tissue. To disrupt this physical barrier, matrix metalloproteinases (MMPs), cleave one or more ECM constituents allowing extravasation of cells into, and out of, damaged sites. Specifically, MMP-2 (gelatinase A, Type N collagenase) and MMP-9 (Gelatinase B, Type IV collagenase) cleave type N collagens and gelatin, two important constituents of the basement membrane [428, 429]. Inhibiting MMP activity could be detrimental in immunity and in the process of re-epithelialization [430]; however, in pathological fibrotic responses, neutralization of specific MMPs either with small molecule inhibitors [431] or by influencing TIMP expression may help restore this imbalance.

Non-selective inhibition of MMPs results in decreased lung injury after high-pressure ventilation due to a reduction in the inflammatory response [295, 296]. However, our results indicate an important role for MMPs in the repair phase after VILI. Moreover, different MMPs may have opposite effects, and blanket inhibition is as likely to inhibit essential pathways as it is pathologic ones. For example, it has been previously shown that absence of MMP-9 worsens VILI [432], and other authors have shown a similar protective role of MMP-9 in different models of lung injury [433-435]. Indeed the increased levels of MMPs during repair in our study, in spite of a decrease in physiologic lung damage indices, suggest that these molecules may have an important role in tissue repair. Indeed the rapid increase in MMPs in our study, and subsequent decline to normal levels, together with lung functional and structural restoration, highlight

the critical point of timing in relation to tissue remodeling and therapeutic intervention. Preventive inhibition of MMPs may protect against VILI [295], but blocking these enzymes during the repair phase may be detrimental.

10.2.5 The myofibroblast – role in recovery following VILI

The key effector cell in fibrogenesis is the myofibroblast; these spindle- or stellate-shaped cells localize to fibrotic foci and other sites of active fibrosis, and are the primary cell type responsible for the synthesis and deposition of ECM and the resultant structural remodeling that leads to the loss of alveolar function in pulmonary fibrosis. They may be derived by activation/proliferation of resident lung fibroblasts, epithelial-mesenchymal differentiation, or recruitment of circulating fibroblastic stem cells (fibrocytes) [408]. Of note, Heise et al have recently shown that cyclic mechanical stretch induces EMT in alveolar type II epithelial cells, associated with increased expression of low molecular weight hyaluronan [436]. The quantity of activated myofibroblasts [437] determines the amount of collagen deposition during wound repair. Conversely, the removal of myofibroblasts is essential to terminate collagen deposition [438].

Our studies indicate that stretch induced lung injury results in early (at 6 hours) recruitment of myofibroblasts into lung. Despite the recruitment of significant amounts of cells, this did not result in an overall increase in lung collagen. This implies that the balance of collagen production and removal during repair from VILI remained constant. These results do not preclude the idea that further or more severe episodes of lung stretch, or concomitant injury such as infection, may upset this balance or cause persistence of the myofibroblast with resultant excess matrix deposition

10.2.6 Collagen levels in lung are not increased after a single episode of severe injury

Collagen fibers are the main component of the ECM. Type III collagen fiber is flexible and susceptible to breakdown; type I is comprised of thicker and cross-linked fibrils [439-441]. Their turnover is a dynamic process that is necessary for the maintenance of the normal lung architecture. Ultimately, collagen accumulation depends not only on its synthesis, but also on its degradation .[440, 441]

Despite the demonstration of conditions that favour the development of pulmonary fibrosis after VILI in this model, overall levels of collagen in lung tissue remained unchanged. However, a pro-inflammatory, pro-fibrotic environment exists after VILI, with elevations in pro-fibrotic cytokines, MMPs and collagen secreting fibroblasts. Pro-collagen peptide I mRNA levels were found to be elevated days after VILI, but later expression was suppressed. The failure to demonstrate increases in lung tissue collagen at different times after injury is indicative of a well balanced repair process. The potential to disrupt this process with further episodes of injury remains obvious.

10.2.7 Elastic fiber disruption may attract neutrophils

Elastic fibers provide support for the alveolar patency and lung elastic recoil. The importance of elastin in VILI and ALI has not been studied; however, it was noted over 40 years ago with the advent of the elastase:antielastase theory for the pathogenesis of emphysema, which, remarkably, remains the prevailing hypothesis today [442]. Although all ECM components are degraded by

inflammatory cell proteinases in COPD, elastin is distinguished by the difficulty in restoring a functional elastic fiber in an adult [443]. With injury, although most matrix components undergo physiologic turnover, the longer-lived elastic fibers may be less capable of normal repair. Despite bursts of elastin synthesis in animal models, elastic fibers are disorganized [443]. In addition, proteolytic fragments of elastin serve as monocyte chemokines, fueling continued macrophage accumulation in COPD. In the early 1980s, independent studies by Senior and coworkers [444, 445] and Hunninghake and colleagues [446] demonstrated that elastase-generated fragments were chemotactic for monocytes and fibroblasts. Cigarette smoke induces constitutive macrophages present in lungs to produce MMP-12, which in turn cleaves elastin into fragments chemotactic for monocytes. This positive feedback loop perpetuates macrophage accumulation and lung destruction. Whether this system is operative in VILI and ALI has not been determined.

Our study demonstrated that the amount of elastic fibers in lung parenchyma was similar in all groups, but elastic fiber fragmentation and disorganization were present in the alveoli of animals after VILI. The fragmentation of elastic fibers in alveoli may be due to inappropriate repair or to mechanical distortion of damaged fibers induced by mechanical stretch. Alternatively, MMP-12, which was elevated in lung up to 96 hours after VILI, may play a similar role as in COPD, and the influx of inflammatory cells seen in our model may occur mainly or in part as a result of elastin fiber disruption.

10.2.8 Keratinocyte Growth Factor – role in ordered repair versus fibrosis

KGF is expressed predominantly by mesenchymal cells, and its receptor (KGFR) is expressed only in epithelial cells. This epithelial specificity suggests that KGF may play an important role in mesothelial-epithelial interactions [385]. The role of endogenous KGF in acute lung injury has not been well studied. However, it seems likely, on the basis of the key role that endogenous KGF has been shown to play in wound healing in the skin [447, 448], that endogenous KGF plays an important role in epithelial repair in the lung also.

Our study demonstrated a late increase (14 days) in levels of KGF after VILI. This peak was associated with restoration of alveolar structure on histologic section, and suppression of pro-collagen peptide mRNA levels. This is consistent with other studies of endogenous KGF. In neonatal rabbits exposed to hyperoxia, KGF mRNA expression was increased 12-fold in whole lung homogenates at 6 days compared with controls [449]. This rise in KGF mRNA was followed, at 8 – 12 days, by an increase in type II cell proliferation, suggesting that increased expression of KGF led to alveolar epithelial type II cell hyperplasia in response to hyperoxic injury. In rats with acute lung injury due to bleomycin injection, KGF levels in bronchoalveolar lavage (BAL) increased markedly after injury, peaking at 7 – 14 days, coincident with peak type II cell proliferation [301]. Thus, in different injury models, the available evidence indicates that KGF expression is increased late after acute lung injury and may be an important endogenous stimulus for alveolar epithelial proliferation and repair.

There have been very few clinical studies evaluating the role of endogenous KGF in human acute lung injury. Verghese et al. [450] measured levels of KGF in undiluted pulmonary edema fluid sampled from patients with early acute lung injury. Although KGF was detected, there was no difference in levels in patients

with acute lung injury compared with control patients with hydrostatic pulmonary edema. In contrast, Stern et al. [451] collected BAL fluid from patients with acute respiratory distress syndrome (ARDS) later in their course than in the Verghese study. KGF was detected in BAL fluid in 13 of 17 patients with ARDS vs. only 1 of 8 patients with hydrostatic pulmonary edema. Mechanically ventilated patients without ARDS or hydrostatic edema did not have detectable levels of KGF in BAL.

10.3 Summary of insights from VILI repair studies

These studies demonstrate the interrelated roles of inflammatory cells and cytokines, growth factors and the extracellular matrix in restoration of structure and function after mechanical ventilation induced lung injury. The potential to disrupt this finely balanced process is evident. Repeated episodes of injury, or a two-hit model might provide more significant injury and fibroproliferation. While we have drawn inferences regarding causation from our observations, these will require individual study. The role of individual MMPs and the overall balance of MMPs to their tissue inhibitors, the role of elastin disruption, the source and mechanism of fibroblast recruitment and the inhibitory action of KGF on fibroproliferation after lung stretch will each require more detailed analysis.

10.4 The potential of Mesenchymal Stem Cells in ALI

Mesenchymal stem cells represent a therapy that may revolutionize medicine. Ours [452] and other studies have demonstrated a simple intravenous cell therapy that can restore function to damaged or diseased tissue, avoid host

rejection and reduce inflammation throughout the body without the use of immunosuppressive drugs. Specifically, cell therapy utilizing adult mesenchymal stem cells, multipotent cells with the capacity to promote angiogenesis, differentiate to produce multiple types of connective tissue and downregulate an inflammatory response, are the focus of a multitude of clinical studies currently underway. MSCs are being explored to regenerate damaged tissue and treat inflammation, resulting from cardiovascular disease and myocardial infarction (MI), brain and spinal cord injury, stroke, diabetes, cartilage and bone injury, Crohn's disease and graft versus host disease (GvHD) [1]. The results from ours and other studies in ALI provide the young field of MSC therapy with rationale for additional 'steps' forward. This research is beginning to identify the fate and function of MSC following systemic infusion. With evidence for massive cell entrapment in the capillary beds of the lungs, ALI would appear to be an ideal target for this therapy [2,37].

10.5 Results in context: Efficacy of MSCs in other pre-clinical models

The studies of MSCs outlined in this thesis provide important novel insights. Several experimental studies have shown the possible value of allogeneic MSC for a variety of clinical disorders, including myocardial infarction [95, 453], diabetes [454], hepatic failure [94], acute renal failure [93], and sepsis [96, 120]. MSCs have also been demonstrated to reduce mortality, improve alveolar epithelial barrier function and attenuate inflammation and lung injury in diverse pre-clinical ALI animal models including bleomycin-induced lung injury in mice [117], intraperitoneal endotoxin [118], intrapulmonary endotoxin or live *Esherichia coli* bacteria [96, 119], in a mouse caecal ligation and puncture model

of sepsis [120], in hyperoxia-induced bronchopulmonary dysplasia [121, 122], and in the *ex vivo* perfused human lung preparation [123, 124].

Our study is the first to look at the potential for MSCs to repair the injured lung. Others have focused on the acute stages after injury, and the potential for MSCs to modulate the acute inflammatory response. Our study is also the first to use repeated dosing of MSCs, an approach that we consider more likely to be used in clinical practice if MSCs are shown to be safe and effective in human ALI.

10.6 Insights into mechanism of action of MSCs

Early studies appeared to demonstrate MSC engraftment in the lung and trans-differentiation into alveolar cells [162]. However, these results were questioned by multiple groups, who observed only engraftment of leukocyte lineages [163], or efficacy despite low engraftment rates in lung injury models with observed rates of < 1% [117, 164, 165]. Our experiments confirm what has been demonstrated by others, that the mechanism of action of MSCs appears to be predominantly paracrine, and to involve the release of factors that have immunomodulatory, reparative and anti-bacterial effects.

10.6.1 MSC effects on the immune response

MSCs had profound effects on inflammatory cell recruitment in lung after injury and the subsequent inflammatory response in our model of repair from VILI. These effects were repeated with conditioned medium from MSCs, containing their secreted mediators. MSCs have previously been shown to interact with a wide range of immune cells and exert diverse effects on the innate and adaptive

immune responses. These include suppression of T-cell proliferation, NK cell function and inhibition of dendritic cell differentiation [238]. The list of soluble factors that are candidate mediators for MSC immune modulation includes transforming growth factor-β (TGF-β) [241], prostaglandin E_2 (PGE_2) [120], indoleamine 2,3-dioxygenase [209], interleukin-1-receptor antagonist (IL-1ra) [242] and tumour necrosis factor-α-induced protein 6 (TSG-6) [244] among others. Recently Danchuk *et al* [244] demonstrated that human MSCs delivered via either the intravenous or intraperitoneal route significantly attenuated LPS-induced inflammation in the lung. Knockdown of TSG-6 expression in hMSCs by RNA interference abrogated most of their anti-inflammatory effects. In addition, intra-pulmonary delivery of recombinant human TSG-6 reduced LPS-induced inflammation in the lung [244].

10.6.3 MSCs secrete growth factors

Bone marrow derived MSC are known to produce several epithelial specific growth factors. In our experiments we used neutralizing antibodies to examine the contribution of candidate mediators responsible for more efficient wound repair. Inhibition of keratinocyte growth factor, which was secreted in excess by MSCs in comparison to fibroblasts, abolished much of the reparative effects of MSC conditioned medium. KGF secreted by MSCs has demonstrated other beneficial effects in ALI. In the *ex vivo* perfused human lung, the intra-bronchial instillation of human MSC 1 h following endotoxin-induced lung injury restored alveolar fluid clearance, in part by the secretion of keratinocyte growth factor (KGF) [124]. Other MSC secreted growth factors have also been identified. In

primary cultures of human alveolar type II cells, human MSCs grown without cell contact in a Transwell plate restored the increase in epithelial permeability to protein caused by exposure to inflammatory cytokines in part by the secretion of Angiopoietin-1 [240]. Another epithelial specific growth factor secreted by MSC is hepatocyte growth factor (HGF) [239] . Previously, HGF was found to stabilize integrity of pulmonary endothelial cells by the inhibition of Rho GTPase and the prevention of actin stress fiber formation and paracellular gaps among pulmonary endothelial cells injured by thrombin [248]. However, blocking HgF did not alter the reparative capacity of the MSC secretome in our studies.

10.6.4 Role of other secreted mediators

Other soluble factors released by MSCs include VEGF-1, IGF-1, EGF, NO, stromal derived factor-1, macrophage inflammatory protein-1a and -1b and erythropoietin [354]. These molecules are known to be important for cell survival, proliferation and neovascularization during tissue repair and wound healing.

Further limiting the damage from inflammation in MSC-transplanted mice could be the ability of MSCs to regulate the oxidative state of the local environment. It has been demonstrated that MSCs secrete antioxidant molecules such as glutathione and disulfide cysteine, to maintain redox homeostasis, as seen when conditioned media from MSCs were able to rescue oxidized cells and in an endotoxin model of lung injury [249].

Thus much of current evidence for MSC mediated disease modification has focused on soluble factors. MSCs have the ability to secrete multiple paracrine factors such as growth factors, factors regulating endothelial and epithelial

permeability, anti-inflammatory cytokines, and, more recently, antimicrobial peptides that can potentially treat many of the abnormalities that underlie ALI, including impaired alveolar fluid clearance, alveolar epithelial injury, altered lung endothelial permeability, dysregulated inflammation and infection.

10.6.5 Keratinocyte Growth Factor – a potential therapeutic agent?

The protective effect of exogenous KGF in a model of acute lung injury was first reported in 1995 by Panos et al [386]. In that study, rats pre-treated intratracheally with 5 mg/kg of recombinant human KGF had far better survival and virtually no histological changes when exposed to 120h of hyperoxia compared with untreated animals. Intratracheal KGF has since been shown to have a protective effect in a variety of other lung injury models: in an acid instillation model [387], pre-treatment with intratracheal KGF reduced mortality; in an ANTU model of increased permeability pulmonary edema [388], pretreatment with KGF reduced alveolar-capillary barrier permeability and pulmonary edema formation. Similar beneficial effects on vascular permeability and pulmonary edema formation have been reported in a rat model of ventilator-induced lung injury [389]. Intratracheal KGF has also been shown to ameliorate radiation pneumonitis [390], bleomycin-induced lung injury [455], and Pseudomonas aeruginosa pneumonia [392], when given before the insult. Intravenous KGF (5 mg/kg) has also been shown to protect against bleomycin- and hyperoxia- induced lung injury in mice [456], even though it stimulated less alveolar epithelial proliferation than intra-tracheal KGF.

Several important observations can be made from a comparison of these studies of KGF in lung injury models. First, KGF was protective for a wide variety of

mechanisms of lung injury. Second, the beneficial effects of KGF were multifactorial. These included reduced or absent histological changes, decreased fibrosis and deposition of collagen precursors, reduced physiological indices of lung injury including vascular permeability and formation of pulmonary edema, and improved survival. Of note, KGF enhances the spreading and motility of alveolar epithelial type II cells, suggesting that improved alveolar repair may underlie some of the protective effects of KGF in lung injury [457].

However, in all studies, pretreatment with KGF was necessary for the protective effect. Simultaneous or posttreatment was not efficacious. These observations suggest that the mechanisms by which KGF exerts its protective effects on lung injury are probably multiple, not immediate, and affect multiple cell types within the lung. However, exogenous delivery of KGF, particularly to the injured lung, may not represent an efficient delivery method for this promising growth factor. MSCs, as discussed above, may provide a more reliable vehicle for delivery of this molecule to damaged alveolar epithelium. Our work suggests that either MSCs alone, or MSCs overexpressing KGF, may be the most efficacious therapeutic strategy to maximize the potential of this promising reparative agent.

10.7 Issues in translating MSC therapy for human ALI

MSCs constitute a promising therapeutic strategy for patients suffering from ALI/ARDS. MSCs appear close to clinical translation, given the evidence that they may favourably modulate the immune response to reduce lung injury, while maintaining host immune-competence and also facilitating lung regeneration and repair. The demonstration that human MSCs exert benefit in the endotoxin injured human lung is particularly persuasive. However, gaps remain in our

knowledge regarding the mechanisms of action of MSCs, the optimal MSC administration and dosage regimens, and the safety of MSSs in critically ill patients. It is anticipated that these remaining knowledge deficits will be addressed in ongoing and future studies.

10.7.1 Insights from Clinical Studies

The therapeutic potential of MSCs has been reported in recent years in several fields. Currently, clinical trials using MSCs to treat acute myocardial ischemia (AMI), stroke, liver cirrhosis, amyotrophic lateral sclerosis (ALS), GVHD, fire burns and Crohn's disease have been reported.

A pilot study with 11 patients showed that MSCs were effective for radiation-induced lung injuries that developed after combined chemotherapy and radiation therapy for lymphogranulomatosis or breast cancer [458]. This is the only report on the use of MSCs for any lung disease.

In a Phase I, double-blind, placebo-controlled trial of PROCHYMAL (ex vivo cultured adult human mesenchymal stem cells) conducted by Osiris Therapeutics Inc. (Columbia, MD) in patients with acute myocardial infarction, an improvement in both FEV1 and FVC was noted in treated patients [130]. Although the mechanisms of improvement in pulmonary function in this patient population are not yet understood, these observations stimulated a multicenter, double-blind, placebo- controlled Phase II trial of PROCHYMAL (Osiris Therapeutics Inc., Columbia, MD) for patients with moderate to severe COPD (FEV1/FVC , 0.70; 30% < FEV1 < 70%). The primary goal of the trial, which was initiated in May 2008, is to determine safety of MSC infusions in patients with lung disease. The secondary goal is initial estimation of the potential efficacy of

MSCs for decreasing the chronic inflammation associated with COPD thus improving both pulmonary function and quality of life.

In a randomized clinical trial of MSC therapy for acute MI reported by Chen et al. [459], 69 patients with acute MI after percutaneous coronary intervention were randomized to receive either intracoronary injection of bone-marrow-derived MSCs or control vehicle. MSCs significantly increased the left ventricular ejection fraction three months after transplantation compared with the control group. MSC transplantation was safe with no deaths or malignant arrhythmias [459]. Since then, several clinical trials have been performed to test the safety and efficacy of MSC transplantation for the treatment of MI and chronic ischemic cardiomyopathy [460-462]. These studies have each enrolled a small number of patients, are heterogeneous in their methods and have relatively short follow-up duration. Thus, these studies have fallen short of providing conclusive results.

Studies have demonstrated that intravenous infusion of autologous MSCs to stroke patients is a feasible and safe therapy that may improve functional recovery [398, 463]. In addition, MSCs were tried for multiple sclerosis, amyotrophic lateral sclerosis, Parkinson's disease and metachromatic leukodystrophy [464-466] with some success. Although these preliminary clinical studies are encouraging, further studies are warranted.

MSCs have been applied in the clinic to treat corticoid- resistant life-threatening GVHD [467, 468]. This treatment resulted in a lower transplant-related mortality in patients with complete response one year after MSC infusion compared with patients with partial or no response (37 versus 72%), as well as a higher overall survival two years after HSC transplantation (53 versus 16%). Any possible effect of the immunosuppressive properties of MSCs on the incidence of

infectious complications was not evident in the already immunosuppressed GVHD patients and the overall result was a significant improvement in the survival of these corticoid-resistant GVHD patients as compared with patients treated with other alternatives.

There is much scientific and clinical interest in the potential of MSCs to stimulate wound repair. Mesenchymal stem cell based therapies represent a new treatment for preventing morbidity and disability associated with chronic wounds - an unresolved clinical problem that has shown little improvement over the past decades [469]. Recent studies have demonstrated that treatment of cutaneous wounds with BMSCs accelerates wound healing kinetics and increases epithelialization and angiogenesis [349, 352, 353], suggesting that MSCs enhance wound repair by at least two different mechanisms: differentiation and paracrine interactions with specific cell types in the cutaneous wound [354]. These studies of the clinical potential of MSCs for other diseases provide reassurance regarding the clinical safety of MSCs and suggest translation of MSCs to clinical testing for ARDS is a realistic goal.

10.7.2 Stem Cell Administration Route and Dosage Regimens

The optimal route of delivery for MSCs is a subject of some debate. Most of the experimental studies in ALI to date have been carried out using intratracheal delivery [470]. On the other hand, the pulmonary circulation is an ideal target for intravenous (IV) delivery, given it is the first capillary bed encountered by injected cells. Indeed the pulmonary vascular bed acts as a barrier to MSC delivery to other organs such as the heart, kidney and brain, such that investigators now utilize local injection techniques to target these organs [461,

464]. MSCs home to injured organs, whether the injury occurs in the liver, kidney, or the lung [399], and IV delivered MSCs may have multiple beneficial effects in ALI with associated multiorgan failure. MSCs have been delivered IV in other conditions with a good safety record [471]. Thus, the IV route may prove the most efficacious mode of delivery.

As mentioned above, MSCs modulate immune cell functions in a dose-dependent manner *in vitro*. Similarly a strong direct correlation was found between the number of cells applied and the therapeutic outcomes in treating chronic wound and heart infarction [349, 472]. The ideal dose selection of MSCs for critically ill patients with ALI remains a matter of conjecture. Extrapolation from animal studies and from human studies of MSC administration in other disease states may be used as a guide. For example, 1-2 million cells/kg has been used safely in healthy subjects and in patients with disease [471]. However, these doses will need validation in the critical care setting. It has been suggested that treatment could be given over three consecutive days [399] as has been used in a trial of autologous endothelial progenitor cells in patients with end stage pulmonary hypertension [473]. However, obviously the optimal dose of stem cells differs when different diseases are treated. In addition, the dose may be influenced by other factors, such as state of illness, type of MSCs, route of cell delivery, viability and purity of MSCs and condition of the patient.

Current clinical trials and animal studies have indicated that the early phase of injury or acute/subacute phases of diseases may be the optimal time window for stem cell therapy. Behr *et al*. [474] investigated the engraftment of autologous MSCs injected into the renal artery in an ovine model of ischemia/ reperfusion-induced injury to assess the consequences of delayed cell transplantation.

Results showed there was a significant increase in engraftment of tubules by MSCs when cells were injected early after injury. Similarly animals with stroke who received MSCs on post-ischemic days recovered significantly better than animals treated with MSCs 30 days after ischemia [475]. Our data suggest that MSCs may be effective when the injury has become established. In addition, our study is the first to use repeated dosing in ALI, highlighting the safety and efficacy of this dosing option. Finally, our data regarding upregulation of IL-10 only when MSCs are given systemically raises the possibility that beneficial immune-modulation may be optimal when given intravenously, rather then locally.

10.7.3 Lack of mechanistic knowledge

Despite an explosion of mechanistic studies across a broad range of disease areas, a consensus on MSC mechanism of action is far from clear. This is borne out by the diverse array of paracrine mediators responsible for therapeutic effects as outlined. Research on MSCs is confused by the marked differences in MSCs from mice and human MSCs in terms of properties such as cell surface epitopes, ease of expansion, and genomic stability [476]. It is also becoming increasingly apparent that different inflammatory environments can profoundly influence MSC behavior [477]. Furthermore, there is growing evidence that MSCs are heterogeneous and that different MSC subtypes exist [478]. Our studies, which utilized a heterogenous MSC population, provide further evidence for a paracrine mechanism of action, with KGF. Although isolating these paracrine factors, as we and others have done, raises the intruiging possibility of bypassing

the need for a cell therapy, it is unlikely that all of the beneficial effects of MSCs could be packaged and administered without the cell.

10.7.4 Need for culture expansion

One of the limitations of cell therapy for clinical use is the insufficient number of cells that can be isolated from tissues to achieve therapeutic effect. *Ex-vivo* expansion of MSCs, therefore, is a good therapeutic option. However, MSCs may give rise to more restricted self-renewing progenitors when they are passaged, and gradually lose their differentiation potential until a state of complete restriction to the fibroblast is reached [479]. Homing receptors such as CXCR4, which is a chemotactic receptor for SDF-1 and crucial for their migration capability, might diminish as cells are continually passaged [480]. This may explain why freshly isolated MSCs have greater homing ability compared with their culture-expanded counterparts [481]. Therefore a balance between culture expansion and early passage number is advisable. In our studies we used MSCs at passage 2-4. This provided the capacity for population multiplication, while limiting these doublings in order to maintain therapeutic effect. It remains to be seen if longer lived and expanded cultures will have similar efficacy.

In addition, culture conditions, including culture density, culture surface composition [130], oxygen levels [482] and temperature [483] can profoundly influence phenotype and behavior of MSCs.

10.7.5 Tumourigencity

In contrast to embryonic stem cells, human adult stem cells are thought to be extremely resistant to transformation [484]. It is well recognized that DNA mutation may happen in late-passage MSCs [485]. MSCs have, however, also shown limited *ex vivo* expansion potential in normal conditions, a fact that increases their safety profile [486]. Spontaneous transformation of un-manipulated human MSCs has been described [487-489]. Nevertheless, many laboratories have been unable to reproduce these results, indicating genetic or karyotypic alterations rather than immortalization or transformation [490-492]. Recently, the first transformation described was ruled out by the authors, who demonstrated culture cross-contaminations [493]. In any case, these data should introduce a note of caution in the clinical use of MSCs. All current clinical trials expand MSCs as little as possible to maintain the original features while generating sufficient numbers to enable therapeutic interventions; any culture showing signs of alterations would therefore be discarded. These data indicate the need for greater knowledge of human adult stem cell biology and inter-individual variation in order to unlock the immense therapeutic potential of MSCs.

10.7.6 Pulmonary fibrosis

The potential for MSC therapy to contribute to fibroproliferative ARDS remains a potential concern, since bone marrow cells have been implicated in the fibrotic process. In bleomycin-induced pulmonary fibrosis, Hashimoto and colleagues demonstrated that bone marrow progenitor cells were recruited to injured areas and differentiated into fibroblasts [494]. In pulmonary fibrosis induced by irradiation, circulating cells of bone marrow origin contribute to the fibrotic

process [495]. However in animal models of pulmonary fibrosis induced by bleomycin, MSCs ameliorate the fibrotic process, resulting in reduced lung expression of pro-fibrotic cytokines and stimulated production of growth factors involved in endogenous stem cell mobilization from bone marrow, helping the repair process [117, 165, 242]. MSCs transfected to over-express the growth factor KGF also leads to a reduction in lung fibrogenesis [496].

10.8 Summary and conclusion

ALI/ARDS is a highly complex disease process. Earlier concepts of distinct disease phases, from an early 'pro-inflammatory' to a later 'fibrotic' phase now appear to be an over-simplification. It is increasingly apparent that these phases largely co-exist, with evidence of 'pro-inflammatory' responses leading to host damage, an impaired immune response to pathogens, and of repair and fibrosis all present in the complex milieu that is clinical ALI/ARDS. Given this, it is perhaps not surprising that strategies targeted at single aspects of the disease process have been unsuccessful. This suggests the need to consider more complex therapeutic approaches, aimed at reducing early injury while maintaining host immune competence, and facilitating (or at least not inhibiting) lung regeneration and repair. MSCs offer considerable hope as a therapy for ALI/ARDS. They are immunomodulatory, antibacterial, enhance pulmonary oedema clearance, and as we have demonstrated, are regenerative. We have demonstrated their ability to restore epithelial and endothelial function via secretion of paracrine factors. Through investigation of MSC biology, discovery of their therapeutic mechanisms within animal models and testing their

therapeutic potential within human trials, we will hopefully achieve many more steps forward to make MSC therapy a new clinical paradigm.

11.0 Publications, Presentations and Awards

11.1 Original articles

Curley G, Contreras M, O'Toole B, Higgins B, O'Kane C, McAuley D, Laffey JG. Evolution of the inflammatory and fibroproliferative responses during resolution and repair following Ventilator Induced Lung Injury. **Anesthesiology. 2011 Nov;115(5):1022-32**

Curley GF, Hayes M, Ansari B, Shaw G, Ryan A, Barry F, O'Brien T, O'Toole D, Laffey JG. Mesenchymal stem cells enhance recovery and repair following ventilator-induced lung injury in the rat. **Thorax. 2011 Nov 21 Epub**

Curley GF, Ansari B, Hayes M, Devaney J, Barry F, O'Brien T, O'Toole D, Laffey JG. Effects of intra-tracheal Mesenchymal Stem Cells therapy during recovery and resolution following Ventilator Induced Lung Injury. **Undergoing peer review at Critical Care Medicine, submitted February 2012.**

11.2 Reviews and commentary

Curley GF, Kevin LG, Laffey JG. Mechanical ventilation: taking its toll on the lung. **Anesthesiology. 2009 Oct;111(4):701-3**

Hayes M, Curley GF, Laffey JG. Lung stem cells - from an evolving understanding to a paradigm shift? **Stem Cell Res Ther. 2011 Oct 20;2(5):41**

Hayes M, Curley G, Laffey JG. Mesenchymal stem cells - a promising therapy for Acute Respiratory Distress Syndrome **F1000 Med Rep. 2012;4:2. Epub 2012 Jan 3**

Hayes M, Curley G, Laffey JG. Stem cell therapies for ALI/ARDS – hope or hype? **Critical Care. Accepted for publication January 2012**

11.3 Invited Lectures

Société de Réanimation de langue Française (French Intensive Care Society), International Congress, Paris, January 2012
Technologies of the future: Mesenchymal Stem Cells for Acute Lung Injury

11.4 Oral Presentations

European Society for Intensive Care Medicine, Berlin, October 2011
Intratracheal Delivery of Mesenchymal Stem Cells enhance repair following Ventilator Induced Lung Injury

American Thoracic Society International Conference, Denver, May 2011.
Mesenchymal Stem Cells enhance repair following Ventilator Induced Lung Injury

Delaney Medal Research Presentation, Dublin, March 2011
Mesenchymal Stem Cells enhance repair following Ventilator Induced Lung Injury

Canada Critical Care Forum, Toronto, Canada, November, 2010.
Mesenchymal Stem Cells enhance repair following Ventilator Induced Lung Injury

UK and Ireland Acute Lung Injury Group Annual Meeting, London, UK. October 2010

Mesenchymal Stem Cells and Ventilator Induced Lung Injury

Current Controversies in Anaesthesia and Peri-operative Medicine, Dingle, 2010.

Mesenchymal Stem Cells and Ventilator Induced Lung Injury

European Society of Intensive Care Medicine Annual Congress, Barcelona, October 2010

Mesenchymal Stem Cells enhance repair following Ventilator Induced Lung Injury

Western Anaesthesia Symposium, Westport, Co Mayo, Ireland. April 2010.

The role of mesenchymal stem cells during repair from Ventilator Induced Lung Injury.

University College London/ Intensive Care Society of Ireland Autumn Meeting. Dingle, Co Kerry, Ireland. October 2009

Time course of lung injury, inflammation, fibrosis and repair following Ventilator Induced Lung Injury

Molecular Medicine Ireland, Clinical Scientist Fellowship Programme, Annual Meeting. Galway, Ireland. Sept 2009

Evaluating strategies for repair from Ventilator Induced Lung Injury

Intensive Care Society of Ireland, Annual Scientific Meeting, Dublin, June 2009

Characterising the repair phase from Ventilator Induced Lung Injury

11.5 Poster Presentations

Tissue Engineering and Regenerative Medicine International Society EU Chapter meeting, Galway, Ireland, June 2010
Evaluating the fibroproliferative response to Ventilator Induced Lung Injury

American Thoracic Society International Conference, New Orleans, May 2010
Time course of lung injury, inflammation, fibrosis and repair following Ventilator Induced Lung Injury

International Symposium on Intensive Care and Emergency Medicine, Brussels, Belgium, March 2010
Evaluating the fibroproliferative response to Ventilator Induced Lung Injury

Western Anaesthesia Symposium. Westport, Co Mayo, Ireland. April 2009
Developing an animal model of repair of Ventilator Induced Lung Injury

11.6 Awards

Notable Abstract, European Society of Intensive Care Medicine Annual Congress, Barcelona, 2010

Best Presentation, University College London Current Controversies in Anaesthesia and Peri-operative Care, Dingle, 2010

Best Abstract and Presentation Award, Critical Care Canada Forum, Toronto, Canada, 2010

American Thoracic Society Respiratory Structure and Function Assembly Abstract Excellence Award, ATS International Conference Denver 2011

Best oral presentation, Intensive Care Society of Ireland, Annual Congress, June 2011

11.7 Funding Awards

Molecular Medicine Ireland, Clinical Scientist Fellowship Programme Grant Award 2008-2011. Laboratory based structured PhD programme including equipment grant, consumables grant, travel stipend and wages. Value €250,000 over three years.

Intensive Care Society of Ireland Research Award 2009. Value €5000

Intensive Care Society of Ireland Research Award 2011. Value €5000

12.0 References

1. **Rubenfeld GD, Caldwell E, Peabody E, Weaver J, Martin DP, Neff M, Stern EJ, Hudson LD: Incidence and outcomes of acute lung injury. *N Engl J Med* 2005, 353(16):1685-1693.**
2. **Blank R, Napolitano LM: Epidemiology of ARDS and ALI. *Crit Care Clin* 2011, 27(3):439-458.**
3. **Phua J, Badia JR, Adhikari NK, Friedrich JO, Fowler RA, Singh JM, Scales DC, Stather DR, Li A, Jones A *et al*: Has mortality from acute respiratory distress syndrome decreased over time?: A systematic review. *Am J Respir Crit Care Med* 2009, 179(3):220-227.**
4. **Ware LB, Matthay MA: The acute respiratory distress syndrome. *N Engl J Med* 2000, 342(18):1334-1349.**
5. **Bigatello LM, Pesenti A: Ventilator-induced lung injury: less ventilation, less injury. *Anesthesiology* 2009, 111(4):699-700.**
6. **Moriondo A, Mukenge S, Negrini D: Transmural pressure in rat initial subpleural lymphatics during spontaneous or mechanical ventilation. *Am J Physiol Heart Circ Physiol* 2005, 289(1):H263-269.**
7. **Tremblay L, Valenza F, Ribeiro SP, Li J, Slutsky AS: Injurious ventilatory strategies increase cytokines and c-fos m-RNA expression in an isolated rat lung model. *J Clin Invest* 1997, 99(5):944-952.**
8. **Frank JA, Gutierrez JA, Jones KD, Allen L, Dobbs L, Matthay MA: Low tidal volume reduces epithelial and endothelial injury in acid-injured rat lungs. *Am J Respir Crit Care Med* 2002, 165(2):242-249.**
9. **Tremblay LN, Slutsky AS: Ventilator-induced lung injury: from the bench to the bedside. *Intensive Care Med* 2006, 32(1):24-33.**
10. **Gattinoni L, Pesenti A, Avalli L, Rossi F, Bombino M: Pressure-volume curve of total respiratory system in acute respiratory failure. Computed tomographic scan study. *Am Rev Respir Dis* 1987, 136(3):730-736.**
11. **Maunder RJ, Shuman WP, McHugh JW, Marglin SI, Butler J: Preservation of normal lung regions in the adult respiratory distress syndrome. Analysis by computed tomography. *JAMA* 1986, 255(18):2463-2465.**
12. **Tsuchida S, Engelberts D, Peltekova V, Hopkins N, Frndova H, Babyn P, McKerlie C, Post M, McLoughlin P, Kavanagh BP: Atelectasis causes alveolar injury in nonatelectatic lung regions. *Am J Respir Crit Care Med* 2006, 174(3):279-289.**

13. **Greenfield LJ, Ebert PA, Benson DW: EFFECT OF POSITIVE PRESSURE VENTILATION ON SURFACE TENSION PROPERTIES OF LUNG EXTRACTS. *Anesthesiology* 1964, 25:312-316.**
14. **Sladen A, Laver MB, Pontoppidan H: Pulmonary complications and water retention in prolonged mechanical ventilation. *N Engl J Med* 1968, 279(9):448-453.**
15. **Webb HH, Tierney DF: Experimental pulmonary edema due to intermittent positive pressure ventilation with high inflation pressures. Protection by positive end-expiratory pressure. *Am Rev Respir Dis* 1974, 110(5):556-565.**
16. **Dreyfuss D, Basset G, Soler P, Saumon G: Intermittent positive-pressure hyperventilation with high inflation pressures produces pulmonary microvascular injury in rats. *Am Rev Respir Dis* 1985, 132(4):880-884.**
17. **Dreyfuss D, Soler P, Basset G, Saumon G: High inflation pressure pulmonary edema. Respective effects of high airway pressure, high tidal volume, and positive end-expiratory pressure. *Am Rev Respir Dis* 1988, 137(5):1159-1164.**
18. **Dreyfuss D, Soler P, Saumon G: Spontaneous resolution of pulmonary edema caused by short periods of cyclic overinflation. *J Appl Physiol* 1992, 72(6):2081-2089.**
19. **Kolobow T, Moretti MP, Fumagalli R, Mascheroni D, Prato P, Chen V, Joris M: Severe impairment in lung function induced by high peak airway pressure during mechanical ventilation. An experimental study. *Am Rev Respir Dis* 1987, 135(2):312-315.**
20. **Tsuno K, Prato P, Kolobow T: Acute lung injury from mechanical ventilation at moderately high airway pressures. *J Appl Physiol* 1990, 69(3):956-961.**
21. **John E, McDevitt M, Wilborn W, Cassady G: Ultrastructure of the lung after ventilation. *Br J Exp Pathol* 1982, 63(4):401-407.**
22. **Cooper JA, van der Zee H, Line BR, Malik AB: Relationship of end-expiratory pressure, lung volume, and 99mTc-DTPA clearance. *J Appl Physiol* 1987, 63(4):1586-1590.**
23. **O'Brodovich H, Coates G, Marrin M: Effect of inspiratory resistance and PEEP on 99mTc-DTPA clearance. *J Appl Physiol* 1986, 60(5):1461-1465.**
24. **Marks JD, Luce JM, Lazar NM, Wu JN, Lipavsky A, Murray JF: Effect of increases in lung volume on clearance of aerosolized solute from human lungs. *J Appl Physiol* 1985, 59(4):1242-1248.**
25. **Nolop KB, Maxwell DL, Royston D, Hughes JM: Effect of raised thoracic pressure and volume on 99mTc-DTPA clearance in humans. *J Appl Physiol* 1986, 60(5):1493-1497.**
26. **Egan EA: Response of alveolar epithelial solute permeability to changes in lung inflation. *J Appl Physiol* 1980, 49(6):1032-1036.**
27. **Ramanathan R, Mason GR, Raj JU: Effect of mechanical ventilation and barotrauma on pulmonary clearance of 99mtechnetium diethylenetriamine pentaacetate in lambs. *Pediatr Res* 1990, 27(1):70-74.**

28. **Parker JC, Townsley MI, Rippe B, Taylor AE, Thigpen J: Increased microvascular permeability in dog lungs due to high peak airway pressures.** ***J Appl Physiol*** **1984, 57(6):1809-1816.**
29. **Mead J, Takishima T, Leith D: Stress distribution in lungs: a model of pulmonary elasticity.** ***J Appl Physiol*** **1970, 28(5):596-608.**
30. **Omlor G, Niehaus GD, Maron MB: Effect of peak inspiratory pressure on the filtration coefficient in the isolated perfused rat lung.** ***J Appl Physiol*** **1993, 74(6):3068-3072.**
31. **Julien M, Flick MR, Hoeffel JM, Murray JF: Accurate reference measurement for postmortem lung water.** ***J Appl Physiol*** **1984, 56(1):248-253.**
32. **Martynowicz MA, Minor TA, Walters BJ, Hubmayr RD: Regional expansion of oleic acid-injured lungs.** ***Am J Respir Crit Care Med*** **1999, 160(1):250-258.**
33. **Dreyfuss D, Martin-Lefevre L, Saumon G: Hyperinflation-induced lung injury during alveolar flooding in rats: effect of perfluorocarbon instillation.** ***Am J Respir Crit Care Med*** **1999, 159(6):1752-1757.**
34. **Lecuona E, Saldias F, Comellas A, Ridge K, Guerrero C, Sznajder JI: Ventilator-associated lung injury decreases lung ability to clear edema in rats.** ***Am J Respir Crit Care Med*** **1999, 159(2):603-609.**
35. **Hernandez LA, Peevy KJ, Moise AA, Parker JC: Chest wall restriction limits high airway pressure-induced lung injury in young rabbits.** ***J Appl Physiol*** **1989, 66(5):2364-2368.**
36. **Adkins WK, Hernandez LA, Coker PJ, Buchanan B, Parker JC: Age effects susceptibility to pulmonary barotrauma in rabbits.** ***Crit Care Med*** **1991, 19(3):390-393.**
37. **Carlton DP, Cummings JJ, Scheerer RG, Poulain FR, Bland RD: Lung overexpansion increases pulmonary microvascular protein permeability in young lambs.** ***J Appl Physiol*** **1990, 69(2):577-583.**
38. **Dreyfuss D, Saumon G: Ventilator-induced lung injury: lessons from experimental studies.** ***Am J Respir Crit Care Med*** **1998, 157(1):294-323.**
39. **Corbridge TC, Wood LD, Crawford GP, Chudoba MJ, Yanos J, Sznajder JI: Adverse effects of large tidal volume and low PEEP in canine acid aspiration.** ***Am Rev Respir Dis*** **1990, 142(2):311-315.**
40. **Colmenero-Ruiz M, Fernandez-Mondejar E, Fernandez-Sacristan MA, Rivera-Fernandez R, Vazquez-Mata G: PEEP and low tidal volume ventilation reduce lung water in porcine pulmonary edema.** ***Am J Respir Crit Care Med*** **1997, 155(3):964-970.**
41. **Bshouty Z, Ali J, Younes M: Effect of tidal volume and PEEP on rate of edema formation in in situ perfused canine lobes.** ***J Appl Physiol*** **1988, 64(5):1900-1907.**
42. **Muscedere JG, Mullen JB, Gan K, Slutsky AS: Tidal ventilation at low airway pressures can augment lung injury.** ***Am J Respir Crit Care Med*** **1994, 149(5):1327-1334.**
43. **Naureckas ET, Dawson CA, Gerber BS, Gaver DP, 3rd, Gerber HL, Linehan JH, Solway J, Samsel RW: Airway reopening pressure in isolated rat lungs.** ***J Appl Physiol*** **1994, 76(3):1372-1377.**

44. Bilek AM, Dee KC, Gaver DP, 3rd: Mechanisms of surface-tension-induced epithelial cell damage in a model of pulmonary airway reopening. ***J Appl Physiol*** **2003, 94(2):770-783.**

45. Slutsky AS, Tremblay LN: Multiple system organ failure. Is mechanical ventilation a contributing factor? ***Am J Respir Crit Care Med*** **1998, 157(6 Pt 1):1721-1725.**

46. Ranieri VM, Suter PM, Tortorella C, De Tullio R, Dayer JM, Brienza A, Bruno F, Slutsky AS: Effect of mechanical ventilation on inflammatory mediators in patients with acute respiratory distress syndrome: a randomized controlled trial. ***JAMA*** **1999, 282(1):54-61.**

47. ARDSNet: Ventilation with lower tidal volumes as compared with traditional tidal volumes for acute lung injury and the acute respiratory distress syndrome. The Acute Respiratory Distress Syndrome Network. ***N Engl J Med*** **2000, 342(18):1301-1308.**

48. Meduri GU, Headley S, Kohler G, Stentz F, Tolley E, Umberger R, Leeper K: Persistent elevation of inflammatory cytokines predicts a poor outcome in ARDS. Plasma IL-1 beta and IL-6 levels are consistent and efficient predictors of outcome over time. ***Chest*** **1995, 107(4):1062-1073.**

49. Goodman RB, Strieter RM, Martin DP, Steinberg KP, Milberg JA, Maunder RJ, Kunkel SL, Walz A, Hudson LD, Martin TR: Inflammatory cytokines in patients with persistence of the acute respiratory distress syndrome. ***Am J Respir Crit Care Med*** **1996, 154(3 Pt 1):602-611.**

50. Imanaka H, Shimaoka M, Matsuura N, Nishimura M, Ohta N, Kiyono H: Ventilator-induced lung injury is associated with neutrophil infiltration, macrophage activation, and TGF-beta 1 mRNA upregulation in rat lungs. ***Anesth Analg*** **2001, 92(2):428-436.**

51. Imai Y, Kawano T, Iwamoto S, Nakagawa S, Takata M, Miyasaka K: Intratracheal anti-tumor necrosis factor-alpha antibody attenuates ventilator-induced lung injury in rabbits. ***J Appl Physiol*** **1999, 87(2):510-515.**

52. Narimanbekov IO, Rozycki HJ: Effect of IL-1 blockade on inflammatory manifestations of acute ventilator-induced lung injury in a rabbit model. ***Exp Lung Res*** **1995, 21(2):239-254.**

53. Quinn DA, Moufarrej RK, Volokhov A, Hales CA: Interactions of lung stretch, hyperoxia, and MIP-2 production in ventilator-induced lung injury. ***J Appl Physiol*** **2002, 93(2):517-525.**

54. Haitsma JJ, Uhlig S, Goggel R, Verbrugge SJ, Lachmann U, Lachmann B: Ventilator-induced lung injury leads to loss of alveolar and systemic compartmentalization of tumor necrosis factor-alpha. ***Intensive Care Med*** **2000, 26(10):1515-1522.**

55. Ricard JD, Dreyfuss D, Saumon G: Production of inflammatory cytokines in ventilator-induced lung injury: a reappraisal. ***Am J Respir Crit Care Med*** **2001, 163(5):1176-1180.**

56. Verbrugge SJ, Uhlig S, Neggers SJ, Martin C, Held HD, Haitsma JJ, Lachmann B: Different ventilation strategies affect lung function but do not increase tumor necrosis factor-alpha and prostacyclin

production in lavaged rat lungs in vivo. *Anesthesiology* 1999, 91(6):1834-1843.

57. Debs RJ, Fuchs HJ, Philip R, Montgomery AB, Brunette EN, Liggitt D, Patton JS, Shellito JE: Lung-specific delivery of cytokines induces sustained pulmonary and systemic immunomodulation in rats. *J Immunol* 1988, 140(10):3482-3488.

58. Wrigge H, Zinserling J, Stuber F, von Spiegel T, Hering R, Wetegrove S, Hoeft A, Putensen C: Effects of mechanical ventilation on release of cytokines into systemic circulation in patients with normal pulmonary function. *Anesthesiology* 2000, 93(6):1413-1417.

59. Vaneker M, Halbertsma FJ, van Egmond J, Netea MG, Dijkman HB, Snijdelaar DG, Joosten LA, van der Hoeven JG, Scheffer GJ: Mechanical ventilation in healthy mice induces reversible pulmonary and systemic cytokine elevation with preserved alveolar integrity: an in vivo model using clinical relevant ventilation settings. *Anesthesiology* 2007, 107(3):419-426.

60. Jaecklin T, Otulakowski G, Kavanagh BP: Do soluble mediators cause ventilator-induced lung injury and multi-organ failure? *Intensive Care Med* 2010, 36(5):750-757.

61. Pugin J, Dunn I, Jolliet P, Tassaux D, Magnenat JL, Nicod LP, Chevrolet JC: Activation of human macrophages by mechanical ventilation in vitro. *Am J Physiol* 1998, 275(6 Pt 1):L1040-1050.

62. Dunn I, Pugin J: Mechanical ventilation of various human lung cells in vitro: identification of the macrophage as the main producer of inflammatory mediators. *Chest* 1999, 116(1 Suppl):95S-97S.

63. Kurdowska A, Miller EJ, Noble JM, Baughman RP, Matthay MA, Brelsford WG, Cohen AB: Anti-IL-8 autoantibodies in alveolar fluid from patients with the adult respiratory distress syndrome. *J Immunol* 1996, 157(6):2699-2706.

64. Miller EJ, Cohen AB, Matthay MA: Increased interleukin-8 concentrations in the pulmonary edema fluid of patients with acute respiratory distress syndrome from sepsis. *Crit Care Med* 1996, 24(9):1448-1454.

65. Downey GP, Dong Q, Kruger J, Dedhar S, Cherapanov V: Regulation of neutrophil activation in acute lung injury. *Chest* 1999, 116(1 Suppl):46S-54S.

66. Tremblay LN, Slutsky AS: Ventilator-induced injury: from barotrauma to biotrauma. *Proc Assoc Am Physicians* 1998, 110(6):482-488.

67. Kawano T, Mori S, Cybulsky M, Burger R, Ballin A, Cutz E, Bryan AC: Effect of granulocyte depletion in a ventilated surfactant-depleted lung. *J Appl Physiol* 1987, 62(1):27-33.

68. Zhang H, Downey GP, Suter PM, Slutsky AS, Ranieri VM: Conventional mechanical ventilation is associated with bronchoalveolar lavage-induced activation of polymorphonuclear leukocytes: a possible mechanism to explain the systemic consequences of ventilator-induced lung injury in patients with ARDS. *Anesthesiology* 2002, 97(6):1426-1433.

69. Taniguchi LU, Caldini EG, Velasco IT, Negri EM: Cytoskeleton and mechanotransduction in the pathophysiology of ventilator-induced lung injury. ***J Bras Pneumol*** **2010, 36(3):363-371.**

70. Parker JC, Ivey CL, Tucker JA: Gadolinium prevents high airway pressure-induced permeability increases in isolated rat lungs. ***J Appl Physiol*** **1998, 84(4):1113-1118.**

71. Parker JC, Ivey CL, Tucker A: Phosphotyrosine phosphatase and tyrosine kinase inhibition modulate airway pressure-induced lung injury. ***J Appl Physiol*** **1998, 85(5):1753-1761.**

72. Grembowicz KP, Sprague D, McNeil PL: Temporary disruption of the plasma membrane is required for c-fos expression in response to mechanical stress. ***Mol Biol Cell*** **1999, 10(4):1247-1257.**

73. Gajic O, Lee J, Doerr CH, Berrios JC, Myers JL, Hubmayr RD: Ventilator-induced cell wounding and repair in the intact lung. ***Am J Respir Crit Care Med*** **2003, 167(8):1057-1063.**

74. Jaecklin T, Engelberts D, Otulakowski G, O'Brodovich H, Post M, Kavanagh BP: Lung-derived soluble mediators are pathogenic in ventilator-induced lung injury. ***Am J Physiol Lung Cell Mol Physiol*** **2011, 300(4):L648-658.**

75. Pierson D: Barotrauma and bronchpleural fistula. In: ***Principle and Practice of Mechanical Ventilation.*** **Edited by Tobin M, 2 edn. New York: McGraw-Hill; 2006: 813-836.**

76. Tobin MJ: Culmination of an era in research on the acute respiratory distress syndrome. ***N Engl J Med*** **2000, 342(18):1360-1361.**

77. Amato MB, Barbas CS, Medeiros DM, Magaldi RB, Schettino GP, Lorenzi-Filho G, Kairalla RA, Deheinzelin D, Munoz C, Oliveira R ***et al*****: Effect of a protective-ventilation strategy on mortality in the acute respiratory distress syndrome.** ***N Engl J Med*** **1998, 338(6):347-354.**

78. Stewart TE, Meade MO, Cook DJ, Granton JT, Hodder RV, Lapinsky SE, Mazer CD, McLean RF, Rogovein TS, Schouten BD ***et al*****: Evaluation of a ventilation strategy to prevent barotrauma in patients at high risk for acute respiratory distress syndrome. Pressure- and Volume-Limited Ventilation Strategy Group.** ***N Engl J Med*** **1998, 338(6):355-361.**

79. Curley MA, Hibberd PL, Fineman LD, Wypij D, Shih MC, Thompson JE, Grant MJ, Barr FE, Cvijanovich NZ, Sorce L ***et al*****: Effect of prone positioning on clinical outcomes in children with acute lung injury: a randomized controlled trial.** ***JAMA*** **2005, 294(2):229-237.**

80. Meade MO, Cook DJ, Guyatt GH, Slutsky AS, Arabi YM, Cooper DJ, Davies AR, Hand LE, Zhou Q, Thabane L ***et al*****: Ventilation strategy using low tidal volumes, recruitment maneuvers, and high positive end-expiratory pressure for acute lung injury and acute respiratory distress syndrome: a randomized controlled trial.** ***JAMA*** **2008, 299(6):637-645.**

81. Terragni PP, Rosboch G, Tealdi A, Corno E, Menaldo E, Davini O, Gandini G, Herrmann P, Mascia L, Quintel M ***et al*****: Tidal hyperinflation during low tidal volume ventilation in acute respiratory distress syndrome.** ***Am J Respir Crit Care Med*** **2007, 175(2):160-166.**

82. **Gattinoni L, Caironi P, Pelosi P, Goodman LR: What has computed tomography taught us about the acute respiratory distress syndrome? *Am J Respir Crit Care Med* 2001, 164(9):1701-1711.**
83. **Laffey JG, Engelberts D, Kavanagh BP: Injurious effects of hypocapnic alkalosis in the isolated lung. *Am J Respir Crit Care Med* 2000, 162 (2):399-405.**
84. **Gattinoni L, Pesenti A: The concept of "baby lung". *Intensive Care Med* 2005, 31(6):776-784.**
85. **Fanelli V, Mascia L, Puntorieri V, Assenzio B, Elia V, Fornaro G, Martin EL, Bosco M, Delsedime L, Fiore T *et al*: Pulmonary atelectasis during low stretch ventilation: "open lung" versus "lung rest" strategy. *Crit Care Med* 2009, 37(3):1046-1053.**
86. **Duggan M, Kavanagh BP: Pulmonary atelectasis: a pathogenic perioperative entity. *Anesthesiology* 2005, 102(4):838-854.**
87. **Meduri GU: The role of the host defence response in the progression and outcome of ARDS: pathophysiological correlations and response to glucocorticoid treatment. *Eur Respir J* 1996, 9(12):2650-2670.**
88. **Berthiaume Y, Lesur O, Dagenais A: Treatment of adult respiratory distress syndrome: plea for rescue therapy of the alveolar epithelium. *Thorax* 1999, 54(2):150-160.**
89. **Geiser T: Mechanisms of alveolar epithelial repair in acute lung injury--a translational approach. *Swiss Med Wkly* 2003, 133(43-44):586-590.**
90. **Fuchs E, Tumbar T, Guasch G: Socializing with the neighbors: stem cells and their niche. *Cell* 2004, 116(6):769-778.**
91. **Rawlins EL, Hogan BL: Epithelial stem cells of the lung: privileged few or opportunities for many? *Development* 2006, 133(13):2455-2465.**
92. **Stripp BR: Hierarchical organization of lung progenitor cells: is there an adult lung tissue stem cell? *Proc Am Thorac Soc* 2008, 5(6):695-698.**
93. **Togel F, Hu Z, Weiss K, Isaac J, Lange C, Westenfelder C: Administered mesenchymal stem cells protect against ischemic acute renal failure through differentiation-independent mechanisms. *Am J Physiol Renal Physiol* 2005, 289(1):F31-42.**
94. **Parekkadan B, van Poll D, Suganuma K, Carter EA, Berthiaume F, Tilles AW, Yarmush ML: Mesenchymal stem cell-derived molecules reverse fulminant hepatic failure. *PLoS One* 2007, 2(9):e941.**
95. **Lee RH, Pulin AA, Seo MJ, Kota DJ, Ylostalo J, Larson BL, Semprun-Prieto L, Delafontaine P, Prockop DJ: Intravenous hMSCs improve myocardial infarction in mice because cells embolized in lung are activated to secrete the anti-inflammatory protein TSG-6. *Cell Stem Cell* 2009, 5(1):54-63.**
96. **Mei SH, Haitsma JJ, Dos Santos CC, Deng Y, Lai PF, Slutsky AS, Liles WC, Stewart DJ: Mesenchymal stem cells reduce inflammation while enhancing bacterial clearance and improving survival in sepsis. *Am J Respir Crit Care Med* 2010, 182(8):1047-1057.**
97. **Krasnodembskaya A, Song Y, Fang X, Gupta N, Serikov V, Lee JW, Matthay MA: Antibacterial effect of human mesenchymal stem cells**

is mediated in part from secretion of the antimicrobial peptide LL-37. *Stem Cells* 2010, 28(12):2229-2238.

98. Chapel A, Bertho JM, Bensidhoum M, Fouillard L, Young RG, Frick J, Demarquay C, Cuvelier F, Mathieu E, Trompier F *et al*: Mesenchymal stem cells home to injured tissues when co-infused with hematopoietic cells to treat a radiation-induced multi-organ failure syndrome. *J Gene Med* 2003, 5(12):1028-1038.

99. Mei SH, McCarter SD, Deng Y, Parker CH, Liles WC, Stewart DJ: Prevention of LPS-induced acute lung injury in mice by mesenchymal stem cells overexpressing angiopoietin 1. *PLoS Med* 2007, 4(9):e269.

100. Friedenstein AJ, Chailakhjan RK, Lalykina KS: The development of fibroblast colonies in monolayer cultures of guinea-pig bone marrow and spleen cells. *Cell Tissue Kinet* 1970, 3(4):393-403.

101. Caplan AI: Mesenchymal stem cells. *J Orthop Res* 1991, 9(5):641-650.

102. Pittenger MF, Mackay AM, Beck SC, Jaiswal RK, Douglas R, Mosca JD, Moorman MA, Simonetti DW, Craig S, Marshak DR: Multilineage potential of adult human mesenchymal stem cells. *Science* 1999, 284(5411):143-147.

103. Erices A, Conget P, Minguell JJ: Mesenchymal progenitor cells in human umbilical cord blood. *Br J Haematol* 2000, 109(1):235-242.

104. Gronthos S, Mankani M, Brahim J, Robey PG, Shi S: Postnatal human dental pulp stem cells (DPSCs) in vitro and in vivo. *Proc Natl Acad Sci U S A* 2000, 97(25):13625-13630.

105. Williams JT, Southerland SS, Souza J, Calcutt AF, Cartledge RG: Cells isolated from adult human skeletal muscle capable of differentiating into multiple mesodermal phenotypes. *Am Surg* 1999, 65(1):22-26.

106. Zuk PA, Zhu M, Ashjian P, De Ugarte DA, Huang JI, Mizuno H, Alfonso ZC, Fraser JK, Benhaim P, Hedrick MH: Human adipose tissue is a source of multipotent stem cells. *Mol Biol Cell* 2002, 13(12):4279-4295.

107. Horwitz EM, Le Blanc K, Dominici M, Mueller I, Slaper-Cortenbach I, Marini FC, Deans RJ, Krause DS, Keating A: Clarification of the nomenclature for MSC: The International Society for Cellular Therapy position statement. *Cytotherapy* 2005, 7(5):393-395.

108. Gronthos S, Zannettino AC, Hay SJ, Shi S, Graves SE, Kortesidis A, Simmons PJ: Molecular and cellular characterisation of highly purified stromal stem cells derived from human bone marrow. *J Cell Sci* 2003, 116(Pt 9):1827-1835.

109. D'Ippolito G, Diabira S, Howard GA, Menei P, Roos BA, Schiller PC: Marrow-isolated adult multilineage inducible (MIAMI) cells, a unique population of postnatal young and old human cells with extensive expansion and differentiation potential. *J Cell Sci* 2004, 117(Pt 14):2971-2981.

110. Reyes M, Lund T, Lenvik T, Aguiar D, Koodie L, Verfaillie CM: Purification and ex vivo expansion of postnatal human marrow mesodermal progenitor cells. *Blood* 2001, 98(9):2615-2625.

111. Caplan AI: Why are MSCs therapeutic? New data: new insight. *J Pathol* 2009, 217(2):318-324.

112. Crisan M, Yap S, Casteilla L, Chen CW, Corselli M, Park TS, Andriolo G, Sun B, Zheng B, Zhang L *et al*: A perivascular origin for mesenchymal stem cells in multiple human organs. *Cell Stem Cell* 2008, 3(3):301-313.

113. da Silva Meirelles L, Caplan AI, Nardi NB: In search of the in vivo identity of mesenchymal stem cells. *Stem Cells* 2008, 26(9):2287-2299.

114. Takashima Y, Era T, Nakao K, Kondo S, Kasuga M, Smith AG, Nishikawa S: Neuroepithelial cells supply an initial transient wave of MSC differentiation. *Cell* 2007, 129(7):1377-1388.

115. Dominici M, Le Blanc K, Mueller I, Slaper-Cortenbach I, Marini F, Krause D, Deans R, Keating A, Prockop D, Horwitz E: Minimal criteria for defining multipotent mesenchymal stromal cells. The International Society for Cellular Therapy position statement. *Cytotherapy* 2006, 8(4):315-317.

116. Russell KC, Phinney DG, Lacey MR, Barrilleaux BL, Meyertholen KE, O'Connor KC: In vitro high-capacity assay to quantify the clonal heterogeneity in trilineage potential of mesenchymal stem cells reveals a complex hierarchy of lineage commitment. *Stem Cells* 2010, 28(4):788-798.

117. Ortiz La, Gambelli F, McBride C, Gaupp D, Baddoo M, Kaminski N, Phinney DG: Mesenchymal stem cell engraftment in lung is enhanced in response to bleomycin exposure and ameliorates its fibrotic effects. *Proceedings of the National Academy of Sciences of the United States of America* 2003, 100(14):8407-8411.

118. Xu J, Woods CR, Mora AL, Joodi R, Brigham KL, Iyer S, Rojas M: Prevention of endotoxin-induced systemic response by bone marrow-derived mesenchymal stem cells in mice. *American journal of physiology Lung cellular and molecular physiology* 2007, 293(1):L131-141.

119. Gupta N, Su X, Popov B, Lee JW, Serikov V, Matthay MA: Intrapulmonary delivery of bone marrow-derived mesenchymal stem cells improves survival and attenuates endotoxin-induced acute lung injury in mice. *Journal of immunology (Baltimore, Md : 1950)* 2007, 179(3):1855-1863.

120. Nemeth K, Leelahavanichkul A, Yuen PS, Mayer B, Parmelee A, Doi K, Robey PG, Leelahavanichkul K, Koller BH, Brown JM *et al*: Bone marrow stromal cells attenuate sepsis via prostaglandin E(2)-dependent reprogramming of host macrophages to increase their interleukin-10 production. *Nat Med* 2009, 15(1):42-49.

121. van Haaften T, Byrne R, Bonnet S, Rochefort GY, Akabutu J, Bouchentouf M, Rey-Parra GJ, Galipeau J, Haromy A, Eaton F *et al*: Airway delivery of mesenchymal stem cells prevents arrested alveolar growth in neonatal lung injury in rats. *Am J Respir Crit Care Med* 2009, 180(11):1131-1142.

122. Aslam M, Baveja R, Liang OD, Fernandez-Gonzalez A, Lee C, Mitsialis SA, Kourembanas S: Bone marrow stromal cells attenuate lung injury in a murine model of neonatal chronic lung disease. *Am J Respir Crit Care Med* 2009, 180(11):1122-1130.

123. **Frank JA, Briot R, Lee JW, Ishizaka A, Uchida T, Matthay MA: Physiological and biochemical markers of alveolar epithelial barrier dysfunction in perfused human lungs.** ***American journal of physiology Lung cellular and molecular physiology*** **2007, 293(1):L52-59.**
124. **Lee JW, Fang X, Gupta N, Serikov V, Matthay Ma: Allogeneic human mesenchymal stem cells for treatment of E. coli endotoxin-induced acute lung injury in the ex vivo perfused human lung.** ***Proceedings of the National Academy of Sciences of the United States of America*** **2009, 106(38):16357-16362.**
125. **Ware LB, Matthay MA: The Acute Respiratory Distress Syndrome.** ***New England Journal of Medicine*** **2000, 342(18):1334-1349.**
126. **Bruno S, Grange C, Deregibus MC, Calogero RA, Saviozzi S, Collino F, Morando L, Busca A, Falda M, Bussolati B** ***et al*****: Mesenchymal stem cell-derived microvesicles protect against acute tubular injury.** ***Journal of the American Society of Nephrology : JASN*** **2009, 20(5):1053-1067.**
127. **Gatti S, Bruno S, Deregibus MC, Sordi A, Cantaluppi V, Tetta C, Camussi G: Microvesicles derived from human adult mesenchymal stem cells protect against ischaemia-reperfusion-induced acute and chronic kidney injury.** ***Nephrol Dial Transplant*** **2011, 26(5):1474-1483.**
128. **Kanazawa H, Fujimoto Y, Teratani T, Iwasaki J, Kasahara N, Negishi K, Tsuruyama T, Uemoto S, Kobayashi E: Bone marrow-derived mesenchymal stem cells ameliorate hepatic ischemia reperfusion injury in a rat model.** ***PLoS One*****, 6(4):e19195.**
129. **Kharaziha P, Hellstrom PM, Noorinayer B, Farzaneh F, Aghajani K, Jafari F, Telkabadi M, Atashi A, Honardoost M, Zali MR** ***et al*****: Improvement of liver function in liver cirrhosis patients after autologous mesenchymal stem cell injection: a phase I-II clinical trial.** ***Eur J Gastroenterol Hepatol*** **2009, 21(10):1199-1205.**
130. **Hare JM, Traverse JH, Henry TD, Dib N, Strumpf RK, Schulman SP, Gerstenblith G, DeMaria AN, Denktas AE, Gammon RS** ***et al*****: A randomized, double-blind, placebo-controlled, dose-escalation study of intravenous adult human mesenchymal stem cells (prochymal) after acute myocardial infarction.** ***J Am Coll Cardiol*** **2009, 54(24):2277-2286.**
131. **Eisner MD, Thompson T, Hudson LD, Luce JM, Hayden D, Schoenfeld D, Matthay MA: Efficacy of low tidal volume ventilation in patients with different clinical risk factors for acute lung injury and the acute respiratory distress syndrome.** ***American journal of respiratory and critical care medicine*** **2001, 164(2):231-236.**
132. **Doyle RL, Szaflarski N, Modin GW, Wiener-Kronish JP, Matthay MA: Identification of patients with acute lung injury. Predictors of mortality.** ***American journal of respiratory and critical care medicine*** **1995, 152(6 Pt 1):1818-1824.**
133. **Krasnodembskaya A, Song Y, Fang X, Gupta N, Serikov V, Lee J-W, Matthay Ma: Antibacterial effect of human mesenchymal stem cells is mediated in part from secretion of the antimicrobial peptide LL-37.** ***Stem cells (Dayton, Ohio)*****, 28(12):2229-2238.**

134. **Chapel A, Bertho JM, Bensidhoum M, Fouillard L, Young RG, Frick J, Demarquay C, Cuvelier Fdr, Mathieu E, Trompier Fo *et al*: Mesenchymal stem cells home to injured tissues when co-infused with hematopoietic cells to treat a radiation-induced multi-organ failure syndrome. *The journal of gene medicine* 2003, 5(12):1028-1038.**
135. **Mei SHJ, McCarter SD, Deng Y, Parker CH, Liles WC, Stewart DJ: Prevention of LPS-induced acute lung injury in mice by mesenchymal stem cells overexpressing angiopoietin 1. *PLoS medicine* 2007, 4(9):e269-e269.**
136. **MacLoughlin RJ, Higgins BD, Laffey JG, O'Brien T: Optimized aerosol delivery to a mechanically ventilated rodent. *Journal of aerosol medicine and pulmonary drug delivery* 2009, 22(4):323-332.**
137. **Lee JW, Fang X, Gupta N, Serikov V, Matthay MA: Allogeneic human mesenchymal stem cells for treatment of E. coli endotoxin-induced acute lung injury in the ex vivo perfused human lung. *Proc Natl Acad Sci U S A* 2009, 106(38):16357-16362.**
138. **Granero-Molto F, Weis JA, Miga MI, Landis B, Myers TJ, O'Rear L, Longobardi L, Jansen ED, Mortlock DP, Spagnoli A: Regenerative effects of transplanted mesenchymal stem cells in fracture healing. *Stem Cells* 2009, 27(8):1887-1898.**
139. **Morigi M, Imberti B, Zoja C, Corna D, Tomasoni S, Abbate M, Rottoli D, Angioletti S, Benigni A, Perico N *et al*: Mesenchymal stem cells are renotropic, helping to repair the kidney and improve function in acute renal failure. *J Am Soc Nephrol* 2004, 15(7):1794-1804.**
140. **Barbash IM, Chouraqui P, Baron J, Feinberg MS, Etzion S, Tessone A, Miller L, Guetta E, Zipori D, Kedes LH *et al*: Systemic delivery of bone marrow-derived mesenchymal stem cells to the infarcted myocardium: feasibility, cell migration, and body distribution. *Circulation* 2003, 108(7):863-868.**
141. **Li Y, Chen J, Wang L, Lu M, Chopp M: Treatment of stroke in rat with intracarotid administration of marrow stromal cells. *Neurology* 2001, 56(12):1666-1672.**
142. **Francois S, Bensidhoum M, Mouiseddine M, Mazurier C, Allenet B, Semont A, Frick J, Sache A, Bouchet S, Thierry D *et al*: Local irradiation not only induces homing of human mesenchymal stem cells at exposed sites but promotes their widespread engraftment to multiple organs: a study of their quantitative distribution after irradiation damage. *Stem Cells* 2006, 24(4):1020-1029.**
143. **Rochefort GY, Delorme B, Lopez A, Herault O, Bonnet P, Charbord P, Eder V, Domenech J: Multipotential mesenchymal stem cells are mobilized into peripheral blood by hypoxia. *Stem Cells* 2006, 24(10):2202-2208.**
144. **Granero-Molto F, Weis JA, Longobardi L, Spagnoli A: Role of mesenchymal stem cells in regenerative medicine: application to bone and cartilage repair. *Expert Opin Biol Ther* 2008, 8(3):255-268.**
145. **Lapidot T, Dar A, Kollet O: How do stem cells find their way home? *Blood* 2005, 106(6):1901-1910.**

146. **Cho HH, Kyoung KM, Seo MJ, Kim YJ, Bae YC, Jung JS: Overexpression of CXCR4 increases migration and proliferation of human adipose tissue stromal cells.** ***Stem Cells Dev*** **2006, 15(6):853-864.**
147. **Cheng Z, Ou L, Zhou X, Li F, Jia X, Zhang Y, Liu X, Li Y, Ward CA, Melo LG** ***et al*****: Targeted migration of mesenchymal stem cells modified with CXCR4 gene to infarcted myocardium improves cardiac performance.** ***Mol Ther*** **2008, 16(3):571-579.**
148. **Hiasa K, Ishibashi M, Ohtani K, Inoue S, Zhao Q, Kitamoto S, Sata M, Ichiki T, Takeshita A, Egashira K: Gene transfer of stromal cell-derived factor-1alpha enhances ischemic vasculogenesis and angiogenesis via vascular endothelial growth factor/endothelial nitric oxide synthase-related pathway: next-generation chemokine therapy for therapeutic neovascularization.** ***Circulation*** **2004, 109(20):2454-2461.**
149. **Abbott JD, Huang Y, Liu D, Hickey R, Krause DS, Giordano FJ: Stromal cell-derived factor-1alpha plays a critical role in stem cell recruitment to the heart after myocardial infarction but is not sufficient to induce homing in the absence of injury.** ***Circulation*** **2004, 110(21):3300-3305.**
150. **Ip JE, Wu Y, Huang J, Zhang L, Pratt RE, Dzau VJ: Mesenchymal stem cells use integrin beta1 not CXC chemokine receptor 4 for myocardial migration and engraftment.** ***Mol Biol Cell*** **2007, 18(8):2873-2882.**
151. **Kumar S, Ponnazhagan S: Bone homing of mesenchymal stem cells by ectopic alpha 4 integrin expression.** ***FASEB J*** **2007, 21(14):3917-3927.**
152. **Sasaki M, Abe R, Fujita Y, Ando S, Inokuma D, Shimizu H: Mesenchymal stem cells are recruited into wounded skin and contribute to wound repair by transdifferentiation into multiple skin cell type.** ***J Immunol*** **2008, 180(4):2581-2587.**
153. **Dwyer RM, Potter-Beirne SM, Harrington KA, Lowery AJ, Hennessy E, Murphy JM, Barry FP, O'Brien T, Kerin MJ: Monocyte chemotactic protein-1 secreted by primary breast tumors stimulates migration of mesenchymal stem cells.** ***Clin Cancer Res*** **2007, 13(17):5020-5027.**
154. **Schmidt A, Ladage D, Steingen C, Brixius K, Schinkothe T, Klinz FJ, Schwinger RH, Mehlhorn U, Bloch W: Mesenchymal stem cells transmigrate over the endothelial barrier.** ***Eur J Cell Biol*** **2006, 85(11):1179-1188.**
155. **Eguchi G, Kodama R: Transdifferentiation.** ***Curr Opin Cell Biol*** **1993, 5(6):1023-1028.**
156. **Beresford WA: Direct transdifferentiation: can cells change their phenotype without dividing?** ***Cell Differ Dev*** **1990, 29(2):81-93.**
157. **Sanchez-Ramos J, Song S, Cardozo-Pelaez F, Hazzi C, Stedeford T, Willing A, Freeman TB, Saporta S, Janssen W, Patel N** ***et al*****: Adult bone marrow stromal cells differentiate into neural cells in vitro.** ***Exp Neurol*** **2000, 164(2):247-256.**
158. **Kreja L, Brenner RE, Tautzenberger A, Liedert A, Friemert B, Ehrnthaller C, Huber-Lang M, Ignatius A: Non-resorbing osteoclasts**

induce migration and osteogenic differentiation of mesenchymal stem cells. *J Cell Biochem* 2010, 109(2):347-355.

159. Chao KC, Chao KF, Fu YS, Liu SH: Islet-like clusters derived from mesenchymal stem cells in Wharton's Jelly of the human umbilical cord for transplantation to control type 1 diabetes. *PLoS One* 2008, 3(1):e1451.

160. Paunescu V, Deak E, Herman D, Siska IR, Tanasie G, Bunu C, Anghel S, Tatu CA, Oprea TI, Henschler R *et al*: In vitro differentiation of human mesenchymal stem cells to epithelial lineage. *J Cell Mol Med* 2007, 11(3):502-508.

161. Gong Z, Niklason LE: Small-diameter human vessel wall engineered from bone marrow-derived mesenchymal stem cells (hMSCs). *FASEB J* 2008, 22(6):1635-1648.

162. Krause DS, Theise ND, Collector MI, Henegariu O, Hwang S, Gardner R, Neutzel S, Sharkis SJ: Multi-organ, multi-lineage engraftment by a single bone marrow-derived stem cell. *Cell* 2001, 105(3):369-377.

163. Wagers AJ, Sherwood RI, Christensen JL, Weissman IL: Little evidence for developmental plasticity of adult hematopoietic stem cells. *Science* 2002, 297(5590):2256-2259.

164. Kotton DN, Fabian AJ, Mulligan RC: Failure of bone marrow to reconstitute lung epithelium. *American journal of respiratory cell and molecular biology* 2005, 33(4):328-334.

165. Rojas M, Xu J, Woods CR, Mora AL, Spears W, Roman J, Brigham KL: Bone marrow-derived mesenchymal stem cells in repair of the injured lung. *American journal of respiratory cell and molecular biology* 2005, 33(2):145-152.

166. Theise ND, Krause DS, Sharkis S: Comment on "Little evidence for developmental plasticity of adult hematopoietic stem cells". *Science* 2003, 299(5611):1317; author reply 1317.

167. Lange C, Togel F, Ittrich H, Clayton F, Nolte-Ernsting C, Zander AR, Westenfelder C: Administered mesenchymal stem cells enhance recovery from ischemia/reperfusion-induced acute renal failure in rats. *Kidney Int* 2005, 68(4):1613-1617.

168. Wu JY, Scadden DT, Kronenberg HM: Role of the osteoblast lineage in the bone marrow hematopoietic niches. *J Bone Miner Res* 2009, 24(5):759-764.

169. Tolar J, Le Blanc K, Keating A, Blazar BR: Concise review: hitting the right spot with mesenchymal stromal cells. *Stem Cells* 2010, 28(8):1446-1455.

170. Barry FP, Murphy JM, English K, Mahon BP: Immunogenicity of adult mesenchymal stem cells: lessons from the fetal allograft. *Stem Cells Dev* 2005, 14(3):252-265.

171. Uccelli A, Moretta L, Pistoia V: Mesenchymal stem cells in health and disease. *Nat Rev Immunol* 2008, 8(9):726-736.

172. Ankrum J, Karp JM: Mesenchymal stem cell therapy: Two steps forward, one step back. *Trends Mol Med* 2010, 16(5):203-209.

173. Tu Z, Li Q, Bu H, Lin F: Mesenchymal stem cells inhibit complement activation by secreting factor H. *Stem Cells Dev* 2010, 19(11):1803-1809.

174. **Komoda H, Okura H, Lee CM, Sougawa N, Iwayama T, Hashikawa T, Saga A, Yamamoto-Kakuta A, Ichinose A, Murakami S *et al*: Reduction of N-glycolylneuraminic acid xenoantigen on human adipose tissue-derived stromal cells/mesenchymal stem cells leads to safer and more useful cell sources for various stem cell therapies. *Tissue Eng Part A* 2010, 16(4):1143-1155.**
175. **Schraufstatter IU, Discipio RG, Zhao M, Khaldoyanidi SK: C3a and C5a are chemotactic factors for human mesenchymal stem cells, which cause prolonged ERK1/2 phosphorylation. *J Immunol* 2009, 182(6):3827-3836.**
176. **Rasmusson I, Ringden O, Sundberg B, Le Blanc K: Mesenchymal stem cells inhibit the formation of cytotoxic T lymphocytes, but not activated cytotoxic T lymphocytes or natural killer cells. *Transplantation* 2003, 76(8):1208-1213.**
177. **Aggarwal S, Pittenger MF: Human mesenchymal stem cells modulate allogeneic immune cell responses. *Blood* 2005, 105(4):1815-1822.**
178. **Poggi A, Prevosto C, Massaro AM, Negrini S, Urbani S, Pierri I, Saccardi R, Gobbi M, Zocchi MR: Interaction between human NK cells and bone marrow stromal cells induces NK cell triggering: role of NKp30 and NKG2D receptors. *J Immunol* 2005, 175(10):6352-6360.**
179. **Sotiropoulou PA, Perez SA, Gritzapis AD, Baxevanis CN, Papamichail M: Interactions between human mesenchymal stem cells and natural killer cells. *Stem Cells* 2006, 24(1):74-85.**
180. **Spaggiari GM, Capobianco A, Becchetti S, Mingari MC, Moretta L: Mesenchymal stem cell-natural killer cell interactions: evidence that activated NK cells are capable of killing MSCs, whereas MSCs can inhibit IL-2-induced NK-cell proliferation. *Blood* 2006, 107(4):1484-1490.**
181. **Raffaghello L, Bianchi G, Bertolotto M, Montecucco F, Busca A, Dallegri F, Ottonello L, Pistoia V: Human mesenchymal stem cells inhibit neutrophil apoptosis: a model for neutrophil preservation in the bone marrow niche. *Stem Cells* 2008, 26(1):151-162.**
182. **Tesar V: Monocyte 'reprogramming' and mortality in septic patients with acute kidney injury. *Blood Purif* 2008, 26(2):186-187.**
183. **Stout RD, Watkins SK, Suttles J: Functional plasticity of macrophages: in situ reprogramming of tumor-associated macrophages. *J Leukoc Biol* 2009, 86(5):1105-1109.**
184. **Geissmann F, Manz MG, Jung S, Sieweke MH, Merad M, Ley K: Development of monocytes, macrophages, and dendritic cells. *Science* 2010, 327(5966):656-661.**
185. **Ohtaki H, Ylostalo JH, Foraker JE, Robinson AP, Reger RL, Shioda S, Prockop DJ: Stem/progenitor cells from bone marrow decrease neuronal death in global ischemia by modulation of inflammatory/immune responses. *Proc Natl Acad Sci U S A* 2008, 105(38):14638-14643.**
186. **Kim J, Hematti P: Mesenchymal stem cell-educated macrophages: a novel type of alternatively activated macrophages. *Experimental hematology* 2009, 37(12):1445-1453.**

187. **Pevsner-Fischer M, Morad V, Cohen-Sfady M, Rousso-Noori L, Zanin-Zhorov A, Cohen S, Cohen IR, Zipori D: Toll-like receptors and their ligands control mesenchymal stem cell functions. *Blood* 2007, 109(4):1422-1432.**
188. **Liotta F, Angeli R, Cosmi L, Fili L, Manuelli C, Frosali F, Mazzinghi B, Maggi L, Pasini A, Lisi V *et al*: Toll-like receptors 3 and 4 are expressed by human bone marrow-derived mesenchymal stem cells and can inhibit their T-cell modulatory activity by impairing Notch signaling. *Stem Cells* 2008, 26(1):279-289.**
189. **Tomchuck SL, Zwezdaryk KJ, Coffelt SB, Waterman RS, Danka ES, Scandurro AB: Toll-like receptors on human mesenchymal stem cells drive their migration and immunomodulating responses. *Stem cells (Dayton, Ohio)* 2008, 26(1):99-107.**
190. **Opitz CA, Litzenburger UM, Lutz C, Lanz TV, Tritschler I, Koppel A, Tolosa E, Hoberg M, Anderl J, Aicher WK *et al*: Toll-like receptor engagement enhances the immunosuppressive properties of human bone marrow-derived mesenchymal stem cells by inducing indoleamine-2,3-dioxygenase-1 via interferon-beta and protein kinase R. *Stem Cells* 2009, 27(4):909-919.**
191. **Wang ZJ, Zhang FM, Wang LS, Yao YW, Zhao Q, Gao X: Lipopolysaccharides can protect mesenchymal stem cells (MSCs) from oxidative stress-induced apoptosis and enhance proliferation of MSCs via Toll-like receptor(TLR)-4 and PI3K/Akt. *Cell Biol Int* 2009, 33(6):665-674.**
192. **Romieu-Mourez R, Francois M, Boivin MN, Bouchentouf M, Spaner DE, Galipeau J: Cytokine modulation of TLR expression and activation in mesenchymal stromal cells leads to a proinflammatory phenotype. *J Immunol* 2009, 182(12):7963-7973.**
193. **English K, Barry FP, Field-Corbett CP, Mahon BP: IFN-gamma and TNF-alpha differentially regulate immunomodulation by murine mesenchymal stem cells. *Immunol Lett* 2007, 110(2):91-100.**
194. **Beyth S, Borovsky Z, Mevorach D, Liebergall M, Gazit Z, Aslan H, Galun E, Rachmilewitz J: Human mesenchymal stem cells alter antigen-presenting cell maturation and induce T-cell unresponsiveness. *Blood* 2005, 105(5):2214-2219.**
195. **Nauta AJ, Kruisselbrink AB, Lurvink E, Willemze R, Fibbe WE: Mesenchymal stem cells inhibit generation and function of both CD34+-derived and monocyte-derived dendritic cells. *J Immunol* 2006, 177(4):2080-2087.**
196. **Djouad F, Charbonnier LM, Bouffi C, Louis-Plence P, Bony C, Apparailly F, Cantos C, Jorgensen C, Noel D: Mesenchymal stem cells inhibit the differentiation of dendritic cells through an interleukin-6-dependent mechanism. *Stem Cells* 2007, 25(8):2025-2032.**
197. **Zhang W, Ge W, Li C, You S, Liao L, Han Q, Deng W, Zhao RC: Effects of mesenchymal stem cells on differentiation, maturation, and function of human monocyte-derived dendritic cells. *Stem Cells Dev* 2004, 13(3):263-271.**
198. **Masteller EL, Warner MR, Tang Q, Tarbell KV, McDevitt H, Bluestone JA: Expansion of functional endogenous antigen-specific CD4+CD25+**

regulatory T cells from nonobese diabetic mice. *J Immunol* 2005, 175(5):3053-3059.

199. Babu S, Blauvelt CP, Kumaraswami V, Nutman TB: Regulatory networks induced by live parasites impair both Th1 and Th2 pathways in patent lymphatic filariasis: implications for parasite persistence. *J Immunol* 2006, 176(5):3248-3256.

200. Walsh KP, Brady MT, Finlay CM, Boon L, Mills KH: Infection with a helminth parasite attenuates autoimmunity through TGF-beta-mediated suppression of Th17 and Th1 responses. *J Immunol* 2009, 183(3):1577-1586.

201. Shevach EM, Thornton A, Suri-Payer E: T lymphocyte-mediated control of autoimmunity. *Novartis Found Symp* 1998, 215:200-211; discussion 211-230.

202. Cobbold SP, Adams E, Farquhar CA, Nolan KF, Howie D, Lui KO, Fairchild PJ, Mellor AL, Ron D, Waldmann H: Infectious tolerance via the consumption of essential amino acids and mTOR signaling. *Proc Natl Acad Sci U S A* 2009, 106(29):12055-12060.

203. Miao CH, Harmeling BR, Ziegler SF, Yen BC, Torgerson T, Chen L, Yau RJ, Peng B, Thompson AR, Ochs HD *et al*: CD4+FOXP3+ regulatory T cells confer long-term regulation of factor VIII-specific immune responses in plasmid-mediated gene therapy-treated hemophilia mice. *Blood* 2009, 114(19):4034-4044.

204. Prevosto C, Zancolli M, Canevali P, Zocchi MR, Poggi A: Generation of CD4+ or CD8+ regulatory T cells upon mesenchymal stem cell-lymphocyte interaction. *Haematologica* 2007, 92(7):881-888.

205. English K, Ryan JM, Tobin L, Murphy MJ, Barry FP, Mahon BP: Cell contact, prostaglandin E(2) and transforming growth factor beta 1 play non-redundant roles in human mesenchymal stem cell induction of CD4+CD25(High) forkhead box P3+ regulatory T cells. *Clin Exp Immunol* 2009, 156(1):149-160.

206. Ghannam S, Pene J, Torcy-Moquet G, Jorgensen C, Yssel H: Mesenchymal stem cells inhibit human Th17 cell differentiation and function and induce a T regulatory cell phenotype. *J Immunol* 2010, 185(1):302-312.

207. Di Ianni M, Del Papa B, De Ioanni M, Moretti L, Bonifacio E, Cecchini D, Sportoletti P, Falzetti F, Tabilio A: Mesenchymal cells recruit and regulate T regulatory cells. *Exp Hematol* 2008, 36(3):309-318.

208. Nauta AJ, Fibbe WE: Immunomodulatory properties of mesenchymal stromal cells. *Blood* 2007, 110(10):3499-3506.

209. Meisel R, Zibert A, Laryea M, Gobel U, Daubener W, Dilloo D: Human bone marrow stromal cells inhibit allogeneic T-cell responses by indoleamine 2,3-dioxygenase-mediated tryptophan degradation. *Blood* 2004, 103(12):4619-4621.

210. Krampera M, Glennie S, Dyson J, Scott D, Laylor R, Simpson E, Dazzi F: Bone marrow mesenchymal stem cells inhibit the response of naive and memory antigen-specific T cells to their cognate peptide. *Blood* 2003, 101(9):3722-3729.

211. Corcione A, Benvenuto F, Ferretti E, Giunti D, Cappiello V, Cazzanti F, Risso M, Gualandi F, Mancardi GL, Pistoia V *et al*: Human

mesenchymal stem cells modulate B-cell functions. *Blood* 2006, 107(1):367-372.

212. Comoli P, Ginevri F, Maccario R, Avanzini MA, Marconi M, Groff A, Cometa A, Cioni M, Porretti L, Barberi W *et al*: Human mesenchymal stem cells inhibit antibody production induced in vitro by allostimulation. *Nephrol Dial Transplant* 2008, 23(4):1196-1202.

213. Tabera S, Perez-Simon JA, Diez-Campelo M, Sanchez-Abarca LI, Blanco B, Lopez A, Benito A, Ocio E, Sanchez-Guijo FM, Canizo C *et al*: The effect of mesenchymal stem cells on the viability, proliferation and differentiation of B-lymphocytes. *Haematologica* 2008, 93(9):1301-1309.

214. Rafei M, Hsieh J, Fortier S, Li M, Yuan S, Birman E, Forner K, Boivin MN, Doody K, Tremblay M *et al*: Mesenchymal stromal cell-derived CCL2 suppresses plasma cell immunoglobulin production via STAT3 inactivation and PAX5 induction. *Blood* 2008, 112(13):4991-4998.

215. Schena F, Gambini C, Gregorio A, Mosconi M, Reverberi D, Gattorno M, Casazza S, Uccelli A, Moretta L, Martini A *et al*: Interferon-gamma-dependent inhibition of B cell activation by bone marrow-derived mesenchymal stem cells in a murine model of systemic lupus erythematosus. *Arthritis Rheum* 2010, 62(9):2776-2786.

216. Rasmusson I, Le Blanc K, Sundberg B, Ringden O: Mesenchymal stem cells stimulate antibody secretion in human B cells. *Scand J Immunol* 2007, 65(4):336-343.

217. Traggiai E, Volpi S, Schena F, Gattorno M, Ferlito F, Moretta L, Martini A: Bone marrow-derived mesenchymal stem cells induce both polyclonal expansion and differentiation of B cells isolated from healthy donors and systemic lupus erythematosus patients. *Stem Cells* 2008, 26(2):562-569.

218. Bartholomew A, Sturgeon C, Siatskas M, Ferrer K, McIntosh K, Patil S, Hardy W, Devine S, Ucker D, Deans R *et al*: Mesenchymal stem cells suppress lymphocyte proliferation in vitro and prolong skin graft survival in vivo. *Exp Hematol* 2002, 30(1):42-48.

219. Lazarus HM, Koc ON, Devine SM, Curtin P, Maziarz RT, Holland HK, Shpall EJ, McCarthy P, Atkinson K, Cooper BW *et al*: Cotransplantation of HLA-identical sibling culture-expanded mesenchymal stem cells and hematopoietic stem cells in hematologic malignancy patients. *Biol Blood Marrow Transplant* 2005, 11(5):389-398.

220. Zappia E, Casazza S, Pedemonte E, Benvenuto F, Bonanni I, Gerdoni E, Giunti D, Ceravolo A, Cazzanti F, Frassoni F *et al*: Mesenchymal stem cells ameliorate experimental autoimmune encephalomyelitis inducing T-cell anergy. *Blood* 2005, 106(5):1755-1761.

221. Rafei M, Campeau PM, Aguilar-Mahecha A, Buchanan M, Williams P, Birman E, Yuan S, Young YK, Boivin MN, Forner K *et al*: Mesenchymal stromal cells ameliorate experimental autoimmune encephalomyelitis by inhibiting CD4 Th17 T cells in a CC chemokine ligand 2-dependent manner. *J Immunol* 2009, 182(10):5994-6002.

222. Isakova IA, Dufour J, Lanclos C, Bruhn J, Phinney DG: Cell-dose-dependent increases in circulating levels of immune effector cells in

rhesus macaques following intracranial injection of allogeneic MSCs. *Exp Hematol* 2010, 38(10):957-967 e951.

223. Zangi L, Margalit R, Reich-Zeliger S, Bachar-Lustig E, Beilhack A, Negrin R, Reisner Y: Direct imaging of immune rejection and memory induction by allogeneic mesenchymal stromal cells. *Stem Cells* 2009, 27(11):2865-2874.

224. Camp DM, Loeffler DA, Farrah DM, Borneman JN, LeWitt PA: Cellular immune response to intrastriatally implanted allogeneic bone marrow stromal cells in a rat model of Parkinson's disease. *J Neuroinflammation* 2009, 6:17.

225. Cho PS, Messina DJ, Hirsh EL, Chi N, Goldman SN, Lo DP, Harris IR, Popma SH, Sachs DH, Huang CA: Immunogenicity of umbilical cord tissue derived cells. *Blood* 2008, 111(1):430-438.

226. Badillo AT, Beggs KJ, Javazon EH, Tebbets JC, Flake AW: Murine bone marrow stromal progenitor cells elicit an in vivo cellular and humoral alloimmune response. *Biol Blood Marrow Transplant* 2007, 13(4):412-422.

227. Poncelet AJ, Vercruysse J, Saliez A, Gianello P: Although pig allogeneic mesenchymal stem cells are not immunogenic in vitro, intracardiac injection elicits an immune response in vivo. *Transplantation* 2007, 83(6):783-790.

228. Nauta AJ, Westerhuis G, Kruisselbrink AB, Lurvink EG, Willemze R, Fibbe WE: Donor-derived mesenchymal stem cells are immunogenic in an allogeneic host and stimulate donor graft rejection in a nonmyeloablative setting. *Blood* 2006, 108(6):2114-2120.

229. Beggs KJ, Lyubimov A, Borneman JN, Bartholomew A, Moseley A, Dodds R, Archambault MP, Smith AK, McIntosh KR: Immunologic consequences of multiple, high-dose administration of allogeneic mesenchymal stem cells to baboons. *Cell Transplant* 2006, 15(8-9):711-721.

230. Eliopoulos N, Stagg J, Lejeune L, Pommey S, Galipeau J: Allogeneic marrow stromal cells are immune rejected by MHC class I- and class II-mismatched recipient mice. *Blood* 2005, 106(13):4057-4065.

231. Togel F, Cohen A, Zhang P, Yang Y, Hu Z, Westenfelder C: Autologous and allogeneic marrow stromal cells are safe and effective for the treatment of acute kidney injury. *Stem Cells Dev* 2009, 18(3):475-485.

232. Poncelet AJ, Nizet Y, Vercruysse J, Hiel AL, Saliez A, Gianello P: Inhibition of humoral response to allogeneic porcine mesenchymal stem cell with 12 days of tacrolimus. *Transplantation* 2008, 86(11):1586-1595.

233. Ge W, Jiang J, Baroja ML, Arp J, Zassoko R, Liu W, Bartholomew A, Garcia B, Wang H: Infusion of mesenchymal stem cells and rapamycin synergize to attenuate alloimmune responses and promote cardiac allograft tolerance. *Am J Transplant* 2009, 9(8):1760-1772.

234. Le Blanc K, Tammik C, Rosendahl K, Zetterberg E, Ringden O: HLA expression and immunologic properties of differentiated and

undifferentiated mesenchymal stem cells. *Exp Hematol* 2003, 31(10):890-896.

235. Le Blanc K, Tammik L, Sundberg B, Haynesworth SE, Ringden O: Mesenchymal stem cells inhibit and stimulate mixed lymphocyte cultures and mitogenic responses independently of the major histocompatibility complex. *Scand J Immunol* 2003, 57(1):11-20.

236. Ryan JM, Barry F, Murphy JM, Mahon BP: Interferon-gamma does not break, but promotes the immunosuppressive capacity of adult human mesenchymal stem cells. *Clin Exp Immunol* 2007, 149(2):353-363.

237. Polchert D, Sobinsky J, Douglas G, Kidd M, Moadsiri A, Reina E, Genrich K, Mehrotra S, Setty S, Smith B *et al*: IFN-gamma activation of mesenchymal stem cells for treatment and prevention of graft versus host disease. *Eur J Immunol* 2008, 38(6):1745-1755.

238. Griffin MD, Ritter T, Mahon BP: Immunological aspects of allogeneic mesenchymal stem cell therapies. *Hum Gene Ther* 2010, 21(12):1641-1655.

239. Neuss S, Becher E, Woltje M, Tietze L, Jahnen-Dechent W: Functional expression of HGF and HGF receptor/c-met in adult human mesenchymal stem cells suggests a role in cell mobilization, tissue repair, and wound healing. *Stem Cells* 2004, 22(3):405-414.

240. Fang X, Neyrinck AP, Matthay MA, Lee JW: Allogeneic human mesenchymal stem cells restore epithelial protein permeability in cultured human alveolar type II cells by secretion of angiopoietin-1. *J Biol Chem* 2010, 285(34):26211-26222.

241. Nemeth K, Keane-Myers A, Brown JM, Metcalfe DD, Gorham JD, Bundoc VG, Hodges MG, Jelinek I, Madala S, Karpati S *et al*: Bone marrow stromal cells use TGF-beta to suppress allergic responses in a mouse model of ragweed-induced asthma. *Proc Natl Acad Sci U S A* 2010, 107(12):5652-5657.

242. Ortiz La, Dutreil M, Fattman C, Pandey AC, Torres G, Go K, Phinney DG: Interleukin 1 receptor antagonist mediates the antiinflammatory and antifibrotic effect of mesenchymal stem cells during lung injury. *Proceedings of the National Academy of Sciences of the United States of America* 2007, 104(26):11002-11007.

243. Geiser T, Atabai K, Jarreau PH, Ware LB, Pugin J, Matthay MA: Pulmonary edema fluid from patients with acute lung injury augments in vitro alveolar epithelial repair by an IL-1beta-dependent mechanism. *Am J Respir Crit Care Med* 2001, 163(6):1384-1388.

244. Danchuk S, Ylostalo JH, Hossain F, Sorge R, Ramsey A, Bonvillain RW, Lasky JA, Bunnell BA, Welsh DA, Prockop DJ *et al*: Human multipotent stromal cells attenuate lipopolysaccharide-induced acute lung injury in mice via secretion of tumor necrosis factor-alpha-induced protein 6. *Stem Cell Res Ther* 2011, 2(3):27.

245. Xu J, Qu J, Cao L, Sai Y, Chen C, He L, Yu L: Mesenchymal stem cell-based angiopoietin-1 gene therapy for acute lung injury induced by lipopolysaccharide in mice. *Journal of Pathology, The* 2008(December 2007):472-481.

246. McCarter SD, Mei SH, Lai PF, Zhang QW, Parker CH, Suen RS, Hood RD, Zhao YD, Deng Y, Han RN *et al*: Cell-based angiopoietin-1 gene therapy for acute lung injury. *Am J Respir Crit Care Med* 2007, 175(10):1014-1026.
247. Son BR, Marquez-Curtis LA, Kucia M, Wysoczynski M, Turner AR, Ratajczak J, Ratajczak MZ, Janowska-Wieczorek A: Migration of bone marrow and cord blood mesenchymal stem cells in vitro is regulated by stromal-derived factor-1-CXCR4 and hepatocyte growth factor-c-met axes and involves matrix metalloproteinases. *Stem Cells* 2006, 24(5):1254-1264.
248. Birukova AA, Alekseeva E, Mikaelyan A, Birukov KG: HGF attenuates thrombin-induced endothelial permeability by Tiam1-mediated activation of the Rac pathway and by Tiam1/Rac-dependent inhibition of the Rho pathway. *FASEB J* 2007, 21(11):2776-2786.
249. Iyer SS, Co C, Rojas M: Mesenchymal stem cells and inflammatory lung diseases. *Panminerva Med* 2009, 51(1):5-16.
250. Augello A, Tasso R, Negrini SM, Amateis A, Indiveri F, Cancedda R, Pennesi G: Bone marrow mesenchymal progenitor cells inhibit lymphocyte proliferation by activation of the programmed death 1 pathway. *Eur J Immunol* 2005, 35(5):1482-1490.
251. Costello J, Higgins B, Contreras M, Chonghaile MN, Hassett P, O'Toole D, Laffey JG: Hypercapnic acidosis attenuates shock and lung injury in early and prolonged systemic sepsis. *Crit Care Med* 2009, 37(8):2412-2420.
252. Higgins BD, Costello J, Contreras M, Hassett P, D OT, Laffey JG: Differential effects of buffered hypercapnia versus hypercapnic acidosis on shock and lung injury induced by systemic sepsis. *Anesthesiology* 2009, 111(6):1317-1326.
253. Gill SE, Huizar I, Bench EM, Sussman SW, Wang Y, Khokha R, Parks WC: Tissue inhibitor of metalloproteinases 3 regulates resolution of inflammation following acute lung injury. *Am J Pathol* 2010, 176(1):64-73.
254. O'Kane CM, Elkington PT, Jones MD, Caviedes L, Tovar M, Gilman RH, Stamp G, Friedland JS: STAT3, p38 MAP Kinase and NF-{kappa}B Drive Unopposed Monocyte-dependent Fibroblast MMP-1 Secretion in Tuberculosis. *Am J Resp Cell Mol Biol* 2009, epub ahead of print:2009-0211OC.
255. O'Toole D, Hassett P, Contreras M, Higgins BD, McKeown ST, McAuley DF, O'Brien T, Laffey JG: Hypercapnic acidosis attenuates pulmonary epithelial wound repair by an NF-kappaB dependent mechanism. *Thorax* 2009, 64(11):976-982.
256. Ashcroft T, Simpson JM, Timbrell V: Simple method of estimating severity of pulmonary fibrosis on a numerical scale. *J Clin Pathol* 1988, 41(4):467-470.
257. Meirelles Lda S, Nardi NB: Murine marrow-derived mesenchymal stem cell: isolation, in vitro expansion, and characterization. *Br J Haematol* 2003, 123(4):702-711.
258. Phinney DG, Kopen G, Isaacson RL, Prockop DJ: Plastic adherent stromal cells from the bone marrow of commonly used strains of

inbred mice: variations in yield, growth, and differentiation. *J Cell Biochem* 1999, 72(4):570-585.

259. Todaro GJ, Lazar GK, Green H: The initiation of cell division in a contact-inhibited mammalian cell line. *J Cell Physiol* 1965, 66(3):325-333.

260. Selden SC, 3rd, Rabinovitch PS, Schwartz SM: Effects of cytoskeletal disrupting agents on replication of bovine endothelium. *J Cell Physiol* 1981, 108(2):195-211.

261. Egan LJ, de Lecea A, Lehrman ED, Myhre GM, Eckmann L, Kagnoff MF: Nuclear factor-kappa B activation promotes restitution of wounded intestinal epithelial monolayers. *Am J Physiol Cell Physiol* 2003, 285(5):C1028-1035.

262. Bernard GR, Artigas A, Brigham KL, Carlet J, Falke K, Hudson L, Lamy M, LeGall JR, Morris A, Spragg R: Report of the American-European Consensus conference on acute respiratory distress syndrome: definitions, mechanisms, relevant outcomes, and clinical trial coordination. Consensus Committee. *J Crit Care* 1994, 9(1):72-81.

263. Matute-Bello G, Downey G, Moore BB, Groshong SD, Matthay MA, Slutsky AS, Kuebler WM: An official American Thoracic Society workshop report: features and measurements of experimental acute lung injury in animals. *Am J Respir Cell Mol Biol* 2011, 44(5):725-738.

264. Hamanaka K, Jian MY, Weber DS, Alvarez DF, Townsley MI, Al-Mehdi AB, King JA, Liedtke W, Parker JC: TRPV4 initiates the acute calcium-dependent permeability increase during ventilator-induced lung injury in isolated mouse lungs. *Am J Physiol Lung Cell Mol Physiol* 2007, 293(4):L923-932.

265. Sakashita A, Nishimura Y, Nishiuma T, Takenaka K, Kobayashi K, Kotani Y, Yokoyama M: Neutrophil elastase inhibitor (sivelestat) attenuates subsequent ventilator-induced lung injury in mice. *Eur J Pharmacol* 2007, 571(1):62-71.

266. Dries DJ, Adams AB, Marini JJ: Time course of physiologic variables in response to ventilator-induced lung injury. *Respir Care* 2007, 52(1):31-37.

267. Ni Chonghaile M, Higgins BD, Costello JF, Laffey JG: Hypercapnic acidosis attenuates severe acute bacterial pneumonia-induced lung injury by a neutrophil-independent mechanism. *Crit Care Med* 2008, 36(12):3135-3144.

268. O'Croinin DF, Nichol AD, Hopkins N, Boylan J, O'Brien S, O'Connor C, Laffey JG, McLoughlin P: Sustained hypercapnic acidosis during pulmonary infection increases bacterial load and worsens lung injury. *Crit Care Med* 2008, 36(7):2128-2135.

269. Matute-Bello G, Frevert CW, Kajikawa O, Skerrett SJ, Goodman RB, Park DR, Martin TR: Septic shock and acute lung injury in rabbits with peritonitis: failure of the neutrophil response to localized infection. *Am J Respir Crit Care Med* 2001, 163(1):234-243.

270. Tsuno K, Miura K, Takeya M, Kolobow T, Morioka T: Histopathologic pulmonary changes from mechanical ventilation at high peak airway pressures. *Am Rev Respir Dis* 1991, 143(5 Pt 1):1115-1120.

271. Borelli M, Kolobow T, Spatola R, Prato P, Tsuno K: Severe acute respiratory failure managed with continuous positive airway pressure and partial extracorporeal carbon dioxide removal by an artificial membrane lung. A controlled, randomized animal study. *Am Rev Respir Dis* 1988, 138(6):1480-1487.
272. Matute-Bello G, Frevert CW, Martin TR: Animal models of acute lung injury. *Am J Physiol Lung Cell Mol Physiol* 2008, 295(3):L379-399.
273. Gomez CR, Hirano S, Cutro BT, Birjandi S, Baila H, Nomellini V, Kovacs EJ: Advanced age exacerbates the pulmonary inflammatory response after lipopolysaccharide exposure. *Crit Care Med* 2007, 35(1):246-251.
274. Fleg JL, Strait J: Age-associated changes in cardiovascular structure and function: a fertile milieu for future disease. *Heart Fail Rev* 2011.
275. Rossi AP, Watson NL, Newman AB, Harris TB, Kritchevsky SB, Bauer DC, Satterfield S, Goodpaster BH, Zamboni M: Effects of body composition and adipose tissue distribution on respiratory function in elderly men and women: the health, aging, and body composition study. *J Gerontol A Biol Sci Med Sci* 2011, 66(7):801-808.
276. Miller RA: The aging immune system: primer and prospectus. *Science* 1996, 273(5271):70-74.
277. Ershler WB, Keller ET: Age-associated increased interleukin-6 gene expression, late-life diseases, and frailty. *Annu Rev Med* 2000, 51:245-270.
278. Meyer KC: Aging. *Proc Am Thorac Soc* 2005, 2(5):433-439.
279. Saito H, Sherwood ER, Varma TK, Evers BM: Effects of aging on mortality, hypothermia, and cytokine induction in mice with endotoxemia or sepsis. *Mech Ageing Dev* 2003, 124(10-12):1047-1058.
280. Peevy KJ, Hernandez LA, Moise AA, Parker JC: Barotrauma and microvascular injury in lungs of nonadult rabbits: effect of ventilation pattern. *Crit Care Med* 1990, 18(6):634-637.
281. Cilley RE, Wang JY, Coran AG: Lung injury produced by moderate lung overinflation in rats. *J Pediatr Surg* 1993, 28(3):488-493; discussion 494-485.
282. Crosby LM, Waters CM: Epithelial repair mechanisms in the lung. *Am J Physiol Lung Cell Mol Physiol* 2010, 298(6):L715-731.
283. Vaneker M, Joosten LA, Heunks LM, Snijdelaar DG, Halbertsma FJ, van Egmond J, Netea MG, van der Hoeven JG, Scheffer GJ: Low-tidal-volume mechanical ventilation induces a toll-like receptor 4-dependent inflammatory response in healthy mice. *Anesthesiology* 2008, 109(3):465-472.
284. Charles PE, Tissieres P, Barbar SD, Croisier D, Dufour J, Dunn-Siegrist I, Chavanet P, Pugin J: Mild-stretch mechanical ventilation up-regulates toll-like receptor 2 and sensitizes the lung to bacterial lipopeptide. *Crit Care* 2011, 15(4):R181.
285. Ventilation with lower tidal volumes as compared with traditional tidal volumes for acute lung injury and the acute respiratory distress syndrome. The Acute Respiratory Distress Syndrome Network. *N Engl J Med* 2000, 342(18):1301-1308.

286. Chesnutt AN, Matthay MA, Tibayan FA, Clark JG: Early detection of type III procollagen peptide in acute lung injury. Pathogenetic and prognostic significance. *Am J Respir Crit Care Med* 1997, 156(3 Pt 1):840-845.

287. Pittet JF, Griffiths MJ, Geiser T, Kaminski N, Dalton SL, Huang X, Brown LA, Gotwals PJ, Koteliansky VE, Matthay MA *et al*: TGF-beta is a critical mediator of acute lung injury. *J Clin Invest* 2001, 107(12):1537-1544.

288. Munger JS, Huang X, Kawakatsu H, Griffiths MJ, Dalton SL, Wu J, Pittet JF, Kaminski N, Garat C, Matthay MA *et al*: The integrin alpha v beta 6 binds and activates latent TGF beta 1: a mechanism for regulating pulmonary inflammation and fibrosis. *Cell* 1999, 96(3):319-328.

289. Dhainaut JF, Charpentier J, Chiche JD: Transforming growth factor-beta: a mediator of cell regulation in acute respiratory distress syndrome. *Crit Care Med* 2003, 31(4 Suppl):S258-264.

290. Kaminski N, Allard JD, Pittet JF, Zuo F, Griffiths MJ, Morris D, Huang X, Sheppard D, Heller RA: Global analysis of gene expression in pulmonary fibrosis reveals distinct programs regulating lung inflammation and fibrosis. *Proc Natl Acad Sci U S A* 2000, 97(4):1778-1783.

291. Marshall RP, Bellingan G, Webb S, Puddicombe A, Goldsack N, McAnulty RJ, Laurent GJ: Fibroproliferation occurs early in the acute respiratory distress syndrome and impacts on outcome. *Am J Respir Crit Care Med* 2000, 162(5):1783-1788.

292. Demoule A, Decailliot F, Jonson B, Christov C, Maitre B, Touqui L, Brochard L, Delclaux C: Relationship between pressure-volume curve and markers for collagen turn-over in early acute respiratory distress syndrome. *Intensive Care Med* 2006, 32(3):413-420.

293. Ricou B, Nicod L, Lacraz S, Welgus HG, Suter PM, Dayer JM: Matrix metalloproteinases and TIMP in acute respiratory distress syndrome. *Am J Respir Crit Care Med* 1996, 154(2 Pt 1):346-352.

294. Fligiel SE, Standiford T, Fligiel HM, Tashkin D, Strieter RM, Warner RL, Johnson KJ, Varani J: Matrix metalloproteinases and matrix metalloproteinase inhibitors in acute lung injury. *Hum Pathol* 2006, 37(4):422-430.

295. Foda HD, Rollo EE, Drews M, Conner C, Appelt K, Shalinsky DR, Zucker S: Ventilator-induced lung injury upregulates and activates gelatinases and EMMPRIN: attenuation by the synthetic matrix metalloproteinase inhibitor, Prinomastat (AG3340). *Am J Respir Cell Mol Biol* 2001, 25(6):717-724.

296. Kim JH, Suk MH, Yoon DW, Lee SH, Hur GY, Jung KH, Jeong HC, Lee SY, Suh IB, Shin C *et al*: Inhibition of matrix metalloproteinase-9 prevents neutrophilic inflammation in ventilator-induced lung injury. *Am J Physiol Lung Cell Mol Physiol* 2006, 291(4):L580-587.

297. Nin N, Lorente JA, de Paula M, El Assar M, Vallejo S, Penuelas O, Fernandez-Segoviano P, Ferruelo A, Sanchez-Ferrer A, Esteban A: Rats surviving injurious mechanical ventilation show reversible pulmonary, vascular and inflammatory changes. *Intensive Care Med* 2008, 34(5):948-956.

298. Higgins BD, Costello J, Contreras M, Hassett P, D OT, Laffey JG: Differential Effects of Buffered Hypercapnia versus Hypercapnic Acidosis on Shock and Lung Injury Induced by Systemic Sepsis. *Anesthesiology* 2009, 111(6):1317-1326.

299. Ni Chonghaile M, Higgins BD, Costello J, Laffey JG: Hypercapnic acidosis attenuates lung injury induced by established bacterial pneumonia. *Anesthesiology* 2008, 109(5):837-848.

300. Smith PK, Krohn RI, Hermanson GT, Mallia AK, Gartner FH, Provenzano MD, Fujimoto EK, Goeke NM, Olson BJ, Klenk DC: Measurement of protein using bicinchoninic acid. *Analytical biochemistry* 1985, 150(1):76-85.

301. Adamson IY, Bakowska J: Relationship of keratinocyte growth factor and hepatocyte growth factor levels in rat lung lavage fluid to epithelial cell regeneration after bleomycin. *Am J Pathol* 1999, 155(3):949-954.

302. Elkington PT, Green JA, Emerson JE, Lopez-Pascua LD, Boyle JJ, O'Kane CM, Friedland JS: Synergistic Up-Regulation of Epithelial Cell Matrix Metalloproteinase-9 Secretion in Tuberculosis. *Am J Resp Cell Mol Biol* 2007, 37(4):431-437.

303. Elkington PTG, Nuttall RK, Boyle JJ, O'Kane CM, Horncastle DE, Edwards DR, Friedland JS: Mycobacterium tuberculosis, but Not Vaccine BCG, Specifically Upregulates Matrix Metalloproteinase-1. *Am J Respir Crit Care Med* 2005, 172(12):1596-1604.

304. O'Kane CM, Elkington PT, Jones MD, Caviedes L, Tovar M, Gilman RH, Stamp G, Friedland JS: STAT3, p38 MAP Kinase and NF-{kappa}B Drive Unopposed Monocyte-dependent Fibroblast MMP-1 Secretion in Tuberculosis. *Am J Resp Cell Mol Biol* 2010, 43(4):465-474.

305. Laffey JG, Honan D, Hopkins N, Hyvelin JM, Boylan JF, McLoughlin P: Hypercapnic acidosis attenuates endotoxin-induced acute lung injury. *Am J Respir Crit Care Med* 2004, 169(1):46-56.

306. O'Croinin DF, Hopkins NO, Moore MM, Boylan JF, McLoughlin P, Laffey JG: Hypercapnic acidosis does not modulate the severity of bacterial pneumonia-induced lung injury. *Crit Care Med* 2005, 33(11):2606-2612.

307. Fredriksson K, Liu XD, Lundahl J, Klominek J, Rennard SI, Skold CM: Red blood cells increase secretion of matrix metalloproteinases from human lung fibroblasts in vitro. *Am J Physiol - Lung Cell Mol Physiol* 2006, 290(2):L326-333.

308. Nielsen BS, Egeblad M, Rank F, Askautrud HA, Pennington CJ, Pedersen TX, Christensen IJ, Edwards DR, Werb Z, Lund LR: Matrix Metalloproteinase 13 Is Induced in Fibroblasts in Polyomavirus Middle T Antigen-Driven Mammary Carcinoma without Influencing Tumor Progression. *PloS one* 2008, 3(8):e2959.

309. Wilcox ME, Herridge MS: Long-term outcomes in patients surviving acute respiratory distress syndrome. *Seminars in respiratory and critical care medicine* 2010, 31(1):55-65.

310. Kolb M, Margetts PJ, Anthony DC, Pitossi F, Gauldie J: Transient expression of IL-1beta induces acute lung injury and chronic repair

leading to pulmonary fibrosis. *The Journal of clinical investigation* 2001, 107(12):1529-1536.

311. Sime PJ, Marr RA, Gauldie D, Xing Z, Hewlett BR, Graham FL, Gauldie J: Transfer of tumor necrosis factor-alpha to rat lung induces severe pulmonary inflammation and patchy interstitial fibrogenesis with induction of transforming growth factor-beta1 and myofibroblasts. *Am J Pathol* 1998, 153(3):825-832.

312. Vaneker M, Heunks LM, Joosten LA, van Hees HW, Snijdelaar DG, Halbertsma FJ, van Egmond J, Netea MG, van der Hoeven JG, Scheffer GJ: Mechanical ventilation induces a Toll/interleukin-1 receptor domain-containing adapter-inducing interferon beta-dependent inflammatory response in healthy mice. *Anesthesiology* 2009, 111(4):836-843.

313. D'Alessio FR, Tsushima K, Aggarwal NR, West EE, Willett MH, Britos MF, Pipeling MR, Brower RG, Tuder RM, McDyer JF *et al*: CD4+CD25+Foxp3+ Tregs resolve experimental lung injury in mice and are present in humans with acute lung injury. *The Journal of clinical investigation* 2009, 119(10):2898-2913.

314. Morris PE, Glass J, Cross R, Cohen DA: Role of T-lymphocytes in the resolution of endotoxin-induced lung injury. *Inflammation* 1997, 21(3):269-278.

315. Meszaros AJ, Reichner JS, Albina JE: Macrophage-induced neutrophil apoptosis. *J Immunol* 2000, 165(1):435-441.

316. Jennings JH, Linderman DJ, Hu B, Sonstein J, Curtis JL: Monocytes recruited to the lungs of mice during immune inflammation ingest apoptotic cells poorly. *Am J Respir Cell Mol Biol* 2005, 32(2):108-117.

317. Clark IM, Swingler TE, Sampieri CL, Edwards DR: The regulation of matrix metalloproteinases and their inhibitors. *Int J Biochem Cell Biol* 2008, 40(6-7):1362-1378.

318. Lanchou J, Corbel M, Tanguy M, Germain N, Boichot E, Theret N, Clement B, Lagente V, Malledant Y: Imbalance between matrix metalloproteinases (MMP-9 and MMP-2) and tissue inhibitors of metalloproteinases (TIMP-1 and TIMP-2) in acute respiratory distress syndrome patients. *Crit Care Med* 2003, 31(2):536-542.

319. O'Kane CM, McKeown S, Perkins GD, Bassford CR, Gao F, Thickett DR, McAuley DF: Salbutamol up-regulates matrix metalloproteinase-9 in the alveolar space in the acute respiratory distress syndrome. *Crit Care Med* 2009, 37(7):2242-2249.

320. Quintero PA, Knolle MD, Cala LF, Zhuang Y, Owen CA: Matrix Metalloproteinase-8 Inactivates Macrophage Inflammatory Protein-1{alpha} To Reduce Acute Lung Inflammation and Injury in Mice. *J Immunol* 2010, 184(3):1575-1588.

321. Mott JD, Khalifah RG, Nagase H, Shield CFr, Hudson JK, Hudson BG: Nonenzymatic glycation of type IV collagen and matrix metalloproteinase susceptibility. *Kidney Int* 1997, 52(5):1302-1312.

322. Manicone AM, Huizar I, McGuire JK: Matrilysin (Matrix Metalloproteinase-7) regulates anti-inflammatory and antifibrotic pulmonary dendritic cells that express CD103 (alpha(E)beta(7)-integrin). *Am J Pathol* 2009, 175(6):2319-2331.

323. Negrini D, Tenstad O, Passi A, Wiig H: Differential degradation of matrix proteoglycans and edema development in rabbit lung. *Am J Physiol Lung Cell Mol Physiol* 2006, 290(3):L470-477.
324. Cosgrove GP, du Bois RM: Matrix metalloproteinase-7 expression in fibrosing lung disease: restoring the balance. *Chest* 2008, 133(5):1058-1060.
325. Moriondo A, Pelosi P, Passi A, Viola M, Marcozzi C, Severgnini P, Ottani V, Quaranta M, Negrini D: Proteoglycan fragmentation and respiratory mechanics in mechanically ventilated healthy rats. *J Appl Physiol* 2007, 103(3):747-756.
326. Konigshoff M, Balsara N, Pfaff EM, Kramer M, Chrobak I, Seeger W, Eickelberg O: Functional Wnt signaling is increased in idiopathic pulmonary fibrosis. *PLoS One* 2008, 3(5):e2142.
327. Haseneen NA, Vaday GG, Zucker S, Foda HD: Mechanical stretch induces MMP-2 release and activation in lung endothelium: role of EMMPRIN. *Am J Physiol Lung Cell Mol Physiol* 2003, 284(3):L541-547.
328. Selman M, Ruiz V, Cabrera S, Segura L, Ramirez R, Barrios R, Pardo A: TIMP-1, -2, -3, and -4 in idiopathic pulmonary fibrosis. A prevailing nondegradative lung microenvironment? *Am J Physiol Lung Cell Mol Physiol* 2000, 279(3):L562-574.
329. Manoury B, Nenan S, Leclerc O, Guenon I, Boichot E, Planquois JM, Bertrand CP, Lagente V: The absence of reactive oxygen species production protects mice against bleomycin-induced pulmonary fibrosis. *Respir Res* 2005, 6:11.
330. Ruiz V, Ordonez RM, Berumen J, Ramirez R, Uhal B, Becerril C, Pardo A, Selman M: Unbalanced collagenases/TIMP-1 expression and epithelial apoptosis in experimental lung fibrosis. *Am J Physiol Lung Cell Mol Physiol* 2003, 285(5):L1026-1036.
331. Hautamaki RD, Kobayashi DK, Senior RM, Shapiro SD: Requirement for macrophage elastase for cigarette smoke-induced emphysema in mice. *Science* 1997, 277(5334):2002-2004.
332. Molet S, Belleguic C, Lena H, Germain N, Bertrand CP, Shapiro SD, Planquois JM, Delaval P, Lagente V: Increase in macrophage elastase (MMP-12) in lungs from patients with chronic obstructive pulmonary disease. *Inflamm Res* 2005, 54(1):31-36.
333. Churg A, Wang RD, Tai H, Wang X, Xie C, Wright JL: Tumor necrosis factor-alpha drives 70% of cigarette smoke-induced emphysema in the mouse. *Am J Respir Crit Care Med* 2004, 170(5):492-498.
334. Nenan S, Planquois JM, Berna P, De Mendez I, Hitier S, Shapiro SD, Boichot E, Lagente V, Bertrand CP: Analysis of the inflammatory response induced by rhMMP-12 catalytic domain instilled in mouse airways. *Int Immunopharmacol* 2005, 5(3):511-524.
335. Lanone S, Zheng T, Zhu Z, Liu W, Lee CG, Ma B, Chen Q, Homer RJ, Wang J, Rabach LA *et al*: Overlapping and enzyme-specific contributions of matrix metalloproteinases-9 and -12 in IL-13-induced inflammation and remodeling. *J Clin Invest* 2002, 110(4):463-474.
336. Heise RL, Stober V, Cheluvaraju C, Hollingsworth JW, Garantziotis S: Mechanical stretch induces epithelial-mesenchymal transition in

alveolar epithelia via hyaluronan activation of innate immunity. *J Biol Chem* 2011.

337. Zupancich E, Paparella D, Turani F, Munch C, Rossi A, Massaccesi S, Ranieri VM: Mechanical ventilation affects inflammatory mediators in patients undergoing cardiopulmonary bypass for cardiac surgery: a randomized clinical trial. *J Thorac Cardiovasc Surg* 2005, 130(2):378-383.

338. Fernandez-Perez ER, Keegan MT, Brown DR, Hubmayr RD, Gajic O: Intraoperative tidal volume as a risk factor for respiratory failure after pneumonectomy. *Anesthesiology* 2006, 105(1):14-18.

339. Gajic O, Frutos-Vivar F, Esteban A, Hubmayr RD, Anzueto A: Ventilator settings as a risk factor for acute respiratory distress syndrome in mechanically ventilated patients. *Intensive Care Med* 2005, 31(7):922-926.

340. Verbrugge SJ, Bohm SH, Gommers D, Zimmerman LJ, Lachmann B: Surfactant impairment after mechanical ventilation with large alveolar surface area changes and effects of positive end-expiratory pressure. *Br J Anaesth* 1998, 80(3):360-364.

341. Prella M, Feihl F, Domenighetti G: Effects of short-term pressure-controlled ventilation on gas exchange, airway pressures, and gas distribution in patients with acute lung injury/ARDS: comparison with volume-controlled ventilation. *Chest* 2002, 122(4):1382-1388.

342. Rubenfeld GD, Herridge MS: Epidemiology and outcomes of acute lung injury. *Chest* 2007, 131(2):554-562.

343. McIntyre RC, Jr., Pulido EJ, Bensard DD, Shames BD, Abraham E: Thirty years of clinical trials in acute respiratory distress syndrome. *Crit Care Med* 2000, 28(9):3314-3331.

344. Zambon M, Vincent JL: Mortality rates for patients with acute lung injury/ARDS have decreased over time. *Chest* 2008, 133(5):1120-1127.

345. Apa: American Psychiatric Association. Diagnostic and Statistical Manual of Mental Disorders 4th Edition. Washington, DC; 2000.

346. Vlahakis NE, Hubmayr RD: Cellular stress failure in ventilator-injured lungs. *Am J Respir Crit Care Med* 2005, 171(12):1328-1342.

347. Prockop DJ: Marrow stromal cells as stem cells for nonhematopoietic tissues. *Science* 1997, 276(5309):71-74.

348. Prockop DJ: Repair of tissues by adult stem/progenitor cells (MSCs): controversies, myths, and changing paradigms. *Mol Ther* 2009, 17(6):939-946.

349. Falanga V, Iwamoto S, Chartier M, Yufit T, Butmarc J, Kouttab N, Shrayer D, Carson P: Autologous bone marrow-derived cultured mesenchymal stem cells delivered in a fibrin spray accelerate healing in murine and human cutaneous wounds. *Tissue Eng* 2007, 13(6):1299-1312.

350. Lataillade JJ, Doucet C, Bey E, Carsin H, Huet C, Clairand I, Bottollier-Depois JF, Chapel A, Ernou I, Gourven M *et al*: New approach to radiation burn treatment by dosimetry-guided surgery combined with autologous mesenchymal stem cell therapy. *Regen Med* 2007, 2(5):785-794.

351. Yoshikawa T, Mitsuno H, Nonaka I, Sen Y, Kawanishi K, Inada Y, Takakura Y, Okuchi K, Nonomura A: Wound therapy by marrow mesenchymal cell transplantation. *Plast Reconstr Surg* 2008, 121(3):860-877.

352. McFarlin K, Gao X, Liu YB, Dulchavsky DS, Kwon D, Arbab AS, Bansal M, Li Y, Chopp M, Dulchavsky SA *et al*: Bone marrow-derived mesenchymal stromal cells accelerate wound healing in the rat. *Wound Repair Regen* 2006, 14(4):471-478.

353. Wu Y, Chen L, Scott PG, Tredget EE: Mesenchymal stem cells enhance wound healing through differentiation and angiogenesis. *Stem Cells* 2007, 25(10):2648-2659.

354. Chen L, Tredget EE, Wu PY, Wu Y: Paracrine factors of mesenchymal stem cells recruit macrophages and endothelial lineage cells and enhance wound healing. *PLoS One* 2008, 3(4):e1886.

355. Gupta N, Su X, Popov B, Lee JW, Serikov V, Matthay MA: Intrapulmonary delivery of bone marrow-derived mesenchymal stem cells improves survival and attenuates endotoxin-induced acute lung injury in mice. *J Immunol* 2007, 179(3):1855-1863.

356. Ortiz LA, Dutreil M, Fattman C, Pandey AC, Torres G, Go K, Phinney DG: Interleukin 1 receptor antagonist mediates the antiinflammatory and antifibrotic effect of mesenchymal stem cells during lung injury. *Proc Natl Acad Sci U S A* 2007, 104(26):11002-11007.

357. Xu J, Woods CR, Mora AL, Joodi R, Brigham KL, Iyer S, Rojas M: Prevention of endotoxin-induced systemic response by bone marrow-derived mesenchymal stem cells in mice. *Am J Physiol Lung Cell Mol Physiol* 2007, 293(1):L131-141.

358. Prockop DJ, Kota DJ, Bazhanov N, Reger RL: Evolving paradigms for repair of tissues by adult stem/progenitor cells (MSCs). *J Cell Mol Med* 2010, 14(9):2190-2199.

359. O'Croinin DF, Nichol AD, Hopkins N, Boylan J, O'Brien S, O'Connor C, Laffey JG, McLoughlin P: Sustained hypercapnic acidosis during pulmonary infection increases bacterial load and worsens lung injury*. *Crit Care Med* 2008, 36(7):2128-2135.

360. Friedenstein AJ, Petrakova KV, Kurolesova AI, Frolova GP: Heterotopic of bone marrow. Analysis of precursor cells for osteogenic and hematopoietic tissues. *Transplantation* 1968, 6(2):230-247.

361. Glennie S, Soeiro I, Dyson PJ, Lam EW, Dazzi F: Bone marrow mesenchymal stem cells induce division arrest anergy of activated T cells. *Blood* 2005, 105(7):2821-2827.

362. Ajuebor MN, Das AM, Virag L, Flower RJ, Szabo C, Perretti M: Role of resident peritoneal macrophages and mast cells in chemokine production and neutrophil migration in acute inflammation: evidence for an inhibitory loop involving endogenous IL-10. *J Immunol* 1999, 162(3):1685-1691.

363. Matthay MA, Wiener-Kronish JP: Intact epithelial barrier function is critical for the resolution of alveolar edema in humans. *Am Rev Respir Dis* 1990, 142(6 Pt 1):1250-1257.

364. Ware LB, Matthay MA: Alveolar fluid clearance is impaired in the majority of patients with acute lung injury and the acute respiratory distress syndrome. *Am J Respir Crit Care Med* 2001, 163(6):1376-1383.

365. Lee JW, Gupta N, Serikov V, Matthay MA: Potential application of mesenchymal stem cells in acute lung injury. *Expert Opin Biol Ther* 2009, 9(10):1259-1270.

366. Yano T, Mason RJ, Pan T, Deterding RR, Nielsen LD, Shannon JM: KGF regulates pulmonary epithelial proliferation and surfactant protein gene expression in adult rat lung. *Am J Physiol Lung Cell Mol Physiol* 2000, 279(6):L1146-1158.

367. Ware LB, Matthay MA: Keratinocyte and hepatocyte growth factors in the lung: roles in lung development, inflammation, and repair. *Am J Physiol Lung Cell Mol Physiol* 2002, 282(5):L924-940.

368. Wang Y, Folkesson HG, Jayr C, Ware LB, Matthay MA: Alveolar epithelial fluid transport can be simultaneously upregulated by both KGF and beta-agonist therapy. *J Appl Physiol* 1999, 87(5):1852-1860.

369. Guery BP, Mason CM, Dobard EP, Beaucaire G, Summer WR, Nelson S: Keratinocyte growth factor increases transalveolar sodium reabsorption in normal and injured rat lungs. *Am J Respir Crit Care Med* 1997, 155(5):1777-1784.

370. Block GJ, Ohkouchi S, Fung F, Frenkel J, Gregory C, Pochampally R, Dimattia G, Sullivan DE, Prockop DJ: Multipotent Stromal Cells (MSCs) are Activated to Reduce Apoptosis in Part by Upregulation and Secretion of Stanniocalcin-1 (STC-1). *Stem Cells* 2008.

371. Gnecchi M, He H, Noiseux N, Liang OD, Zhang L, Morello F, Mu H, Melo LG, Pratt RE, Ingwall JS *et al*: Evidence supporting paracrine hypothesis for Akt-modified mesenchymal stem cell-mediated cardiac protection and functional improvement. *FASEB J* 2006, 20(6):661-669.

372. Katsha AM, Ohkouchi S, Xin H, Kanehira M, Sun R, Nukiwa T, Saijo Y: Paracrine factors of multipotent stromal cells ameliorate lung injury in an elastase-induced emphysema model. *Mol Ther* 2011, 19(1):196-203.

373. Yagi H, Soto-Gutierrez A, Kitagawa Y, Tilles AW, Tompkins RG, Yarmush ML: Bone marrow mesenchymal stromal cells attenuate organ injury induced by LPS and burn. *Cell Transplant* 2010, 19(6):823-830.

374. Haack-Sorensen M, Bindslev L, Mortensen S, Friis T, Kastrup J: The influence of freezing and storage on the characteristics and functions of human mesenchymal stromal cells isolated for clinical use. *Cytotherapy* 2007, 9(4):328-337.

375. Vajta G, Nagy ZP: Are programmable freezers still needed in the embryo laboratory? Review on vitrification. *Reprod Biomed Online* 2006, 12(6):779-796.

376. Perry BC, Zhou D, Wu X, Yang FC, Byers MA, Chu TM, Hockema JJ, Woods EJ, Goebel WS: Collection, cryopreservation, and characterization of human dental pulp-derived mesenchymal stem

cells for banking and clinical use. *Tissue Eng Part C Methods* 2008, 14(2):149-156.
377. Lucas R, Verin AD, Black SM, Catravas JD: Regulators of endothelial and epithelial barrier integrity and function in acute lung injury. *Biochem Pharmacol* 2009, 77(12):1763-1772.
378. Dos Santos CC: Advances in mechanisms of repair and remodelling in acute lung injury. *Intensive Care Med* 2008, 34(4):619-630.
379. Gardner A, Borthwick LA, Fisher AJ: Lung epithelial wound healing in health and disease. *Expert Rev Respir Med* 2010, 4(5):647-660.
380. Phinney DG, Prockop DJ: Concise review: mesenchymal stem/multipotent stromal cells: the state of transdifferentiation and modes of tissue repair--current views. *Stem Cells* 2007, 25(11):2896-2902.
381. Lee JW, Fang X, Krasnodembskaya A, Howard JP, Matthay MA: Concise review: Mesenchymal stem cells for acute lung injury: role of paracrine soluble factors. *Stem Cells* 2011, 29(6):913-919.
382. Martin C, Papazian L, Payan MJ, Saux P, Gouin F: Pulmonary fibrosis correlates with outcome in adult respiratory distress syndrome. A study in mechanically ventilated patients. *Chest* 1995, 107(1):196-200.
383. Moodley Y, Manuelpillai U, Weiss DJ: Cellular therapies for lung disease: a distant horizon. *Respirology (Carlton, Vic)*, 16(2):223-237.
384. Rubin JS, Osada H, Finch PW, Taylor WG, Rudikoff S, Aaronson SA: Purification and characterization of a newly identified growth factor specific for epithelial cells. *Proc Natl Acad Sci U S A* 1989, 86(3):802-806.
385. Danilenko DM: Preclinical and early clinical development of keratinocyte growth factor, an epithelial-specific tissue growth factor. *Toxicol Pathol* 1999, 27(1):64-71.
386. Panos RJ, Bak PM, Simonet WS, Rubin JS, Smith LJ: Intratracheal instillation of keratinocyte growth factor decreases hyperoxia-induced mortality in rats. *J Clin Invest* 1995, 96(4):2026-2033.
387. Yano T, Deterding RR, Simonet WS, Shannon JM, Mason RJ: Keratinocyte growth factor reduces lung damage due to acid instillation in rats. *Am J Respir Cell Mol Biol* 1996, 15(4):433-442.
388. Mason CM, Guery BP, Summer WR, Nelson S: Keratinocyte growth factor attenuates lung leak induced by alpha-naphthylthiourea in rats. *Crit Care Med* 1996, 24(6):925-931.
389. Welsh DA, Summer WR, Dobard EP, Nelson S, Mason CM: Keratinocyte growth factor prevents ventilator-induced lung injury in an ex vivo rat model. *Am J Respir Crit Care Med* 2000, 162(3 Pt 1):1081-1086.
390. Yi ES, Williams ST, Lee H, Malicki DM, Chin EM, Yin S, Tarpley J, Ulich TR: Keratinocyte growth factor ameliorates radiation- and bleomycin-induced lung injury and mortality. *Am J Pathol* 1996, 149(6):1963-1970.
391. Sugahara K, Iyama K, Kuroda MJ, Sano K: Double intratracheal instillation of keratinocyte growth factor prevents bleomycin-induced lung fibrosis in rats. *J Pathol* 1998, 186(1):90-98.

392. Viget NB, Guery BP, Ader F, Neviere R, Alfandari S, Creuzy C, Roussel-Delvallez M, Foucher C, Mason CM, Beaucaire G *et al*: Keratinocyte growth factor protects against Pseudomonas aeruginosa-induced lung injury. *Am J Physiol Lung Cell Mol Physiol* 2000, 279(6):L1199-1209.

393. Fehrenbach H, Kasper M, Tschernig T, Pan T, Schuh D, Shannon JM, Muller M, Mason RJ: Keratinocyte growth factor-induced hyperplasia of rat alveolar type II cells in vivo is resolved by differentiation into type I cells and by apoptosis. *Eur Respir J* 1999, 14(3):534-544.

394. Ulich TR, Yi ES, Longmuir K, Yin S, Biltz R, Morris CF, Housley RM, Pierce GF: Keratinocyte growth factor is a growth factor for type II pneumocytes in vivo. *J Clin Invest* 1994, 93(3):1298-1306.

395. Bachofen M, Weibel ER: Structural alterations of lung parenchyma in the adult respiratory distress syndrome. *Clin Chest Med* 1982, 3(1):35-56.

396. Curley G, Hayes M, Shaw G, Ryan A, Barry F, O'Brien T, O'Toole T, Laffey J: Mesenchymal Stem Cells enhance recovery and repair following Ventilator Induced Lung Injury in the Rat. *Thorax* 2011, In Press.

397. Le Blanc K, Frassoni F, Ball L, Locatelli F, Roelofs H, Lewis I, Lanino E, Sundberg B, Bernardo ME, Remberger M *et al*: Mesenchymal stem cells for treatment of steroid-resistant, severe, acute graft-versus-host disease: a phase II study. *Lancet* 2008, 371(9624):1579-1586.

398. Lee JS, Hong JM, Moon GJ, Lee PH, Ahn YH, Bang OY: A long-term follow-up study of intravenous autologous mesenchymal stem cell transplantation in patients with ischemic stroke. *Stem Cells* 2010, 28(6):1099-1106.

399. Matthay MA, Thompson BT, Read EJ, McKenna DH, Jr., Liu KD, Calfee CS, Lee JW: Therapeutic potential of mesenchymal stem cells for severe acute lung injury. *Chest* 2010, 138(4):965-972.

400. Burst VR, Gillis M, Putsch F, Herzog R, Fischer JH, Heid P, Muller-Ehmsen J, Schenk K, Fries JW, Baldamus CA *et al*: Poor cell survival limits the beneficial impact of mesenchymal stem cell transplantation on acute kidney injury. *Nephron Exp Nephrol* 2010, 114(3):e107-116.

401. Curley GF, Contreras M, Higgins B, O'Kane C, McAuley DF, O'Toole D, Laffey JG: Evolution of the Inflammatory and Fibroproliferative Responses during Resolution and Repair Following Ventilator-induced Lung Injury in the Rat. *Anesthesiology* 2011.

402. Kotton DN, Ma BY, Cardoso WV, Sanderson EA, Summer RS, Williams MC, Fine A: Bone marrow-derived cells as progenitors of lung alveolar epithelium. *Development* 2001, 128(24):5181-5188.

403. Freyman T, Polin G, Osman H, Crary J, Lu M, Cheng L, Palasis M, Wilensky RL: A quantitative, randomized study evaluating three methods of mesenchymal stem cell delivery following myocardial infarction. *Eur Heart J* 2006, 27(9):1114-1122.

404. Kraitchman DL, Tatsumi M, Gilson WD, Ishimori T, Kedziorek D, Walczak P, Segars WP, Chen HH, Fritzges D, Izbudak I *et al*: Dynamic

imaging of allogeneic mesenchymal stem cells trafficking to myocardial infarction. *Circulation* 2005, 112(10):1451-1461.

405. Beers MF, Morrisey EE: The three R's of lung health and disease: repair, remodeling, and regeneration. *J Clin Invest* 2011, 121(6):2065-2073.

406. Papazian L, Doddoli C, Chetaille B, Gernez Y, Thirion X, Roch A, Donati Y, Bonnety M, Zandotti C, Thomas P: A contributive result of open-lung biopsy improves survival in acute respiratory distress syndrome patients. *Crit Care Med* 2007, 35(3):755-762.

407. Lopez AD, Avasarala S, Grewal S, Murali AK, London L: Differential role of the Fas/Fas ligand apoptotic pathway in inflammation and lung fibrosis associated with reovirus 1/L-induced bronchiolitis obliterans organizing pneumonia and acute respiratory distress syndrome. *J Immunol* 2009, 183(12):8244-8257.

408. Scotton CJ, Chambers RC: Molecular targets in pulmonary fibrosis: the myofibroblast in focus. *Chest* 2007, 132(4):1311-1321.

409. Kim KK, Kugler MC, Wolters PJ, Robillard L, Galvez MG, Brumwell AN, Sheppard D, Chapman HA: Alveolar epithelial cell mesenchymal transition develops in vivo during pulmonary fibrosis and is regulated by the extracellular matrix. *Proc Natl Acad Sci U S A* 2006, 103(35):13180-13185.

410. Kuwano K: Epithelial cell apoptosis and lung remodeling. *Cell Mol Immunol* 2007, 4(6):419-429.

411. Wilson MR, Choudhury S, Goddard ME, O'Dea KP, Nicholson AG, Takata M: High tidal volume upregulates intrapulmonary cytokines in an in vivo mouse model of ventilator-induced lung injury. *J Appl Physiol* 2003, 95(4):1385-1393.

412. Yoshikawa S, King JA, Lausch RN, Penton AM, Eyal FG, Parker JC: Acute ventilator-induced vascular permeability and cytokine responses in isolated and in situ mouse lungs. *J Appl Physiol* 2004, 97(6):2190-2199.

413. Stuber F, Wrigge H, Schroeder S, Wetegrove S, Zinserling J, Hoeft A, Putensen C: Kinetic and reversibility of mechanical ventilation-associated pulmonary and systemic inflammatory response in patients with acute lung injury. *Intensive Care Med* 2002, 28(7):834-841.

414. Parsons PE, Eisner MD, Thompson BT, Matthay MA, Ancukiewicz M, Bernard GR, Wheeler AP: Lower tidal volume ventilation and plasma cytokine markers of inflammation in patients with acute lung injury. *Crit Care Med* 2005, 33(1):1-6; discussion 230-232.

415. Parsons PE, Matthay MA, Ware LB, Eisner MD: Elevated plasma levels of soluble TNF receptors are associated with morbidity and mortality in patients with acute lung injury. *Am J Physiol Lung Cell Mol Physiol* 2005, 288(3):L426-431.

416. Hong SB, Huang Y, Moreno-Vinasco L, Sammani S, Moitra J, Barnard JW, Ma SF, Mirzapoiazova T, Evenoski C, Reeves RR *et al*: Essential role of pre-B-cell colony enhancing factor in ventilator-induced lung injury. *Am J Respir Crit Care Med* 2008, 178(6):605-617.

417. Wolthuis EK, Vlaar AP, Choi G, Roelofs JJ, Haitsma JJ, van der Poll T, Juffermans NP, Zweers MM, Schultz MJ: Recombinant human soluble tumor necrosis factor-alpha receptor fusion protein partly attenuates ventilator-induced lung injury. *Shock* 2009, 31(3):262-266.
418. Chiang CH, Pai HI, Liu SL: Ventilator-induced lung injury (VILI) promotes ischemia/reperfusion lung injury (I/R) and NF-kappaB antibody attenuates both injuries. *Resuscitation* 2008, 79(1):147-154.
419. Held HD, Boettcher S, Hamann L, Uhlig S: Ventilation-induced chemokine and cytokine release is associated with activation of nuclear factor-kappaB and is blocked by steroids. *Am J Respir Crit Care Med* 2001, 163(3 Pt 1):711-716.
420. Wilson MR, Goddard ME, O'Dea KP, Choudhury S, Takata M: Differential roles of p55 and p75 tumor necrosis factor receptors on stretch-induced pulmonary edema in mice. *Am J Physiol Lung Cell Mol Physiol* 2007, 293(1):L60-68.
421. Sime PJ, Xing Z, Graham FL, Csaky KG, Gauldie J: Adenovector-mediated gene transfer of active transforming growth factor-beta1 induces prolonged severe fibrosis in rat lung. *J Clin Invest* 1997, 100(4):768-776.
422. Border WA, Ruoslahti E: Transforming growth factor-beta in disease: the dark side of tissue repair. *J Clin Invest* 1992, 90(1):1-7.
423. Giri SN, Hyde DM, Hollinger MA: Effect of antibody to transforming growth factor beta on bleomycin induced accumulation of lung collagen in mice. *Thorax* 1993, 48(10):959-966.
424. Broekelmann TJ, Limper AH, Colby TV, McDonald JA: Transforming growth factor beta 1 is present at sites of extracellular matrix gene expression in human pulmonary fibrosis. *Proc Natl Acad Sci U S A* 1991, 88(15):6642-6646.
425. Hamacher J, Lucas R, Lijnen HR, Buschke S, Dunant Y, Wendel A, Grau GE, Suter PM, Ricou B: Tumor necrosis factor-alpha and angiostatin are mediators of endothelial cytotoxicity in bronchoalveolar lavages of patients with acute respiratory distress syndrome. *Am J Respir Crit Care Med* 2002, 166(5):651-656.
426. Hurst VI, Goldberg PL, Minnear FL, Heimark RL, Vincent PA: Rearrangement of adherens junctions by transforming growth factor-beta1: role of contraction. *Am J Physiol* 1999, 276(4 Pt 1):L582-595.
427. Gill SE, Parks WC: Metalloproteinases and their inhibitors: regulators of wound healing. *Int J Biochem Cell Biol* 2008, 40(6-7):1334-1347.
428. Murphy G, Docherty AJ: The matrix metalloproteinases and their inhibitors. *Am J Respir Cell Mol Biol* 1992, 7(2):120-125.
429. Hoshino M, Nakamura Y, Sim J, Shimojo J, Isogai S: Bronchial subepithelial fibrosis and expression of matrix metalloproteinase-9 in asthmatic airway inflammation. *J Allergy Clin Immunol* 1998, 102(5):783-788.

430. Agren MS: Matrix metalloproteinases (MMPs) are required for re-epithelialization of cutaneous wounds. ***Arch Dermatol Res*** **1999, 291(11):583-590.**
431. Mirastschijski U, Haaksma CJ, Tomasek JJ, Agren MS: Matrix metalloproteinase inhibitor GM 6001 attenuates keratinocyte migration, contraction and myofibroblast formation in skin wounds. ***Exp Cell Res*** **2004, 299(2):465-475.**
432. Albaiceta GM, Gutierrez-Fernandez A, Parra D, Astudillo A, Garcia-Prieto E, Taboada F, Fueyo A: Lack of matrix metalloproteinase-9 worsens ventilator-induced lung injury. ***Am J Physiol Lung Cell Mol Physiol*** **2008, 294(3):L535-543.**
433. Renckens R, Roelofs JJ, Florquin S, de Vos AF, Lijnen HR, van't Veer C, van der Poll T: Matrix metalloproteinase-9 deficiency impairs host defense against abdominal sepsis. ***J Immunol*** **2006, 176(6):3735-3741.**
434. Lukkarinen H, Hogmalm A, Lappalainen U, Bry K: Matrix metalloproteinase-9 deficiency worsens lung injury in a model of bronchopulmonary dysplasia. ***Am J Respir Cell Mol Biol*** **2009, 41(1):59-68.**
435. Cabrera S, Gaxiola M, Arreola JL, Ramirez R, Jara P, D'Armiento J, Richards T, Selman M, Pardo A: Overexpression of MMP9 in macrophages attenuates pulmonary fibrosis induced by bleomycin. ***Int J Biochem Cell Biol*** **2007, 39(12):2324-2338.**
436. Heise RL, Stober V, Cheluvaraju C, Hollingsworth JW, Garantziotis S: Mechanical stretch induces epithelial-mesenchymal transition in alveolar epithelia via hyaluronan activation of innate immunity. ***J Biol Chem*** **2011, 286(20):17435-17444.**
437. Thannickal VJ, Horowitz JC: Evolving concepts of apoptosis in idiopathic pulmonary fibrosis. ***Proc Am Thorac Soc*** **2006, 3(4):350-356.**
438. Fattman CL: Apoptosis in pulmonary fibrosis: too much or not enough? ***Antioxid Redox Signal*** **2008, 10(2):379-385.**
439. Rocco PR, Negri EM, Kurtz PM, Vasconcellos FP, Silva GH, Capelozzi VL, Romero PV, Zin WA: Lung tissue mechanics and extracellular matrix remodeling in acute lung injury. ***Am J Respir Crit Care Med*** **2001, 164(6):1067-1071.**
440. Santos FB, Nagato LK, Boechem NM, Negri EM, Guimaraes A, Capelozzi VL, Faffe DS, Zin WA, Rocco PR: Time course of lung parenchyma remodeling in pulmonary and extrapulmonary acute lung injury. ***J Appl Physiol*** **2006, 100(1):98-106.**
441. Rocco PR, Souza AB, Faffe DS, Passaro CP, Santos FB, Negri EM, Lima JG, Contador RS, Capelozzi VL, Zin WA: Effect of corticosteroid on lung parenchyma remodeling at an early phase of acute lung injury. ***Am J Respir Crit Care Med*** **2003, 168(6):677-684.**
442. Shapiro SD, Ingenito EP: The pathogenesis of chronic obstructive pulmonary disease: advances in the past 100 years. ***Am J Respir Cell Mol Biol*** **2005, 32(5):367-372.**
443. Kielty CM: Elastic fibres in health and disease. ***Expert Rev Mol Med*** **2006, 8(19):1-23.**

444. Senior RM, Griffin GL, Mecham RP: Chemotactic activity of elastin-derived peptides. *J Clin Invest* 1980, 66(4):859-862.
445. Senior RM, Griffin GL, Mecham RP, Wrenn DS, Prasad KU, Urry DW: Val-Gly-Val-Ala-Pro-Gly, a repeating peptide in elastin, is chemotactic for fibroblasts and monocytes. *J Cell Biol* 1984, 99(3):870-874.
446. Hunninghake GW, Davidson JM, Rennard S, Szapiel S, Gadek JE, Crystal RG: Elastin fragments attract macrophage precursors to diseased sites in pulmonary emphysema. *Science* 1981, 212(4497):925-927.
447. Marchese C, Chedid M, Dirsch OR, Csaky KG, Santanelli F, Latini C, LaRochelle WJ, Torrisi MR, Aaronson SA: Modulation of keratinocyte growth factor and its receptor in reepithelializing human skin. *J Exp Med* 1995, 182(5):1369-1376.
448. Werner S, Smola H, Liao X, Longaker MT, Krieg T, Hofschneider PH, Williams LT: The function of KGF in morphogenesis of epithelium and reepithelialization of wounds. *Science* 1994, 266(5186):819-822.
449. Charafeddine L, D'Angio CT, Richards JL, Stripp BR, Finkelstein JN, Orlowski CC, LoMonaco MB, Paxhia A, Ryan RM: Hyperoxia increases keratinocyte growth factor mRNA expression in neonatal rabbit lung. *Am J Physiol* 1999, 276(1 Pt 1):L105-113.
450. Verghese GM, McCormick-Shannon K, Mason RJ, Matthay MA: Hepatocyte growth factor and keratinocyte growth factor in the pulmonary edema fluid of patients with acute lung injury. Biologic and clinical significance. *Am J Respir Crit Care Med* 1998, 158(2):386-394.
451. Stern JB, Fierobe L, Paugam C, Rolland C, Dehoux M, Petiet A, Dombret MC, Mantz J, Aubier M, Crestani B: Keratinocyte growth factor and hepatocyte growth factor in bronchoalveolar lavage fluid in acute respiratory distress syndrome patients. *Crit Care Med* 2000, 28(7):2326-2333.
452. Curley GF, Hayes M, Ansari B, Shaw G, Ryan A, Barry F, O'Brien T, O'Toole D, Laffey JG: Mesenchymal stem cells enhance recovery and repair following ventilator-induced lung injury in the rat. *Thorax* 2011.
453. Miyahara Y, Nagaya N, Kataoka M, Yanagawa B, Tanaka K, Hao H, Ishino K, Ishida H, Shimizu T, Kangawa K *et al*: Monolayered mesenchymal stem cells repair scarred myocardium after myocardial infarction. *Nat Med* 2006, 12(4):459-465.
454. Lee RH, Seo MJ, Reger RL, Spees JL, Pulin AA, Olson SD, Prockop DJ: Multipotent stromal cells from human marrow home to and promote repair of pancreatic islets and renal glomeruli in diabetic NOD/scid mice. *Proc Natl Acad Sci U S A* 2006, 103(46):17438-17443.
455. Yi ES, Salgado M, Williams S, Kim SJ, Masliah E, Yin S, Ulich TR: Keratinocyte growth factor decreases pulmonary edema, transforming growth factor-beta and platelet-derived growth factor-BB expression, and alveolar type II cell loss in bleomycin-induced lung injury. *Inflammation* 1998, 22(3):315-325.

456. Guo J, Yi ES, Havill AM, Sarosi I, Whitcomb L, Yin S, Middleton SC, Piguet P, Ulich TR: Intravenous keratinocyte growth factor protects against experimental pulmonary injury. *Am J Physiol* 1998, 275(4 Pt 1):L800-805.

457. Waters CM, Savla U: Keratinocyte growth factor accelerates wound closure in airway epithelium during cyclic mechanical strain. *J Cell Physiol* 1999, 181(3):424-432.

458. Kursova LV, Konoplyannikov AG, Pasov VV, Ivanova IN, Poluektova MV, Konoplyannikova OA: Possibilities for the use of autologous mesenchymal stem cells in the therapy of radiation-induced lung injuries. *Bull Exp Biol Med* 2009, 147(4):542-546.

459. Chen SL, Fang WW, Ye F, Liu YH, Qian J, Shan SJ, Zhang JJ, Chunhua RZ, Liao LM, Lin S *et al*: Effect on left ventricular function of intracoronary transplantation of autologous bone marrow mesenchymal stem cell in patients with acute myocardial infarction. *Am J Cardiol* 2004, 94(1):92-95.

460. Katritsis DG, Sotiropoulou PA, Karvouni E, Karabinos I, Korovesis S, Perez SA, Voridis EM, Papamichail M: Transcoronary transplantation of autologous mesenchymal stem cells and endothelial progenitors into infarcted human myocardium. *Catheter Cardiovasc Interv* 2005, 65(3):321-329.

461. Chen S, Liu Z, Tian N, Zhang J, Yei F, Duan B, Zhu Z, Lin S, Kwan TW: Intracoronary transplantation of autologous bone marrow mesenchymal stem cells for ischemic cardiomyopathy due to isolated chronic occluded left anterior descending artery. *J Invasive Cardiol* 2006, 18(11):552-556.

462. Ripa RS, Haack-Sorensen M, Wang Y, Jorgensen E, Mortensen S, Bindslev L, Friis T, Kastrup J: Bone marrow derived mesenchymal cell mobilization by granulocyte-colony stimulating factor after acute myocardial infarction: results from the Stem Cells in Myocardial Infarction (STEMMI) trial. *Circulation* 2007, 116(11 Suppl):I24-30.

463. Bang OY, Lee JS, Lee PH, Lee G: Autologous mesenchymal stem cell transplantation in stroke patients. *Ann Neurol* 2005, 57(6):874-882.

464. Mazzini L, Mareschi K, Ferrero I, Vassallo E, Oliveri G, Boccaletti R, Testa L, Livigni S, Fagioli F: Autologous mesenchymal stem cells: clinical applications in amyotrophic lateral sclerosis. *Neurol Res* 2006, 28(5):523-526.

465. Koc ON, Day J, Nieder M, Gerson SL, Lazarus HM, Krivit W: Allogeneic mesenchymal stem cell infusion for treatment of metachromatic leukodystrophy (MLD) and Hurler syndrome (MPS-IH). *Bone Marrow Transplant* 2002, 30(4):215-222.

466. Venkataramana NK, Kumar SK, Balaraju S, Radhakrishnan RC, Bansal A, Dixit A, Rao DK, Das M, Jan M, Gupta PK *et al*: Open-labeled study of unilateral autologous bone-marrow-derived mesenchymal stem cell transplantation in Parkinson's disease. *Transl Res* 2010, 155(2):62-70.

467. Le Blanc K, Rasmusson I, Sundberg B, Gotherstrom C, Hassan M, Uzunel M, Ringden O: Treatment of severe acute graft-versus-host

disease with third party haploidentical mesenchymal stem cells. *Lancet* 2004, 363(9419):1439-1441.

468. Ringden O, Uzunel M, Rasmusson I, Remberger M, Sundberg B, Lonnies H, Marschall HU, Dlugosz A, Szakos A, Hassan Z *et al*: Mesenchymal stem cells for treatment of therapy-resistant graft-versus-host disease. *Transplantation* 2006, 81(10):1390-1397.

469. Boulton AJ, Vileikyte L, Ragnarson-Tennvall G, Apelqvist J: The global burden of diabetic foot disease. *Lancet* 2005, 366(9498):1719-1724.

470. Matthay MA, Goolaerts A, Howard JP, Lee JW: Mesenchymal stem cells for acute lung injury: preclinical evidence. *Crit Care Med* 2010, 38(10 Suppl):S569-573.

471. Wang J, Liao L, Tan J: Mesenchymal-stem-cell-based experimental and clinical trials: current status and open questions. *Expert Opin Biol Ther* 2011, 11(7):893-909.

472. Henning RJ, Burgos JD, Vasko M, Alvarado F, Sanberg CD, Sanberg PR, Morgan MB: Human cord blood cells and myocardial infarction: effect of dose and route of administration on infarct size. *Cell Transplant* 2007, 16(9):907-917.

473. Ghofrani HA, Barst RJ, Benza RL, Champion HC, Fagan KA, Grimminger F, Humbert M, Simonneau G, Stewart DJ, Ventura C *et al*: Future perspectives for the treatment of pulmonary arterial hypertension. *J Am Coll Cardiol* 2009, 54(1 Suppl):S108-117.

474. Behr L, Hekmati M, Fromont G, Borenstein N, Noel LH, Lelievre-Pegorier M, Laborde K: Intra renal arterial injection of autologous mesenchymal stem cells in an ovine model in the postischemic kidney. *Nephron Physiol* 2007, 107(3):p65-76.

475. de Vasconcelos Dos Santos A, da Costa Reis J, Diaz Paredes B, Moraes L, Jasmin, Giraldi-Guimaraes A, Mendez-Otero R: Therapeutic window for treatment of cortical ischemia with bone marrow-derived cells in rats. *Brain Res* 2010, 1306:149-158.

476. Meisel R, Brockers S, Heseler K, Degistirici O, Bulle H, Woite C, Stuhlsatz S, Schwippert W, Jager M, Sorg R *et al*: Human but not murine multipotent mesenchymal stromal cells exhibit broad-spectrum antimicrobial effector function mediated by indoleamine 2,3-dioxygenase. *Leukemia* 2011, 25(4):648-654.

477. Gregory CA, Ylostalo J, Prockop DJ: Adult bone marrow stem/progenitor cells (MSCs) are preconditioned by microenvironmental "niches" in culture: a two-stage hypothesis for regulation of MSC fate. *Sci STKE* 2005, 2005(294):pe37.

478. Lee RH, Hsu SC, Munoz J, Jung JS, Lee NR, Pochampally R, Prockop DJ: A subset of human rapidly self-renewing marrow stromal cells preferentially engraft in mice. *Blood* 2006, 107(5):2153-2161.

479. Sarugaser R, Hanoun L, Keating A, Stanford WL, Davies JE: Human mesenchymal stem cells self-renew and differentiate according to a deterministic hierarchy. *PLoS One* 2009, 4(8):e6498.

480. Karp JM, Leng Teo GS: Mesenchymal stem cell homing: the devil is in the details. *Cell Stem Cell* 2009, 4(3):206-216.

481. Rombouts WJ, Ploemacher RE: Primary murine MSC show highly efficient homing to the bone marrow but lose homing ability following culture. *Leukemia* 2003, 17(1):160-170.
482. Das R, Jahr H, van Osch GJ, Farrell E: The role of hypoxia in bone marrow-derived mesenchymal stem cells: considerations for regenerative medicine approaches. *Tissue Eng Part B Rev* 2010, 16(2):159-168.
483. Stolzing A, Scutt A: Effect of reduced culture temperature on antioxidant defences of mesenchymal stem cells. *Free Radic Biol Med* 2006, 41(2):326-338.
484. Garcia-Gomez I, Elvira G, Zapata AG, Lamana ML, Ramirez M, Castro JG, Arranz MG, Vicente A, Bueren J, Garcia-Olmo D: Mesenchymal stem cells: biological properties and clinical applications. *Expert Opin Biol Ther* 2010, 10(10):1453-1468.
485. Schallmoser K, Bartmann C, Rohde E, Bork S, Guelly C, Obenauf AC, Reinisch A, Horn P, Ho AD, Strunk D *et al*: Replicative senescence-associated gene expression changes in mesenchymal stromal cells are similar under different culture conditions. *Haematologica* 2010, 95(6):867-874.
486. Muraglia A, Cancedda R, Quarto R: Clonal mesenchymal progenitors from human bone marrow differentiate in vitro according to a hierarchical model. *J Cell Sci* 2000, 113 (Pt 7):1161-1166.
487. Rubio D, Garcia-Castro J, Martin MC, de la Fuente R, Cigudosa JC, Lloyd AC, Bernad A: Spontaneous human adult stem cell transformation. *Cancer Res* 2005, 65(8):3035-3039.
488. Rosland GV, Svendsen A, Torsvik A, Sobala E, McCormack E, Immervoll H, Mysliwietz J, Tonn JC, Goldbrunner R, Lonning PE *et al*: Long-term cultures of bone marrow-derived human mesenchymal stem cells frequently undergo spontaneous malignant transformation. *Cancer Res* 2009, 69(13):5331-5339.
489. Wang Y, Huso DL, Harrington J, Kellner J, Jeong DK, Turney J, McNiece IK: Outgrowth of a transformed cell population derived from normal human BM mesenchymal stem cell culture. *Cytotherapy* 2005, 7(6):509-519.
490. Bernardo ME, Zaffaroni N, Novara F, Cometa AM, Avanzini MA, Moretta A, Montagna D, Maccario R, Villa R, Daidone MG *et al*: Human bone marrow derived mesenchymal stem cells do not undergo transformation after long-term in vitro culture and do not exhibit telomere maintenance mechanisms. *Cancer Res* 2007, 67(19):9142-9149.
491. Grimes BR, Steiner CM, Merfeld-Clauss S, Traktuev DO, Smith D, Reese A, Breman AM, Thurston VC, Vance GH, Johnstone BH *et al*: Interphase FISH demonstrates that human adipose stromal cells maintain a high level of genomic stability in long-term culture. *Stem Cells Dev* 2009, 18(5):717-724.
492. Kim J, Kang JW, Park JH, Choi Y, Choi KS, Park KD, Baek DH, Seong SK, Min HK, Kim HS: Biological characterization of long-term cultured human mesenchymal stem cells. *Arch Pharm Res* 2009, 32(1):117-126.

493. Garcia S, Bernad A, Martin MC, Cigudosa JC, Garcia-Castro J, de la Fuente R: Pitfalls in spontaneous in vitro transformation of human mesenchymal stem cells. *Exp Cell Res* 2010, 316(9):1648-1650.

494. Hashimoto N, Jin H, Liu T, Chensue SW, Phan SH: Bone marrow-derived progenitor cells in pulmonary fibrosis. *J Clin Invest* 2004, 113(2):243-252.

495. Epperly MW, Guo H, Gretton JE, Greenberger JS: Bone marrow origin of myofibroblasts in irradiation pulmonary fibrosis. *Am J Respir Cell Mol Biol* 2003, 29(2):213-224.

496. Aguilar S, Scotton CJ, McNulty K, Nye E, Stamp G, Laurent G, Bonnet D, Janes SM: Bone marrow stem cells expressing keratinocyte growth factor via an inducible lentivirus protects against bleomycin-induced pulmonary fibrosis. *PLoS One* 2009, 4(11):e8013.